UDK 66:54(05) CODEN HMIDA 8 ISSN 0367–598 X

2

Hemijska industrija

Vol. 70

Časopis Saveza hemijskih inženjera Srbije

Chemical Industry

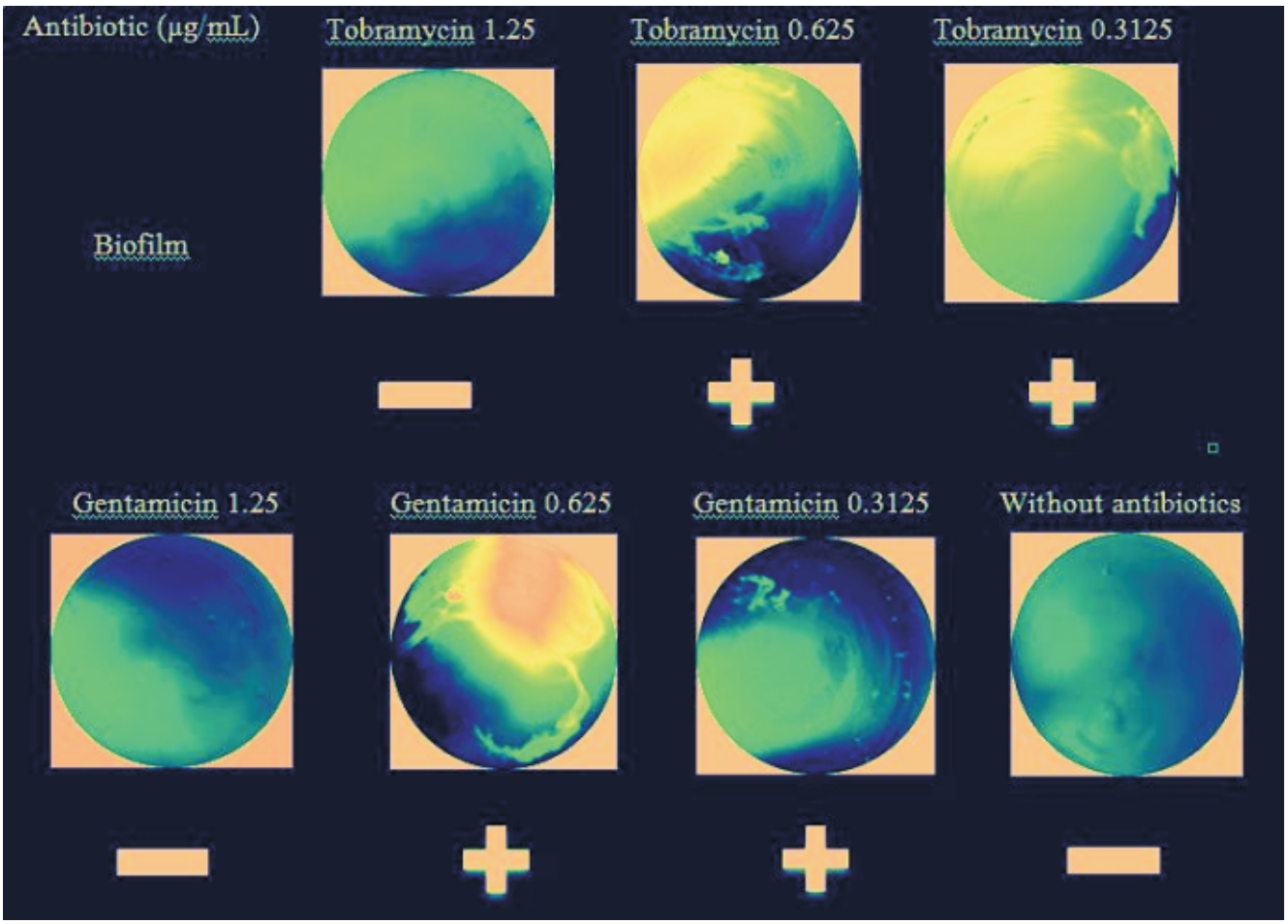

BEOGRAD, MART-APRIL 2016. HMIDA 8, 70 (2) 113-224 (2016)

GENERALNI POKROVITELJ

Hemofarm

HEMOFARM KONCERN

VRŠAC, Beogradski put bb, tel. 013/821-345, 821-027, 821-129
BEOGRAD, Prote Mateje 70, tel. 011/344-26-63, faks: 344-17-87
E-pošta: info@hemofarm.com

Aktivnosti Saveza hemijskih inženjera Srbije pomažu:

MINISTARSTVO PROSVETE, NAUKE I TEHNOLOŠKOG RAZVOJA REPUBLIKE SRBIJE

Tehnološko-metalurški fakultet Univerziteta u Beogradu, Beograd

Prirodno-matematički fakultet Univerziteta u Novom Sadu, Novi Sad

Hemijski fakutet Univerziteta u Beogradu Beograd

ITNMS
Institut za tehnologiju nuklearnih i drugih mineralnih sirovina, Beograd

Institut za opštu i fizičku hemiju, Beograd

Tehnološki fakultet Univerziteta u Novom Sadu, Novi Sad

Hipol
Hipol a.d., Odžaci

NU Institut za hemiju, tehnologiju i metalurgiju Univerziteta u Beogradu, Beograd

Tehnološki fakultet Univerziteta u Nišu, Leskovac

Fakultet tehničkih nauka, Kosovska Mitrovica

Chemical Industry
Химическая промышленность

Hemijska industrija

Časopis Saveza hemijskih inženjera Srbije
Journal of the Association of Chemical Engineers of Serbia
Журнал Союза химических инженеров Сербии

VOL. 70 **Beograd, mart–april 2016** **Broj 2**

Izdavač
Savez hemijskih inženjera Srbije
Beograd, Kneza Miloša 9/I

Glavni urednik
Branko Bugarski
Zamenica glavnog i odgovornog urednika
Nevenka Bošković-Vragolović
Urednici
Katarina Jeremić, Ivana Banković-Ilić, Maja Obradović, Dušan Mijin, Dragan Povrenović, orica Knežević Jugović

Članovi uredništva
Nikolaj Ostrovski, Milorad Cakić, Željko Čupić, Katarina Jeremić, Miodrag Lazić, Slobodan Petrović, Milovan Purenović, Aleksandar Spasić, Dragoslav Stoiljković, Radmila Šećerov-Sokolović, Slobodan Šerbanović, Nikola Nikačević, Svetomir Milojević

Članovi uredništva iz inostranstva
Dragomir Bukur (SAD), Jiri Hanika (Češka Republika), Valerij Meshalkin (Rusija), Ljubiša Radović (SAD), Constantinos Vayenas (Grčka)

Likovno-grafičko rešenje naslovne strane
Milan Jovanović

Redakcija
11000 Beograd, Kneza Miloša 9/I
Tel/fax: 011/3240-018
E-pošta: shi@ache.org.rs
www.ache.org.rs

Izlazi dvomesečno, rukopisi se ne vraćaju

Za izdavača
Tatijana Duduković

Sekretar redakcije
Slavica Desnica

Izdavanje časopisa pomaže
Republika Srbija, Ministarstvo prosvete, nauke i tehnološkog razvoja

Uplata pretplate i oglasnog prostora vrši se na tekući račun Saveza hemijskih inženjera Srbije, Beograd, broj 205-2172-71, Komercijalna banka a.d., Beograd

Kompjuterska priprema
Vladimir Panić

Štampa
Razvojno-istraživački centar grafičkog inženjerstva, Tehnološko-metalurški fakultet, Univerzitet u Beogradu, Karnegijeva 4, 11000 Beograd

Indeksiranje
Radovi koji se publikuju u časopisu *Hemijska Industrija* ideksiraju se preko *Thompson Reuters Scietific®* servisa *Science Citation Index - Expanded™* i *Journal Citation Report (JCR)*

SADRŽAJ/CONTENTS

SADRŽAJ nastavak
CONTENTS continued

Edible mycorrhizal species *Lactarius controversus* Pers. 1800 as a source of antioxidant and cytotoxic agents

Aleksandra R. Novaković[1], Maja A. Karaman[2], Ivan Lj. Milovanović[1], Miona M. Belović[1], Milena J. Rašeta[3], Tanja I. Radusin[1], Nebojša M. Ilić[1]

[1]*Institute of Food Technology, University of Novi Sad, Novi Sad, Serbia*
[2]*Department of Biology and Ecology, Faculty of Sciences, University of Novi Sad, Novi Sad, Serbia*
[3]*Department of Chemistry, Biochemistry and Environmental Protection, Faculty of Sciences, University of Novi Sad, Novi Sad, Serbia*

Abstract
The aim of this work was to study chemical profile and antioxidant and cytotoxic activities of ethanol and water extracts of *Lactarius controversus* (Pers.) 1800 mushroom species growing in eastern Serbia. The chemical characterization of phenolic compounds performed by HPLC–MS/MS demonstrated the presence of quinic acid among others. Determination of antioxidant activity, including radical scavenging effects on DPPH$^{\bullet}$, NO$^{\bullet}$, $^{\bullet}$OH and SOA radicals and ferric reducing ability was investigated. The highest DPPH radical scavenging effect was obtained for water extract (LcAq) while ethanol extract (LcEtOH) demonstrated the highest FRAP activity. Hexane extract applied in antibacterial assay against three pathogenic strains demonstrated antibacterial effect only against *S. aureus* ATCC25922. Anti-proliferative properties against estrogen dependent MCF 7 breast cancer cell lines using MTT showed higher activity for ethanolic extract.

Keywords: *Lactarius controversus*, phenolic compounds, quinic acid, antioxidants, cytotoxic agents.

Available online at the Journal website: http://www.ache.org.rs/HI/

SCIENTIFIC PAPER

UDC 582.28(497.11-11):54:543.544

Hem. Ind. **70** (2) 113–122 (2016)

doi: 10.2298/HEMIND141229017N

For thousands of years, traditional oriental medicine has used natural products, including medicinal and toxic mushrooms, for curing and disease prevention. Most of medicinal mushroom preparations were used in a form of tonics, food or powder with unknown side-effects. Nowadays, wild-growing mushrooms still comprise a vast and largely untapped source of powerful new pharmaceutical products for the mankind in the future [1]. The number of mushroom species on Earth is estimated to approximately 140,000 species, while only 10% of them have been already determined. According to estimates that only 5% of the total known species, which is about 7000 species, are with detected and potential benefits for mankind, means that mushrooms are still insufficiently explored sources of bioactive compounds [2–5]. Mushrooms contain a variety of complex compounds derived from secondary metabolism such as phenolic compounds, polyketides, triterpenoids and steroids which are specific to each mushroom species and strain and have specific medicinal effects on humans, including antimicrobial, antitumor, antioxidant etc. [6,7]. Many such compounds have been used in the treatment of cancer [8,9]. Furthermore, evidence-based studies suggest that there is a relationship between the physiopathology of several chronic diseases (*e.g.*, cancer) and oxidative stress development. Therefore, the use of foods rich in antioxidants, such as phytochemical and mycochemical protectors, may be the most relevant factor in the prevention of oxidative stress related diseases [10]. Moreover, there is a continuous need for discovery of new molecules that are able to effectively reduce cancer which is the leading cause of death in Europe in 2006 [11].

Some literature data suggest that *L. controversus* is inedible species [12], but in Serbia this species is used as food, after obligatory cooking procedure before consumption.

In the present work we studied whether the autochthonous mushroom species *Lactarius controversus* Pers. 1800 possesses antioxidant, antibacterial and antiproliferative properties. To our knowledge, this is the first report dealing with the antioxidant growth inhibitory properties of *L. controversus* against MCF 7 breast cancer cell line.

EXPERIMENTAL

Standards and reagents

Folin–Ciocalteu (FC) reagent, anhydrous sodium carbonate, gallic acid, aluminium trichloride hexahydrate, sodium acetate trihydrate, quercetin hydrate, 2,2--diphenyl-1-picrylhydrazyl (DPPH$^{\bullet}$), anhydrous iron(III)

Correspondence: A. Novaković, Institute of Food Technology, University of Novi Sad, Bulevar cara Lazara 1, 21000 Novi Sad, Serbia.
E-mail: aleksandra.novakovic@fins.uns.ac.rs
Paper received: 29 December, 2014
Paper accepted: 6 March, 2015

chloride, 2,4,6-Tris(2-pyridyl)-s-triazine (TPTZ), 2-thiobarbituric acid, disodium hydrogen phosphate, thiazolyl blue tetrazolium bromide, phenazine methosulfate (PMS), and β-nicotinamide adenine dinucleotide (NADH), 3-(4,5-dimethylthiazole-2-yl)-2,5-diphenyltetrazolium bromide (MTT), dimethyl sulfoxide (DMSO), sulforhodamine B (SRB), and trichloroacetic acid (TCA) were purchased from Sigma-Aldrich (Steinheim, Germany). Dulbecco's Modified Eagle's Medium with 4.5% of glucose (DMEM) and fetal calf serum (FCS) were purchased from PAA Laboratories (Pasching, Austria). Ascorbic acid, potassium dihydrogen phosphate, sodium nitroprusside dihidrate (SNP), naphthylethylenediamine dihydrochloride (NEDA), sulfanilamide (SA) 35% hydrogen peroxide, iron(II) sulfate heptahydrate, trichloracetic acid, and ethylenediaminetetraacetic acid (EDTA) were purchased from Lach-ner (Neratovice, Czech Republic). 2-Deoxy-D-ribose was obtained from Alfa Aesar (Karlsruhe, Germany). Reference standards of the phenolic compounds were obtained from Sigma–Aldrich Chem (Steinheim, Germany), Fluka Chemie GmbH (Buchs, Switzerland) or from Chromadex (Santa Ana, USA). HPLC gradient grade methanol was purchased from J. T. Baker (Deventer, The Netherlands), and p.a. formic acid and DMSO from Merck (Darmstadt, Germany). Deionized water was produced using a Millipore water purification system.

Mushroom samples

Lactarius controversus was collected from Sikola area in Serbia during the year 2012. After the identification of the species, a voucher specimen (12-00663) was deposited at the Herbarium Buns, Faculty of Sciences Department of Biology and Ecology, University of Novi Sad. The mushroom samples were pre-frozen at –20 °C and freeze-dried (Martin Christ GmbH, Germany). Freeze dried samples were ground to a fine powder, wrapped in plastic bags and stored in the dark at room temperature prior to analysis.

Extraction

The whole freeze dried and powdered sporocarps of *L. controversus* (10 g) were extracted with the following solvents: ethanol (EtOH), methanol (MeOH) or hexane (Hex) and distilled water (Aq) for 24 h on a shaker (Thermofisher Scientific, USA) at 120 rpm at room temperature (25 °C). The extracts were filtered through Whatman No.4 filter paper and the solvents were removed by rotary evaporation in vacuum at 40 °C (Bűchi, Switzerland). The extracts obtained (LcEtOH, LcMeOH, LcHex) were stored in refrigerator at 4 °C, while aqueous extract (LcAq) was stored at –20 °C prior to analysis. Dry residues were redissolved in DMSO to obtain LcAq, LcEtOH, for determination of antioxidant and anti-proliferative activities (5 mg/ml), and LcHex was used for evaluation of antibacterial activity.

HPLC–MS/MS screening of the phenolic compounds

For HPLC–MS/MS determination of the phenolic profile, method developed by Orčić *et al*. [13] was used. The Agilent 1200 series liquid chromatograph was used for separation of all analytes, using a Zorbax Eclipse XDB-C18 RR 4.6 mm×50 mm×1.8 mm (Agilent Technologies) reversed-phase column held at 40 °C. Detection was carried out by Agilent series 6410A triple-quadrupole mass spectrometer with electrospray ionization (ESI). MassHunter ver. B.03.01. software (Agilent Technologies) was used for instruments control and data analysis. The binary mobile phase consisted of 0.05% formic acid (A) and methanol (B) and was delivered at a flow rate of 1 ml/min. Gradient elution was performed using the following solvent gradient: starting with 70% A/30% B, reaching 30% A/70% B in 6.00 min, then 100% B at 9.00 min, holding until 12.00 min, with reequilibration time of 3 min. The injection volume for all samples was 5 µL. ESI parameters were: drying gas (N2) temperature, 350 °C; flow, 9 L/min; nebulizer gas pressure, 40 psi; capillary voltage, 4 kV, negative polarity. All compounds were quantified in dynamic MRM mode (multiple reaction monitoring mode). Compound-specific, optimized MS/ /MS parameters are given in Table 1. The mix of stock solutions was prepared, with concentration of each compound being 100 µg/ml, and then, subsequently serially diluted in methanol–water (1:1), giving working standard solutions with concentration ranging from 0.0015 do 25.0 µg/ml, which were used for construction of the calibration curves. Concentrations of standard compounds in extracts were determined from the peak areas by using the equation for linear regression obtained from the calibration curves (R2 gt; 0.995).

Total phenolic content

Total phenolic content (TP) in the ethanol and water extracts was determined according to method by Singleton *et al*. [14] adapted for plate reader (Multiskan Ascent, Thermo Electron Corporation). 125 µl of 0,1M Folin–Ciocalteu reagent was added to 25 µl of diluted extracts. After 10 min, 100 µl of 7.5% sodium carbonate was added and reaction mixture was incubated for 2 h. Absorbance was read at 690 nm after finished incubation period. In order to eliminate the interferences, correction was prepared by replacing the volume of reagents with the same volume of distilled water. Standard curve was prepared for gallic acid, and total phenolic content was expressed as mg gallic acid equivalents (GAE)/g of dry weight. Experiments were performed in triplicate.

Total flavonoid content

The flavonoid (TF) content of investigated extracts was measured spectrophotometrically in a 96-well

Table 1. Optimized dynamic MRM parameters

Compound	t_R / min	Precursor (*m*/*z*)	Product (*m*/*z*)	$V_{fragmentor}$ / V	$V_{collision}$ / V
Gallic acid	0.58	169	125	90	10
Catechin	0.74	289	245	150	10
Protocatechuic acid	0.79	153	109	105	9
5-*O*-Caffeoylquinic acid	0.80	353	191	100	10
Epigallocatechin gallate	0.81	457	169	165	16
Epicatechin	0.95	289	245	150	10
Gentisic acid	1.03	153	109	100	9
p-Hydroxybenzoic acid	1.08	137	93	80	10
Esculetin	1.13	177	133	105	15
Caffeic acid	1.18	179	135	100	10
Vanillic acid	1.24	167	108	100	15
Syringic acid	1.31	197	182	90	7
p-Coumaric acid	1.69	163	119	90	9
Umbelliferone	1.73	161	133	120	19
Scopoletin	1.77	191	176	80	8
Ferulic acid	1.90	193	134	90	11
Vitexin	1.90	431	311	200	22
Sinapic acid	1.92	223	193	100	17
Luteolin 7-*O*-glucoside	2.13	447	285	230	30
Hyperoside	2.16	463	300	200	30
Quercetin 3-*O*-glucoside	2.25	463	300	210	30
Rutin	2.33	609	300	135	42
Apiin	2.60	563	269	250	36
o-Coumaric acid	2.62	163	119	100	5
Myricetin	2.67	317	179	150	20
Quercitrin	2.75	447	300	190	27
Kaempferol 3-*O*-glucoside	2.80	447	284	190	30
Apigenin 7-*O*-glucoside	2.81	431	268	135	41
Secoisolariciresinol	2.90	361	165	130	26
3,4-Dimethoxycinnamic acid	2.99	207	103	110	7
Baicalein	3.40	445	269	140	22
Daidzein	3.43	253	208	145	31
Matairesinol	3.66	357	122	130	24
Quercetin	3.74	301	151	130	15
Naringenin	3.87	271	151	130	16
Cinnamic acid	3.91	147	103	100	5
Luteolin	4.03	285	133	135	25
Genistein	4.12	269	133	145	32
Kaepferol	4.55	285	285	130	0
Apigenin	4.71	269	117	130	25
Isorhamnetin	4.79	315	300	160	21
Chrysoeriol	4.82	299	284	125	20
Baicalein	5.15	269	269	165	0
Amentoflavone	5.78	537	375	220	35

plate reader using modified method by Chang *et al*. [15]. 30 µl of sample was mixed with 90 µl of methanol, 6 µl of 0.75 M aluminium trichloride, 6 µl of 1 M sodium acetate and 170 µl of distilled water. Absorbance was measured at 414 nm after 30 min of incubation. Correction was prepared in the way indicated above, with aluminium trichloride solution replaced with the equivalent volume of distilled water. Standard

curve was prepared using quercetin. Experiments were repeated three times, and results were expressed as mg quercetin equivalents (QE)/g of dry weight.

DPPH radical scavenging activity

Spectrophotometrical determination of free radical scavenging activity was based on the monitoring of DPPH radical transformation in the presence of antioxidants according to Espin *et al*. [16]. The reaction mixture in the wells consisted of 10 µl of sample, 60 µl of DPPH solution and 180 µl of methanol. Control contained ethanol instead of sample, and correction contained 10 µl of sample and 240 µl of methanol. After 60 min of incubation in the dark at room temperature, the absorbance was measured using plate reader at 540 nm. Each sample was tested at five different concentrations to obtain IC_{50}, and experiments were performed in triplicate.

Ferric reducing antioxidant power (FRAP)

FRAP test was performed according to modified procedure of Benzie and Strain [17]. The FRAP reagent consisted of 300 mM acetate buffer (pH 3.6), 10 mM TPTZ in 40 mM HCl and 20 mM $FeCl_3$ in the volume ratio 10:1:1. 10 µl of sample, 225 µl of FRAP reagent and 22,5 µl of distilled water were added in 96-well plate. Extract was replaced by the same volume of ethanol in control, and correction contained distilled water instead of FRAP reagent. Absorbance was measured after 6 min at 620 nm. Ascorbic acid was used to construct the standard curve, and results were expressed as mg ascorbic acid equivalents (AAE)/g of dry weight. Each analysis was performed three times.

Nitric oxide radical scavenging capacity

Nitric oxide scavenging capacity was determined according to the procedure of Green *et al*. [18]. The reaction mixtures in the test tubes consisted of 30 µl tomato extract, 500 µl SNP, and 500 µl of phosphate buffer, pH 7.4. Control contained equivalent volume of ethanol, while the reagents were replaced by the phosphate buffer in the correction. Test tubes were incubated at room temperature for 90 min, under light exposure. After incubation, 1 ml of Griess reagent (0.2% solution of NEDA and 2% solution of SA in 4% phosphoric acid in the volume ratio 1:1) was added to samples, corrections, and control. Aliquots of 250 µl were transferred to the plate, and their absorbance was measured using plate reader at 540 nm. Samples were tested at five different concentrations to obtain IC_{50}, and experiments were performed in triplicate.

Superoxide anion radical scavenging capacity

Superoxide anion radical scavenging capacity of extracts was determined by measuring their ability to neutralize superoxide anion radicals generated during aerobic reduction of nitro blue tetrazolium by NADH mediated by PMS [19]. 100 µl of 677 µM NADH, 100 µl of 60 µM PMS, 200 µl of 144 µM NBT and 1,1 ml of phosphate buffer (pH 8.3) were mixed with 10 µl of extract in the test tube. Control contained ethanol instead of extract, and correction contained 10 µl of extract and 1,5 ml of phosphate buffer. After 5 minutes of incubation, aliquots of 250 µl were transferred to the plate, and their absorbance was measured at 540 nm. Five different concentrations of each sample were tested to obtain IC_{50}, and experiments were performed in triplicate.

Hydroxyl radical scavenging capacity

The content of OH radicals was determined from the degradation reaction of 2-deoxy d-ribose into fragments [20], while the malonyl dialdehyde (MDA) reaction with TBA reagent was determined spectrophotometrically at 532 nm. Each reaction was performed at five different concentrations using 10 µL of fungal extract (33.3–1000 µg/mL) to obtain IC_{50}, and experiments were performed in triplicate.

Antibacterial activity

In vitro antibacterial susceptibility assay was done for LcHex extract after dissolving in 5% DMSO to reach final extract concentration of 0,5%. Standard American Type Culture Collection (ATCC) strains of two Gram--positive bacteria, *Staphylococcus aureus* ATCC25922, *Bacillus subtilis* ATCC6633 and one Gram-negative bacteria, *Escherichia coli* ATCC25923were used.

Two-fold assay in 96-well microplates (Spektar, Čačak, Serbia) for determination of minimal inhibitory concentration (*MIC*) and minimal bactericidal concentration (*MBC*) values was employed. Pure bacterial strains were subcultured on nutrient agar slants at 37 °C 24 h, while suspensions of the tested strains were corresponding to McFarland 0.5 optical density $\approx 1.5\times10^8$ CFU/mL. 50 µl of extract was added to 50 µl of Műeller Hinton Broth (Torlak, Belgrade, Serbia) seeded with 1 µl bacterial suspensions. Evaluation of antibacterial activity was done according to the CLSI procedure (2008) modified by Karaman *et al.* [21] applying extract concentration in the final range from 0.78 to 25.0 mg/mL. After incubation at 3 °C for 18–24 h, *MIC* was determined as the lowest extract concentration preventing visible bacterial growth while the complete absence of growth was considered as *MBC*. It was confirmed by sub-culturing aliquots of 100 µL working solutions on Müeller Hinton agar plates and incubated at 35 °C overnight. Last two wells were free from tested extracts, and hence served as a growth control (positive control) and with 5% DMSO as a negative control. Reference antibiotics (ampicillin and gentamicin) were applied as control standards. All analysis were carried out in triplicate (n = 3).

Evaluation of anti-proliferative activity

Cells

MCF-7 cells were grown in Dulbecco's modified Eagle's medium with 4.5% of glucose (DMEM, PAA Laboratories) supplemented with 10% fetal calf serum (FCS). For the experiment, the cells were seeded in a 96-well microplate (5000 cells per well). After 24 h incubation, the growth medium was replaced with 100 µl of medium containing samples at four different concentrations (33.3, 100, 300 and 900 µg/mL). Untreated cells served as the control, and DMSO was used as a positive control. The effects of the extracts on the growth of human tumor cell line were evaluated according to the two procedures.

MTT Assay

After 24 and 72 h, the cell viability was determined by the proliferation test MTT assay [22], which is based on the colour reaction of mitochondrial dehydrogenase in living cells with MTT reagent. At the end of the treatment period, MTT was added to each well (50 µg/100 µl /well), which was then incubated at 37 °C in 5% CO_2 for 3 h. The coloured crystals of produced formazan were dissolved in 100 µl acidified isopropanol (0.04 M HCl in isopropanol). The absorbance was measured at 540 nm and 690 nm on plate reader (Multiskan Ascent, Thermo Electron Corporation, USA).

SRB (sulforhodamine B) Assay

This colorimetric assay estimates cell number indirectly, by staining cellular protein with the protein--binding dye SRB, in adapted procedure by Skehan *et al*. [23]. After incubation period, the cells were fixed adding cold 50% trichloroacetic acid (TCA) and incubated for 1 h at 4 °C. Wells were washed with deionized water and dried; sulforhodamine solution (0.4% in 1% acetic acid) was then added to each plate well and incubated for 30 min at room temperature. Unbound SRB was removed by washing with 1% acetic acid. Plates were air dried, the bound SRB was solubilised with 10 mM Tris (pH 10.5) and absorbance was measured at 492 and 690 nm in the microplate reader. The results were expressed in EC_{50} values (sample concentration that inhibited 50% of the net cell growth). DMSO was used as positive control.

Percentage of cytotoxicity was calculated as the ratio of treated group absorbance and the control group absorbance, multiplied by 100. Experiments were performed twice in triplicate, and the obtained results were expressed as IC_{50} values (sample concentration that inhibited 50% of the net cell growth). IC_{50} values were calculated from the cytotoxicity (%) – extract concentration (µg/mL) plot using the Origin v. 6.0 graphing and data analysis software (1999).

Statistical analysis

Results were expressed as mean ± standard deviation (*SD*). Statistical analysis was performed using Statistica software system (StatSoft, Inc. (2013), version 12.0 (www.statsoft.com)). Significant differences between two groups were determined by Student's *t*-test. Pearson correlation coefficients were calculated between content of antioxidant compounds in extracts and their antioxidant and antiproliferative activity in different assays. Cluster analysis was performed using Mahalanobius distances.

RESULTS AND DISCUSSION

LC–MS/MS determination of phenolic compounds

Forty-five phenolic compounds were recorded using HPLC–MS/MS technique (Table 1), and only quinic acid was identified and quantified (8.9 µg/g d.w.), while concentrations of other detected compounds were under the limits of quantification (*LOQ*) of the method. According to the obtained results we cannot claim that other detected compounds, which could not be quantified in this work, are not present in examined extracts, but we could expect them to be present in amount lower than listed *LOQ*.

Quinic acid is a crystalline acid that is usually obtained from plants and it is a versatile starting material for the synthesis of new pharmaceuticals [25]. It was found in some species from genus *Lactarius*, *L. volemus* in previous studies [26]. Previous research [25,27,28] showed that quinic acid is a common constituent of human diet, capable of conversion into tryptophan and nicotinamide *via* the micro flora of the gastro intestinal (GI) tract, thus providing *in situ* physiological source of these essential metabolic ingredients to humans [25,27,29].

Antioxidant activity

Antioxidant activity is manifested in a wide variety of actions, such as inhibition of oxidizing enzymes, chelating of transition metals, transfer of hydrogen or a single electron to radicals, singlet oxygen deactivation, or enzymatic detoxification of reactive oxygen species [30,31].

The overall antioxidant activity should be evaluated by different methods in order to extensively characterize the antioxidant potential of pure compounds or extracts [32]. Therefore, water and ethanol extracts of *L. controversus* were examined with regard to scavenging capacity towards, $DPPH^{\bullet}$, $NO^{\bullet}$, $^{\bullet}OH$ and SOA radicals and ferric reducing power.

The results for antioxidant activity of analyzed extracts are shown in Table 2. Although both extracts possessed antioxidant properties, water extract provides higher antioxidant activity (IC_{50} = 219.37 µg/ml) than

*Table 2. Antioxidant activity of L. controversus extracts and their total phenolic and total flavonoid content; *,**: significant differences between two groups were determined by student's t-test (p < 0.001)*

Parameter	LCEtOH	LCAq
Antiradical assays[a], IC_{50} / µg ml^{-1}		
DPPH$^{\bullet}$	355.64*±41.5	219.37**±5.7
NO$^{\bullet}$	52.61*±5.7	90.2*±24.4
SOA	128*±6.6	4.41**±4.4
OH$^{\bullet}$	12.05*±3.9	12.80*±1.1
Antioxidant assay[b]		
FRAP	10.93*±0.9	3.0**±0.8
Total content[c]		
TP	45.84*±0.9	3.50**±0.9
TF	25.05*±0.31	1.20**±0.3

[a]Results are expressed as IC_{50} (µg/ml) – concentration of extracts that caused 50% (25%) of activity in assays (in NO assay); [b]ferric reducing antioxidant power (*FRAP*) is expressed as mg ascorbic acid equivalents/g extract dry weight (mg AAE/g d.w.); [c]total phenol content (*TP*) was expressed as mg gallic acid equivalents/g extract dry weight (mg GAE /g d.w.) and total flavonoid content (*TF*) was expressed in mg quercetine equivalents/g extract dry weight (mg QE/g d.w.)

ethanol extract for the DPPH and SOA assay, while ethanolic extract showed higher activity than water extract according to reducing power capacity (*FRAP*). Moreover, both analyzed extracts did not differ significantly only in $^{\bullet}$OH and NO$^{\bullet}$ assay according to IC_{50} values. Investigated extracts showed higher activities for DPPH assay than *L. piperatus* and methanol extract of *L. deliciosus* [30].

Results showed that ethanol extract contained more total phenols than water extract (Table 2).These results showed higher values than in the previous studies for the genus *Lactarius* [33]. The content of flavonoids between extracts did not differ significantly. Phenols are expected to be the key components accounting for the demonstrated results that are statistically determined *via* correlations (Table 3).

Antibacterial activity

Hexane extract provides antibacterial activity against only one strain *S. aureus*at concentration of 3.12 mg/ml for *MIC* and 6.25 mg/ml for *MBC*. Analyzed extract showed lower activities than antibiotics (gentamicin and ampicillin: *MIC*, 2.5 and 8 µg/ml and *MBC*, 10 and 128 µg/ml, respectively). These results are in agreement with previous data for chloroformic extracts [21].

Antiproliferative activity

Antiproliferative activity of water and ethanol extracts of *L.controversus* against MCF 7 human breast cancer cell line evaluated by MTT and SRB assays are presented in Table 4. Under the experimental conditions both extracts showed cytotoxic activity in two different assays applied at the highest concentration (900 µg/mg), percentage of cytotoxic inhibition was in the range from 53.12%-LcAq to 95.35%-LcEtOH after 24 h and from 36.15%-LcAq to 79.96-LcEtOH after 72 h. In particular, LcEtOH displayed the strongest growth inhibitory activity after 24 h acute phase (IC_{50} = 166.42 µg/ml). Differences in IC_{50} values obtained for the same samples by the two assays can probably be attributed to the difference in sensitivity of targets they reflect, since they measure distinct biological parameters in living cells. While SRB assay does not depend on enzymatic activity but on protein content of the cells, in MTT assay the results reflect the activity of mitochondrial dehydrogenase which is more sensitive parameter, and therefore in many cases with changes detectable in lower concentrations. However, the effects observed for each sample also strongly depend on the specific mixture of compounds present in the sample, their interaction and action of their metabolites that induce specific and often unexpected cellular responses.

*Table 3. Cytotoxic activities of L. controversus extracts on MCF7 (IC_{50}; µg/ml); *: correlations are significant at p < 0.05; **: correlations are significant at p < 0.01; ***: correlations are significant at p < 0.001*

Extract	MTT assay		SRB assay	
	24 h	72 h	24 h	72 h
LCAq	306.17*±15.5	<900*	623.80*±49.81	249.02**±44.8
LCEtOH	166.42**±3.1	302.74**±9.6	526.98*±35.4	696.37*±8.4

[a]Total flavonoid content (*TF*) was expressed in mg quercetine equivalents/g extract dry weight (mg QE/g d.w.); [b]total phenol content (*TP*) was expressed as mg gallic acid equivalents/g extract dry weight (mg GAE/g d.w.)

*Table 4.Correlation between antiproliferative assays and antioxidant assays and total phenolicand total flavonoid content in crude extracts; *: correlations are significant at p < 0.05; **: correlations are significant at p < 0.01; ***: correlations are significant at p < 0.001*

Parameter	MTT assay		*TF*[a]	*TP*[b]
	24 h	72 h		
DPPH	–0.8031	–0.8387	0.8839*	0.9515**
FRAP	–0.9549**	–0.9486**	0.9623**	0.9038*
$NO^{\bullet}$	0.4338	0.5974	–0.6044	–0.3017
$OH^{\cdot}$	0.1122	0.0736	–0.0490	–0.0672
SOA	–0.9767***	–0.9951***	0.9789***	0.7105
TF	–0.9621**	–0.9939***	–	–
TP	–0.7568	–0.7546	–	–

[a]Total flavonoid content (*TF*) was expressed in mg quercetine equivalents/g extract dry weight (mg QE/g d.w.); [b]total phenol content (*TP*) was expressed as mg gallic acid equivalents/g extract dry weight (mg GAE/g d.w.)

Cluster analysis was done in order to classify extracts with different examined concentrations (33.3, 100, 300 and 900 µg/ml) on the basis of percentage of cytotoxic inhibition, depending on the treatments applied, *e.g.*, incubation time exposure (24h and 72h). In this study, we calculated Mahalanobis distance between samples, which were used for cluster analysis (Fig. 1). All samples were clustered into two major groups which separated LcEtOH 900 µg/ml (57% CI to 91% CI at both incubation times) from others which were divided in two main groups, (IIb – water extract except LcEtOH at 300 µg/ml , and IIa – ethanolic extract except LcAq at 33.3 µg/ml). In previous studies, *L. controversus* collected in Portugal was described in the literature as an ergosterol producer (58.6 mg/100 gf.w.) [12]. Therefore, it could be assumed that sterols and similar compounds (triterpenoids) may be a major class of active constituents contributing to *in vitro* cytotoxicity against cancer cells [9].

Correlation analysis between obtained IC_{50} values in antioxidant assays, and total phenolic and flavonoid content and cytotoxic activity are presented in Table 4. The highest significant positive correlation was observed for DPPH, FRAP and SOA assays with *TP* and *TF* contents. The observed correlations are in agreement with the data of Kalogeropoulos *et al.* [34], who reported that antioxidant activity of wild growing mushrooms correlated well with total phenolic acids and flavonoid content. SOA assay showed the strongest significant negative correlation with cytotoxic activity for both incubation times and FRAP assay.

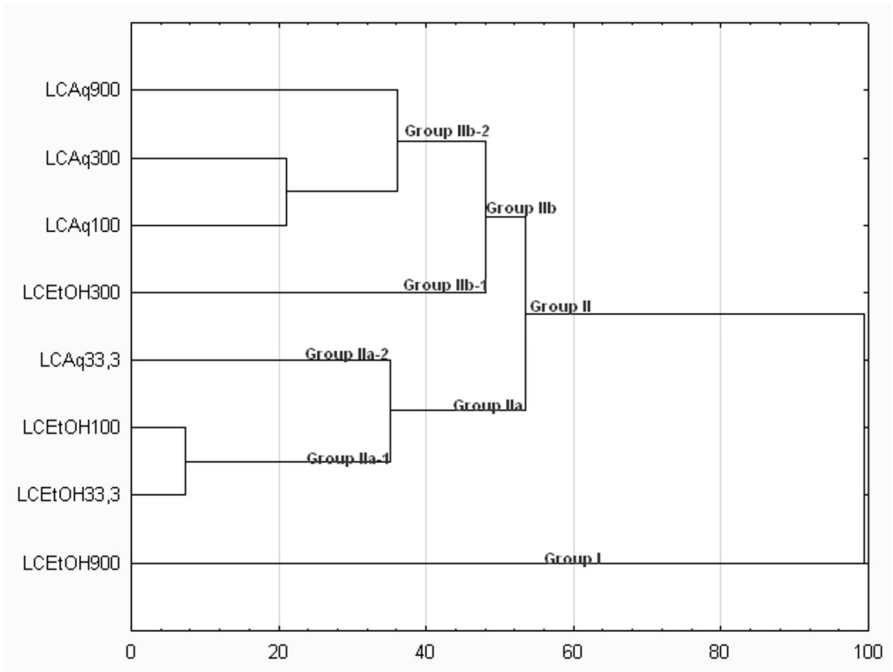

Figure 1. Diagram of cluster analysis based on cytotoxic activities.

MTT assay results significantly correlated negatively with TF, especially after 72h (–0.9939).These negative linear correlations proved that the highest antioxidant (lowest IC_{50}) activities showed higher cytotoxic effects.

CONCLUSION

In summary, quinic acid (8.9 µg/g d.w.) was identified and quantified by HPLC-MS/MS in methanol extract of *L. controversus* which confirms that this species is a potentially good source of nutraceuticals. Both ethanol and water extracts of *L. controversus* possessed antioxidant activity, with water extract being the most potent in DPPH and SOA assays and ethanol extract in FRAP assay. In antiproliferative assay both extracts showed activity against MCF 7 cell line, although ethanol extract was more potent. To our knowledge, this is the first report describing antioxidant, antibacterial activity, and growth inhibitory properties of *L. controversus*. Our results revealed that the ethanol and water extracts *L. controversus* showed anticancer, antioxidant, and low antibiotic capacities. Together, these activities indicate that these mushrooms are promising sources of bioactive compounds.

Acknowledgement

This paper is the result of research within the projects III 46001 and 172058, financed by the Ministry of Education, Science and Technological Development, Republic of Serbia. The authors would like to thank Prof. Goran Anačkov, PhD, for his valuable support in statistical analysis performance.

REFERENCES

[1] I.C.F.R. Ferreira, J.A. Vaz, M.H. Vasconcelos, A. Martins, Compounds from wild mushrooms with antitumor potential, Anti-Cancer Agents Med. Chem. **10** (2010) 424–436.

[2] D.L. Hawksworth, Mushrooms: the extent of the unexplored potential, Int. J. Med. Mushrooms **3** (2001).

[3] I.C.F.R. Ferreira, L. Barros, R. Abreu, Antioxidants in wild mushrooms, Curr. Med. Chem. **16** (2009) 1543–1560.

[4] F.S. Reis, A. Martins, L. Barros, I.C.F.R. Ferreira, Antioxidant properties and phenolic profile of the most widely appreciated cultivated mushrooms: A comparative study between *in vivo*and *in vitro*samples, Food Chem. Toxicol. **50** (2012) 1201–1207.

[5] A.R. Leal, L. Barros, J. Barreira, M. J.Sousa, A. Martins, C. Santos-Buelga, I.C.F.R. Ferreira, Portuguese wild mushrooms at the "pharma–nutrition" interface: Nutritional characterization and antioxidant properties, Food Res. Int. **50** (2013) 1–9.

[6] S.P. Wasser, A.L. Weis, Medicinal properties of substances occurring in higher basidiomycetes mushrooms: current perspectives, Int. J. Med. Mushrooms **1** (1999) 31–62.

[7] B.-Z. Zaidman, M. Yassin, J. Mahajna, S.P. Wasser, Medicinal mushroom modulators of molecular targets as cancer therapeutics, Appl. Microbiol. Biotechnol. **67** (2005) 453–468.

[8] D.D. De Silva, S. Rapior, E. Sudarman, M. Stadler, J. Xu, S.A. Alias, K.D. Hyde, Bioactive metabolites from macrofungi: ethnopharmacology, biological activities and chemistry, Fungal Divers. **62** (2013) 1–40.

[9] R.R. M.Paterson, *Ganoderma*–A therapeutic fungal biofactory, Phytochemistry **67** (2006) 1985–2001.

[10] J.A. Vaz, S.A. Heleno, A. Martins, G.M. Almeida, M.H. Vasconcelos, I.C.F.R. Ferreira, Wild mushrooms*Clitocybe alexandri* and *Lepista inversa*: *In vitro*antioxidant activity and growth inhibition of human tumour cell lines, Food Chem. Toxicol. **48** (2010) 2881–2884.

[11] J. Ferlay, P.Autier, M. Boniol, M. Heanue, M. Colombet, P. Boyle, Estimates of the cancer incidence and mortality in Europe in 2006, Ann. Oncol. **18** (2007) 581–592.

[12] L.M. Carvalho, F. Carvalho, M. de Lourdes Bastos, P. Baptista, N. Moreira, A.R. Monforte, A.C.S. Ferreira, P.G. de Pinho, Non-targeted and targeted analysis of wild toxic and edible mushrooms using gas chromatography–ion trap mass spectrometry, Talanta **118** (2014) 292–303.

[13] D. Orčić, M.Francišković, K. Bekvalac, E. Svirčev, I. Beara, M. Lesjak, N.Mimica-Dukić, Quantitative determination of plant phenolics in *Urtica dioica* extracts by high-performance liquid chromatography coupled with tandem mass spectrometric detection, Food Chem. **143** (2014) 48–53.

[14] V.L. Singleton, R. Orthofer, R.M. Lamuela-Raventos, Analysis of total phenols and other oxidation substrates and antioxidants by means of Folin-Ciocalteu reagent, Methods Enzymol. **299** *(*1999) 152–178.

[15] C.C. Chang, M.H. Yang, H.M. Wen, J.C. Chern, Estimation of total flavonoid content in propolis by two complementary colorimetric methods, J. Food Drug Anal. **10** (2002) 178–182.

[16] J.C. Espín, C. Soler-Rivas, H.J. Wichers, Characterization of the total free radical scavenger capacity of vegetable oils and oil fractions using 2, 2-diphenyl-1-picrylhydrazyl radical, J. Agric. Food Chem. **48** (2000) 648–656.

[17] I.F. Benzie, J.J. Strain, Ferric reducing/antioxidant power assay: Direct measure of total antioxidant activity of biological fluids and modified version for simultaneous measurement of total antioxidant power and ascorbic acid concentration, Methods Enzymol. **299** (1999) 15–27.

[18] L.C. Green, D.A. Wagner, J. Glogowski, P.L. Skipper, J.S. Wishnok, S.R. Tannenbaum, Analysis of nitrate, nitrite, and [^{15}N] nitrate in biological fluids, Anal. Biochem. **126** (1982) 131–138.

[19] M. Nishikimi, N. Appaji Rao, K. Yagi, The occurrence of superoxide anion in the reaction of reduced phenazine methosulfate and molecular oxygen, Biochem. Biophys. Res. Commun. **46** (1972) 849–854.

[20] K.H. Cheeseman, A.Beavis, H. Esterbauer, Hydroxyl-radical-induced iron-catalysed degradation of 2-deoxyri-

bose. Quantitative determination of malondialdehyde, Biochem. J. **252** (1988) 649–653.

[21] M.Karaman, N. Mimica-Dukic, P. Knezevic, Z. Svircev, M. Matavulj, Antibacterial properties of selected lignicolous mushrooms and fungi from northern Serbia, Int. J. Med. Mushrooms **11** (2009) 269–279.

[22] T. Mosmann,Rapid colorimetric assay for cellular growth and survival: Application to proliferation and cytotoxicity assays, J. Immunol. Methods **65** (1983) 55–63.

[23] P. Skehan, R. Storeng, D. Scudiero, A. Monks, J. MacMahon, D. Vistica, J.T. Warren, H. Bokesch, S. Kenney, M.R. Boyd, New Colorimetric Cytotoxicity Assay for Anticancer-Drug Screening, J. Nat. Cancer Inst. **82** (1990) 1107–1112.

[24] Statistica (Data Analysis Software System), version 12.0. StatSoft Inc., Tulsa, OK, USA, 2013 (www.statsoft.com).

[25] R.W. Pero, H. Lund, T. Leanderson, Antioxidant metabolism induced by quinic acid. Increased urinary excretion of tryptophan and nicotinamide, Phytother. Res. **23** (2009) 335–346.

[26] L. Barros, C. Pereira, I.F.R. Ferreira, Optimized Analysis of Organic Acids in Edible Mushrooms from Portugal by Ultra Fast Liquid Chromatography and Photodiode Array Detection, Food Anal. Methods **6** (2013) 309–316.

[27] R.W. Pero, H. Lund, Dietary quinic acid supplied as the nutritional supplement AIO + AC-11® leads to induction of micromolar levels of nicotinamide and tryptophan in the urine, Phytother. Res. **25** (2011) 851–857.

[28] Y. Soh, J.A. Kim, N.W. Sohn, K.R. Lee, S.Y. Kim, Protective effects of quinic acid derivatives on tetrahydropapaveroline-induced cell death in C6 glioma cells, Biol. Pharm. Bull. **26** (2003) 803–807.

[29] R.W. Pero, Health Consequences of Catabolic Synthesis of Hippuric Acid in Humans, Curr. Clin. Pharmacol. **5** (2010) 67–73.

[30] L. Barros, M. Dueñas, I.C. Ferreira, P. Baptista, C. Santos--Buelga, Phenolic acids determination by HPLC–DAD––ESI/MS in sixteen different Portuguese wild mushrooms species, Food Chem. Toxicol. **47** (2009) 1076––1079.

[31] B. Halliwell, Antioxidants in human health and disease, Annu. Rev. Nutr. **16** (1996) 33–50.

[32] R.L.Prior, X. Wu, K. Schaich, Standardized Methods for the Determination of Antioxidant Capacity and Phenolics in Foods and Dietary Supplements, J. Agric. Food Chem. **53** (2005) 4290–4302.

[33] C. Sarikurkcu, B. Tepe, M. Yamac, Evaluation of the antioxidant activity of four edible mushrooms from the Central Anatolia, Eskisehir–Turkey: *Lactarius deterrimus*,*Suillus collitinus*, *Boletus edulis*, *Xerocomus chrysentero*, Bioresour. Technol. **99** (2008) 6651–6655.

[34] N. Kalogeropoulos, A.E. Yanni, G. Koutrotsios, M. Aloupi, Bioactive microconstituents and antioxidant properties of wild edible mushrooms from the island of Lesvos, Greece, Food Chem. Toxicol. **55** (2013) 378–385.

IZVOD

JESTIVA MIKORIZNA VRSTA *Lactarius controversus* PERS. 1800 KAO IZVOR ANTIOKSIDATIVNIH I CITOTOKSIČNIH AGENASA

Aleksandra R. Novaković[1], Maja A. Karaman[2], Ivan Lj Milovanović[1], Miona M. Belović[1], Milena J. Rašeta[3], Tanja I. Radusin[1], Nebojša M. Ilić[1]

[1]*Institut za prehrambene tehnologije, Univerzitet u Novom Sadu, Bulevar cara Lazara 1, 21000 Novi Sad, Srbija*
[2]*Departman za biologiju i ekologiju, Prirodno–matematički fakultet, Univerzitet u Novom Sadu, Trg Dositeja Obradovića 3, 21000 Novi Sad, Srbija*
[3]*Departman za hemiju, biohemijui zaštitu okoline, Prirodno–matematički fakultet, Univerzitet u Novom Sadu, Trg Dositeja Obradovića 3, 21000 Novi Sad, Srbija*

(Naučni rad)

Lactarius controversus Pers. 1800 je vrsta gljive sa veoma oštrim ukusom, ali se može koristiti u ljudskoj ishrani nakon kuvanja. Cilj ovog rada je bio da se prouči hemijski profil i antioksidativna i citotoksična aktivnost etanolnih i vodenih ekstrakata ove samonikle vrste sa lokacije iz istočne Srbije. Sadržaj ukupnih fenola i flavonoida je imao više vrednosti za etanolne ekstrakte (45,84 mg GAE/g d.w. i 3,50 mg QE/g d.w).Takođe je ispitana i antioksidativna aktivnost, uključujući aktivnost protiv $DPPH^{\bullet}$, $NO^{\bullet}$, $^{\bullet}OH$ i SOA radikala i sposobnost redukcije gvožđa. Najveću aktivnost protiv $DPPH^{\bullet}$ je imao vodeni ekstrakt (IC_{50} = 219,37 µg/ml) dok je etanolni ekstrakt demonstrirao najveću FRAP aktivnost od 10,93 mg AAE/g. Hemijska karakterizacija fenolnih jedinjenja izvedena pomoću HPLC–MS/MS je pokazala prisustvo hininske kiseline (8,9 µg/g d.w.). Heksanski ekstrakt primenjen u antibakterijskom testu duplog razblaženja, protiv tri patogena soja, je pokazao antibakterijsko dejstvo samo protiv *S. aureus* ATCC25922, postižući *MIC* i *MBC* od 3,12 i 6,25 mg/ml, redom. Antiproliferativno dejstvo na estrogen zavisnu MCF 7 ćelijsku liniju raka dojke određeno pomoću MTT testa je bilo jače za etanolne ekstrakte (166,42±3,1 µg/ml). Podaci dobijeni u ovi testovima ukazuju da je ova vrsta gljive obećavajući izvor bioaktivnih jedinjenja sa antioksidativnim i citotoksičnim dejstvom.

Ključne reči: *Lactarius controversus* • Fenolna jedinjenja • Hinska kiselina • Antioksidanti • Citotoksični agensi

The impact of isatin derivatives on antibiotic production by *Streptomyces hygroscopicus* CH-7

Jovan T. Ćirić[1], Sandra S. Konstantinović[1], Slavica B. Ilić[1], Gordana Gojgić-Cvijović[2], Dragiša S. Savić[1], Vlada B. Veljković[1]

[1]*Faculty of Technology, University of Niš, Leskovac, Serbia*
[2]*Institute of Chemistry, Technology and Metallurgy, Department of Chemistry, University of Belgrade, Belgrade, Serbia*

Abstract
The effect of isatin derivatives as a nitrogen source on antibiotic (hexaene H-85 and azalomycine B) production by *Streptomyces hygroscopicus* CH-7 was studied. Isatin-3-hydrazone, 5-chloroisatin-3-hydrazone, isatin-3-tosylhydrazone, 5-chloroisatin-3-tosylhydrazone, isatin-3-(4`-hidroxy)benzoilhydrazone and 5-chloroisatin-3-(4'-hidroxy)benzoylhydrazone were synthesized in a crude glycerol, obtained during the biodiesel production from edible sunflower oil. The highest concentration of Hexaene H-85 is achieved with 5-chloroisatin-3-hydrazone (197 μg/cm^3) in medium, while isatin-3-hydrazone has the greatest impact on azalomycine B production (72 μg/cm^3).

Keywords: isatin derivatives, *Streptomyces hygroscopicus*, hexaene H-85, azalomycine.

Available online at the Journal website: http://www.ache.org.rs/HI/

SCIENTIFIC PAPER

UDC 547.75:615.33:579.873.7

Hem. Ind. **70** (2) 123–128 (2016)

doi: 10.2298/HEMIND141127019C

A large number of bacteria and fungi have the ability to produce secondary metabolites. Microorganisms are the main sources of bioactive components, of which more than 60% are produced by Actinomycetales, 28% by moulds and about 11% by nonfilamentous organisms. Antibiotics are the most important secondary metabolites [1,2], and about three-quarters of known antibiotics with different chemical structures are produced by Actinomycetales [3,4]. Species of the genus Streptomyces are known as one of the best antibiotic producers [5], whereby some strains can produce more than 180 different secondary metabolites [6].

Streptomyces hygroscopicus CH-7 produces antibiotics such as hexaene H-85, nigericin and azalomycine B. By changing the conditions of fermentation process and the composition of the nutrient medium at an early stage of trial, it is possible to increase the yield of antibiotics [7,8].

The production of antibiotics by *Streptomyces* species depends on the growth phase. The secondary metabolism occurs when growth is limited, when nutrients are worn-out or their availability is reduced. The nature of limiting nutrient is very important, and essential ingredients of substrate are carbon, nitrogen and phosphorus. Other nutrients, such as mineral substances, have an impact on production, but their absence is not essential [9,10].

Correspondence: S.S. Konstantinović, Faculty of Technology, University of Niš, Bulevar oslobodjenja 124, Leskovac 16000, Serbia.
E-mail: sakisandra12@yahoo.com
Paper received: 27 November, 2014
Paper accepted: 17 March, 2015

Isatin derivatives possess different biological activity, such as antimicrobial, anticonvulsative, anticancer, antiHIV, etc. [11,12]. The usage of some isatin derivatives, such as isatin-3-thiosemicarbazone, isatin-3--semicarbazone and isatin-3-phenylhydrazone as a nitrogen source for antibiotic production of *S. hygroscopicus* CH-7 significantly increased hexaene H-85 and azalomycine B production [9,13,14]. Since those isatin derivatives were synthesized in crude glycerol as a green solvent, and similar compounds have a positive effect on antibiotic production, the idea was to replace a part of tryptophan with isatin products and gained even better results in hexaene H-85 and azalomycine B production.

MATERIALS AND METHODS

Organism, media and growth conditions

A strain *Streptomyces hygroscopicus* CH-7 (NCAIM (P) B-001336) was gained from the Microbial Collection at Faculty of Chemistry and Institute of Chemistry, Technology and Metallurgy in Belgrade, Serbia [15,16]. The culture was stored at 4 °C at soybean medium containing the following: 15 g/dm^3 glucose; 10 g/dm^3 soybean; 3 g/dm^3 $CaCO_3$; 3 g/ dm^3 NaCl; 2 g/ dm^3 agar (pH 7.2). Flasks (250 ml) that contained 50 ml of this media were inoculated with 0.1 ml of spore suspension and incubated at 30 °C with shaking at 200 rpm. The fermentation media were inoculated with 5 vol.% of a preculture after 48 h growth and incubated at 30 °C for 240 h under the standard condition of aeration and agitation (200 rpm). The composition of media used for fermentation were: basal medium (M_1, 15 g/dm^3 glucose; 10 g/dm^3 soybean; 5 g/dm^3 yeast extract; 3 g/dm^3 $CaCO_3$; 3 g/dm^3 NaCl; 0.5 g/dm^3 $MgSO_4 \cdot 7H_2O$; 0.5

g/dm^3 $(NH_4)_2HPO_4$; 1 g/dm^3 K_2HPO_4); medium with tryptophan (M_2, 15 g/dm^3 glucose; 15 g/dm^3 tryptophan; 3 g/dm^3 $CaCO_3$; 3 g/dm^3 NaCl; 0.5 g/dm^3 $MgSO_4 \times 7H_2O$; 0.5 g/dm^3 $(NH_4)_2HPO_4$; 1 g/dm^3 K_2HPO_4) and media with isatin derivatives (15 g/dm^3 glucose; 10 g/dm^3 isatin derivatives; 5 g/dm^3 tryptophan; 3 g/dm^3 $CaCO_3$; 3 g/dm^3 NaCl; 0.5 g/dm^3 $MgSO_4 \times 7H_2O$; 0.5 g/dm^3 $(NH_4)_2HPO_4$; 1 g/dm^3 K_2HPO_4).

The results were obtained by measuring absorbance at λ_{max} = 364 nm (Hexaene H-85) and λ_{max} = 252 nm (azalomycine B) with Perkin-Elmer Lambda 15 UV/Vis spectrophotometer [15,16]. Microbial growth was determined by measuring dry weights of cells [16].

Synthesis of isatin derivatives in the crude glycerol

All chemicals, except crude glycerol, were of analytical grade and used without further purification. They were purchased from Sigma Aldrich. The crude glycerol, a by-product in the production of biodiesel from sunflower oil, was obtained from the Laboratory for Chemical Engineering, Faculty of Technology, Leskovac. The excess of methanol was removed from the crude glycerol by distillation. After distillation, the acidity of crude glycerol was adjusted to pH 5 by addition of 85% phosphoric acid. The inorganic salts formed in this stage were then removed by centrifugation at 400 rpm for 15 min.

Isatin derivatives were synthesized by the reaction of equimolar amounts of isatin and amine components in the crude glycerol as a green solvent [17]. The mixture was refluxed at 80 °C. The products, precipitated as a colored solid, were filtered and washed out with water.

RESULTS AND DISCUSSION

To achieve better concentration of antibiotics, soybean and yeast extract in basal medium were replaced with tryptophan (15 g/dm^3) and mixtures of tryptophan (5 g/dm^3) and isatin derivatives (10 g/dm^3). Amino acids are known as a good nitrogen source [18,19], as well as tryptophan, which was already used for antibiotic production by *Streptomyces hygroscopicus* CH-7 [14]. Tryptophan is similar to the isatin (indole moiety is constitutional part of their structure), and therefore, in this paper, isatin derivatives were used as a nitrogen sources for antibiotic production by *S. hygroscopicus* CH-7. Isatin derivatives (Fig. 1) were synthesized by using „green method“ in a crude glycerol obtained as a by-product in biodiesel production.

Table 1 shows the effect of tryptophan and isatin-3--hydrazone, 5-chloroisatin-3-hydrazone, isatin-3-tosylhydrazone, 5-chloroisatin-3-tosylhydrazone, isatin-3--(4'-hidroxy)benzoylhydrazone and 5-chloroisatin-3-(4'--hidroxy)benzoilhydrazone on concentration of dry biomass and antibiotics, while the kinetic of fermentation is shown in Figures 2–4.

Figure 2 shows the variation of dry biomass during the fermentation. Independently of nitrogen source, the concentration of dry biomass increased during the first 72 h of fermentation, after which it began to decrease. The highest concentration of dry biomass was

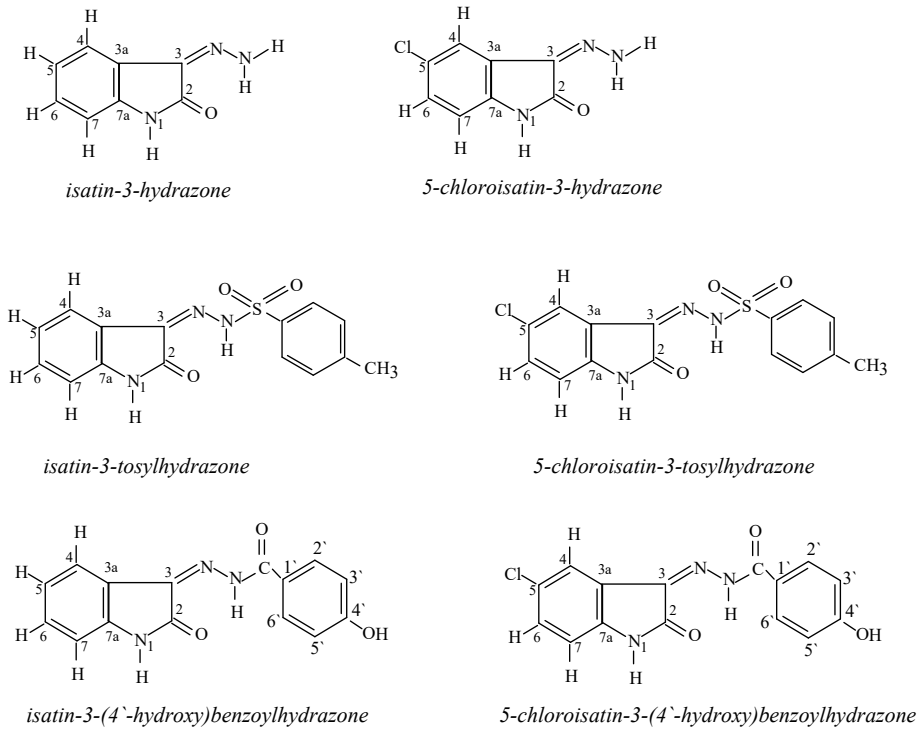

Fig. 1. Chemical structure of isatin derivatives synthesized in the crude glycerol as a green solvent.

Table 1. The effect of tryptophan and isatin derivatives as a nitrogen source on the maximum dry biomass concentration (X_{max}) and the maximum antibiotic concentration (c_{max})

Nitrogen source	Dry biomass X_{max} / g dm^{-3}	Hexaene H-85 c_{Hmax} / μg cm^{-3}	Azalomycine B c_{Emax} / μg cm^{-3}
M_1	9.0	114	36
M_2	8.3	156	48
5-chloroisatin-3-hydrazone + tryptophan (10 g/dm^3+5 g/dm^3)	8.6	197	61
5-chloroisatin-3-tosylhydrazone + tryptophan (10g/dm^3+5g/dm^3)	8.0	172	54
Isatin-3-tosylhydrazone + tryptophan (10g/dm^3+5g/dm^3)	8.1	165	67
Isatin-3-hydrazone + tryptophan (10g/dm^3+5g/dm^3)	9.0	183	72
Isatin-3-(4`-hidroxy)benzoylhydrazone + tryptophan (10g/dm^3+5g/dm^3)	8.2	145	49
5-chloroisatin-3-(4`-hidroxy)benzoilhydrazone + tryptophan (10g/dm^3+5g/dm^3)	7.9	162	51

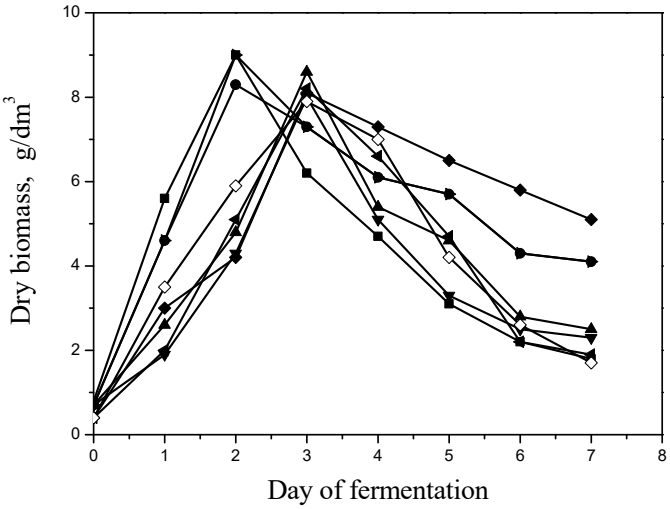

Fig. 2. Variation of dry biomass concentration during the fermentation of Streptomyces hygroscopicus CH-7 in basal medium (■) and media with tryptophan (●); 5-chloroisatin-3-hydrazone (▲); 5-chloroisatin-3-tosylhydrazone (▼); isatin-3-tosylhydrazone (♦); isatin-3-hydrazone (►); isatin-3-(4 -hidroxy)benzoilhydrazone (◄); 5-chloroisatin-3-(4 -hidroxy)benzoilhydrazone (◊).

achieved in medium M_1 and medium modified with isatin-3-hydrazone, after 48 h (9.0 g/dm^3). Comparing to all tested media, the lowest value of dry biomass was achieved with 5-chloroisatin-3-tosylhydrazone (8.0 g/dm^3).

The results obtained during the ferementation show that isatin derivatives have different impact on antibiotic production by *Streptomyces hygroscopicus* CH-7 (Table 1 and Fig. 3). The concentration of hexaene H-85 increases in first 48 h and reaches the highest values (197 μg/cm^3) with 5-chloroisatin-3-hydrazone as a nitrogen source in 4th day of fermentation. This is 72% higher, while the yield of hexaene H-85 in medium with 5-chloroisatin-3-tosylhydrazone is higher for 51% than value for medium M_1, actually 26 and 11% higher than medium M_2. Higher values for antibiotic concentration, comparing to basal medium and medium with tryptophan were also obtained in media with isatin-3--tosylhydrazone (165 μg/cm^3) and isatin-3-hydrazone (183 μg/cm^3). The highest concentration of hexaene H-85 in a medium with tryptophan is achieved during the 72 h of fermentation (156 μg/cm^3), which is 36% higher than in medium with soybean and yeast extract.

The variation of azalomycine B during the fermentation is given in a Fig. 4. The highest concentration of azalomycine B in basal medium was reached after 72 h of fermentation (36 μg/cm^3) and in the media with tryptophan and isatin derivatives during 72–96 h. The increase of azalomycine B concentration in the medium with tryptophan is 33% higher than basal medium (Table 1). The addition of 5-chloroisatin-3-hydrazone and 5-chloroisatin-3-tosylhydrazone stimulates azalomycine B production, with maximum 61 and 54 μg/cm^3, respectively. The higher yield was achieved in media with isatin-3-tosylhydrazone (67 μg/cm^3) and isatin-3--hydrazone (72 μg/cm^3).

It`s very difficult to find a connection between the structure of isatin derivatives and antibiotic production. The results show that isatin-3-hydrazone and 5-chloroisatin-3-hydrazone have greater influence on hexaene H-85 production. The main structure of those compounds is identical, and the only difference is in sub-

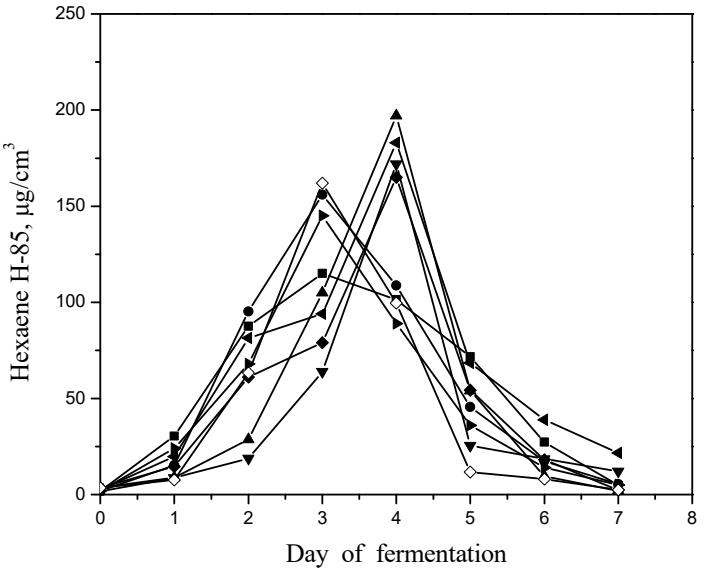

Fig. 3. Variation of Hexaene H-85 concentration during the fermentation in basal medium (■) and media with tryptophan (•); 5-chloroisatin-3-hydrazone (▲); 5-chloroisatin-3-tosylhydrazone (▼); isatin-3-tosylhydrazone (♦); isatin-3-hydrazone (►); isatin-3-(4`-hidroxy)benzoilhydrazone (◄); 5-chloroisatin-3-(4`-hidroxy)benzoilhydrazone (◊).

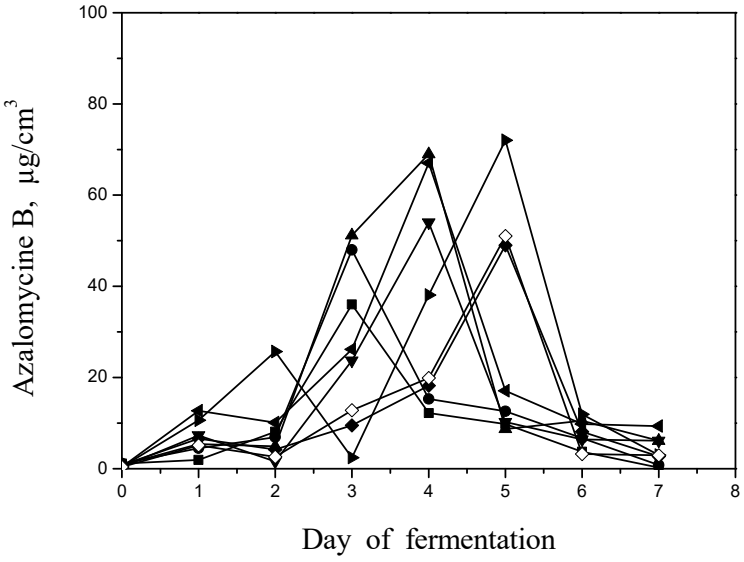

Fig. 4. Variation of Azalomycine B concentration during the fermentation in basal medium (■) and media with tryptophan (•); 5-chloroisatin-3-hydrazone (▲); 5-chloroisatin-3-tosylhydrazone (▼); isatin-3-tosylhydrazone (♦); isatin-3-hydrazone (►); isatin-3-(4`-hidroxy)benzoilhydrazone (◄); 5-chloroisatin-3-(4`-hidroxy)benzoilhydrazone (◊).

stituent at position 5, which means that chloro-ion does not have a negative effect on antibiotic production.

On the other hand, isatin derivatives with no chloro substituent in position 5 (isatin-3-tosylhydrazone and isatin-3-hydrazone), have a better influence on azalomycine B production. Isatin-3-hydrazone has the best impact on azalomycine B production. It`s main difference with isatin-3-tosylhydrazone is in SO_2 group and aromatic moiety, which means that those groups reduce azalomycine B production.

CONCLUSIONS

Comparing to the results obtained for similar nitrogen sources [13,14] the impact of isatin-3-hydrazone, 5-chloroisatin-3-hydrazone, isatin-3-tosylhydrazone, 5-chloroisatin-3-tosylhydrazone, isatin-3-(4'-hidroxy)-benzoylhydrazone and 5-chloroisatin-3-(4'-hidroxy)benzoylhydrazone on antibiotic production is lower than those achieved for isatin-3-thiosemicarbazone, isatin-3--semicarbazone and isatin-3-phenylhydrazone [13,14]. Those were expected, especially with isatin-3-thiosemi-

carbazone and isatin-3-semicarbazone**,** since their structure is the most similar with tryptophan.

Acknowledgements

This work has been funded by the Ministry of Education, Science and Technological Development of the Republic of Serbia (Project III 45001).

REFERENCES

[1] Y. Okami, K. Hotta, Search and discovery of new antibiotics, Actinomycetes in biotechnology, Academic Press, 1988, pp. 33–67.

[2] G. Lancini, R. Lorenzetti, iotechnology of antibiotics and other bioactive microbial metabolites, Plenum Press, New York, 1993, pp. 1, 29, 95, 133, 145.

[3] H. Schrempf, Streptomycetaceae: Life Style, Genome, Metabolism and Habitats. In: Encyclopedia of Life Sciences (ELS). John Wiley & Sons Ltd, Chichester, 2008.

[4] J. Berdy, Bioactive Microbial Metabolites, J. Antibiot. **58** (2005) 1–26.

[5] B. Mythili, M.P. Ayyappa Das, Studies on Antimicrobial Activity of Streptomycin spp. Isolates from Tea Plantation Soil, Res. J. Agricul. Scien. **2** (2011) 104–106.

[6] A.L. Demain, Pharmaceutically active secondary metabolites of microorganisms, Appl. Microbial. Biot. **52** (1999) 455–463.

[7] S.B. Ilić, S.S. Konstantinović, G. Gojgić-Cvijović, D.S. Savić, V.B. Veljković, The impact of glycerol and some carbohydrates on antibiotic production by *Streptomyces hygroscopicus* CH-7, Med. Chem. Res. **22** (2013) 934––937.

[8] J.T. Ćirić, S.B. Ilić, S.S. Konstantinović, V.B. Veljkovic, G. Gojgić-Cvijović, D.S. Savić, The fermentation of glycerol by *Streptomyces hygroscopius* CH-7 bacteria, Savremene tehnologije **2** (2012) 20–25.

[9] S.B. Ilić, Uticaj sastava i reoloških svojstava hranljive podloge na kinetiku produkcije antibiotika pomoću bakterije *Streptomyces hygroscopicus* CH-7, Doktorska disertacija, Tehnološki fakultet, Univerzitet u Nišu, Leskovac, 2010.

[10] T. Neumann, W. Piepersberg, J. Distler, Decision phase regulation of streptomycin production in *Streptomyces griseus*, Microbiology **142** (1996) 1953–1963.

[11] S.S. Konstantinović, Sinteza, struktura i antimikrobna aktivnost koordinacionih jedinjenja izatin-Schiff-ovih baza, Doktorska disertacija, Prirodno-Matematički fakultet, Univerzitet u Nišu, Niš, 2007.

[12] S.S. Konstantinović, B.C. Radovanović, S.P. Sovilj, S.S. Stanojević, Antimicrobial activity of some isatin-3-thiosemicarbazone complexes, J. Serb. Chem. Soc. **72** (2008) 7–13.

[13] S.B. Ilić, S.S. Konstantinović, V.B. Veljković, D.S. Savić, G. Gojgić-Cvijović, The impact of different carbon and nitrogen sources on antibiotic production by *Streptomyces hygroscopicus* CH-7 in: Current Research, Technology and Education Topics in Applied Microbiology and Microbial Biotechnology, Formatex, Spain, 2010.

[14] S.B. Ilić, S.S. Konstantinović, D.S. Savić, V.B. Veljković, G. Gojgić-Cvijović, The impact of Schiff bases on antibiotic production by *Streptomyces hygroscopicus*, Med. Chem. Res. **19** (2010) 690–697.

[15] J. Vučetić, I. Karadžić, G. Gojgić-Cvijović, E. Radovanović, Improving hexaene H-85 production by *Streptomyces hygroscopicus*, J. Serb. Chem. Soc. **59** (1994) 973–980.

[16] I. Karadžić, G. Gojgić-Cvijović, J. Vučetić, Hexaene H-85, A hexaene H-85 macrolide complex, J. Antibiot. **12** (1991) 1452–1453.

[17] M. Jovanović, S. Konstantinović, S. Ilić, V. Veljković, The synthesis of vanillin- semicarbazone in crude glycerol as a green solvent, Adv. Technol. **2** (2013) 38–44.

[18] M. Mahesh, N. Meenakshi, Effect of carbon and nitrogen source for the production of tetracycline analysis by using HPLC, Int. J. Adv. Biotechnol. Res. **4** (2013) 218––223.

[19] S. Rattleff, Heterologous protein production in *Streptomyces lividans*, Phd thesis, Technical University of Denmark, Denmark, 2013.

IZVOD

UTICAJ DERIVATA IZATINA NA PRODUKCIJU ANTIBIOTIKA POMOĆU *Streptomyces hygroscopicus* CH-7

Jovan T. Ćirić[1], Sandra S. Konstantinović[1], Slavica B. Ilić[1], Gordana Gojgić-Cvijović[2], Dragiša S. Savić[1], Vlada B. Veljković[1]

Tehnološki fakultet u Leskovcu, Univerzitet u Nišu, Bulevar oslobođenja 124, 16000 Leskovac, Srbija
[2]Institut za hemiju, tehnologiju i metalurgiju, Njegoševa 12, P.O. Box 815, Beograd 11000, Srbija

(Naučni rad)

Intenzivna istraživanja poslednjih godina vrše se na polju poboljšanja produkcije sekundarnih metabolita sa različitom aktivnošću i primenom u biotehnologiji. Streptomiceta *Steptomyces hygroscopicus* raste i produkuje sekundarne metabolite na podlogama različitog sastava. Izvor azota značajno utiče kako na primarni tako i na sekundarni metabolizam, odnosno na rast, razvoj i produkciju sekundarnih metabolita. Pri fermentaciji u tečnoj podlozi, ovaj soj proizvodi smešu antibiotika. U ovom radu je proučavan uticaj derivata izatina, kao izvora azota na produkciju antibiotika heksaena H-85 i azalomicina B pomoću soja *Streptomyces hygroscopicus* CH-7. Derivati izatina poseduju različite biološke aktivnost i dosadašnjim istraživanjima je ustanovljeno da imaju stimulativno dejstvo kako na primarni tako i na sekundarni metabolizam. Izatin-3-tozilhidrazon, izatin-3-hidrazon, izatin-3-(4`-hidroksi)benzoilhidrazon, 5-hloroizatin-3-(4`-hidroksi)benzoilhidrazon, 5-hloroizatin-3-tozilhidrazon i 5-hloroizatin-3-hidrazon su sintetisani u sirovom glicerolu dobijenom tokom procesa proizvodnje biodizela od jestivog suncokretovog ulja. Najviša koncentracija Heksaena H-85 je postignuta u podlozi sa 5-hloroizatin-3-hidrazonom (197 μg/cm^3) dok je izatin-3-hidrazon imao najveći uticaj na produkciju azalomicina B (72 μg/cm^3).

Ključne reči: Derivati izatina • *Streptomyces hygroscopicus* • Heksaena H-85 • Azalomicina B

Linamarase production by some microbial isolates and a comparison of the rate of degradation of cassava cyanide by microbial and cassava linamarases

Ogbonnaya Nwokoro

Industrial Microbiology and Biotechnology Laboratory, Department of Microbiology, University of Nigeria, Nsukka, Nigeria

Abstract

Production of linamarase and the effects of media composition on enzyme production were studied. A total of eight linamarase-producing bacteria were isolated from fermenting cassava tubers and soil samples. Selection of the isolates was based on their fast growth in media containing 800 mg/L potassium cyanide solution. Eight of the isolates which showed very fast growth in the growth medium as demonstrated by increase in their optical density readings to at least 0.6 in the cyanide containing media were selected for further studies. The isolates were identified as *Lactobacillus plantarum, Lactobacillus fermentum, Lactobacillus amylovorus, Lactobacillus cellobiosus, Leuconostoc mesenteroides, Pseudomonas stutzeri, Bacillus pumilus* and *Bacillus subtilis.* All the isolates were grown in media containing Tween 80 solution and in control media without the surfactant. Best enzyme activity of 6.82 U/mL was obtained in the medium containing Tween 80 solution and *Lactobacillus fermentum* as the test bacterium. Comparatively, linamarase production by the isolates in media without Tween 80 showed lower enzyme productivity. Cassava endogenous and microbial enzymes were tested for their abilities to hydrolyze cyanide in cassava flour samples pretreated to either remove the endogenous or microbial enzyme. Residual cyanide in cassava flour samples treated with linamarase of *Lactobacillus plantarum* was undetected in 30 h, while in contrast, the residual cyanide in cassava flour samples treated with endogenous linamarase was 0.39 mg/10 g cassava flour after 80 h. Residual cyanide in the untreated control sample was 1.98 mg HCN /10 g cassava flour after 80 h. The results from this finding demonstrated improved cassava cyanide degradation with microbial linamarase as compared to endogenous cassava linamarase. Massive inoculation of fermenting cassava tubers with the isolates reported in this study would enable better control of the cassava fermentation process and may lead to the production of standardized and non-toxic cassava food products.

Keywords: linamarase, cassava cyanide reduction, microorganisms, surfactant.

Available online at the Journal website: http://www.ache.org.rs/HI/

SCIENTIFIC PAPER

UDC 579:547:66.0:66.094.941

Hem. Ind. **70** (2) 129–136 (2016)

doi: 10.2298/HEMIND141028021O

Cassava, the vital food in the tropical areas of Africa, Asia and Latin America is the third most important source of calories in the tropics after rice and corn [1]. Cassava is toxic as it contains large amounts of cyanogenic glucosides, linamarin and lotaustralin [2–4]. Daily consumption of foodstuffs which still contain residual levels of these cyanogenic compounds can result in chronic diseases such as goitre, cretinism, tropical atoxic neuropathy and tropical diabetes [5,6].

Cassava processing allows the reduction of toxic endogenous cyanogens which are present in variable concentrations in cassava tubers by volatilization of HCN present in the cassava tubers and consequent reduction of the cyanide levels. During the consequent fermentation, roots are softened, the disintegration of the tissue structures result in the contact of linamarin with linamarase and subsequent hydrolysis to glucose and cyanohydrins which easily break down to ketone and hydrocyanic acid [7]. Retting is one of the simplest methods for the processing of cassava tubers into various African staple foods. In some conditions, retting may take considerably longer periods particularly with tubers older than 24 months and some of the tubers steeped under this condition may fail to soften. Other processing techniques such as cooking, sun-drying, oven-drying and roasting have been developed in different parts of the world to reduce the cyanide content of cassava-based foods to an acceptable level. However none has achieved a complete detoxification [8]. The rate of fermentation depends on the processing method, size of cut tubers and the age of roots. With the increasing demand for foods due to a rapid population growth in many developing countries, the need has arisen to reduce the process time for retting of cassava roots.

Correspondence: ogbonnaya.nwokoro@unn.edu.ng
Paper received: 28 October, 2014
Paper accepted: 3 March, 2015

Linamarase, β-D-glucosidase (EC.3.2.1.21) is an enzyme that converts cassava cyanide to hydrogen cyanide (HCN) that either dissolves readily in water or is released into the air. They constitute a group of well studied hydrolases that have been isolated from members of all three domains of life, *i.e.*, eukaryotes, bacteria and archae. The principal reaction catalysed by this class of enzymes is the hydrolytic cleavage of β-glucosidic linkages of low molecular mass glucosides [9]. Apart from hydrolysis, β-glucosidases can catalyse reverse hydrolysis, giving glucose disaccharides and trisaccharides as products when using the glucose as substrate. Linamarase, is found in the leaves and roots of plants such as cassava, lima beans and flax, and are also produced by microorganisms. When the cellular structure of cyanogenic plants is disrupted, the intracellular glucoside becomes exposed to the extracellular enzymes linamarase. Linamarin, is first hydrolysed by linamarase to produce β-D-glucopyranose and 2-hydroxyisolentyronotrite or acetone-cyanohydrin, after which the latter is degraded to acetone and hydrogen cyanide (Fig. 1).

The aim of the present work is to comparatively study the effect of some media on the production of microbial linamarase and an assessment of the rate of cassava cyanide degradation by linamarase from microbial and cassava sources.

MATERIALS AND METHODS

Chemicals and reagents

Potassium cyanide (KCN), magnesium chloride ($MgCl_2 \cdot 2H_2O$), sodium carbonate (Na_2CO_3), potassium chloride (KCl), calcium chloride ($CaCl_2$), ferric sulphate ($FeSO_4 \cdot 7H_2O$), magnesium sulphate ($MgSO_4 \cdot 7H_2O$), zinc sulphate ($ZnSO_4$), mercuric chloride ($HgCl_2$), linamarin, ammonium sulphate $(NH_4)_2SO_4$), manufacturer: BDH Chemicals Ltd., Poole, England. Sodium dihydrogen phosphate (NaH_2PO_4), sodium hydrogen phosphate (Na_2HPO_4), potassium hydrogen phosphate (K_2HPO_4), sodium chloride (NaCl), manufacturer: Sigma-Aldrich Chemie Gmbh, Steinheim, Germany. Cupper sulphate ($CuSO_4$ x $5H_2O$), manganese sulphate ($MnSO_4 \cdot 5H_2O$), manufacturer: Bio-Lab UK Ltd., Cockspur Street, London. Sodium hydroxide (NaOH) manufacturer, Nexill World Chem Chadwell Health, Essex England. Potassium hydroxide (KOH) manufacturer: Avondale Laboratories, Banbury, Oxon, England. Picric acid, manufacturer: Qualikems Fine Chemicals PVT. Ltd., India. Glucose manufacturer: May and Baker Ltd., Dagenham, England. Nutrient agar, MRS agar, yeast extract, peptone, manufacturer: Oxoid, Ltd. UK. Tween 80, manufacturer, Difco Laboratory, USA.

Isolation of microorganisms from fermenting cassava tubers and soil samples

Fermenting cassava tuber (*ca.* 10 g) was aseptically removed, homogenized in distilled water in a sterile blender and stirred with a sterile glass rod. Then, 1 mL of the homogenate was withdrawn with a sterile pipette into 9 mL 0.1% peptone water diluents and mixed. About 0.1 mL was aseptically withdrawn with a sterile pipette and inoculated onto Nutrient agar for the isolation of bacteria and MRS agar for the isolation of lactic acid bacteria. The plates were incubated for for 24 h at 35 °C.

Soil samples (*ca.* 20 g) were collected from a cassava processing mill and 1 g of soil was added into a conical flask containing 10 mL of distilled water. The mixture was thoroughly shaken and 1 mL was serially diluted in normal saline diluents. The dilutions (0.1 mL) were plated out on Nutrient agar plates and incubated for 24 h at 35 °C. Pure cultures of the isolates were obtained by streaking onto fresh agar plates. The cultures were given arbitrary codes and stored at 4 °C.

Preparation of modified local media

Banana broth (BB) – peeled ripe banana fruit (200 g) was homogenized with mortar and pestle in one liter of distilled water and filtered with a stainless steel mesh.

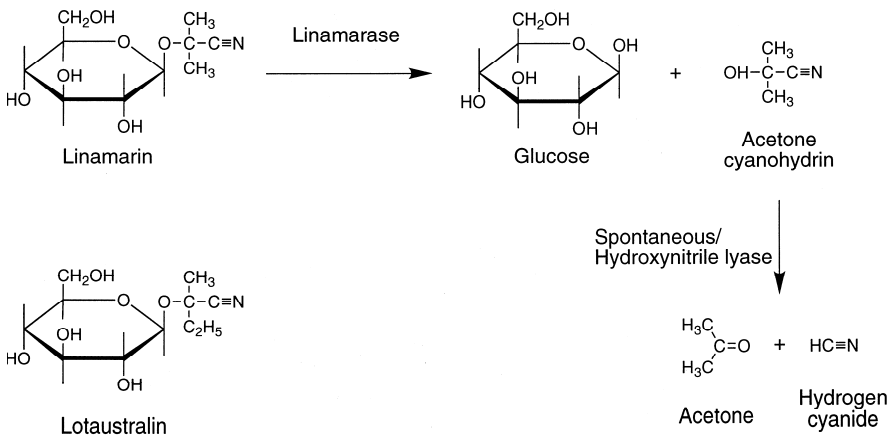

Figure 1. Breakdown of cyanogenic glucosides of cassava by linamarase.

The filtrate was re-filtered with a Whatman No. 1 filter paper. The broth was fortified with 0.1% ammonium sulphate and sterilized by autoclaving at 121 °C for 10 min.

Orange broth (OB) – fully-ripped oranges (200 g) were peeled and ground with a Corona mill (Medellin, Colombia) after removing the seeds in one liter of distilled water, and filtered with a stainless steel mesh. The filtrate was re-filtered with a Whatman No. 1 filter and fortified with 0.1% ammonium sulphate and sterilized by autoclaving at 121 °C for 10 min.

Tomatoj broth (TJB) – fresh tomato fruits (200 g) were homogenized in distilled water and filtered with a stainless steel mesh. The filtrate was re-filtered with a Whatman No. 1 filter paper and made up to 100 ml with distilled water. The broth was fortified with 0.1% ammonium sulphate and autoclaved at 121 °C for 10 min.

Screening the isolates for their resistance to cyanide

Test tubes each containing 5 mL of screening medium (yeasts extract, 0.5%; peptone 0.7%, glucose, 2% in 100 mL of distilled water) were autoclaved at 121 °C for 15 min. Then, aliquots (0.1 mL), potassium cyanide (KCN) solution (800 mg/L) which was sterilized by tyndallization according to Collins and Lyne [10] was added into each test tube containing the screening medium. A loopful of each bacterial isolate was inoculated into each test tube. The test tubes were incubated at room temperature (30±2 °C) for 2 days. The sensitivity/ resistance of each isolate to cyanide were monitored with a Spectrumlab 23A spectrophotometer at 600 nm against distilled water blank. Isolates that gave OD readings of at least 0.6 after 2 d incubation period were selected for further work. The isolates were identified respectively as *Lactobacillus plantarum, Lactobacillus fermentum, Lactobacillus amylovorus, Lactobacillus cellobiosus, Leuconostoc mesenteroides, Pseudomonas stutzeri, Bacillus pumilus* and *Bacillus subtilis* based on the taxonomic descriptions given by Holt *et al.* [11] and Skinner and Lovelock [12].

Development of inocula of lactic acid bacterial isolates. Inoculum was prepared from a stock culture by transferring to an Erlenmeyer flask (250 ml) containing 100 ml of medium described by Okafor and Ejiofor [13]: NaCl, 0.3%; $(NH_4)_2SO_4$, 0.1%; KH_2PO_4, 0.05%; $MgSO_4$, 0.02%; $CaCl_2$, 0.02%; lactose, 3%; linamarin, 0.15%. The medium was sterilized at 121 °C for 15 min. The inoculum was grown for 24 h in a Gallenkamp orbital incubator at 50*g* at 30 °C. The cells were collected by centrifugation at 2515*g* for 15 min in a Gallenkamp junior centrifuge, washed and diluted with sterile distilled water to an optical density of 0.1 measured in a Spectrumlab 23A spectrophotometer at 600 nm.

Development of inoculum of Pseudomonas sutzeri. The medium for multiplication of *Pseudomonas sutzeri* had the following composition per litre of distilled water: K_2HPO_4, 1 g; $MgSO_4 \cdot 7H_2O$, 0.2 g; $CaCl_2$, 0.01 g; NaCl, 0.01 g; $MnSO_4$, 2 mg; $CuSO_4 \cdot 5H_2O$, 0.2 mg; $ZnSO_4$, 0.2 mg; glucose, 2 g; tryptone, 1 g; and linamarin, 3 g. The medium was sterilized at 121 °C for 15 min. The inoculum was grown for 24 h in a Gallenkamp orbital incubator at 50*g* at 30 °C. The cells were collected by centrifugation at 2515*g* for 15 min, washed and diluted with sterile distilled water to an optical density of 0.1 measured in a Spectrumlab 23A spectrophotometer at 600 nm.

Development of inocula of Bacillus pumilus and Bacillus subtilis. The medium contained the following per litre: linamarin 3 g; peptone, 10 g; KCl, 1.0 g; $MgCl_2 \cdot 2H_2O$, 0.2 g; $CaCl_2 \cdot 2H_2O$, 0.25 g; $FeSO_4 \cdot 7H_2O$, 5 mg; $MnSO_4 \cdot 5H_2O$, 1 mg; Na_2HPO_4 5.26 g; NaH_2PO_4 5.4 g. The medium was sterilized at 121 °C for 15 min. The inoculum was grown for 24 h in a Gallenkamp orbital incubator at 50*g* at 30 °C. The cells were collected by centrifugation at 2515*g* for 15 min, washed and diluted with sterile distilled water to an optical density of 0.1 measured in a Spectrumlab 23A spectrophotometer at 600 nm.

Cultivation of bacteria

Lactic acid bacterial isolates were grown in the following media: OB, TJB, BB and MRS broth. *Pseudomonas stutzeri*, *Bacillus pumilus* and *Bacillus subtilis* were cultured in OB, TJB, BB and Nutrient broth. The isolates were added into 100 mL media containing 2% linamarin solution and incubated at 32±2 °C for 24 h. At the end of the incubation period, the culture was centrifuged at 2515*g* for 10 min. The effects of Tween 80 on the production and activity of the linamarase were studied by adding 0.1% Tween 80 into each duplicate culture flasks at the time of incubation. At the end of the incubation period, the culture was centrifuged at 2515*g* for 10 min.

Bacterial enzyme extraction

The harvested cells were washed with 0.2 M phosphate buffer (pH 6.5) and the washed cell suspension was disrupted by sonication for 10 min. using Biologics Ultrasonic homogenizer, model 150VT (115V/60Hz). Following disruption, the mixture was centrifuged at 2515*g* for 15 min. The supernatants of the two centrifugations were combined and suspended in 0.2 M phosphate buffer (pH 6.5). Ammonium sulphate was added with stirring to 40% saturation followed by centrifugation at 2515*g* for 10 min. Linamarase activity was then determined.

Extraction of endogenous cassava linamarase enzyme. Fresh cassava peel (100 g) was homogenized in 300 mL 0.2 M phosphate buffer (pH 6.5) using a mortar and pestle chilled by ice. The homogenate was centrifuged at 2515*g* for 15 min. The supernatant was

applied to a column of Sephadex G-25 (7 cm×62 cm) pre equilibrated with phosphate buffer (pH 6.5) and eluted with the same buffer to remove lower molecular weight compounds. Fractions were collected from the column and measured for linamarase activity.

Comparison of the rate of detoxification of cassava flour by microbial and endogenous cassava linamarases

Cassava tubers (NR 8082) were employed for this assay. The cassava tubers were peeled with knife and washed with tap water. The tubers were cut into cubes of approximately 10 cm and sun dried. The dried cassava tubers were milled with a mechanical greater.

To determine the effects of endogenous linamarase activity on the cyanogenic glucoside of cassava, cassava flour (10 g) contained in glass bottles was sterilized with 0.1% $HgCl_2$ solution for 5 min, rinsed with distilled water and finally treated with 1% of hypochlorite solution for 5 min. To wash off the effects of these chemicals, the cassava flour was finally rinsed for 15 min in sterile distilled water.

To assess the role of microbial fermentation on the degradation of the cyanogenic glucoside of cassava, 1, 5-gluconolactone (an inhibitor of endogenous glucosidase enzyme) was added to cassava flour at 10% concentration [14]. The effect of the inhibitor was removed by treating the cassava pulp with 50% ethanol solution and rinsing with sterile distilled water.

Buffered linamarase enzymes of both microbial and cassava origin (20 mL each) were added into 10 g of treated cassava flour contained in glass bottles. Samples of untreated and uninoculated cassava flour (10 g) served as control. Then 2 mL of 2% KOH and 1mL of picric acid:Na_2CO_3:H_2O, 1 mL:5 g:200 mL, contained in test tube were suspended in each bottle just before the bottles were sealed. The system was incubated at intervals of 10 h for 80 h at 30 °C. The HCN liberated from the cassava flour was absorbed by the alkaline picrate solution in the test tube [14]. After incubation, the reaction was stopped by placing the bottles in iced water. The colour that developed was read at 510 nm. Cyanide levels were extrapolated from KCN standard curve.

Analyses

Cyanide was determined by a modification of the alkaline picric acid method of Williams and Edwards [15] as follows: various quantities of standard (50, 100, 150 and 200 μg/ml) solution of KCN were added into tubes containing 2 ml of 2% KOH and 1ml of picric acid:Na_2CO_3:H_2O, 1 mL:5 g:200 mL. The tubes were incubated for 10 min in a 37 °C water bath, cooled for 20 min in a refrigerator and read in a Spectrum lab 23A spectrophotometer at 510 nm. The readings were used to draw a standard curve for micrograms KCN per mL against absorbance.

Linamarase activity was assayed by determining the HCN librated from linamarase as follows: 0.5 ml of enzyme solution in 0.2 M phosphate buffer (pH 6.5) contained in Eppendorf tubes was added to 0.5 ml of 1 mM buffered (same buffer) solution of linamarin (BDH, Poole, England). After 20 min of incubation at 32±2 °C, 2 mL of 2% KOH and 1 ml of picric acid:Na_2CO_3:H_2O (1 mL:5 g:200 mL) were added into the reaction mixture. The reaction was stopped by placing the tubes in iced water. The red colour that developed was read at 510 nm in a spectrophotometer. Under the above conditions, one unit of activity was defined as the amount of enzyme that released 1 μg HCN in 10 min under the assay condition.

Statistical analysis

The results are presented as the mean values of duplicate sampling. The significance of the tests was evaluated by analysis of variance (ANOVA). Significance of the test was accepted at ($p < 0.05$)

RESULTS AND DISCUSSION

Eight bacterial isolates which exhibited increased growth in the cyanide-containing medium were selected. The isolates designated RDS 6, RDS 12, RDS 13, RDS 20, RDS 26, RDS 28, RDS 31 and RDS 34 were selected for further studies because they grew and gave optical density readings of at least 0.6 in the cyanide containing medium (Table 1). The isolates were identified respectively as *Lactobacillus plantarum, Lactobacillus fermentum, Lactobacillus amylovorus, Lactobacillus cellobiosus, Leuconostoc mesenteroides, Pseudomonas stutzeri, Bacillus pumilus* and *Bacillus subtilis.*

Some nutritional factors relating to the production of linamarase enzyme by the isolates were investigated (Tables 2 and 3). There were no significant ($p > 0.05$) differences in the ability of standard media to cause more enzyme productivity by the isolates in comparison to locally formulated media. Under the conditions used, the enzyme activity that developed in the culture was higher in the presence of Tween 80 solution than in control experiments without Tween 80. Linamarase production by the isolates in media without Tween 80 showed the best enzyme activity of 2.67 U/mL produced with *Pseudomonas stutzeri* as the test organism. In comparison, best enzyme activity of 6.82 U/mL was obtained in the medium containing Tween 80 solution and *Lactobacillus fermentum* as the test bacterium. Incorporation of Tween 80 significantly ($p < 0.05$) increased the linamarase productivity of the isolates in all the media tested. This report agrees with the findings of Abalaka and Garba [16] who reported

increases in linamarase production in microbial culture media containing Tween 80 solution.

Table 1. Growth of the isolates in a medium containing 800 mg/L KCN solution

S/N	Isolate	OD at 600 nm
1	RDS 1	0.37
2	RDS 2	0.19
3	RDS 3	0.06
4	RDS 4	0.14
5	RDS 5	0.33
6	RDS 6	0.67
7	RDS 7	0.32
8	RDS 8	0.08
9	RDS 9	0.34
10	RDS 10	0.17
11	RDS 11	0.55
12	RDS 12	0.61
13	RDS 13	0.60
14	RDS 14	0.50
15	RDS 15	0.18
16	RDS 16	0.18
17	RDS 17	0.45
18	RDS 18	0.33
19	RDS 19	0.51
20	RDS 20	0.64
21	RDS 21	0.11
22	RDS 22	0.55
23	RDS 23	0.57
24	RDS 24	0.33
25	RDS 25	0.16
26	RDS 26	0.65
27	RDS 27	0.34
28	RDS 28	0.68
29	RDS 29	0.39
30	RDS 30	0.13
31	RDS 31	0.67
32	RDS 32	0.24
33	RDS 33	0.41
34	RDS 34	0.66
35	RDS 35	0.35
36	RDS 36	0.22
37	RDS 37	0.54
38	RDS 38	0.59
39	RDS 39	0.30
40	RDS 40	0.46

There are various reports on the simulative effects of surfactants in fermentation broth of microorganisms, thus resulting in many fold increases in the production and secretion of enzymes such as amylase [17,18], glucosetransferase [19], cellulase [20,21]; phytase [22], lignase [23], protease [24–26]. The surfactant may have improved cell wall permeability through disruption of lipid layer [27], thereby increasing the uptake of nutrient into the organisms and secretion of enzyme into the culture media.

This present work compared the rate of detoxification of cassava flour by microbial and endogenous cassava linamarases. The degradation of cyanogenic glucoside of cassava was studied in cassava flour pretreated to either prevent microbial enzyme activity or endogenous linamarase activity. The rate of disappearance of the cyanogenic glucosides as determined by the residual cyanide in the cassava flour was compared with the untreated control in which 1.98 mg HCN/10 g cassava flour remained unbroken after 80 h (Fig. 2). The residual cyanide in cassava flour samples treated with linamarase of *Lactobacillus plantarum* was undetectedin 30 h. In contrast, the residual cyanide in cassava flour samples treated with endogenous linamarase was 0.39 mg/10 g cassava flour after 80 h.

Two possible mechanisms of degradation of cassava linamarin are the introduction of microbial linamarase to cassava and cell wall – degrading enzymes that permit contact between the compartmentally separated linamarin and endogenous linamarase of cassava [28]. Gueguen *et al.* [29] reported that cassava is detoxified during processing by the endogenous linamarase present in the enlarged cassava root during grating of the root but the quantity of enzyme released is not sufficient to break down the glucoside present in the root completely. The authors suggested that the endogenous linamarase of the root could be supplemented from a microbial source exogenous to the roots to ensure exogenous to the roots to ensure a greater breakdown of the linamarin. Mkpong *et al.* [30] and Ikediobi and Onyike [31] reported that the endogenous linamarase content could not permit the complete breakdown of linamarin. Ikediobi and Onyike [31] and Okafor and Ejiofor [13] demonstrated that it is possible to reduce the cassava toxicity by the addition of an exogenous linamarase during the fermentation. Petruccioli *et al.* [32], reported in 1999 that addition of *Mucor circinelloides* crude linamarase during cassava tuber fermentation shortened and enhanced the detoxification process leading to a complete hydrolysis of cassava cyanogenic glucoside. In contrast, Giraud *et al.* [33] observed that inoculation of cassava pulp with a strain of lactic acid bacteria possessing a strong linamarase activity did not appear to contribute to cassava detoxification. The authors concluded that the amount of cassava indigenous linamarase released during the grating stage was sufficient to permit complete and rapid hydrolysis of cassava linamarin. This report agrees with Vasconcelos *et al.* [34] who stated that 95% of initial linamarin was hydrolyzed 3 h after grating the

Table 2. Production of linamarase by the isolates in different media without Tween 80 solution – total activity units in 40% $(NH_4)_2SO_4$ fraction (mean ± SD)

Isolate	Banana broth	Orange broth	Tomato juice broth	MRS broth	Czapek dox broth	Nutrient broth
Lactobacillus plantarum	0.26±0.028	1.33±0.41	2.18±0.099	2.11±0.180	0.12±0.042	0.17±0.042
Lactobacillus fermentum	0.29±0.048	0.76±0.021	2.08±0.056	2.13±0.014	0.43±0.021	0.16±0.014
Lactobacillus amylovorus	0.21±0.028	0.53±0.070	1.58±0.184	1.88±0.550	0.24±0.198	0.09±0.057
Lactobacillus cellobiosus	0.39±0.127	0.46±0.090	1.40±0.400	1.31±0.020	0.26±0.093	0.18±0.028
Leuconostoc mesenteroides	0.20±0.127	0.88±0.113	2.06±0.350	1.46±0.085	0.35±0.078	0.30±0.100
Pseudomonas stutzeri	2.67±0.099	1.77±0.042	0.12±0.042	0.15±0.085	0.48±0.099	2.36±0.240
Bacilus pumilus	2.46±0.099	1.61±0.040	0.08±0.071	0.19±0.170	0.23±0.042	2.55±0.35
Bacilus subtilis	2.18±0.098	2.40±0.032	0.15±0.040	0.28±0.099	2.56±0.052	0.42±0.042

Table 3. Production of linamarase by the isolates in different media with Tween 80 solution – total activity units in 40% $(NH_4)_2SO_4$ fraction (mean ± SD)

Isolate	Banana broth	Orange broth	Tomato juice broth	MRS broth	Czapek dox broth	Nutrient broth
Lactobacillus plantarum	3.43±0.042	2.53±0.100	5.96±0.230	5.62±0.420	1.94±0.570	2.22±0.230
Lactobacillus fermentum	2.09±0.049	3.66±0.44	6.82±0.82	4.88±0.049	4.16±0.035	2.67±0.047
Lactobacillus amylovorus	2.60±0.070	2.86±0.300	5.65±0.040	4.80±0.680	2.46±0.070	2.85±0.510
Lactobacillus cellobiosus	4.92±0.140	4.34±0.070	4.21±0.160	5.28±0.170	3.13±0.180	3.58±0.040
Leuconostoc mesenteroides	3.44±0.180	3.57±0.040	5.18±0.240	4.65±0.210	2.89±0.170	2.07±0.100
Pseudomonas stutzeri	4.29±0.610	4.25±0.042	3.37±0.060	2.91±0.140	4.61±0.110	5.16±0.240
Bacilus pumilus	6.61±0.590	5.90±0.300	2.84±0.310	3.40±0.170	4.93±0.042	6.09±0.090
Bacilus subtilis	5.78±0.170	6.17±0.400	2.63±0.200	3.88±0.130	5.11±0.230	2.40±0.030

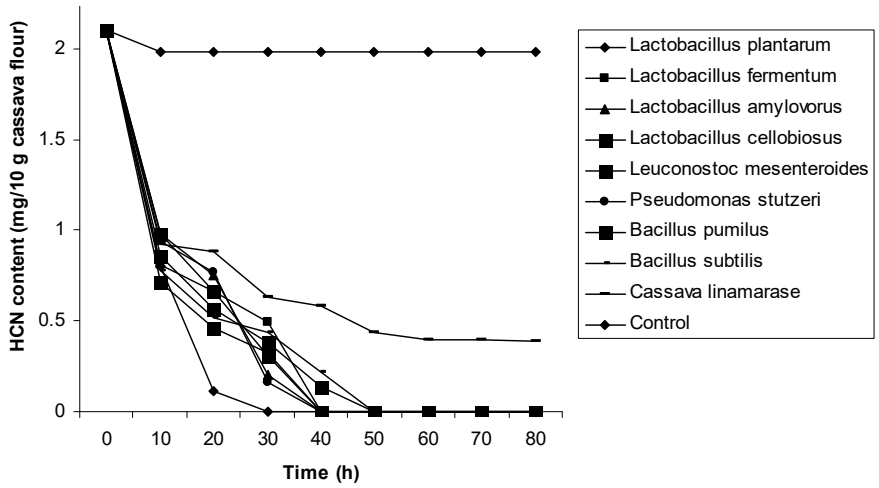

Figure 2. Comparison of the rate of detoxification of cassava flour by microbial and endogenous cassava linamarase enzymes.

roots. Maduagwu [35] observed that the degradation of cyanogenic glucoside in mashed cassava roots during fermentation was essentially effected by endogenous linamarase and that the role of microbial linamarase activity was complementary.

CONCLUSION

Eight linamarase-producing bacteria were selected based on their high growth in media containing 800 mg/L potassium cyanide solution. The isolates showed very high growth in the growth medium as demonstrated by increase in their optical density readings to at least 0.6. The isolates were identified as *Lactobacillus plantarum, Lactobacillus fermentum, Lactobacillus amylovorus, Lactobacillus cellobiosus, Leuconostoc mesenteroides, Pseudomonas stutzeri, Bacillus pumilus* and *Bacillus subtilis.* All the isolates were grown in media containing Tween 80 solution and in control media without the surfactant. Best enzyme activity of 6.82 U/mL was obtained in the medium containing Tween 80 solution and *Lactobacillus fermentum* as the test bacterium. Linamarase production by the isolates in media without Tween 80 was much lower

than in media with the surfactant. Residual cyanide in cassava flour samples treated with linamarase of *Lactobacillus plantarum* was undetected in 30 h; while in contrast, the residual cyanide in cassava flour samples treated with endogenous cassava linamarase was 0.39 mg/10 g cassava flour after 80 h. Residual cyanide in the untreated control sample was 1.98 mg HCN/10 g cassava flour after 80 h.

REFERENCES

[1] K. Murugan, K.Y. Sekar, S. Al-Sohaibani, Detoxification of cyanide in cassava flour by linamarase of *Bacillus subtilis* KM05 isolated from cassava peel, Afr. J. Biotechnol. **11** (2012) 7232–7237.

[2] D.D. Roger, E.N. Jean-Justin, E. Francois-Xvier, Nutritive value, toxicological and hygienic quality of some cassava-based products consumed in Cameroon, Pak. J. Nutrition **6** (2007) 404–408.

[3] S. Soryotha, K.L. Kyu, K. Ratanakhanokchai, Purification and detection of linamarin from cassava root cortex by high performance liquid chromatography, Food Chem. **104** (2007) 1750–1754.

[4] S. Soryotha, K.L. Kyu, K. Ratanakhanokchai, An efficient treatment for detoxification process of cassava starch by plant cell wall-degrading enzymes, J Biosc. Bioeng. **109** (2010) 9–14.

[5] M. Ernesto, A.P. Cardoso, D. Nicala, M.R. Mirione, F. Massaza, J. Cliff, M.R. Haque, J.H. Bradbury, Persistent *konzo* and cyanogens toxicity from cassava in northern Mozambique, Acta Trop. **82** (2002) 357–362.

[6] I. Ahaotu, C.C. Ogueke, C.I. Owuamanam, N.N. Ahaotu, J.N. Nwosu, Fermentation of underwatered cassava pulp by linamarase producing microorganisms: effect of nutritional composition and residual cyanide, American J. Food Nutr. **3** (2013) 1–8.

[7] R.D. Cooke, An enzymatic assay for the total cyanide content of cassava (*Manihot esculenta* Crantz), J. Sci. Food Agric. **29** (1978) 345–352.

[8] A.P. Cardoso, E. Mirione, M. Ernesto, F. Massaza, J. Cliff, R.M. Haque, H.J. Bradbury, Processing of cassava roots to remove cyanogens, J. Food Comp. Analysis **18** (2005) 451–460.

[9] O. Nwokoro, F. O. Anya, Linamarase enzyme from *Lactobacillus delbrueckii* NRRL B-763: Purification and some properties of a β-glucosidase, J. Mex. Chem. Soc. **55** (2011) 246–250.

[10] C.H. Collins, P.M. Lyne, Microbiological Methods, Butherworths, London, 1970.

[11] J.G. Holt, N.R. Krieg, P.H.A. Sneath, J.T. Staley, S.T. Williams, Bergey's Manual of Determinative Bacteriology, 9th ed., Williams and Wilkins, Baltimore, MD, 1994.

[12] F.A. Skinner, D.W. Lovelock, Identification Methods for Microbiologists, Second edition, Academic Press, London, 1979.

[13] N. Okafor, A.N. Ejiofor, The linamarase of *Leuconostoc mesenteroides*: production, isolation and some properties, J. Sci. Food Agric. **36**(1985):669–678.

[14] T. Wood, The isolation, properties and enzymatic breakdown of linamarin from cassava, J. Sci. Food Agric. **17**(1965):85–90.

[15] H.J. Willians, T.G. Edwards, Estimation of cyanide with alcaline picrate, J. Sci. Food Agric. **31** (1980) 15–22.

[16] J.A. Abalaka, Garba, S.A., Influence of media composition on linamarase production by some fungi, Agric Biol. Chem. **53** (1989) 561–563.

[17] R.M. Reedy, P.G.G. Reedy, G. Seenayya, Enhanced production of the thermostable ß-amylase and pullulanase in the presence of surfactants by *Clostridium thermosulfurogenes* SV2, Process Biochem. **34** (1999) 87–92.

[18] E. Thies, T. Jenkins, F. Stutzenberger, Effects of detergent Tween 80 on *Thermomonospora curvata*, World J. Microbiol. Biotechnol. **10** (1994) 657–663.

[19] Y. Umesaki, Y. Kawai, M. Mutai, Effect of Tween 80 on glucosyl transferase production in *Streptococcus mutants*, Appl. Environ. Microbiol. **34** (1977) 115–119.

[20] A.G. Pardo, Effect of surfactants on cellulose production by *Nectria catalinensis*, Curr. Microbiol. **33** (1996) 275––278.

[21] H. Hwang, C.H. Lee, S.W. Kim, H.G. Sung, S.Y. Lee, S.S. Lee, H. Hong, Y. Kwak, J.K. Ha, Effects of mixtures of Tween 80 and cellulolytic enzymes on nutrient digestion and cellulolytic bacterial adhesion, Asian-Aust J. Anim Sci **21** (2008) 1604 – 1609.

[22] A. Ebune, S. Al-Asheh, Z. Duvnjak, Effects of phosphate, surfactants and glucose on phytase production and hydrolysis of phytic acid in canola meal by *Aspergillus ficum* during solid-state fermentation, Bioresour. Technol. **54** (1995) 241–247.

[23] A. Jager, S. Coran, T.K. Kirk, production of lignases and degradation of lignin in agitated submerged culture of *Phanerochaete chrysosporium*, Appl. Environ. Microbiol. **50** (1985) 1274–1278.

[24] H.S. Joo, C.G. Kumar, G.C. Park, K.T. Kim, S.R. Paik, C.S. Chan, Optimization of the production of an extracelluar alkaline protease from *Bacillus horikoshii*, Process Biochem. **37**(2002):139–144.

[25] G.M. Kamande, J. Baah, K.J.T. Cheng, T.A. McAllister, J.A. Shelford, Effects of Tween 60 and Tween 80 on protease activity, thiol group reactivity, protein adsorption and cellulose degradation by rumen microbial enzymes, J. Dairy Sci. **83** (2000) 536–554.

[26] R.N.A. Rahman, L.P. Geok, M. Basrins, A.B. Saleh, Factors affecting the production of organic solvent-tolerant protease by *Pseudomonas aeruginosa* strain K, Bioresour. Technol. **96**(2005):429–436.

[27] R. Goto, Q.K. Beg, P. Lorenz, Hydrophobic moiety of surfactants, 3rd ed. Worth Publications, New York, 1997, p. 3.

[28] A.J.A. Essers, M.H.J. Bennik, M.J.R. Nout, Mechanisms of increased linamarin degradation during solid-substrate fermentation of cassava, World J. Microbiol. Biotechnol. **11** (1995) 266–270.

[29] Y. Gueguen, P. Chemardin, P. Labrot, A. Arnaud, P. Galzy, Purification and characterization of an intracellular β-glucosidase from a new strain of *Lenconostoc*

mesenteroides isolated from cassava, J. Appl. Microbiol. **82** (1997) 469–476.

[30] O.E. Mkpong, H. Yang, G. Chism, R. Sayre, Purification, characterization, and localization of linamarase in cassava, Plant Physiol. **93** (1990) 176–181.

[31] C.O. Ikediobi, E. Onyike, The use of linamarase in gari production. Process Biochem. **17** (1982) 2–5.

[32] M. Petruccioli, L. Brimer, A.R. Cicalini, F. Federici, The linamarase of *Mucor cicinelloides* LU M40 and its detoxifying activity on cassava, J. Appl. Microb. **86** (1999) 302–310.

[33] E. Giraud, L. Gosselin, M. Raimbault, Production of a *Lactobacillus plantarum* starter with linamarase and amylase activities for cassava fermentation, J. Sci. Food Agric. **62** (1993) 77–82.

[34] A.T. Vasconcelos, D.R. Twiddy, A. Westby, P.J.A. Reilly, Detoxification of cassava during gari preparation, Int J. Food Sci. Tech. **25** (1990) 198–203.

[35] E.N. Maduagwu, Differential effects on the cyanogenic glycoside content of fermenting cassava root pulp by β-glucosidase and microbial activities, Toxicol. Lett. **15** (1982) 335–339.

IZVOD

PROIZVODNJA LINAMARAZE POMOĆU MIKROORGANIZAMA I POREĐENJE BRZINE RAZGRADNJE CIJANIDA KASAVE MIKROBNIM LINAMARAZAMA I LINAMARAZAMA KASAVE

Nwokoro Ogbonnaya

Industrial Microbiology and Biotechnology Laboratory, Department of Microbiology, University of Nigeria, Nsukka, Nigeria

(Naučni rad)

U radu je proučena mikrobna proizvodnja linamaraze i uticaj sastava hranljive podloge na proizvodnju enzima. Izolovano je ukupno osam bakterija producenata linamaraze iz krtola kasave i tla. Izbor izolata je izvršen na osnovu kriterijuma brzog rasta u medijumu koji sadrži 800 mg/L kalijum-cijanida. Osam izolata, koji su pokazali vrlo brz rast u hranljivoj podlozi sa cijanidom detektovan rastom optičke gustine do 0,6, izabrani su za dalje istraživanje. Ovi izolati su identifikovani kao: *Lactobacillus plantarum, Lactobacillus fermentum, Lactobacillus amylovorus, Lactobacillus cellobiosus, Leuconostoc mesenteroides, Pseudomonas stutzeri, Bacillus pumilus* i *Bacillus subtilis*. Svi izolati su gajeni u medijumu koji sadrži Tween 80 i u kontrolnom medijumu bez ovog surfaktanta. Najviša enzimska aktivnost od 6,82 U/ml dobijena je u medijumu koji sadrži Tween 80 i sa *Lactobacillus fermentum* kao testiranim mikroorganizmom. Mikrobnom proizvodnjom linamaraze u medijumu bez Tween 80 postignuta je manja enzimska aktivnost. Sposobnost endogenih enzima kasave i mikrobnih enzima da hidrolizuju cijanide brašna kasave je testirana na uzorcima brašna pretretiranim radi uklanjanja enzima prisutnih u brašnu. Cijanidi u brašnu tretiranom linamarazom iz *Lactobacillus plantarum* nakon 30 h nisu bili detektovani, dok je u uzorcima tretiranim endogenim linamarazama kasave nakon 80 h detektovano 0,39 mg/10 g kasavinog brašna. Koncentracija cijanida u kontrolnom uzorku, bez enzima, nakon 80 h je bila 1,98 mg HCN/10 g brašna. Rezultati ovog istraživanja pokazuju da primena mikrobnih linamaraza donosi unapređenje u razgradnji cijanida kasave u odnosu na razgradnju zasnovanu samo na endogenim linamarazama. Inokuliranje fermentišućih krtola kasave mikrobnim izolatima selektovanim u ovom radu će omogućiti bolju kontrolu procesa fermentacije kasave i može da dovede do proizvodnje standardizovanih i netoksičnih prehrambenih proizvoda od kasave.

Ključne reči: Linamaraza • Smanjenje koncentracije cijanida kasave • Mikroorganizmi • Surfactant

Nickel-based catalysts: Dependence of properties on nickel loading and modification with palladium

Vesna D. Nikolić[1], Željko J. Kamberović[2], Marija S. Korać[2], Zoran M. Anđić[3], Aleksandar M. Mihajlović[1], Jelena B. Uljarević[1]

[1]*Innovation Center of the Faculty of Technology and Metallurgy, University of Belgrade, Belgrade, Serbia*
[2]*Faculty of Technology and Metallurgy, University of Belgrade, Belgrade, Serbia*
[3]*Innovation Center of the Faculty of Chemistry, University of Belgrade, Belgrade, Serbia*

Abstract

The aim of this study was comparative analysis of catalysts with 5 and 20 wt.% Ni loading, with and without Pd additive, and it included: determination of reduction degrees, investigation on microstructure by scanning electron microscopy and chemical analysis by energy-dispersive spectroscopy. Ni/Al_2O_3 and $Ni–Pd/Al_2O_3$ catalysts supported on α-Al_2O_3-based foams were synthesized by aerosol assisted impregnation. Impregnation of the foams by ultrasonically aerosolized chlorides was followed by drying at 473 K and hydrogen reduction at 533 and 633 K. Lower Ni loading resulted in higher reduction degrees. Ni loading of 20 wt.% enabled relatively uniform coverage of the foam with a metallic coating. Nearly complete reduction was achieved at both temperatures with activity modifier (Pd). Reduction degrees reached 99.4 and 98.2 wt.% at 533 K for 5 and 20 wt.% of Ni, respectively.

Keywords: catalysts, Ni, Pd, modification, α-Al_2O_3-based foam, aerosol assisted impregnation.

Available online at the Journal website: http://www.ache.org.rs/HI/

SCIENTIFIC PAPER

UDC 544.47:66.097:543:546.47

Hem. Ind. **70** (2) 137–142 (2016)

doi: 10.2298/HEMIND140928090N

Metal-ceramic composite systems have been intensively researched in recent years because properties of a base material can be significantly enhanced by a small quantity of additive. For instance, there are composites such as metals reinforced with ceramic particles, dispersed in a metal matrix. Multiple strengthened $Cu–Al_2O_3$ systems, that could be suitable for using at elevated temperatures, are produced from ultra-fine and nanocomposite $Cu–Al_2O_3$ powders. Those powders can be synthesized by using novel method that includes spray drying of dissolved metal salts [1,2]. Composite catalytic materials with metallic particles dispersed on oxide supports are applied in various heterogeneous catalysis processes [3,4]. As an example, Ni/Al_2O_3 catalysts are commonly used for reforming of hydrocarbons [5–7]. Metallic particles are supported on γ-Al_2O_3 powder [5,8], reticulated α-Al_2O_3 foams [9,10], *etc*. Reticulated ceramic foams have high pore volumes and exhibit good mass transfer, good heat conductivity and low pressure drops for the duration of the fluid flow. Therefore, industrial application of ceramic foams as catalyst support could be favorable [10–12].

Although catalysts based on noble metals are common due to excellent catalytic activity, stability and selectivity [8], they are expensive for using in industry [13]. Ni is an effective alternative for noble metals because of low cost [6,7,14] and excellent catalytic properties [15]. Ni-based catalysts can be rapidly deactivated due to deposits that form on active sites and sintering of Ni at elevated temperatures. However, different supports, synthesis methods and catalytic activity modifiers (additives), improve catalytic activity, deactivation resistance and selectivity [6,7,14,15]. Modification with low amount of Pd (0.01 [16] to 0.3 wt. % [6]) greatly enhances catalysts properties. Catalyst's activity and selectivity can be drastically deteriorated if metals are unevenly dispersed on support [6,16]. Conventional thermochemical methods for Ni-based catalysts synthesis include oxidative calcination and reduction by hydrogen (activation). Calcination causes formation of $NiAl_2O_4$ spinel phase, especially in the case of impregnation and γ-Al_2O_3 support. $NiAl_2O_4$ is hardly reducible and it can inhibit catalytic activity because of low amount of Ni particles [5–7]. As reported by Gayan *et al*. [17], α-Al_2O_3 support minimizes $NiAl_2O_4$ presence in the Ni/Al_2O_3 system obtained by impregnation. Novel methods that involve ultrasonically generated aerosols provide synthesis of fine spherical particles with precise stoichiometry and high purity [18–20]. Ultrasonic spray pyrolysis is favored in large scale production in industry [21]. Gurmen *et al*. [22] pyrolized and reduced ultrasonically aerosolized $NiCl_2$ and $FeCl_2$ solution in hydrogen flow. They obtained fine

Correspondence: V.D. Nikolić, Innovation Center of the Faculty of Technology and Metallurgy, University of Belgrade, Karnegijeva 4, 11120 Belgrade, Serbia.
E-mail: vnikolic@tmf.bg.ac.rs
Paper received: 28 September, 2014
Paper accepted: 23 December, 2014

spherical Fe–Ni particles in a single step, without calcination.

Previously, Ni/Al_2O_3 and $Ni–M/Al_2O_3$ catalysts, modified by additives M = Pd, Cu or Fe, were synthesized by aerosol assisted impregnation [23]. Oxides and chlorides were used as precursors for metals. Reduction of chloride precursor at 633 K, without previous calcination, resulted in optimal morphology of Ni coating. Modification with Pd enabled the highest reduction efficiency of all precursors [23] due to the hydrogen spillover effect [24, 25]. Chloride precursors for Ni–Pd coating reached significantly higher reduction degree (98.2 wt. %) than oxide precursors (20.0 wt. %) at 533 K [23].

On the basis of previously obtained results [23], Ni-based catalysts were synthesized by aerosol assisted impregnation using chlorides as precursors. Catalysts were supported on previously prepared α-Al_2O_3-based foams [26,27]. The aim of the presented research was to investigate dependence of catalysts properties from different Ni loading and from modification by Pd additive. Comparative analysis of the catalysts included determination of reduction degrees in hydrogen stream and microstructure development, which was investigated by scanning electron microscopy (SEM). An additional investigation included point analysis of reduced $Ni–Pd/Al_2O_3$ samples by energy-dispersive spectroscopy (EDS).

EXPERIMENTAL

Non-modified Ni/Al_2O_3 and modified $Ni–Pd/Al_2O_3$ catalysts with 5 and 20 wt.% Ni loading were synthesized by aerosol assisted impregnation method. Considering $Ni–Pd/Al_2O_3$ catalysts, Ni was modified with 0.1 wt.% of Pd. Used materials included: $NiCl_2·6H_2O$, $PdCl_2$ (MERCK, pro analysis) and α-Al_2O_3-based foams. The foams were produced by polymer replication route that is described elsewhere [26,27]. First, the foams were pre-heated at 473 K in a tubular quartz reactor and then impregnated with aerosolized chloride solutions at that temperature. Subsequently, samples were dried at 473 K for 60 min in air. The catalysts were reduced by hydrogen at 533 and 633 K for 90 min. Set-up for the aerosol assisted impregnation and the synthesis method details are presented elsewhere [23].

Reduction degrees of chlorides on the foam surface were determined on the basis of chlorine mass loss before and after hydrogen reduction. After the impregnation and subsequent drying at 473 K for 60 min, the samples were stored in desiccators with silica gel until the mass measurements to prevent absorption of moisture from the air. Mass ratio of chlorides and the foam was a known value. The reduction experiments were performed under static conditions as follows. First, the samples were set into a quartz tube and reaction area was purified by nitrogen flow. Then, nitrogen flow was stopped and hydrogen was introduced into the tube. Hydrogen flow was conducted through system for purification and drying that was consisted of: columns with silica gel, Cu powder and $CaCl_2$ and wash bottle with H_2SO_4. A tubular electric resistance furnace was heated to the selected temperature and then the tube was put in. Measuring of reduction time started at that moment. Reduction of the dried samples was carried out at 533 and 633 K for 90 min (H_2 flow rate 20 L/h). Reduced samples were placed in desiccators, cooled down to room temperature and their mass was determined afterward.

Microstructures of the samples after drying and after reduction experiments were investigated with a JEOL JSM-5800LV scanning electron microscope (SEM) equipped with an energy-dispersive spectrometer (EDS). SEM/EDS point analysis was carried out for $Ni–Pd/Al_2O_3$ catalysts with different metal loading, reduced at 533 K for 90 min.

RESULTS AND DISCUSSION

Reduction degrees of $NiCl_2$ on the foam surface are presented in Table 1.

Table 1. Reduction degrees, wt.%, of $NiCl_2$ on α-Al_2O_3 based foam after 90 min

Sample description	Temperature, K	
	533	633
5 wt.% of Ni	60.2	67.7
20 wt.% of Ni	23.7	35.2

As expected, higher reduction degrees were obtained at 633 than at 533 K for all the samples. However, when Ni loading was lower, significantly higher amount of $NiCl_2$ was reduced at both temperatures due to the better exposure of $NiCl_2$ particles to H_2 flow when $NiCl_2$ content was lower. These results could be explained with microstructures of the samples before and after hydrogen reduction (Figs. 1–3).

SEM photographs of the dried samples are presented in Fig. 1a and b.

After SEM analysis of the dried sample with 5 wt.% Ni loading, presence of relatively unevenly distributed, fine, submicron-sized $NiCl_2$ particles was noted, as shown in Fig. 1a. Agglomerates were not detected. Despite relatively uneven particle distribution, satisfying reduction degrees of $NiCl_2$ were achieved at both temperatures (Table 1). These results could be explained by obtained morphology, because fine particles were non-agglomerated and, consequently, they had good exposure to H_2. In addition, good mass and heat transfer through the foam was one of the reasons for

satisfying reduction degrees. Figure 1b shows microstructure of the dried sample with 20 wt.% Ni loading. Higher $NiCl_2$ amount resulted in formation of cracked $NiCl_2$ crust, which completely covered the foam surface. This crust appeared to be thick on certain sites. A main reason for obtained cracks was dehydration of $NiCl_2 \cdot 6H_2O$ during the drying procedure, while filter-like behavior of the foam provided complete coverage with $NiCl_2$. Higher Ni loading resulted in lower reduction degrees at both temperatures (Table 1), due to absence of small individual $NiCl_2$ particles.

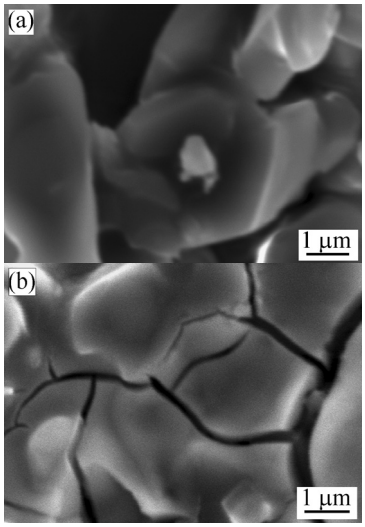

Figure 1. Sample dried at 473 K – $NiCl_2/Al_2O_3$, Ni loading: a) 5 and b) 20 wt.%.

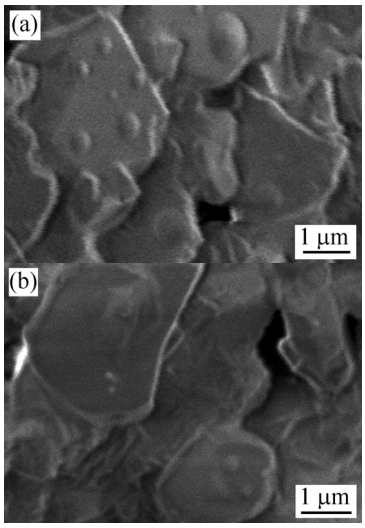

Figure 2. Ni/Al_2O_3 reduced at 533 K, nominal Ni loading: a) 5 and b) 20 wt.%.

SEM photographs of the Ni/Al_2O_3 samples reduced at 533 K are presented in Fig. 2a and b.

SEM photographs of the Ni/Al_2O_3 samples reduced at 633 K are presented in Fig. 3a and b.

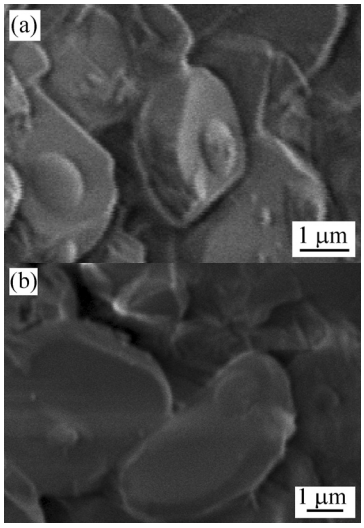

Figure 3. Ni/Al_2O_3 reduced at 633 K, nominal Ni loading: a) 5 and b) 20 wt.%.

After the reduction of Ni/Al_2O_3 with 5 wt.% Ni loading at both temperatures, small, island-like Ni particles were formed. Ni islands were isolated and submicron-sized particles were noted, as presented in Figs. 2a and 3a. No significant changes in the microstructures were noted after the reduction at each temperature. With 20 wt.% Ni loading, the samples reduced at both temperatures had similar microstructures: Ni coating relatively uniformly covered the foam surface, as presented in Figs. 2b and 3b. The reduction with H_2 led to disappearance of visible cracks. Formation of these microstructures could be explained by complex mass transport mechanism that occurred at elevated temperature during the reduction. At the reduction conditions, Ni particles gained sufficient mobility and migrated, which resulted in formation of contacts between particles and their growth. No agglomerates occurred in any of the reduced samples.

Reduction degrees of $NiCl_2$ with added $PdCl_2$, supported on the foam surface, are presented in Table 2.

Table 2. Reduction degrees, wt.%, of $NiCl_2$ with $PdCl_2$ on α-Al_2O_3 based foam after 90 min

Sample description	Temperature, K	
	533	633
5 wt.% Ni, 0.1 wt.% Pd	99.4	99.7
20 wt.% Ni, 0.1 wt.% Pd	98.2	99.6

Results of the reduction experiments showed minor differences in reduction degrees of the $Ni–Pd/Al_2O_3$ samples. All the samples were almost completely reduced at both investigated temperatures (Table 2). Although slightly higher reduction degrees were achieved at 633 K, obtained results indicate that lower reduction temperature can successfully be used for the catalysts synthesis, if the catalysts are modified with

Pd. The main reason for increased reduction efficiency was modification by Pd additive, which caused the hydrogen spillover effect. In general, this effect occurs in the presence of Pd surface, when H_2 molecules dissociate into atoms and rapidly diffuse into crystal lattices of Ni species [24,25].

SEM photographs of Ni–Pd/Al_2O_3 catalysts with 5 and 20 wt.% Ni loading, reduced at 533 K, are presented in Fig. 4a and b, respectively.

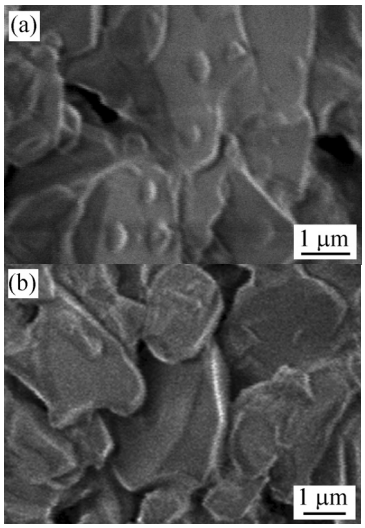

Fig. 4. Ni–Pd/Al_2O_3 reduced at 533 K, nominal Ni loading: a) 5 and b) 20 wt. %.

Similar microstructures were obtained for Ni–Pd/ /Al_2O_3 catalysts, reduced at 533 K, and for Ni/Al_2O_3 catalysts, reduced at 533 and 633 K. Ni–Pd/Al_2O_3 samples with 5 wt.% of Ni had fine, submicron-sized and isolated island-like particles dispersed on the foam surface, as presented in Fig. 4a. With higher Ni loading (20 wt.%), metallic coating relatively evenly covered the foam, as presented in Fig. 4b. Particles agglomeration did not occur in any of the samples. Modification with 0.1 wt.% of Pd enabled almost completed hydrogen reduction at 533 K. Ni-based catalysts prepared by conventional thermochemical methods are calcined before hydrogen reduction. The calcination treatment (*e.g.*, at 823 K [6] or 873–923 K [5, 7]) provides forming of oxide mixtures that contain oxide precursors for catalytically active components. During that treatment, especially in the case of impregnation method, hardly reducible $NiAl_2O_4$ phase is commonly formed [5–7]. In addition, the authors concluded that Ni-based catalysts, prepared by using aerosol assisted impregnation and calcined at 773 K, had undesirable agglomerates on the α-Al_2O_3-based foam surface. Ni-based catalysts prepared by using the same method and obtained from chloride precursors reached significantly higher reduction degrees at same temperatures [23].

Point SEM/EDS analysis was performed for Ni–Pd/ /Al_2O_3 catalysts with different Ni loading, reduced at 533 K. Analyzed points are marked in Fig. 5a and b. The results are presented in Table 3.

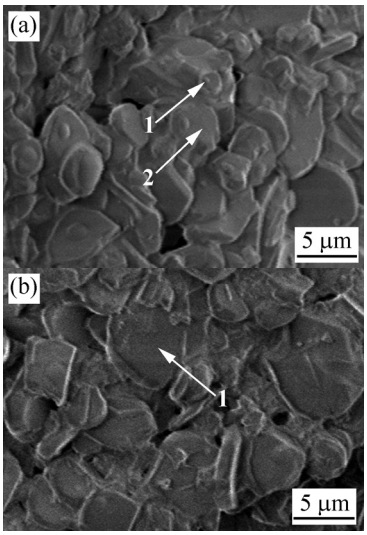

Figure 5. SEM micrographs of Ni–Pd/Al_2O_3 reduced at 533 K, nominal Ni loading: a) 5 and b) 20 wt.%.

Table 3. Point SEM/EDS analysis (wt. %) of Ni–Pd/Al_2O_3 reduced at 533 K

Metal loading	Mark	Ni	Al	Si	O
5 wt.% Ni, 0.1 wt.% Pd	1	93.50	1.97	0.63	3.90
	2	1.50	40.32	5.16	53.02
20 wt.% Ni, 0.1 wt.% Pd	1	94.21	1.53	0.58	3.68

Considering the sample with 5 wt.% Ni loading, island-like metallic particle mainly consisted of Ni. Pd was not detected due to very low concentration. Small amounts of Al, Si and O from the α-Al_2O_3 based foam were also detected. EDS analysis of point with no visible metallic particles showed predominance of elements that correspond to oxides in the α-Al_2O_3 based foam. With Ni loading of 20 wt.%, chemical analysis of a random point revealed that the main element in the metal coating was Ni. Similar to the sample with lower metal content, Pd was not detected because of low concentration. In addition, small amounts of Al, Si and O from the foam were noted. These results confirmed that higher metal loading enabled relatively uniform dispersion of metallic particles over the foam surface.

The conclusion is that Ni–Pd/Al_2O_3 catalysts supported on the α-Al_2O_3 based foams can successfully be produced by hydrogen reduction of chloride instead of oxide precursors, without the calcination step. Chloride precursors for Ni and Pd can be reduced at very low temperature (533 K). Optimal metal loading is 20 wt.%

of Ni modified by 0.1 wt.% Pd due to the relatively even coverage of the foam surface with metallic coating.

CONCLUSION

A comparative analysis of catalysts with 5 and 20 wt.% of Ni, with Pd and without additive, was conducted. The catalysts were supported on α-Al_2O_3-based foams and prepared by aerosol assisted impregnation. Before hydrogen reduction, samples with 5 wt.% of Ni had submicron-sized, non-agglomerated, isolated $NiCl_2$ particles. Cracked $NiCl_2$ crust enveloped the whole foam surface in the case of 20 wt.% of Ni. Higher reduction degrees were reached with lower Ni loading at 533 and 633 K. Reduced Ni/Al_2O_3 and Ni–Pd/Al_2O_3 samples had similar microstructures for the same Ni content. With 5 wt.% of Ni, isolated, island-like, submicron-sized particles were formed. Sample with 20 wt.% of Ni had metallic coating without agglomerates and visible cracks that relatively evenly covered the whole foam surface. Ni–Pd/Al_2O_3 catalysts were nearly completely reduced at both temperatures. Their reduction degrees reached 99.4 and 98.2 wt.% for 5 and 20 wt.% Ni loading, respectively, at 533 K. Optimal metal loading in the produced catalysts is 20 wt.% of Ni and the addition of 0.1 wt.% Pd because the foam surface is relatively uniformly covered with metallic coating. Obtained results indicate that Ni-based catalysts, modified with Pd, can successfully be synthesized without the calcination step and can be reduced at lower temperature.

Acknowledgements

This work was financially supported by the Ministry of Education, Science and Technological Development of the Republic of Serbia and is a result of project No. 34033, Innovative synergy of by-products, waste minimization and clean technologies in metallurgy.

REFERENCES

[1] Z. Anđić, M. Korać, M. Tasić, Ž. Kamberović, K. Raić, Synthesis and sintering of Cu-Al_2O_3 nanocomposite powders produced by a thermochemical route, Metall. Mater. Eng. **13** (2007) 71–81.

[2] M. Korać, Ž. Kamberović, Z. Anđić, M. Filipović, Sintered Materials Based on Copper and Alumina Powders Synthesized by a Novel Method, InTech, Rijeka, 2011.

[3] C. B. Alcock, Thermochemical Processes: Principles and Models, Butterworth-Heinemann, Oxford, 2001.

[4] B.S. Kwak, J. Kim, M. Kang, Hydrogen production from ethanol steam reforming over core–shell structured Ni_xO_y–, Fe_xO_y–, and Co_xO_y–Pd catalysts, Int. J. Hydrogen Energy **35** (2010) 11829–11843.

[5] A.J. Akande, R.O. Idem, A.K. Dalai, Synthesis, characterization and performance evaluation of Ni/Al_2O_3 catalysts for reforming of crude ethanol for hydrogen production, Appl. Catal. A **287** (2005) 159–175.

[6] L.P.R. Profeti, J.A.C. Dias, J.M. Assaf, E.M. Assaf, Hydrogen production by steam reforming of ethanol over Ni-based catalysts promoted with noble metals, J. Power Sources **190** (2009) 525–533.

[7] C.K. Cheng, S.Y. Foo, A.A. Adesina, Steam reforming of glycerol over Ni/Al_2O_3 catalyst, Catal. Today **178** (2011) 25–33.

[8] M.A. Goula, S.K. Kontou, P.E. Tsiakaras, Hydrogen production by ethanol steam reforming over a commercial Pd/γ-Al_2O_3 catalyst, Appl. Catal., B **49** (2004) 135–144.

[9] J. Grosse, B. Dietrich, G. Incera Garrido, P. Habisreuther, N. Zarzalis, H. Martin, M. Kind, B. Kraushaar-Czarnetzki, Morphological characterization of ceramic sponges for applications in chemical engineering, Ind. Eng. Chem. Res. **48** (2009) 10395–10401.

[10] M.V. Twigg, J.T. Richardson, Theory and applications of ceramic foam catalysts, Chem. Eng. Res. Des. **80** (2002) 183–189.

[11] F. Ribeiro, J.M. Silva, E. Silva, M. Fatima Vaz, F.A.C. Oliveira, Catalytic combustion of toluene on Pt zeolite coated cordierite foams, Catal. Today **176** (2011) 93–96.

[12] P. Ciambelli, V. Palma, E. Palo, Comparison of ceramic honeycomb monolith and foam as Ni catalyst carrier for methane autothermal reforming, Catal. Today **155** (2010) 92–100.

[13] D.K. Liguras, D.I. Kondarides, X.E. Verykios, Production of hydrogen for fuel cells by steam reforming of ethanol over supported noble metal catalysts, Appl. Catal., B **43** (2003) 345–354.

[14] Y. Zhang, Y.H. Tang, E.L. Zhang, L.W. Lin, L.Z. Pei, Preparation of Ni/MgO catalysts for carbon nanofibres by self-propagating low temperature combustion process, Mater. Sci.-Poland **28** (2010) 805–815.

[15] A.N. Fatsikostas, D.I. Kondarides, X.E. Verykios, Production of hydrogen for fuel cells by reformation of biomass-derived ethanol, Catal. Today **75** (2002) 145–155.

[16] K. Yoshida, K. Okumura, T. Miyao, S. Naito, S. Ito, K. Kunimori, K. Tomishige, Oxidative steam reforming of methane over Ni/α-Al_2O_3 modified with trace Pd, Appl. Catal., A **351** (2008) 217–225.

[17] P. Gayan, L.F. de Diego, F. Garcia-Labiano, J. Adanez, A. Abad, C. Dueso, Effect of support on reactivity and selectivity of Ni-based oxygen carriers for chemical-looping combustion, Fuel **87** (2008) 2641–2650.

[18] M. Watanabe, H. Yamashita, X. Chen, J. Yamanaka, M. Kotobuki, H. Suzuki, H. Uchida, Nano-sized Ni particles on hollow alumina ball: Catalysts for hydrogen production, Appl. Catal., B **71** (2007) 237–245.

[19] X. Wei, P. Hug, R. Figi, M. Trottmann, A. Weidenkaff, D. Ferri, Catalytic combustion of methane on nano-structured perovskite-type oxides fabricated by ultrasonic spray combustion, Appl. Catal., B **94** (2010) 27–37.

[20] G. Matula, J. Bogović, S. Stopić, B. Friedrich, Scale-up of the Ultrasonic spray pyrolysis (USP) process for nanopowder production (Part 1), PIM International **7** (2013) 75–78.

[21] B. Ebin, E. Arig, B. Ozkal, S. Gurmen, Production and characterization of ZnO nanoparticles and porous particles by ultrasonic spray pyrolysis using a zinc nitrate precursor, Int. J. Min. Metall. Mater. **19** (2012) 651–656.

[22] S. Gurmen, B. Ebin, S. Stopić, B. Friedrich, Nanocrystalline spherical iron–nickel (Fe–Ni) alloy particles prepared by ultrasonic spray pyrolysis and hydrogen reduction (USP-HR), J. Alloys Compd. **480** (2009) 529–533.

[23] V. Nikolić, Ž. Kamberović, Z. Anđić, M. Korać, M. Sokić, V. Maksimović, Influence of the synthesis method and the addition of modifiers on the properties of Ni-based catalysts supported on reticulated ceramic foams, Int. J. Min. Metall. Mater. (2014), DOI: 10.1007/s12613-014--0000-0.

[24] M. Šušić, S. Stopić, I. Ilić, D. Uskoković, Kinetics of hydrogen absorption by nickel powder with added palladium, copper, and nickel from nickel-chloride reduction by hydrogen, Int. J. Hydrogen Energy **22** (1997) 661––667.

[25] C. Amorim, M.A. Keane, Catalytic hydrodechlorination of chloroaromatic gas streams promoted by Pd and Ni: The role of hydrogen spillover, J. Hazard. Mater. **211**––**212** (2011) 208–217.

[26] V. Nikolić, Ž. Kamberović, Z.Andić, M. Korać, A. Vujović, M. Sokić, Alumina based catalytically active components carriers with improved properties, in: Proceedings of the 44th International October Conference on Mining and Metallurgy, Bor, Serbia, 2012, pp. 395–400.

[27] V. Nikolić, Ž. Kamberović, Z. Anđić, M. Korać, M. Sokić, Synthesis of α-Al_2O_3 based foams with improved properties as catalyst carriers, Mater. Tehnol. **48** (2014) 45––50.

IZVOD

Katalizatori na bazi nikla: zavisnost svojstava od sadržaja nikla i modifikacije paladijumom

Vesna D. Nikolić[1], Željko J. Kamberović[2], Marija S. Korać[2], Zoran M. Anđić[3], Aleksandar M. Mihajlović[1], Jelena B. Uljarević[1]

[1]*Inovacioni centar Tehnološko–metalurškog fakulteta, Univerzitet u Beogradu, Beograd, Srbija*
[2]*Tehnološko–metalurški fakultet Univerziteta u Beogradu, Beograd, Srbija*
[3]*Inovacioni centar Hemijskog fakulteta, Univerzitet u Beogradu, Beograd, Srbija*

(Naučni rad)

Cilj predstavljenog istraživanja bila je uporedna analiza svojstava katalizatora na bazi nikla, sa sledećim sadržajem metala: 5 i 20 mas. % Ni, bez dodatka i sa dodatkom Pd. Ni/Al_2O_3 i Ni–Pd/Al_2O_3 katalizatori su sintetisani metodom impregnacije potpomognute ultrazvučnim raspršivanjem. Kao nosači katalitički aktivnih materija korišćene su keramičke pene na bazi α-Al_2O_3. Uporedna analiza svojstava sintetisanih katalizatora obuhvatila je: određivanje stepena redukcije uzoraka u struji vodonika, praćenje razvoja mikrostrukture metodom skenirajuće elektronske mikroskopije i ispitivanje hemijskog sastava u tački metodom energetsko disperzivne spektroskopije. Radi sinteze katalizatora, nosači odn. pene su predgrejane u cevnom reaktoru na 473 K i impregnirane ultrazvučno raspršenim rastvorima hlorida metala. Nakon impregnacije, uzorci su sušeni na 473 K radi dehidratacije, a zatim redukovani u struji vodonika na 533 i 633 K. Kod uzoraka sa nižim sadržajem Ni, dobijeni su viši stepeni redukcije. Svi uzorci sa dodatim Pd, kao modifikatorom aktivnosti, gotovo su u potpunosti bili redukovani na obe ispitivane temperature. Kod ovih uzoraka su na temperaturi od 533 K stepeni redukcije dostigli 99,4 i 98,2 mas.% za sadržaj Ni od 5 i 20 mas.%, redom. Optimalni sastav proizvedenih katalizatora je 20 mas.% Ni i dodatak od 0,1 mas.% Pd, čime se postiže relativno ravnomerna prekrivenost cele površine pene slojem metala. Dobijeni rezultati ukazuju na to da se katalizatori na bazi Ni, modifikovani dodatkom Pd, uspešno mogu sintetisati bez koraka žarenja i redukovati na izuzetno niskoj temperaturi (533 K).

Ključne reči: Katalizatori • Ni • Pd • Modifikovanje • Pena na bazi α-Al_2O_3 • Impregnacija aerosolom

Stimulation of diesel degradation and biosurfactant production by aminoglycosides in a novel oil-degrading bacterium *Pseudomonas luteola* PRO23

Iva M. Atanasković[1], Jelena P. Jovičić Petrović[2], Marjan B. Biočanin[1], Vera M. Karličić[2], Vera B. Raičević[2], Blažo T. Lalević[2]

[1]*University of Belgrade, Faculty of Biology, Belgrade, Serbia*
[2]*University of Belgrade, Faculty of Agriculture, Belgrade-Zemun, Serbia*

Abstract

Bioremediation is promising technology for dealing with oil hydrocarbons contamination. In this research growth kinetics and oil biodegradation efficiency of *Pseudomonas luteola* PRO23, isolated from crude oil-contaminated soil samples, were investigated under different concentrations (5, 10 and 20 g/L) of light and heavy crude oil. More efficient biodegradation and more rapid adaptation and cell growth were obtained in conditions with light oil. The 5 to 10 g/L upgrade of light oil concentration stimulated the microbial growth and the biodegradation efficiency. Further upgrade of light oil concentration and the upgrade of heavy oil concentration both inhibited the microbial growth, as well as biodegradation process. Aminoglycosides stimulated biosurfactant production in *P. luteola* in the range of sub-inhibitory concentrations (0.3125, 0.625 µg/mL). Aminoglycosides also induced biofilm formation. The production of biosurfactants was the most intense during lag phase and continues until stationary phase. Aminoglycosides also induced changes in *P. luteola* growth kinetics. In the presence of aminoglycosides this strain degraded 82% of diesel for 96 h. These results indicated that *P. luteola* PRO23 potentially can be used in bioremediation of crude oil-contaminated environments and that aminoglycosides could stimulate this process.

Keywords: biodegradation, crude oil, aminoglycosides, *Pseudomonas luteola*.

Available online at the Journal website: http://www.ache.org.rs/HI/

SCIENTIFIC PAPER

UDC 665.61:502/504:579.841.1

Hem. Ind. **70** (2) 143–150 (2016)

doi: 10.2298/HEMIND141127020A

Oil pollution accidents have become a common phenomenon and have caused serious environmental problems, such as introduction of toxic compounds in food chains and changes in physical and chemical properties of the soil [1]. One of the highly efficient methods in remediation of oil polluted soil is bioremediation, where contaminants are degraded or transformed to less hazardous compounds through biological processes [2].

Bacteria of the genus *Pseudomonas* are highly capable to adapt on conditions in oil contaminated sites and can use different hydrocarbons as energy sources [3,4]. Therefore, *Pseudomonas* strains are commonly applied in *ex situ* bioremediation methods [5]. In these methods the first step is to isolate and characterize microorganisms that can use the oil contaminant as an energy source. Another step is to define conditions in applied bioreactors which are optimal for microbial growth and biodegradation [6]. These conditions include the type of oil and its concentration [7]. Some oil types stimulate microbial activity with an upgrade of its concentration. This is happening until reaching a specific concentration threshold, afterwards toxic compounds in oil can inhibit microbial growth and the biodegradation process [8]. This raises the importance of defining optimal concentrations for specific oil types.

Furthermore, microbial activity could be stimulated by adding chemical inducers in the bioreactors. For defining such inducers it is crucial to know how the strain of interest adapts to oil as its only carbon source. In genus *Pseudomonas* adaptation is achieved by biosurfactant production and biofilm formation [9]. Biosurfactants allow more efficient oil emulsification, which increases its accessibility for degradation. Biosurfactant production and oil degradation could be stimulated by aminoglycosides [10]. In subinhibitory concentrations aminoglycosides start acting as alternative signaling molecules, modulating gene expression, biosurfactant production and biofilm formation in *Pseudomonas* [11].

The aim of this research was isolation and identification of new oil and diesel degrading bacterial strain, and stimulation of biosurfactant production and diesel degradation using the aminoglycosides in sub-inhibitory concentrations.

Correspondence: B. Lalević, University of Belgrade, Faculty of Agriculture, Department of Microbial Ecology, Nemanjina 6, 11080 Belgrade-Zemun, Serbia.
E-mail: blazol@agrif.bg.ac.rs
Paper received: 27 November, 2014
Paper accepted: 19 March, 2015

MATERIAL AND METHODS

The soil samples were aseptically collected from the zone of used oil re-refining facility in the Belgrade Oil Refinery (Serbia). Isolation of microorganisms resistant on light and heavy crude oil was achieved by diluting 1 g of soil in 100 mL of liquid mineral medium [12], containing 1g/L NH_4NO_3, 0.25g/L K_2HPO_4, 50mL/L soil extract, with addition of 10 g/L light or heavy crude oil (oil drill "Rusija", Serbia). Those enriched suspensions were then incubated on orbital shaker (ES-20, Biosan, Latvia) at 30 °C and 200 rpm for 30 days. Isolation and enumeration of *Pseudomonas* sp. from enrichment suspensions were proceeded on *Pseudomonas* Cetrimide agar with addition of *Pseudomonas* C-N SR0102E supplement (Oxoid). After 48 h of incubation (30 °C) all developed colonies were morphologically identical and further purification and identification was continued on nutrient agar. Ability of the isolate to use crude oil as the only carbon source was investigated by cultivating the strain on solid mineral medium with addition of 10 g/L of heavy or light crude oil. Biosurfactant production was investigated by drop-collapse test [13].

Identification of isolate was performed by API and APIWEB technique (Biomerieux, France).

Effect of different oil type concentrations was studied by cultivating the strain in shaking flask bioreactors [14]. Gas phase–liquid phase ratio in the shaking flasks was 1:1, while the total bioreactor volume was 500 mL. The liquid phase was composed of liquid mineral medium (described above) with 10% of isolated strain suspension. The tested concentrations of oil were: 5, 10 and 20 g/L for each oil type. An un-inoculated shaking flask bioreactor represents control for each oil concentration. For each oil concentration an abiotic control group was created, where no bacterial culture was added to the liquid phase. All bioreactors were incubated (30 °C, 200 rpm) for 6 days. Cell number in liquid phase was measured every 24 h by quantitative plate method. The absorbance (OD_{600}) of the liquid phase was measured using a T70 UV/Vis spectrometer (PG Instruments, UK).

The efficiency of crude oil biodegradation was determined by measuring the residual amount of crude oil present in the experimental and abiotic groups. The remaining oil was extracted from bioreactors after 6 days of incubation by *n*-hexane as previously described [15], where the efficiency of biodegradation was expressed as a percentage of degraded oil and calculated according to previous research [16], as follows:

1) Weight of residual crude oil = weight of beaker containing extracted crude oil – weight of empty beaker;

2) Amount of crude oil degraded = weight of crude oil added in the media – weight of residual crude oil;

3) % degradation = amount of crude oil degraded/amount of crude oil added in the media×100

Different tobramycin and gentamicin concentrations (0.3125–1.25 μg/mL) were used for testing the effect of aminoglycosides on diesel degradation. The bioreactors contained 1g/L of diesel D-2, while the basic liquid mineral medium and incubation conditions were as described previously. Quantitative plate method was used for measuring the microbial growth. Biosurfactant production was simultaneously measured by the oil-spreading test [17]. Diesel degradation was determined after 96 h by *n*-hexane extraction, as described above [15].

RESULTS AND DISCUSSION

Strain characterization

The selected isolate, named PRO23, could grow on solid medium where heavy or light oil was the only carbon source. By drop-collapse test the strains ability to produce biosurfactants was observed (data not shown).

The results of biochemical test showed positive reactions for arginine, citrate, urea, glucose, sucrose, melibiose and arabinose, and negative for oxydase, lysine, ornithine, mannitol, inositol, sorbitol, rhamnose and amygdalin. Based on APIWEB database, this strain shows maximal similarity with species *Pseudomonas luteola*.

Light and heavy crude oil degradation

The strain had adapted to all concentrations of light oil and lower concentrations of heavy oil in period shorter than 24 h (Figs. 1 and 2). The longest lag phase was expressed for the highest concentration of heavy oil. In all conditions log phase of growth is noticeable during the first 48 h of incubation. The highest cell number occurred in conditions with 10 g/L of light oil, where the upgrade of oil concentration from 5 to 10 g/L stimulated the microbial growth. Further upgrade of light oil concentration to 20 g/L, as well as all the upgrades in heavy oil concentration, inhibited the microbial growth. Cell number growth in the first 48 h of incubation was followed by absorbance growth in all experimental groups, but cell number decrease was not followed by absorbance decrease.

The most efficient biodegradation and highest cell number in the lag phase was obtained in 10 g/L of light oil (Fig. 3). In a case of heavy oil as a carbon source, the most efficient biodegradation (29.7 %) was obtained in the lowest oil concentration.

So far, there is no literature data referring to the ability of *P. luteola* to degrade crude oil, but some studies show that it was capable to degrade a selective

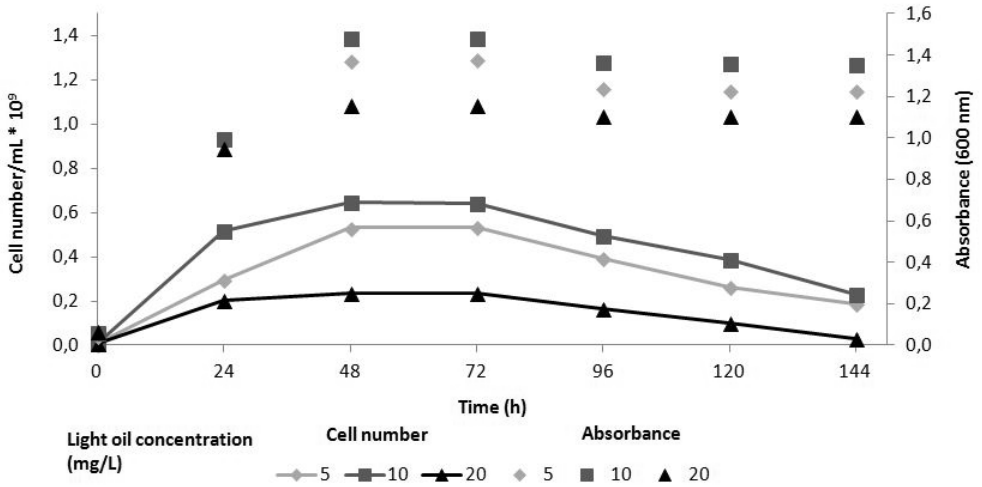

Figure 1. Growth of Pseudomonas luteola PRO23 in the presence of light crude oil.

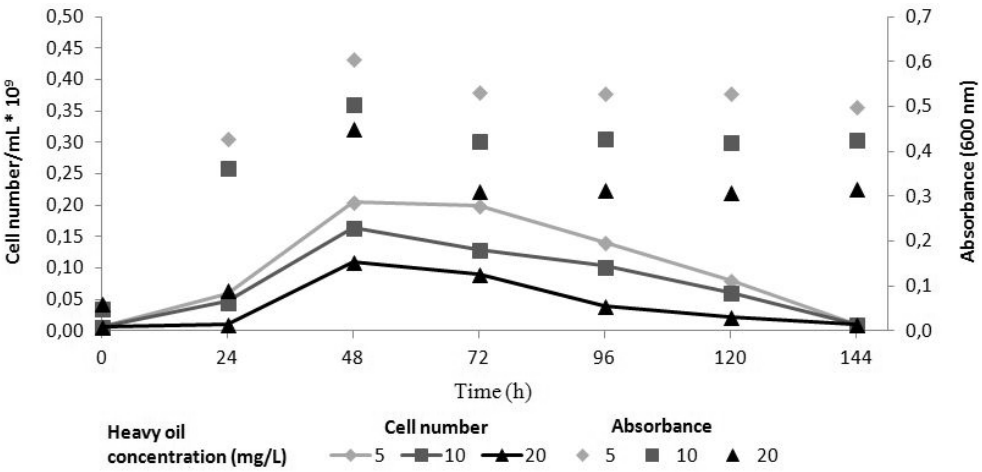

Figure 2. Growth of Pseudomonas luteola PRO23 in the presence of heavy crude oil.

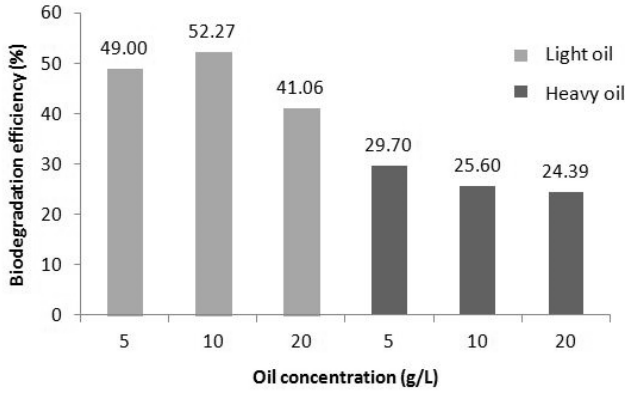

Figure 3. Biodegradation of light and heavy crude oil by Pseudomonas luteola PRO23.

herbicide diclofop-methyl [18], phenolic compounds [19], and decolorize several groups of azo dyes [20].

In genus *Pseudomonas* the main way of adaptation on conditions where the nutrients are hydrophobic is formation of oil in water emulsion with biosurfactants [13]. Higher hydrophobic phase shares [21] and higher viscosity of oil [22] can inhibit the emulsification process. This explains why lag phase was shorter in the light oil and why the highest concentration of heavy oil prolonged it. The highest light and heavy oil concentrations inhibited the microbial growth. In this higher concentration range, some toxic compounds could

express their bacteriostatic effect, which lead to the described growth inhibition. A previous studies show that many crude oil compounds can express bacteriostatic effect for genus *Pseudomonas* after reaching a specific concentration threshold [23]. The bacterial growth was more intensive in conditions with light than in conditions with heavy oil. This can be explained with higher content of small chain alkanes in this type. It is assumed that the isolated strain showed highest affinity for these alkanes, which led to more intensive growth in light oil. This is in accordance with results of previous studies of *Pseudomonas* bacteria [24]. Cell number decrease was not followed by absorbance decrease, which indicates that the changes of the absorbance are the consequence of bacterial growth, as well as oil emulsification and biosurfactant production [25].

Microbial growth stimulation with upgrade in light oil concentration (5 to 10 g/L) was followed by more efficient biodegradation. Heavy oil concentration upgrade induced a decrease in biodegradation efficiency, as well as bacterial growth inhibition.

The isolated strain degraded 41–52% of light and 24–30% of heavy oil in period of 6 days, so it could find a great use in bioremediation technologies.

Stimulation of diesel degradation by aminoglycosides

Tobramycin and gentamicin were added to the bioreactors in three different concentrations. The lowest and the middle concentrations have stimulated biosurfactant production (Fig. 4), biofilm formation (Fig. 5), microbial growth (Fig. 6) and diesel degradation (Fig. 7). Biofilm formation was observed after 48 h of incubation, when a plateau in biosurfactant production was reached (Fig. 5). This stimulatory effect was dose dependent, where 0.625 μg/mL had a higher stimulatory effect than 0.3125 μg/mL. The highest concentration had an inhibitory effect on all of the aforementioned processes. Biofilm induction by aminoglycosides in genus *Pseudomonas* was observed in previous studies [26]. It was also shown that tobramycin could stimulate transcription of biosurfactant production genes in a dose dependent manner [27]. Therefore we suppose that sub-MICs (minimal inhibitory concentrations) of tobramycin and gentamicin have induced biosurfactant production and biofilm formation probably by acting as regulators on a transcriptional level.

Aminoglycosides have also modulated the microbial growth kinetics. The lag phase was shorter and the

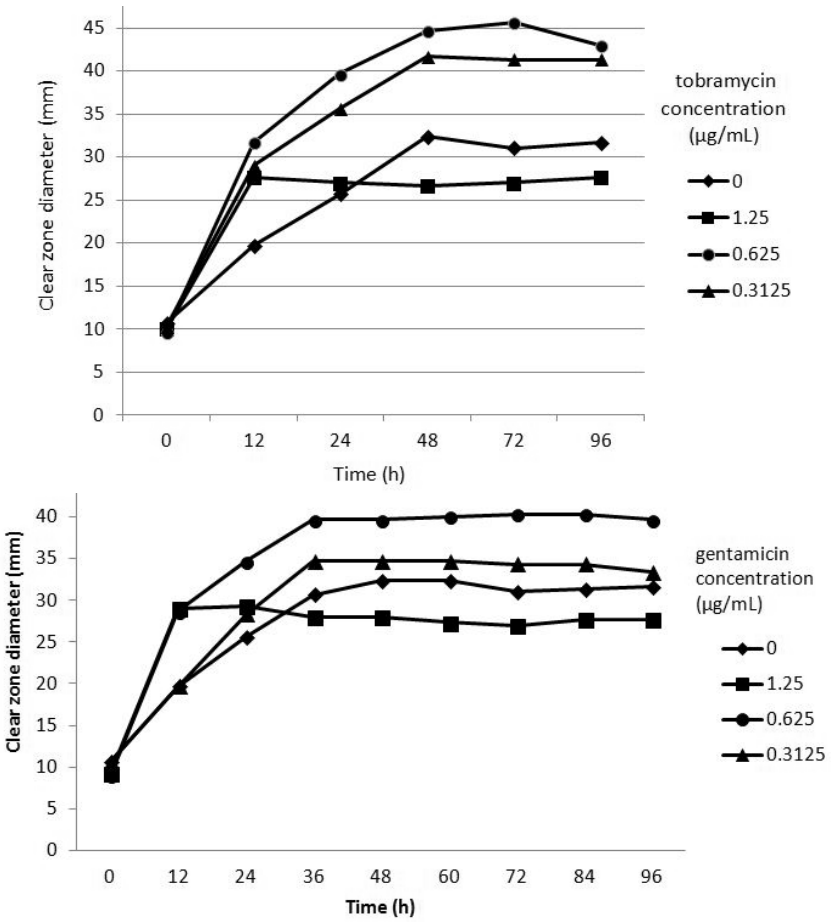

Figure 4. Effect of tobramycin and gentamicin subinhibitory concentrations on biosurfactant production in Pseudomonas luteola PRO23.

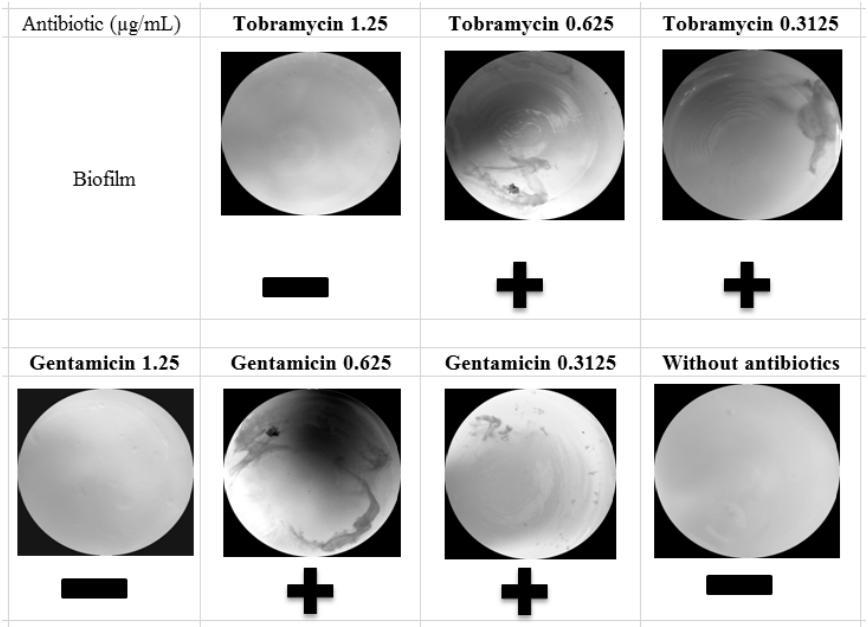

Figure 5. Biofilm appearance in bioreactors after 48h incubation (+); no biofilm appearance (–).

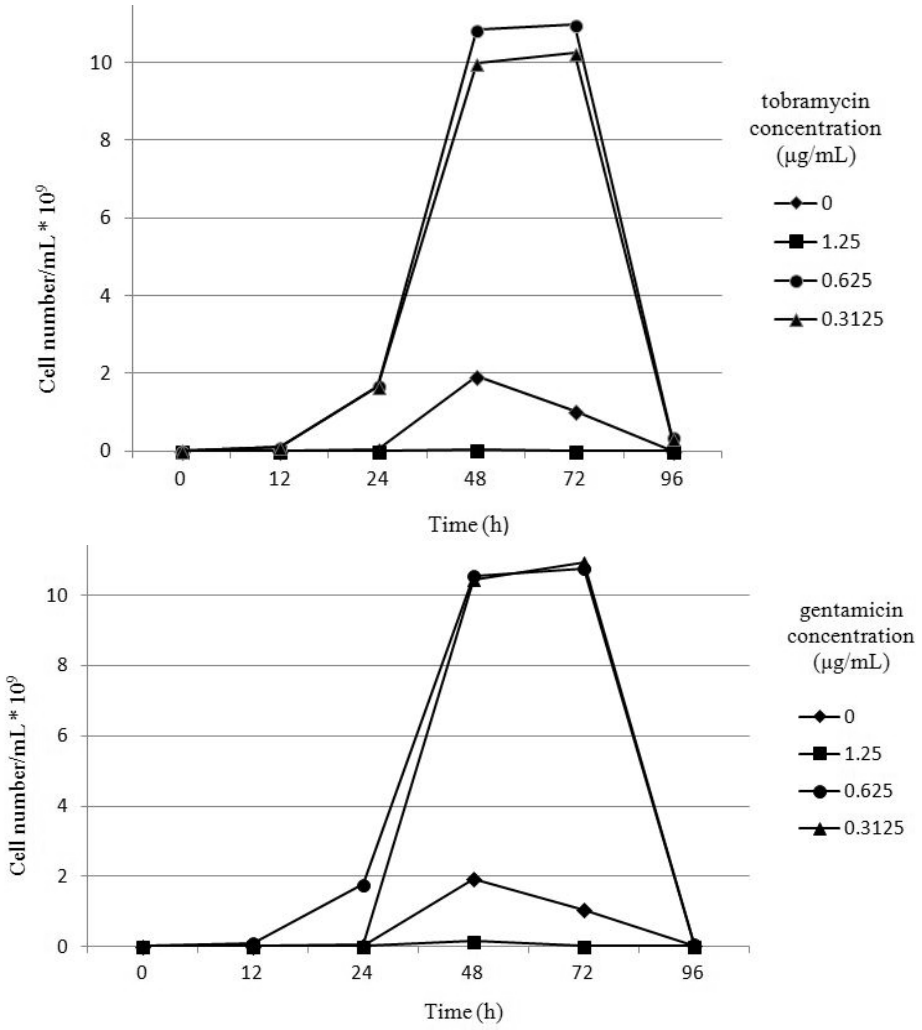

Figure 6. Effect of tobramycin and gentamycin subinhibitory concentrations on growth kinetics in Pseudomonas luteola PRO23.

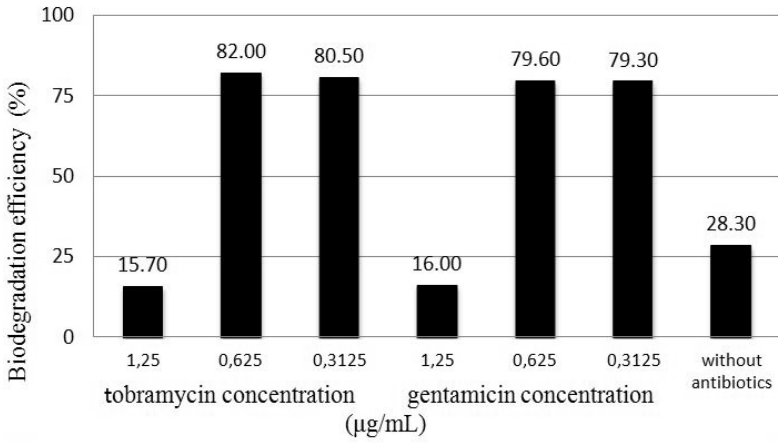

Figure 7. Effect of aminoglycosides on diesel biodegradation efficiency in Pseudomonas luteola PRO23.

higher cell number was reached in the presence of tobramycin and gentamicin sub-MICs (Fig. 6). In these conditions stationary phase was longer then in the control group, probably because biosurfactant production increased the nutrients availability. The optical density of the cultures was growing even in the lag phase, when no growth of bacterial cell number was observed. This *OD* increase is probably caused by biosurfactant production, which starts before the ending of the lag phase. *OD* changes could also be induced by the orange pigmentation of the strain, or other metabolite production. It didn't drop during the decrease of CFUs, which was only observed in biofilm containing bioreactors. *OD* consistency in the liquid phase of biofilm containing cultures was previously described [28].

We also compared the kinetics of biosurfactant production with the growth kinetics. The highest rate of biosurfactant production was observed in the lag phase, when the strain was adapting to diesel as its only nutrient source. The production level reaches a plateau in the stationary phase, although viable cells are still present in the culture. This result is in accordance with previous studies, which show that ramnolipid production stops after reaching a certain threshold [29].

Subinhibitory concentrations of tobramycin and gentamicin have also stimulated diesel biodegradation. The highest rate of biodegradation was observed for 0.625 µg/mL of tobramycin, where 82 % of diesel was degraded in 96 h. This degradation rate was three times higher than in the control group, where no aminoglycoside was present. In previous studies it was shown that biosurfactant production and biofilm formation led to more efficient oil degradation [14]. We suppose that tobramycin and gentamicin stimulate these processes in *P. luteola*, which resulted in better diesel degradation and higher cell growth. Both chemicals had a very similar effect on strains' adaptation to diesel. They exhibit the similar effect probably because they both belong to the same class of antibiotics. Therefore, we propose the structure of aminoglycosides as a reference for new biodegradation inducing agents.

CONCLUSION

Pseudomonas luteola PRO23 strain, isolated from oil contaminated soil, is capable of using light and heavy crude oil as the only carbon and energy source. The strain showed different growth kinetics depending on oil type and concentration. The growth was more intensive in conditions with light oil as a sole carbon source. The most intensive growth was obtained in 10 g/L light oil concentration. The increase of heavy oil concentration and the highest light oil concentration inhibited the microbial growth. According to these results, optimal conditions for *ex situ* oil biodegradation and growth of *P. luteola* PRO23 are 5–10 g/L of light oil type. Aminoglycosides tobramicin and gentamicin stimulated microbial growth in the bioreactors. Growth stimulation was followed by more intense biosurfactant production, biofilm formation and more efficient oil degradation. Therefore aminoglycosides could serve as reference molecules for designing new inducers of bioremediation.

Acknowledgements

This study was partially supported by the Ministry of Education, Science and Technological Development of the Republic of Serbia, grant number TR31080, and by EU Comission project AREA, contract No. 316004.

REFERENCES

[1] B.O. Okonokhua, B. Ikhajiagbe, G.O. Anoliefo, T.O. Emede, The effects of spent engine oil on soil properties and growth of maize (Zea mays L.), J. Appl. Sci. Environ. Manage. **11** (2007) 147–152.

[2] B. Thapa, K.C. Ajay Kumar, A. Ghimire, A review on bioremediation of petroleum hydrocarbon contamin-

ants in soil, Kathmandu Univ. J. Sci. Eng. Technol. **8** (2012) 164–170.

[3] A.O. Nwadinigwe, E.G. Onyeidu, Bioremediation of crude oil-polluted soil using bacteria and poultry manure monitored through soybean productivity, Pol. J. Environ. Stud. **21** (2012) 171–176.

[4] T.T. Tsai, C.M. Kao, R.Y. Surampalli, H.Y. Chien, Enhanced bioremediation of fuel-oil contaminated soils: Laboratory feasibility study, J. Environ. Eng. **135** (2009) 845–853.

[5] M.A.R. Muftah, T. Šolević, M. Antić, V.P. Beškoski, M.M. Vrvić, J. Schwarzbauer, B. Jovančićević, Degradability of n-alkanes during ex situ natural bioremediation of soil contaminated by heavy residual fuel oil (mazut), J. Serb. Chem. Soc. **78** (2013) 1035–1043.

[6] V. Raičević, B. Lalević, D. Dabić, D. Kiković, Lj. Jovanović, M. Nikšić, Mikroorganizmi u remedijaciji zemljišta i voda, Zast. Mater. **2** (2007) 49–52 (in Serbian).

[7] F. Haus, J. German, G.A. Junter GA, Primary biodegrability of mineral base oils in relation to their chemical and physical characteristics, Chemosphere **45** (2001) 983–990.

[8] K. Das, A.K. Mukherjee, Crude petroleum-oil biodegradation effciency of *Bacillus subtilis* and *Pseudomonas aeruginosa* strains isolated from a petroleum-oil contaminated soil from North-East India, Bioresour. Technol. **98** (2006) 1339–1345.

[9] G. Emtiazi, H. Shakarami, I. Nahvi, S.H. Mirdamadian, Utilization of petroleum hydrocarbons by *Pseudomonas* sp. and transformed *Escherichia coli*, Afr. J. Biotechnol. **4** (2005) 172–176.

[10] L.R. Hoffman, D.A. D'Argenio, M.J. MacCoss, Z. Zhang, R.A. Jones, S.I. Miller, Aminoglycoside antibiotics induce bacterial biofilm formation, Nature **436** (2005) 1171––1175.

[11] T. Kievit, Quorum sensing in *Pseudomonas aeruginosa* biofilms, Environ. Microbiol. **11** (2009) 279–288.

[12] J.S. Terzić, Research of biodegradation potential of oil hydrocarbons in soils by detection of catabolytic genes. MSc thesis. Faculty of chemistry, Belgrade (1998).

[13] T. Tugrul, C. Emir, Detecting surfactant-producing microorganisms by the drop collapse test, World J. Microbiol. Biotechnol. **21** (2005) 851–853.

[14] G. Zhang, Y. Wu, X. Qian, Q. Meng Q, Biodegradation of crude oil by *Pseudomonas aeruginosa* in the presence of rhamnolipids, J. Zhejiang Univ. Sci., B **6** (2005) 725–730.

[15] US EPA, Method 1664, Revision A: N-Hexane Extractable Material (HEM; Oil and Grease) and Silica Gel Treated N-Hexane Extractable Material (SGTHEM; Non-polar Material) by Extraction and Gravimetry. US Office of Water, Washington DC, 1999.

[16] K. Sakalle, S. Rajkumar, Isolation of crude oil degrading marine bacteria and assessment for biosurfactant production, Int. J. Microb. **7** (2009), http:// //dx.doi:10.5580/1d0e

[17] N.H. Youssefa, K.E. Duncana, D.P. Naglea, K.N. Savagea, R.M. Knappb, M.J. McInerneya, Comparison of methods to detect biosurfactant production by diverse microorganisms, J. Microbiol. Meth. **56** (2004) 339–347.

[18] L.L. Smith-Greenier, A. Adkins, Degradation of diclofop-methyl by pure cultures of bacteria isolated from Manitoban soils, Can. J. Microbiol. **42** (1996) 227–233.

[19] G. Buitron, A. Gonzalez, L.M. Lopez-Marin, Biodegradation of phenolic compounds by an acclimated activated sludge and isolated bacteria, Water Sci. Technol. **37** (1998) 371–378.

[20] J. Chang, C. Chou, Y. Lin, P. Lin, J. Ho, T. Hu, Kinetic characteristics of bacterial azo-dye decolorization by *Pseudomonas luteola*, Water Res. **35** (2001) 2841–2850.

[21] O.P. Ward, Microbial biosurfactants and biodegradation, In: Ramkrishna sen. (Eds.) Biosurfactants, Chapter 5, Landes Biosciences and Springer Science+Business Media (2010) 65–74.

[22] A. Silset, Emulsion (w/o and o/w) of heavy crude oils. Characterization, stabilization, destabilization and produced water quality. Thesis for the degree of philosophiae doctor, Norwegian University of Science and Technology, Trondhaim, 2008, p. 79.

[23] S.V. Cook, A. Chu, H.R. Goodman, Leachability and toxicity of hydrocarbons, metals and salt contamination from flare pit soil, Water, Air, Soil Pollut. **133** (2001) 297–314.

[24] R.M.P. Silva, A.A. Rodriguez, J.M.G.M. de Oca, D.C. Moreno, Biodegradation of crude oil by *Pseudomonas aeruginosa* AT18 strain, Tecnol. Quim. **26** (2006) 70–77.

[25] Y. Prabhu, P.S. Phale, Biodegradation of phenanthrene by pseudomonas sp. strain PP2: Novel metabolic pathway, role of biosurfactant and cell surface hydrophobicity in hydrocarbon assimilation, Appl. Microbiol. Biotechnol. **61** (2003) 342–351.

[26] W. Khan, S. Bernier, S. Kuchma, J. Hammond, F. Hasan, G. O'Toolel, Aminoglycoside resistance of *Pseudomonas aeruginosa* biofilms modulated by extracellular polysaccharide, Int. Microbiol. **13** (2010) 207–212.

[27] J. Linares, I. Gustafsson, F. Baquero, J. Martinez, Antibiotics as intermicrobial signaling agents instead of weapons, Proc. Natl. Acad. Sci. U.S.A. **103** (2006) 19484––19489.

[28] M. Meyer, V. Roy, W. Bentley, R. Ghodssi, Development and validation of a microfluidic reactor for biofilm monitoring *via* optical methods, J. Micromech. Microeng., **21** (2011) 054023.

[29] Y. Zhang, R. Miller, R., Enhanced octadecane dispersion and biodegradation by a *Pseudomonas* rhamnolipid surfactant (biosurfactant), Appl. Environ. Microbiol. **58** (1992) 3276–3282.

IZVOD

STIMULACIJA DEGRADACIJE DIZELA I PRODUKCIJA BIOSURFAKTANATA POMOĆU AMINOGLIKOZIDA I NOVE BAKTERIJE *Pseudomonas luteola* PRO23 KOJA RAZGRAĐUJE NAFTU

Iva M. Atanasković[1], Jelena P. Jovičić Petrović[2], Marjan B. Biočanin[1], Vera M. Karličić[2], Vera B. Raičević[2], Blažo T. Lalević[2]

[1]*Univerzitet u Beogradu, Biološki fakultet, Beograd, Srbija*
[2]*Univerzitet u Beogradu, Poljoprivredni fakultet, Beograd-Zemun, Srbija*

(Naučni rad)

Jedna od naprednih tehnologija za rešavanje problema kontaminacije naftom je bioremedijacija. U ovim istraživanjima ispitana je kinetika rasta i efikasnost biodegradacije nafte bakterije *Pseudomonas luteola* PRO23, izolovane iz uzoraka zemljišta kontaminiranih sirovom naftom, pri različitim koncentracijama (5, 10 and 20 g/L) lake i teške sirove nafte. U uslovima prisustva lake nafte konstatovana je znatno efikasnija biodegradacija, brža adaptacija i brži rast ćelija. Povećanje koncentracije lake nafte od 5 do 10 g/L stimulisala je mikrobni rast i efikasnost biodegradacije. Dalje povećanje koncentracije lake nafte, kao i povećanje koncentracije teške nafte, inhibiralo je mikrobni rast, kao i biodegradaciju. Aminoglikozidi su stimulisali produkciju biosurfaktanata kod *P. luteola* pri subinhibitornim koncentracijama (0,3125, 0,625 µg/mL). Aminoglikozidi su takođe indukovali stvaranje biofilma. Produkcija biosurfaktanata bila je najintenzivnija tokom lag faze i nastavila se do stacionarne faze. Aminoglikozidi su izazvali promene u kinetici rasta *P. luteola*. U prisustvu aminoglikozida, stepen degradacije dizela u prisustvu ovog soja iznosio je 82% za 96 h. Ovi rezultati ukazuju da *Pseudomonas luteola* PRO23 se potencijalno može koristiti u bioremedijaciji ekosistema kontaminiranog sirovom naftom i da aminoglikozidi mogu da stimulišu ovaj proces.

Ključne reči: Biodegradacija • Sirova nafta • Aminoglikozidi • *Pseudomonas luteola*

Optimization of activation temperature on the preparation of sliced porous activated carbon from date fronds by physical activation

Muhammad Shoaib, Hassan M. Al-Swaidan

Department of Chemistry, College of Science, King Saud University, , Riyadh, Kingdom of Saudi Arabia

Abstract

Saudi Arabia is the major date producer in the world. In order to get the maximum production from date tree there is a need to prune the trees on annual basis and is considered as a serious environmental threat. The single step procedure for the synthesis of porous activated carbon (AC) from Saudi date tree fronds using mixture of gases (N_2 and CO_2) was carried out at different carbonization/activation temperatures staring from 700 to 1000 °C at a ramp rate of 10 °C/min. Alloy 330 horizontal reactor was used in tube furnace. Flow rate of N_2 and CO_2 gases were kept at 150 and 50 ml/min, respectively. Results revealed that at 850 °C larger surface area was achieved and can offer higher potential to produce activated carbon of greater adsorption capacity from date fronds waste. The BET surface area of the activated carbon prepared at 850 °C after 30 min activation time is 1094 m^2/g.

Keywords: activated carbon, physical activation, gaseous mixture, Saudi date fronds, agro waste.

Available online at the Journal website: http://www.ache.org.rs/HI/

PROFESSIONAL PAPER

UDC 661.183:58(532):66

Hem. Ind. **70** (2) 151–157 (2016)

doi: 10.2298/HEMIND140916022S

Any cheap material, with a high carbon content and low in organics, can be used as a raw material for the production of activated carbon (AC) [1]; agricultural by-products have proved to be promising raw materials for the production of activated carbons (ACs) because of their availability at a low price. They can be used for the production of activated carbon (AC) with a high adsorption capacity, considerable mechanical strength, and low ash content [2]. Literature survey indicates that there have been many attempts to obtain low-cost activated carbons (AC) or adsorbent from agricultural wastes [3–7].

Saudi Arabia is the major date producer in the world. In order to get the maximum production from date tree there is a need to prune the trees on annual basis. About twelve million of date-palm trees exist in Saudi Arabia. Approximately about three million trees were cut and then pruned every year. It is reported that about 75,000 tons of palm tree fronds, also consisted of foliar parts and thorns, are left during pruning process [8]. This quantity is either disposed off as waste or burnt and ultimately ends up with a harmful effect to the environment. Carbonaceous material can be used to produce activated carbon. Many studies have been reported for the preparation of activated carbon (AC) through agricultural waste material [9–14]. Therefore, the plenty of this agriculture waste material (palm tree fronds) is available in Saudi Arabia and considered as an ideal source as a precursor for production of activated carbon (AC). For the manufacturing of activated carbon (AC) two methods have been reported, *i.e.*, physical and chemical activation [15–20]. In the present study the aim is to prepare activated carbon (AC) of high surface area and porosity using physical method.

Pyrolysis is one form of energy recovery process, which has the potential to generate char, oil and gas product [21]. Because of the thermal treatment, which removes the moisture and the volatile matter contents of the biomass, the remaining solid char shows different properties than the parent biomass materials. The remarkable differences are mainly in porosity, surface area, pore structures (micro pores, mesopores and macropores) and physicochemical properties such as composition, elemental analysis and ash content. These changes in the properties usually lead to high reactivity, and hence, an alternative usage of char as an adsorbent material becomes possible [22]. Thus, the char becomes an attractive by-product, with applications including production of activated carbons (ACs), which is useful as a sorbent for air pollution control [23]. Activated carbons (ACs) are carbons of highly micro porous form with both high internal surface area and porosity, and commercially the most common adsorbents used for the removal of organic compounds from air and water streams.

EXPERIMENTAL

The fronds were dried at 105 °C for 8 h to reduce the moisture content, sliced with sophisticated wood cutter to a size range of 2–3 mm. Pyrolysis of the palm fronds and activation of the resulting chars were both

Correspondence: H.M. Al-Swaidan, Department of Chemistry, King Saud University, Riyadh 11451, P.O. Box 2455, Saudi Arabia.
E-mail: hswaidan@ksu.edu.sa
Paper received: 16 September, 2014
Paper accepted: 13 February, 2015

carried out in a horizontal stainless-steel tube alloy reactor Alloy 330 (UNS N08330) having ID 30mm, OD 36 mm by Sandmeyer steel company, which was placed in a Carbolyte MTF 12/38/250 tube furnace. During the pyrolysis process, about 10 g of sliced precursor was used in high alumina sample tray to prepare the chars. Grade 5 (99.999%) nitrogen gas at a flow rate of 150 ml/min was passed through the reactor right from the beginning of the pyrolysis process. The furnace temperature was increased at a rate of 10 °C/min from room temperature to 850 °C now activation gas carbon dioxide gas was introduced at a flow rate of 50 ml/min for 30 min. Inside reactor the pressure was maintained at 0.25 bar for all the samples. The prepared activated carbon was characterized by calculating surface area, pore size, pore volume, SEM and FTIR. The schematic of the process is shown below in Fig. 1 [15,24].

RESULT AND DISCUSSION

Proximate and chemical analysis of date fronds

Date palm tree fronds were used as the precursor in the present study. The proximate and chemical analysis of the precursor is given in Table 1.

Proximate analysis of date palm tree fronds was conducted as per the method given in [22]. The method was effectively applied to determine the ash contents, moisture, fixed carbon content and volatile matter in the date palm tree fronds. The properties of the precursor are given in Table 1. To calculate the moisture content in fronds, air dried 1.0 g of date palm tree fronds was loaded in a crucible and placed in an oven at 110 °C for 3 h until total dehydration was occurred. In order to measure the amount of volatile 1.0 g of air dried sample was placed in a muffle furnace at 850 °C for 7 min. The sample was weighed after cooling in the desiccator to get the volatile contents present in the starting material. For the determination of ash content about 1.0 g of starting material was placed in the muffle furnace for 3 h at 750 °C. After 3 h the crucible was placed in desiccators for cooling. The crucible was then weighed to get the ash contents present in the sample. Subtracting the calculated values for moisture, ash content and volatile matter from 100% fixed carbon content was calculated. Chemical composition of date palm tree fronds was conducted as per the method [25] and the results were shown in terms of lignin, hemicellulose and cellulose.

Thermo gravimetric Analysis (TG) of date fronds

Thermo-gravimetric (TG) experiments were carried out by a thermo-gravimetric analyzer (Netzsch STA 409) to study the pyrolysis behavior of date fronds. The dried fronds was directed to analyze in the temperature range of 25–900 °C at heating rate 10 °C/min under nitrogen with a holding time at 900 °C for 15 min. Figure 2 [24] illustrates the TG curve of raw date frond by % weight loss under N_2 atmosphere and at a heating rate of 10 °C/min.

During the first stage, *i.e.*, from 250 to 375 °C cellulose and hemi-cellulose of the fronds decomposed to (acetic acid, methanol and, wood tar) that are considered as a condensable gases and (CO, CO_2, CH_4, H_2 and H_2O) are non-condensable gas. A little loss in wt. % can easily be seen below 250 °C in Fig. 2 [24], as the

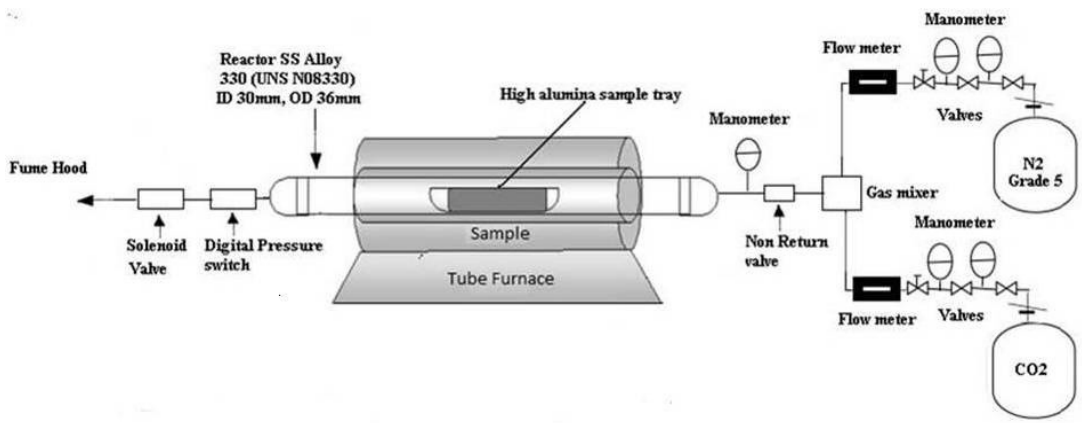

Fig. 1. Schematic of Process [24] ("Reprinted from Biomass and Bioenergy, Vol 73, M. Shoaib, H. M. Al-Swaidan, Optimization and characterization of sliced activated carbon prepared from date palm tree fronds by physical activation, 124-134, Copyright (2015), with permission from Elsevier").

Table 1. Properties of the palm tree fronds

Proximate analysis, wt.%				Chemical composition, %		
Moisture	Volatile	Fixed carbon	Ash	Cellulose	Hemicellulose	Lignin
9.1	74.6	10.3	6.0	44	29.8	26.2

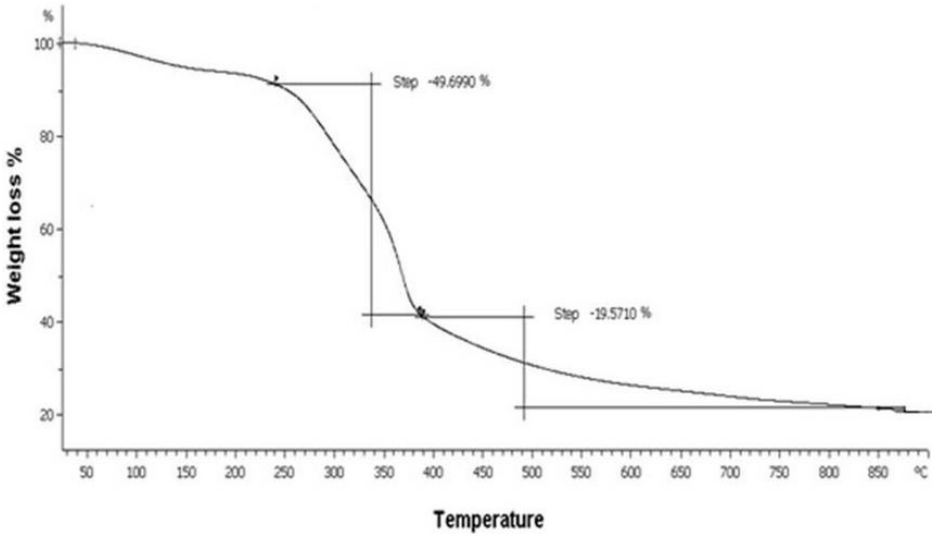

Fig. 2. Thermogravimetric Analysis (TG) of date fronds (this material is reproduced with kind permission of Elsevier) [24] ("Reprinted from Biomass and Bioenergy, Vol 73, M. Shoaib, H. M. Al-Swaidan, Optimization and characterization of sliced activated carbon prepared from date palm tree fronds by physical activation, 124-134, Copyright (2015), with permission from Elsevier").

frond had been dried under 105 °C for 8 h. Curve at temperature over 850 °C showed the weight unchanged at this stage. The carbon at this stage is acceptable as a precursor for producing activated carbon because a carbon with 10–15% volatile is not too tight, and can easily react with activating gas to produce big surface and huge pore volume. So it is apparent that date frond can be as good raw material.

BET surface area, pore size and pore volume

Specific surface areas pore size and pore volumes of the activated carbons were determined by N_2 gas adsorption at 77 K with an automated adsorption instrument (Gemini VII, 2390 Micromeritics). Prior to the determination, the sample (about 0.05 g) was degassed for 45 min at 15 °C under nitrogen to remove moisture and other volatiles from the sample. The surface areas of activated carbon produced at various activation temperatures are shown in Table 2.

Increasing temperature causes increasing release of volatiles and increasing carbon burn off due to carbon–CO_2 reaction. Hence, the yield decreases with increasing temperature. For an activation temperature of 100 °C, the yield has reached at 8.5% and it mainly contains the ash whereas at 850 °C 18.75% yield was obtained with high surface area and pore volume as shown in Table 2. Increasing the activation temperature enhances the existing pores and forms new pores from 700 to 850 °C by continual devolatilization of the chars and carbon burn off due to the carbon–CO_2 reaction, resulting in increasing BET surface area, pore volume, and non-pore volume. A decreasing trend from 900 °C and above was also observed and this is maybe because of the accumulation of carbon in the pores. The pore size may have started increasing and pore fusions might occur, causing decrease in surface area. The highest surface area 1094 $m^2\ g^{-1}$ for AC prepared at 850 °C was obtained.

Fourier transform Infrared spectroscopy (FTIR)

FTIR spectra give details about different functional group information of the materials. Figure 3 illustrates

Table 2. Activation temperature effect on surface area, pore volume, pore size and yield %age of activated carbon; : a-b-c-d-e-f denotes sliced activated carbon: activation temperature (°C), heating ramp rate (°C/min), activation dwell time (min), CO_2 flow rate (ml), reaction vessel pressure (bar)

Sample No.	Sample name	Surface area, m^2/g	Pore volume, cm^3/g	Pore size, Å	Yield, %
1	Raw date frond	2	–	–	–
2	SAC^a-700^b-10^c-30^d-50^e-0.25^f	385	0.1663	17.27	28.42
3	SAC^a-750^b-10^c-30^d-50^e-0.25^f	587	0.2562	17.44	24.65
4	SAC^a-800^b-10^c-30^d-50^e-0.25^f	633	0.2716	17.14	20.62
5	SAC^a-850^b-10^c-30^d-50^e-0.25^f	1094	0.4382	16.09	18.75
6	SAC^a-900^b-10^c-30^d-50^e-0.25^f	727	0.3063	16.83	16.0
7	SAC^a-950^b-10^c-30^d-50^e-0.25^f	515	0.2270	17.38	14.3
8	SAC^a-1000^b-10^c-30^d-50^e-0.25^f	ND	ND	ND	8.5 mainly ash

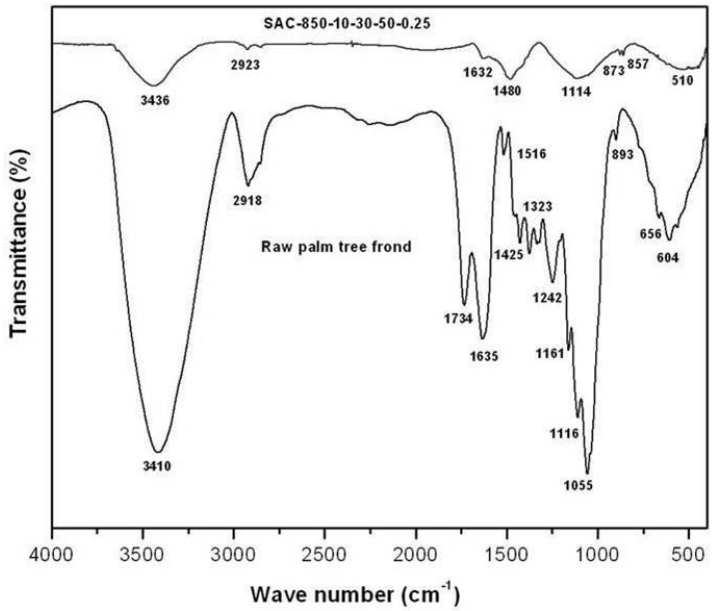

Fig. 3. FTIR spectra for date palm tree frond and SAC-850-10-30-50-0.25 [24] ("Reprinted from Biomass and Bioenergy, Vol 73, M. Shoaib, H.M. Al-Swaidan, Optimization and characterization of sliced activated carbon prepared from date palm tree fronds by physical activation, 124-134, Copyright (2015), with permission from Elsevier").

the FTIR spectra of Raw Date Frond, SAC-850-10-30-50--0.25. Strong absorption band between 3600–3400 cm^{-1} can be seen in all the spectra's shown in Fig. 3 [24], which is the characteristic of OH group and the broadening of the band is due to the high degree of hydrogen bonding. The Raw date frond in Fig. 3 shows the most crowded spectrum. A strong and broad adsorption peak appeared at 3386.23 cm^{-1}, which is due to the stretching of O–H group in the raw date frond sample. Peak observed at 2923.75 cm^{-1} belongs to the alkane C–H stretching. The peak at 1733.44 cm^{-1} is a C=O stretching and a C=C peak also observed around 1618.30 cm^{-1}. The peak at 1425.46–1375.25 corresponds to C–H bends and rock in alkane, respectively. Absorption peaks at 1330.98, 1160.53, 1243.99 and 1055.98 cm^{-1} which is the characteristic of C–O group can also be observed. The spectrum for SAC-850-10-30--50-0.25, in Fig. 3 shows reduction in absorption peaks because most of the groups are reduced at 850 °C.

Scanning electron microscopy (SEM)

SEM analysis was carried out by using Jeol JSM-6380 LA instrument. Figure 4a shows the scanning electron micrographs for the raw date fronds. The image clearly shows the surface is curvy due to cellulose, hemicelluloses and lignin and with less slit like fractures or cracks. Mesoporosity can be seen in Fig.4b. Microporous and mesoporous combination can easily be interpreted in Fig. 4c and small pores, transitional pores, and slit like pores with different shapes could also be clearly identified in Fig. 4d. SEM images account for the higher BET surface area and pore volume.

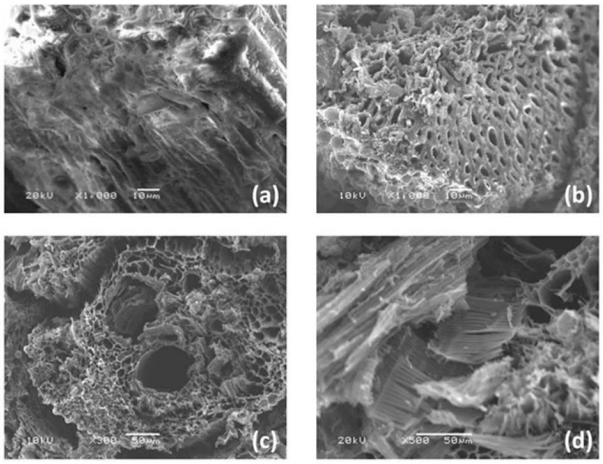

Fig. 4. SEM micrographs showing the surface morphologies of: a) raw date frond, b) mesopores, c) micropores and mesopores and d) slit like pores for SACa-850b-10c-30d-50e-0.25f [24] ("Reprinted from Biomass and Bioenergy, Vol 73, M. Shoaib, H. M. Al-Swaidan, Optimization and characterization of sliced activated carbon prepared from date palm tree fronds by physical activation, 124-134, Copyright (2015), with permission from Elsevier").

Nitrogen adsorption isotherm

The N_2 adsorption isotherms of the selected five activated carbons are presented in Fig. 5. Here the quantity of N_2 adsorbed is plotted against the relative pressure p/p^0 of N_2. It can be seen that the N_2 adsorption isotherm of Sample SAC-850-10-30-50-0.25 shows the maximum adsorption, which indicates predominantly the presence of micro porosity with minor

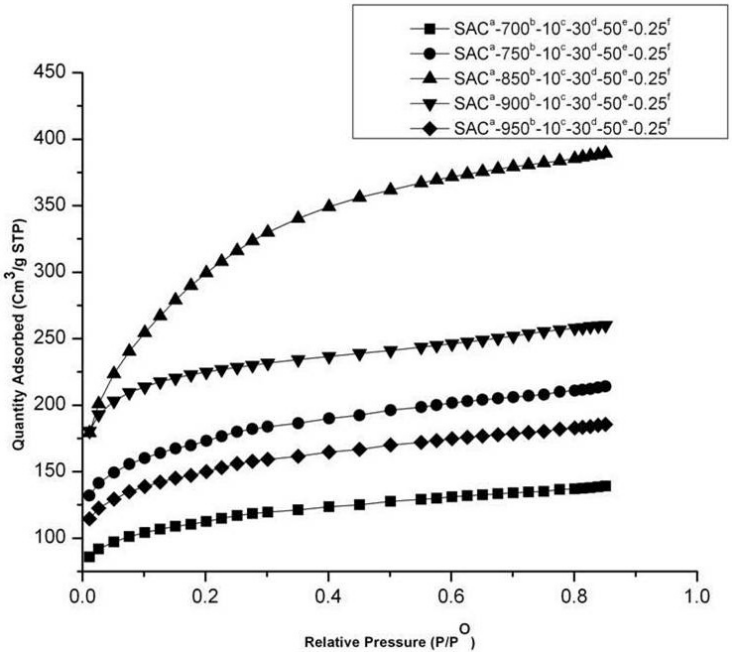

Fig. 5. Adsorption Isotherm for synthesized activated carbon [24] ("Reprinted from Biomass and Bioenergy, Vol 73, M. Shoaib, H. M. Al-Swaidan, Optimization and characterization of sliced activated carbon prepared from date palm tree fronds by physical activation, 124-134, Copyright (2015), with permission from Elsevier").

presence of mesoporosity in the activated carbon. This result is similar to as observed in SEM studies.

Nitrogen adsorption-desorption isotherm

Figure 6 shows the nitrogen adsorption-desorption isotherm at 77 K of the activated carbon prepared from 700 to 950 °C. The effects of temperatures provided different performances of the nitrogen isotherms. All the nitrogen isotherm curves significantly increase in the low-relative pressure (p/p^0 < 0.2) indicating the presence of pore structures with the Type I isotherm indicates the presence of mono layers. However, at higher relative pressure (p/p^0 > 0.2), the knee of nitrogen isotherm curves became more open and steadily

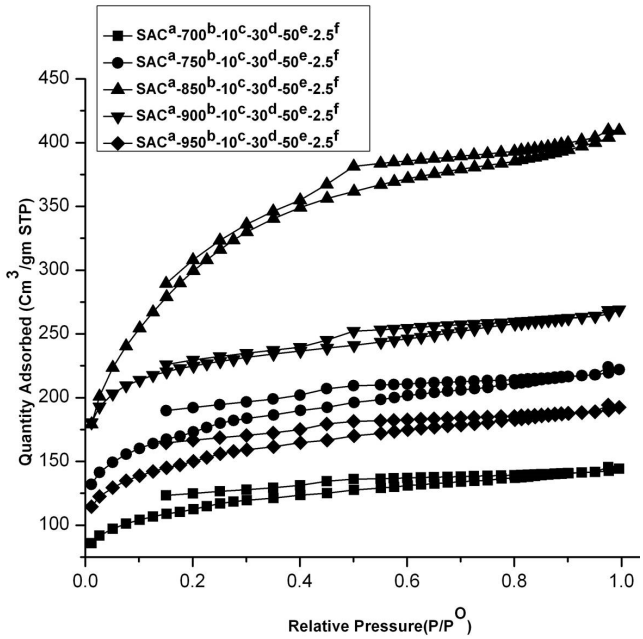

Fig. 6. Nitrogen adsorption desorption isotherm of activated carbon synthesized at various temperatures [24] ("Reprinted from Biomass and Bioenergy, Vol 73, M. Shoaib, H. M. Al-Swaidan, Optimization and characterization of sliced activated carbon prepared from date palm tree fronds by physical activation, 124-134, Copyright (2015), with permission from Elsevier").

increased to the maximum relative pressure (p/p^0 ≈ ≈ 0.9). These results suggested that large amount of nitrogen was adsorbed during the adsorption process indicating the presence of wider porosity (mesopores) with the Type IV isotherm. The entire relative pressure ranges suggested that the nitrogen adsorption exhibited a combination of the Type I and IV isotherms, indicating the presence of micro and mesoporosity in the activated carbon. Additionally, the presence of hysteresis loops with H4 type in the desorption isotherms closure at p/p^0 ≈ 0.4 indicates presence of small mesopores. This hysteresis was associated with capillary condensation in micro and mesopores. This phenomenon shows that the activated carbon production may have a combination of micro and mesopores. The lower curves being an significance of microporosity [26], whereas the upper curves look like a Types H4 that also verifies the presence of slit-shaped pores as shown in SEM images.

CONCLUSION

The optimum activation temperature conditions for the synthesis of activated carbon from date palm tree fronds using the physical activation were a temperature of 850 °C. The above conditions verified that the activation has occurred, BET surface area of 1094 m^2/g has been achieved moreover the synthesized activated carbon has predominantly microporous. SEM images verified the presence of porosities and pore development during the pyrolysis and activation process. Thus, it is feasible to produce high-quality porous activated carbon from date frond agro waste using N_2 carbonization followed by physical activation with CO_2 and N_2 mixture.

Acknowledgements

This research was supported by King Saud University, Deanship of Scientific Research, College of Science Research Center.

REFERENCES

[1] D. Savova, E. Apak, E. Ekinci, F. Yardim, N. Petrova, T. Budinova, Biomass conversion to carbon adsorbents and gas, Biomass Bioenergy **21** (2001) 133–142.

[2] M. Lanzetta, C. di Blasi, Pyrolysis kinetics of wheat and corn straw, J. Anal. Appl. Pyrolysis **44** (1998) 181–192.

[3] M. Ahmedna, W.E. Marshall, R. M. Rao, Production of granular activated carbons from select agricultural by-products and evaluation of their physical, chemical and adsorption properties, Bioresour. Technol. **71** (2000) 113–123.

[4] A. Aygun, S. Yenisoy-Karakas, I. Duman, Production of granular activated carbon from fruit stones and nutshells and evaluation of their physical, chemical, and adsorptionproperties. Micropor. Mesopor. Mater. **66** (2003) 189–195.

[5] E. Cetin, B. Moghtaderi, R. Gupta, T.F Wall, Influence of pyrolysis conditions on the structure and gasification reactivity of biomass chars, Fuel **83** (2004) 2139–2150.

[6] A. Marcilla, S. García-García, M. Asensio, J.A. Conesa, Influence of thermal treatment regime on the density and reactivity of activated carbons from almond shells, Carbon **38** (2000) 429–440.

[7] V. Minkova, S.P. Marinov, R. Zanzi, E. Bjornbom, T. Budinova, M. Stefanova, Thermochemical treatment of biomass in a flow of steam or in a mixture of steam and carbon dioxide, Fuel Process. Technol. **62** (2000) 45–52.

[8] M. Shoaib, H.M. Al-Swaidan, Synthesis of Activated Carbon from Saudi Date Tree. Fronds by Gaseous Mixture (N2 and CO2), J. Chem. Soc. Pak. **36** (2014) 771–774.

[9] S. Balcı, T. Doğu, H. Yücel, J. Chem. Technol. Biotechnol. **60** (1994) 419–426.

[10] J. Laine, S. Yunes, Effect of the preparation method on the pore size distribution of activated carbon from coconut shell, Carbon **30** (1992) 601–604.

[11] Z. Hu, E.F. Vansant, Chemical activation of elutrilithe producing carbon-aluminosilicate composite adsorbent, Carbon **33** (1995) 561–567.

[12] F. Rodriguez-Reinoso, J. M. Martin-Martinaz, M. Molina-Sabio, I. Petez-Lledo, C. Prado-Burguete, Rodriguez-Reinoso, Carbon **23** (1985) 19–24.

[13] K. Gergova, N. Petrov, S. Eser, Adsorption properties and microstructure of activated carbons produced from agricultural by-products by steam pyrolysis, Carbon **32** (1994) 693–702.

[14] J. Rodriguez-Mirasol, T. Cordero, J.J. Rodriguez, High-temperature carbons from kraft lignin, Carbon **31** (1993) 87–95.

[15] M. Shoaib, H.M. Al-Swaidan, Ramp Rate Influence on Synthesis of Sliced Porous Activated Carbon from Date Palm Tree by Physical Activation Method, Asian J. Chem. **26** (2014) 5295–5297.

[16] A. Ahmadpour, D.D. Do, Ahmadpour, The preparation of active carbons from coal by chemical and physical activation, Carbon **34** (1996) 471–479.

[17] T. Kazimierz, S. Teresa, C. Franciszek, J. Anna, Formation of porous structures in activated brown-coal chars using O_2, CO_2 and H_2O as activating agents, Fuel **56** (1977) 121–124.

[18] H. Haykiri-Acma, S. Yaman, S. Kucukbayrak, Gasification of biomass chars in steam–nitrogen mixture, Energy Convers. Manage. **47** (2006) 1004–1013.

[19] V. Fierro, V. Torné-Fernández, A. Celzard, Highly microporous carbons prepared by activation of kraft lignin with KOH, Stud. Surf. Sci. Catal. **160** (2006) 607-614.

[20] J. Yang, Z.M. Shen, Z.B. Hao, Preparation of highly microporous and mesoporous carbon from the mesophase pitch and its carbon foams with KOH, Carbon **42** (2004) 1872–1875.

[21] A.E. Putun, N. Ozbay, E.P. Onal, E. Putun, Fixed-bed pyrolysis of cotton stalk for liquid and solid products, Fuel Process. Technol. **86** (2005) 1207–1219.

[22] M. Fan, W. Marshall, D. Daugaard, R.C. Brown, Steam activation of chars produced from oat hulls and corn stover, Bioresour. Technol. **93** (2004) 103–107.

[23] W.T. Tsai, C.Y. Chang, S.L. Lee, Preparation and characterization of activated carbons from corn cob, Carbon **35** (1997) 1198–2000.

[24] M. Shoaib, H.M. Al-Swaidan, Optimization and characterization of sliced activated carbon prepared from date palm tree fronds by physical activation, Biomass Bioenergy **73** (2015) 124–134.

[25] H. Ammar, M. Abid, S. Abid, Cellulose fibers obtained by organosolv process from date palm rachis (*Phoenix dactylifera* L.), IOP Conf. Series Mater. Sci. Eng. **28** (2012) 012002.

[26] C.F. Chiung, C.Y. Chang, W.T. Tsai, Effects of burn-off and activation temperature on preparation of activated carbon from corn cob agrowaste by CO(2) and steam, J. Colloid Interface Sci. **232** (2000) 45–49.

IZVOD

OPTIMIZACIJA TEMPERATURE AKTIVACIJE ZA PRIPREMU POROZNOG UGLJENIKA DOBIJENOG IZ LISTOVA URME FIZIČKOM AKTIVACIJOM

Muhammad Shoaib, Hassan M. Al-Swaidan

Department of Chemistry, College of Science, King Saud University, P.O. Box 2455, Riyadh 11451, Kingdom of Saudi Arabia

(Stručni rad)

Saudijska Arabija je vodeći proizvođač urmi u svetu. U cilju postizanja maksimalne proizvodnje koristeći drvo urme, postoji potreba da se drveće seče na godišnjem nivou, što se smatra ozbiljnom pretnjom za životnu sredinu. U radu je prikazan jednostavan postupak (u jednom koraku) za sintezu poroznog aktivnog uglja (AC) iz urminog drveta iz Saudijske Arabije, korišćenjem smeše gasova (N_2 i CO_2). Postupak je izveden na različitim temperaturama karbonizacije/aktivacije od 700 to 1000 °C pri brzini od od 10 °C/min. Horizontalni reaktor tipa Alloy 330 je korišćen u cevnoj peći. Protok gasova N_2 i CO_2 je bio 150 i 50 ml/min, redom. Rezultati pokazuju da je za 850 °C dobijena veća površina, i ovi uslovi mogu ponuditi veće mogućnosti za proizvodnju aktivnog uglja sa većim adsopcionim kapacitetom iz otpada od lišća urme. Površina aktivnog uglja, određena BET analizom, dobijenog na 850 °C posle vremena aktivacije od 30 min je iznosila 1094 m^2/g.

Ključne reči: Aktivni ugalj • Fizička aktivacija • Mešavina gasova • Urme iz Saudijske Arabije • Agro otpad

Determination of di(2-ethylhexyl) phthalate in plastic medical devices

Ivana S. Kostić[1], Tatjana D. Anđelković[1], Darko H. Anđelković[1], Tatjana P. Cvetković[2], Dušica D. Pavlović[2]

[1]*University of Niš, Faculty of Sciences and Mathematics, Niš, Serbia*
[2]*University of Niš, Faculty of Medicine, Niš, Serbia*

Abstract

The presence of DEHP in dialysis and infusion sets for peritoneal dialysis and parenteral nutrition, which are made of PVC and other plastic polymeric materials, were investigated. Phthalate determination was carried out by gas chromatography–mass spectrometry method (GC–MS). The results showed that the peritoneal dialysis set (bag and tubing) made of PVC contains DEHP in significant amount, about 31–34%. Solution for peritoneal dialysis which was stored in the investigated PVC bag, contains low amount of DEHP, about 3.72 μg dm^{-3}. Infusion bottles which are made of LDPE, also contain DEHP but in lower amount than PVC bags. LDPE bottle for packaging physiological saline solution (0.9% NaCl) showed higher amount of DEHP than LDPE bottle for packaging Ringer's solution. In contrast, solution stored in bottle with lower DEHP level, *i.e.*, Ringer's solution, contained about three times higher concentration of DEHP than physiological saline solution stored in bottle with higher DEHP level. Concentrations of DEHP in Ringer's solution and physiological saline solution are 17.30 and 5.83 μg dm^{-3}, respectively. The obtained values are under estimated upper-bound dose of DEHP received by adult patients undergoing procedures of peritoneal dialysis and parenteral nutrition.

Keywords: phthalate, plastic material, medical devices, infusion set, peritoneal dialysis set.

Available online at the Journal website: http://www.ache.org.rs/HI/

SCIENTIFIC PAPER

UDC 547.584:678.743:543:615.47

Hem. Ind. **70** (2) 159–164 (2016)

doi: 10.2298/HEMIND141129023K

Phthalates, as diesteres of orto-phthalic acid, are organic lipophilic compounds, which are used as plasticizers. Phthalates are used as plasticizers to increase the softness and flexibility of plastics, notably PVC. But, they are not chemically bound in plastic materials and they can be leached into the environment [1–3]. About one million tonnes of phthalates are produced in Europe per year, and the most dominant phthalates are di-(2-ethylhexyl) phthalate (DEHP), diisodecyl phthalate (DiDP) and diisononyl phthalate (DiNP). In PVC materials, DEHP is the most used plasticizer [4,5].

Humans are exposed to phthalates in numerous ways, by dermal resorption, foodstuff or by inhaling air which contains phthalates. These compounds are present in a wide variety of products, which are often used by people, such as cosmetics, personal care products, food packaging, children toys, water bottles, rainwear, tablecloths, upholstery, etc. [6–10].

PVC medical devices contain on average 20–40% DEHP by weight. A lot of medical devices are made from PVC, such as intravenous bags and tubing, infusion tubing, blood bags, catheters, oxygen masks, peritoneal dialysis bags and tubing, enteral nutrition feeding bags, etc. [10,11]. Medical devices which contain phthalates may be important sources in susceptible subpopulations, including neonatal infants who are undergoing surgical interventions, but also to other hospital patients who receive nutritional supplements intravenously [13]. Phthalates are lipophilic compounds, and can be found in fats due to bioaccumulation process. The tolerable daily intake (*TDI*) values established by the European Food Safety Authority panel (2013) for benzyl butil phthalate (BBP), DEHP and dibutil phthalate (DBP) are 500, 50 and 10 μg/kg of bw per day, respectively [2]. Study of these types of chemical substances has increased in recent years because some of these compounds, such as DBP, BBP and DEHP, are suspected as endocrine disruptors and carcinogenic to humans. There is great concern about the toxicity of DEHP, especially for risk groups. Some of studied effects are mutagenic activity, carcinogenicity, peroxisome proliferation, infertility, etc [9].

DEHP is not chemically bound to the polymer and it can migrate when the medical device comes into contact with certain media such as blood, drugs, saline or water. Also, DEHP can be released when the device is heated. Due to these facts, the major factors determining the degree to which DEHP leaches from medical devices are temperature and storage time. Patients who are undergoing medical procedures, such as blood transfusions and haemodialysis potentially can be exposed to DEHP. When DEHP enters the human body, it is metabolized into various substances that are more readily excreted. The most important metabolite is mono-ethylhexyl phthalate (MEHP). Because conversion of DEHP to MEHP occurs primarily in the intestinal tract, exposures to DEHP by ingestion may be more

Correspondence: I. Kostić, Faculty of Sciences and Mathematics, Višegradska 33, 18000 Niš, Serbia.
E-mail: ivana.kostic83@gmail.com
Paper received: 29 November, 2014
Paper accepted: 16 March, 2015

hazardous than by intravenous exposure, because this path bypasses the intestinal tract. Some studies showed that DEHP can cause liver cancer in laboratory animals. It can be caused through the induction of peroxisome proliferation, which leads to oxidative stress and the generation of electrophilic free radicals, and then indirectly causing damage to DNA damage [14–16].

Phthalates can be detected using different methods, such as mass spectrometry (MS) [17,18], electron capture detection (ECD) [19], and flame ionization detection (FID) [20]. The analysis of phthalates is mostly performed by gas chromatography (GC) and this method presents better sensitivity than HPLC methods. Also, there are different preconcentration methods, such as solid-phase extraction (SPE), solid-phase microextraction (SPME), headspace solid-phase microextraction (HS-SPME), liquid-phase microextraction (LPME) and dispersive liquid-liquid microextraction (DLLME) [22–24]. The most conventional liquid-liquid extraction methods (LLE) performed with hexane, dichloromethane, ethyl acetate or acetone have recovery values in the range between 70 and 100% and is relatively short and easily performed. Because of that, LLE method for extraction and GC for the separation and analysis seem to be the best choices for extraction and detection of phthalates [25] .

Due to the fact that these compounds are present in the environment, the major problem in phthalate determination is the sample contamination during the analysis. This problem can be reduced or even avoided by reduction of number of sample preparation steps [26,27].

The aim of this work was DEHP determination in medical devices, such as dialysis set (bags and tubing) and infusion set (bottles and tubing) which is made of polyvinyl chloride (PVC) and low density polyethylene (LDPE). In this study, we compared PVC and LDPE plastic medical equipment in their capability of leaching DEHP into solutions. DEHP was determined in solutions Dianeal Low Calcium Peritoneal Dialysis Solution (contains 1.5% dextrose and 2.5 meq Ca L^{-1}), physiological saline solution (0.9% NaCl) and Ringer's solution which were stored in the investigated bags and bottles for three years and in the PVC and LDPE plastic medical equipmen by liquid extraction and GC–MS analysis. Based on the obtained results, the migration of phthalates from packaging to the stored infusion/dialysis solutions can be defined.

EXPERIMENTAL

Chemical reagents and instrumentation

High-purity DEHP was purchased from Sigma Aldrich (St. Louis, MO, USA). Dibutil adipate (DBA), which was used as internal standard, was purchased from Fluka (Buchs, Swizerland). HPLC grade *n*-hexane was purchased from Sigma Aldrich.

Preparation of stock and working solutions

Special care was taken to avoid the contamination of sample due to contact of reagents and solvents with plastic laboratory materials during sample preparation. All glassware was washed with hot water and soap, rinsed with ultrapure deionized water and subsequently thoroughly rinsed with dichlormethane. Glassware was then sealed with aluminum foil and stored in a clean environment to avoid adsorption of phthalates from the air. Usage of plastic consumables during the analysis is avoided whenever possible. No laboratory gloves were used during sample preparation and analysis.

All stock and working solutions were prepared in hexane. Individual stock solutions of DEHP and DBA were initially prepared at a concentration of 1 mg cm^{-3}. The stock standard was diluted stepwise with n-hexane to prepare at least 5 concentration levels of intermediate and working standards. Intermediate solutions were prepared by dilution of stock solution, and concentrations of intermediate solutions were 100 and 10 μg cm^{-3}. Working solutions were prepared by dilution of intermediate solutions and by adding DBA at concentration 1 μg cm^{-3}. All solutions were stored at 4 °C.

Sample preparation

Plastic medical devices, which are used for various techniques in medicine, were collected from the local hospital. Samples consisted of filled plastic dialysis bags and tubing from dialysis set (Baxter), infusion bottles (Hemofarm and Zdravlje) and tubing from infusion set (Mediset). Plastic materials were cut into pieces with area of about 1 cm^2. All samples were extracted for 3, 6, 15 and 30 days with 5 ml of *n*-hexane in glass vials.

Individual solutions which are usually present in formulations for peritoneal dialysis and parenteral nutrition were stored in PVC bags and LDPE bottles at room temperature. The analyzed samples were: solution for peritoneal dialysis (1.5% dextrose), physiological saline solution (0.9% NaCl) and Ringer's solution (NaCl, KCl and $CaCl_2$) for parenteral nutrition. Liquid samples were collected in glass flasks and stored at 4 °C until analysis. Since the usual shelf-life of infusion solutions is three years, migration rates of DEHP from plastic containers were measured after a period of 36 months in order to determine the maximum possible leached concentration of DEHP before expiration period of the medical product. The extraction procedure was carried out with 5 cm^3 of hexane for extraction of 500 cm^3 sample. To 500 cm^3 of each sample, 5 cm^3 of hexane was added and mixed 60 min and 24 h. The organic layers were transferred to glass vials, inter-

nal standard was added and aliquots were injected into GC–MS directly with no clean up stage.

GC–MS technique

Determination of phthalates was performed by Hewlett Packard 6890 gas chromatograph equipped with an Agilent 5973 mass selective detector and a DB-5 MS capillary column (30 m×250 mm×0.25 mm, Agilent, USA) for chromatographic separation. The oven is programmed from 60 (1 min) to 220 °C (1 min) at rate of 20 °C min^{-1} and after to 280 °C (4 min) at rate of 5 °C min^{-1}. The gas chromatograph was operated in splitless injection mode. The operating temperature of the MSD was 280 °C with the electronic impact at 70 eV. The MSD was used in the ion-monitoring (SIM) mode at *m*/*z* 149. The identification of target compounds was based on the relative retention time, the presence of target ions and their relative abundance. The quantification ion is *m*/*z* 149 for DEHP. The dwell time was 100 ms.

RESULTS AND DISCUSSION

The chromatogram in Figure 1 shows that the separation of DEHP and DBA, as internal standard, occurred within a running time of 20 min. Retention times for DBA and DEHP were 9.945 and 18.266 min, respectively.

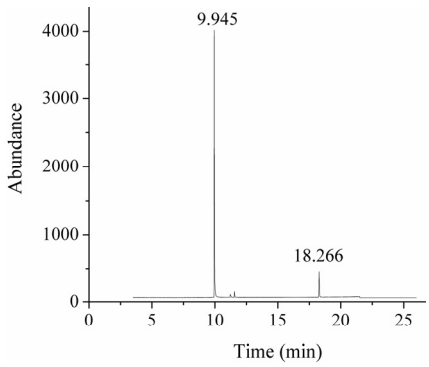

Figure 1. Chromatogram of a standard solution containing DEHP in concentration 0.25 µg cm^{-3} and DBA in concentration 1 µg cm^{-3}.

The analytical curve obtained for DEHP in concentration range 0.25–2.5 µg cm^{-3} is linear for the given range with coefficient of determination, R^2, of 0.9970 and linear equation y = -34868.945 + 170366.584x (Figure 2). Values of standard deviation for both coefficients, intercept and slope, were 1224.711 and 3329.021, respectively. *P*-value for obtained coefficient of determination was $P < 0.0001$.

The hexane extraction of solid samples has been applied for determination of DEHP due to high extraction efficiency for phthalates. The yield of extraction showed that more than 90% of the phthalates in solid samples are extracted in the first 15 days. Presented results are obtained after the extraction procedure which was carried out with the time period of 30 days.

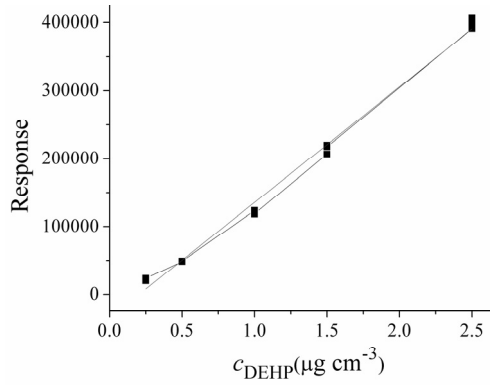

Figure 2. Analytical curve for DEHP for concentration range 0.25–2.5 µg cm^{-3}.

Table 1 presents the amount of plasticizers in the investigated set for peritoneal dialysis. DEHP was found in extracts from the bag and the tubing.

The determined DEHP concentration levels of 33––38% by weight of bag and tubing from peritoneal dialysis set are high but expected, bearing in mind the type of plastic material used for medical device production. The DEHP concentration levels in tubing were higher than DEHP concentration levels in dialysis bag, which is also expected due to more flexibile and soft performances of the tubing material.

Table 2 presents the amount of DEHP extracted from investigated LDPE solid materials. DEHP was found in the obtained extracts from the samples, although in low amounts.

Infusion bottle of physiological saline solution shows the higher concentration of DEHP than infusion bottle of Ringer's solution. But in both cases, about 90% of amount was extracted after 6 days. Despite of

Table 1. Concentration of DEHP in the packaging material (mg g^{-1}) from plastic medical devices (PVC) used for peritoneal dialysis determined for different extraction times (3, 6, 15 and 30 days); SD – standard deviation (n = 3); a–c: values with the same letter within a row are not statistically significant different at the p < 0.05 level (Tukey's HSD test)

Sample	Extraction time, days			
	3	6	15	30
Dialysis bag	23.02±1.24[a]	25.82±1.05[a]	301.00±23.58[b]	324.98±14.17[c]
Tubing from dialysis set	162.63±11.38[a]	319.13±28.37[b]	325.33±8.10[b]	351.18±28.74[b]

Table 2. Concentration of DEHP in the packaging material (mg g^{-1}) from plastic medical devices (LDPE) used for parenteral nutrition determined for different extraction times (3, 6, 15 and 30 days) SD – standard deviation (n = 3); a–c: values with the same letter within a row are not statistically significant different at the p < 0.05 level (Tukey's HSD test)

Sample	Extraction time, days			
	3	6	15	30
Infusion bottle (physiological saline solution)	0.0608±0.0087[a]	0.0706±0.0238[b]	0.0729±0.0013[b]	0.0748±0.0019[b]
Infusion bottle (Ringer's solution)	0.0104±0.0016[a]	0.0277±0.0015[b]	0.0453±0.0033[c]	0.0481±0.0053[c]
Tubing from infusion set	106.05±3.89[a]	112.51±8.79[a]	321.25±3.15[b]	394.49±3.47[c]

that, extraction procedure was carried out for 30 days, due to maximum possible leaching amount determination. Tubing materials show much higher amount of DEHP by weight of sample.

Even though, the investigated plastic LDPE material commonly does not possess plasticizers, the DEHP was found in the infusion bottles and also in the physiological saline solution and Ringer's solution which were stored in the infusion bottles. The contamination of these solutions is higher which is not expected due to low level of phthalate in packaging. This can indicate that the contamination is probably not only from the bottles where they are stored but from the tubing material that are used in their industrial preparation.

The results obtained by liquid–liquid extraction of DEHP from peritoneal dialysis solution and solutions for parenteral nutrition are given in Table 3. Very low amounts were leached by Peritoneal Dialysis Solution from PVC dialysis bag, despite the fact that dialysis bag contains DEHP in high concentration level. Concentration of DEHP in Ringer's solutions is higher than concentration in peritoneal dialysis solution and physiological saline solution. While bottle of physiological saline solution shows higher percentage DEHP than bottle of Ringer's solution, liquid sample from the same bottle shows lower concentration of DEHP.

Table 3. DEHP concentrations (μg dm^{-3}) in peritoneal dialysis solution, physiological saline solution and Ringer's solution stored in PVC bags and LDPE infusion bottles for different extraction times (60 min and 24 h); SD – standard deviation (n = 3); a, b: values with the same letter within a row are not statistically significant different at the p < 0.05 level (Tukey's HSD test)

Sample	Extraction time	
	60 min	24 h
Dialysis solution	3.58±0.29[a]	3.72±0.21[a]
Physiological saline solution	5.83±0.55[a]	8.83±0.19[b]
Ringer's solution	17.30±0.25[a]	21.16±2.51[b]

Difference between values of DEHP concentrations obtained for different extraction times were compared to a critical value in order to see if the difference is significant. The post-hoc test, Tukey's test, was performed and the test compares the difference between each pair of mean values with appropriate adjustment for the multiple testing. The critical value of q was obtained from table values, and it is the point when a mean difference becomes honestly significantly different. Critical values for solid and liquid samples are 3.96 and 3.46, respectively [28]. Values of HSD (honest significant difference) for each pair were computed by Origin© program. Comparing was performed in case $p < 0.05$.

Results obtained after performing Tukey's post-hoc test shows that there is no significant difference between result obtained for 3 days extraction period and 6 day extraction period for dialysis bag, while for tubing from dialysis set, obtained results show that there are significant differences only between results obtained for 3 day extraction period and other extraction periods (6, 15 and 30 days). The same results as for tubing dialysis set were obtained in testing solid samples of infusion bottles with physiological saline solution, while in the case of infusion bottles with Ringer's solution, there is significant difference, except for the extraction period between 15 days and 30 days. Results obtained in testing solid samples of tubing from infusion set show that there is significant difference, except for extraction period between 6 days and 3 days.

Results obtained in testing of liquid samples show that there is significant difference between obtained mean values for 60 min and 24 h extraction period for liquid samples of solutions for parenteral nutrition, while there is no significant difference between obtained mean values for 60 min and 24 h extraction period for liquid samples of dialysis solution.

On average, patient under peritoneal dialysis procedure receives about 8 dm^3 of peritoneal dialysis solution a day and it means that human body receives about 30 μg DEHP in total. This value is under estimated upper-bound dose of DEHP received by adult patients undergoing procedures of peritoneal dialysis 0.01 mg/kg per day (for adult with average body weight 70 kg). Furthermore, a considerable amount of the infused DEHP will be returned upon drainage of the perfusate from the peritoneum. Also, levels of DEHP which were detected in physiological saline solutions and Ringer's solutions are under estimated upper-bound dose of DEHP for these kinds of medical pro-

ducts, 0.005 mg/kg per day (for adult with average body weight 70 kg) [29].

CONCLUSION

A migration of DEHP from set for peritoneal dialysis that are made from PVC into dialysis solution and set for infusion parenteral nutrition that were made from LDPE into infusion solutions has been investigated. Concentrations of DEHP which are determined in peritoneal dialysis solution were about 3.72 µg dm^{-3}. Even though the determined concentrations in the dialysis set are higher than expected, the leached amount of DEHP in the dialysis solution is not significant. Although in low amounts, LDPE bags also showed DEHP in their composition. DEHP leached from PVC into solution is much higher than leached from LDPE bottles. The obtained values are under estimated upper-bound dose of DEHP received by adult patients undergoing procedures of peritoneal dialysis and parenteral nutrition.

The proposed sample preparation and sample extraction methods can be applied for the determination of these compounds in solid samples of different bottles used as medical devices and solutions stored in these bottles and bags. The presence of these compounds in the solid samples can be attributed to the different compositions of the plastic containers.

Control of material which is used for production of the plastic medical devices is essential to avoid human exposure to phthalates.

Acknowledgement

This study was supported by the Ministry of Education, Science and Technological Development of the Republic of Serbia and was performed as a part of Project III 41018.

REFERENCES

[1] T. Fierens, K. Servaes, M. Van Holerbeke, L. Geerts, S. De Henauw, I. Sioen, G. Vanermen, Analysis of phthalates in food products and packaging materials sold on the Belgian market, Food Chem. Toxicol. **50** (2012) 2575–2583.

[2] S. Keresztes, E. Tatar, Zsuzsanna Czegeny, G. Zaray, V.G. Mihucz, Study on the leaching of phthalates from polyethylene terephthalate bottles into mineral water, Sci. total Environ. **458-460** (2013) 451–458.

[3] S. Pradeep, S. Benjamin, Mycelial fungi completely remediate di(2-ethylhexyl)phthalate, the hazardous plasticizer in PVC blood storage bag, J. Hazard. Mater. **235–236** (2012) 69–77.

[4] D. Zhang, H. Lui, Y. Liang, C. Wang, H. Liang, H. Cai, Distribution of phthalate esters in the groundwater of Jianghan plain, Hubei, China, Earth Sci. China **3** (2009) 73–79.

[5] H.M. Koch, B. Rossbach, H. Drexler, J. Angerer, Internal exposure of the general population to DEHP and other phthalates – determination of secondary and primary phthalate monoester metabolites in urine, Environ. Res. **93** (2003) 177–185.

[6] P. Serôdio, J.M.F. Nogueira, Considerations on Ultra-trace Analysis of Phthalates in Drinking Water, Water Res. **40** (2006) 2572–2582.

[7] J. Bošnir, D. Puntarić, A. Galić, I. Škeš, T. Dijanić, M. Klarić, M. Grgić, M. Čurković, Z. Šmit, Migration of phthalates from plastic containers into soft drinks and mineral water, Food Technol. Biotechnol. **45** (2007) 91–95.

[8] G. Latini, Monitoring phthalate exposure in humans, Clin. Chim. Acta **361** (2005) 200.

[9] H.M. Koch, L.M. Gonzales-Reche, J. Angerer, On-line clean-up by multidimensional liquid chromatography–electrospray ionization tandem mass spectrometry for high throughput quantification of primary and secondary phthalate metabolites in human urine, J. Chromatogr., B **784** (2003) 169–182.

[10] Z. Guo, S. Wang, D. Wei, M. Wang, H. Zhang, P. Gai, J. Duan, Development and application of a method for analysis of phthalates in ham sausages by solid-phase extraction and gas chromatography-mass spectrometry, Meat Sci. **84** (2010) 484–490.

[11] H. Liu, W. Den, S. Chan, K.T. Kin, Analysis of trace contamination of phthalate esters in ultrapure water using a modified solid-phase extraction procedure and automated thermal desorption–gas chromatography/ /mass spectrometry, J. Chromatogr., A **1188** (2008) 286–294.

[12] G. Latini, M.Ferri, F. Chiellini, Materials degradation in PVC medical devices, DEHP leaching and neonatal outcomes, Curr. Med. Chem. **17** (2010) 2979–2989.

[13] H.G. Wahl, A. Hoffmann, H-U. Haring, H.M. Liebich, Identification of plasticizers in medical products by a combined direct thermodesorption-cooled injection system and gas chromatography-mass spectrometry, J. Chromatogr., A **847** (1999) 1–7.

[14] F. Gonzalez, M. Peters, R. Cattley, Mechanism of Action of the Nongenotoxic Peroxisome Proliferators: Role of the Peroxisome Proliferator-Activated Receptor α, J. Natl. Cancer I. **90** (1998) 1702–1709.

[15] Swedish National Chemicals Inspectorate, Risk Assessment for bis(2-ethylhexyl) phthalate, February 1999, EINECS-NO: 204-211-0.

[16] M.J. Silva, E. Samandar, J.L. Preau Jr., L.L. Needham, A.M. Calafat, Urinary oxidative metabolites of di(2-ethylhexyl) phthalate in humans, Toxicology **219** (2006) 22–32.

[17] K. Holadova, G. Prokupkova, J. Hajslova, J. Poustka, Headspace SPME of phthalic acid esters from vegetable oil employing solvent based matrix modification, Anal. Chim. Acta **528** (2007) 24–33.

[18] L.K. Sorensen, Determination of phthalates in milk and milk products by liquid chromatography/tandem mass spectrometry, Rapid Commun. Mass Spectrom. **20** (2006) 1135–1143.

[19] X. Li, M. Zhong, S. Xu, C. Sun, Determination of phthalates in water samples using polyaniline-based solid-phase microextraction coupled with gas chromatography, J. Chromatogr., A **1135** (2006) 101–108.

[20] B. Cavaliere, B. Macchione, G. Sindona, A. Tagarelli, Tandem mass spectrometry in food safety assessment : the determination of phthalates in olive oil, J. Chromatogr., A **1205** (2008) 137–143.

[21] D. Xu, X. Deng, E. Fang, X. Zheng, Y. Zhou, L. Lin, L. Chen, M. Wu, Z. Huang, Determination of 23 phthalic acid esters in food by liquid chromatography tandem mass spectrometry, J. Chromatogr., A **1324** (2014) 49–56.

[22] H-Y. Shen, Simultaneous screening and determination eight phthalates in plastic produscts for food use by sonication-assisted extraction/GC-MS methods, Talanta **66** (2005) 734–739.

[23] P. Liang, J. Xu, Q. Li, Application of dispersive liquid–liquid microextraction and high-performance liquid chromatography for the determination of three phthalate esters in water samples, Anal. Chim. Acta **609** (2008) 53–58.

[24] R.Y. Su, X.W. Zhao, Z.Y. Li, Q. Jia, P. Liu, J.B. Jia, Poly(methacrylic acid-co-ethylene glycol dimethacrylate) monolith microextraction coupled with high performance liquid chromatography for the determination of phthalate esters in cosmetics, Anal. Chim. Acta **676** (2010) 103–108.

[25] P. Kueseng, P. Thavarungkul, P. Kanatharana, Trace phthalate and adipate esters contaminated in packaged food, J. Environ. Sci. Heal., B **42** (2007) 569–576.

[26] A. Reid, C. Brougham, A. Fogarty, J. Roche, An investigation into possible sources of phthalate contamination in the environmental analytical laboratory, Intern. J. Environ. Anal. Chem. **87** (2007) 125–133.

[27] C. Perez, M.C. Baricela Alonso, E. Pena Vasquez, P. Herbello Hermelo, P. Barmejo Barera, Phthalates determination in physiological saline solutions by HPLC–ES--MS, Talanta **75** (2008) 1184–1189.

[28] R. Hampton, J. Havel, Introdustory biological statistics, 2nd ed., Waveland Press, Inc., Long Grove, IL, 2006.

[29] [FDA, Safety Assessment of Di(2-ethylhexyl)phthalate (DEHP) Released from PVC Medical Devices, U.S. Food and Drug Administration, 2001, pp. 10–20.

IZVOD

ODREĐIVANJE DIETILHEKSIL FTALATA U PLASTIČNOJ MEDICINSKOJ OPREMI

Ivana S. Kostić[1], Tatjana D. Anđelković[1], Darko H. Anđelković[1], Tatjana P. Cvetković[2], Dušica D. Pavlović[2]

[1]*Univerzitet u Nišu, Prirodno–matematički fakultet, Višegradska 33, 18000 Niš*
[2]*Univerzitet u Nišu, Medicinski fakultet, Bul. Zorana Đinđića 81, 18000 Niš*

(Naučni rad)

Ispitivano je prisustvo dietilheksil-ftalata (DEHP) u medicinskoj opremi napravljenoj od polivinil-hlorida (PVC) i polietilena niske gustine (LDPE) koja se koristi u procesima peritonealne dijalize i parenteralne prehrane. Određivanje ftalata je izvršeno gasnom hromatografijom sa masenom detekcijom (GC–MS). Rezultati su pokazali da set koji se koristi u procesu peritonealne dijalize (kesa sa rastvorom i cevčica) napravljen od PVC sadrži DEHP u značajnoj količini, oko 31–34%. Rastvor za peritonealnu dijalizu, koji je čuvan u ispitivanoj PVC kesi, sadrži malu količinu DEHP, oko 3,72 μg dm^{-3}. Infuzione boce koje su napravljene od polietilena niske gustine (LDPE), takođe sadrže DEHP, ali u manjoj količini u odnosu na PVC kese. LDPE boca u kojoj se nalazio fiziološki rastvor (0,9% NaCl) sadrži veću količinu DEHP od LDPE boce u kojoj se nalazio Ringerov rastvor. Nasuprot tome, rastvori koji se se nalazili u bocama sa nižim sadržajem DEHP, tj. Ringerov rastvor sadrži oko tri puta veću koncentraciju DEHP od fiziološkog rastvora (0,9% NaCl) koji se nalazio u boci sa većim sadržajem DEHP. Određene koncentracije DEHP u Ringerovom rastvoru i fiziološkom rastvoru bile su 17,30 i 5,83 μg dm^{-3}, redom. Dobijeni rezultati su ispod utvrđenih dozvoljenih doza za DEHP kojima je odrastao čovek izložen tokom peritonealne dijalize i parenteralne prehrane.

Ključne reči: Ftalati • Plastični materijali • Medicinska oprema • Infuzioni set • Set za peritonealnu dijalizu

Liquid–liquid equilibrium constant for acetic acid in an olive oil–epoxidized olive oil–acetic acid–hydrogen peroxide–water system

Milovan R. Janković, Olga M. Govedarica, Snežana V. Sinadinović-Fišer, Jelena M. Pavličević, Vesna B. Teofilović, Nevena R. Vukić

Faculty of Technology, University of Novi Sad, Novi Sad, Serbia

Abstract

The liquid–liquid equilibrium constant for acetic acid in a quinary system olive oil–epoxidized olive oil–acetic acid–hydrogen peroxide–water was experimentally determined for temperatures and component ratios relevant for *in situ* epoxidation of plant oils. The values have the constant range from 1.52 to 2.73. To predict the equilibrium constant for acetic acid, the experimental data were correlated with UNIQUAC (universal quasi chemical) and NRTL (non-random two liquid) activity coefficient models. For simplified calculation of the phase equilibrium the insolubility of olive oil and epoxidized olive oil in the water, as well as insolubility of water and hydrogen peroxide in the olive oil and epoxidized olive oil, was assumed. The root mean square deviation (*RMSD*) of the experimental and calculated values of the liquid–liquid equilibrium constant for acetic acid is 0.1910 for the UNIQUAC model and 0.1815 for the NRTL model. For rigorous flash calculation, when the partitioning of all components between the phases was assumed, the *RMSD* for the NRTL model is 0.1749.

Keywords: Liquid–liquid equilibrium, acetic acid, plant oil, epoxidation.

Available online at the Journal website: http://www.ache.org.rs/HI/

SCIENTIFIC PAPER

UDC 66.094.39:665.3:547.292:544.35

Hem. Ind. **70** (2) 165–175 (2016)

doi: 10.2298/HEMIND141210024J

Percarboxylic acid, such as performic or peracetic acid, is a common oxidizing agent in a large scale production of epoxidized plant oils. The percarboxylic acid is generated *in situ* through the acid catalyzed reaction of corresponding organic acid with hydrogen peroxide in an aqueous solution. A soluble mineral acid, usually sulfuric acid, or an acidic cation exchange resin can be used as a catalyst for this reaction [1,2]. Depending on applied catalyst, the reaction system of epoxidation is either two- (oil–water) or three-phase (oil–water–ion exchange resin) system. Thus, it is important to obtain the liquid-liquid equilibrium data for modeling and optimization of the epoxidation process. A rigorous two- or three-phase model of the epoxidation reaction system should include a partition coefficient for organic acid [3–6]. The coefficient is dependent on a liquid–liquid equilibrium constant for organic acid and molar densities of the phases [7–9]. A few authors investigated partitioning of formic acid or acetic acid between the oil and water phases of the epoxidation reaction system. Rangarajan *et al*. determined experimentally the partition coefficient for acetic acid in a soybean oil-acetic acid-water system at 313 and 333 K [3]. On the basis of experimental data for the liquid-liquid equilibrium constant for acetic acid, Sinadinović-Fišer and Janković calculated the partition coefficient for acetic acid in the soybean oil–acetic acid–water system at temperature range of 293–353 K [7]. Campanella *et al*. determined the partition coefficient for formic acid/acetic acid in the soybean oil–formic acid/acetic acid–water system at 313 K [8]. A presence of epoxidized plant oil in the system was taken into account when the liquid-liquid equilibrium constant for acetic acid was investigated for the epoxidized soybean oil–acetic acid–water system [9]. In aforementioned works, neither the changing of the oil phase composition during the reaction of epoxidation, *i.e*., different ratios of plant oil and epoxidized plant oil, nor the presence of hydrogen peroxide in the system was considered. In this work, however, the temperature and composition dependency of the liquid-liquid equilibrium constant for acetic acid (K_A) in a system containing five reaction components was investigated. To predict the liquid–liquid equilibrium constant for acetic acid in an olive oil (OO)–epoxidized olive oil (EOO)–acetic acid (A)–hydrogen peroxide (HP)–water (W) system, the interaction parameters of the UNIQUAC (universal quasi chemical) [10] and NRTL (non-random two liquid) [11] models for the activity coefficient were determined by fitting the experimental data obtained for the equilibrium constant at different temperatures and compositions. The results of simplified and rigorous calculation of the phase equilibrium were compared.

Correspondence: S.V. Sinadinović-Fišer, Faculty of Technology, University of Novi Sad, Bul. cara Lazara 1, 21000 Novi Sad, Serbia.
E-mail: ssfiser@uns.ac.rs
Paper received: 10 December, 2014
Paper accepted: 3 March, 2015

Determination of the liquid–liquid equilibrium constant

For the same reference state in two phases, L_1 and L_2, the liquid–liquid equilibrium condition for component *j* is:

$$\gamma_j^{L_1} x_j^{L_1} = \gamma_j^{L_2} x_j^{L_2} \tag{1}$$

where γ_j^L is the activity coefficient of component *j* in phase L; and x_j^L is the mole fraction of component *j* in phase L.

The mole fraction of component *j* in the phase *L* can be expressed by the following equation:

$$x_j^L = \frac{m_j^L / M_j}{\sum_{k=1}^{NC} m_k^L / M_k} \tag{2}$$

where m_j^L and m_k^L (g) are the masses of component *j* and *k*, respectively, in phase L; M_j and M_k (g/mol) are molecular masses of component *j* and *k*, respectively; and NC is the number of components in the system.

According to Eq. (1), the liquid–liquid equilibrium constant for acetic acid (K_A) in investigated oil-water system is defined as:

$$K_A = \frac{\gamma_A^w}{\gamma_A^o} = \frac{x_A^o}{x_A^w} \tag{3}$$

where used superscripts are for water (w) and oil (o) phases.

The experimental value of the liquid-liquid equilibrium constant for acetic acid can be calculated *via* Eq. (3) using mole fractions (x_A^L).

The predicted value of the equilibrium constant for acetic acid can be obtained also *via* Eq. (3) using activity coefficients (γ_A^L). The activity coefficient of component *j* is the function of phase composition (x_j^L) and temperature (*T*). For investigated system, the coefficients are defined as:

$$\gamma_j^o = f\left(x_{OO}^o, x_{EOO}^o, x_A^o, x_{HP}^o, x_W^o, T\right) \tag{4}$$

$$\gamma_j^w = f\left(x_{OO}^w, x_{EOO}^w, x_A^w, x_{HP}^w, x_W^w, T\right) \tag{5}$$

For the calculation of the equilibrium constant, in this work the UNIQUAC and NRTL models for the activity coefficient were used. Their interaction parameters were determined by fitting the experimental data for the liquid-liquid equilibrium.

The UNIQUAC binary interaction parameter ($\tau_{j,k}$) is expressed as [10]:

$$\tau_{j,k} = e^{\frac{-u_{j,k}}{RT}} \tag{6}$$

where $u_{j,k}$ (J/mol) indicates an adjustable binary parameter for components *j* and *k* in the mixture; and *R* is the universal gas constant.

The NRTL binary interaction parameter ($G_{j,k}$) is given as [11]:

$$G_{j,k} = e^{-\alpha \frac{u_{j,k}}{RT}} \tag{7}$$

A value of the non-randomness parameter (α) of 0.2, which was used in this work, is recommended for the partially miscible liquids [11].

EXPERIMENTAL

Materials and chemicals

Olive oil, product of the Urzante, S.L., Spain, was purchased in supermarket. Glacial acetic acid (>99.8%) was bought from Sigma-Aldrich, Germany, while 30 wt.% aqueous hydrogen peroxide solution, hydrobromic acid and isopropyl alcohol (min 99.5%) were ordered from J.T. Backer, Netherlands. An acid form of sulfonated polystyrene-type cation exchange resin Amberlite IR-120H from Sigma-Aldrich, USA, was used as a catalyst. Alfapanon, Serbia, was a supplier of the aqueous solutions of potassium permanganate (0.1 N), sodium hydroxide (0.1 N) and sodium thiosulfate (0.1 N), while sulfuric acid (p.a.), iodine (p.a.) and bromine (p.a.) were purchased from Centrohem, Serbia. Potassium iodide (extra pure), benzene (p.a.) and chloroform (min 98.5%) were purchased from LachNer, Czech Republic.

Epoxidation procedure

The epoxidation of olive oil was carried out in bulk with peracetic acid formed *in situ* according to the method reported in the literature [12]. Mole ratio of oil unsaturation:acetic acid:hydrogen peroxide was 1:0.5:1.5. The amount of cationic ion exchange resin Amberlite IR-120H used as catalyst was 20 wt.% of acetic acid and hydrogen peroxide solution weight. Olive oil (250 g), glacial acetic acid and catalyst were introduced into a 500 mL three-neck round-bottom flask placed in a water bath and equipped with magnetic stirrer, thermometer, reflux condenser and dropping funnel. The 30% aqueous hydrogen peroxide was dropwise charged into the reaction mixture at temperature of 323±1 K within half an hour. The stirring speed of 1000 rpm was constant. After addition, the temperature of the reaction mixture was increased to 348 K and maintained within ±1 K next 8 h. After removing of the ion exchange resin by filtration, cooled product was centrifuged. Separated oil phase was washed with water (313 K) until pH 7. Water was evaporated at 323 K under the vacuum (about 30 kPa). Stock of epoxidized

olive oil was obtained by blending products of 8 epoxidation runs.

Equilibration procedure

The liquid–liquid equilibrium constant for acetic acid in the system olive oil–epoxidized olive oil–acetic acid–hydrogen peroxide–water was experimentally determined by equilibrating the system components at four temperatures employing seven compositions. A 500 mL three-neck round-bottom flask with weighed masses of olive oil (m_{OO}), epoxidized olive oil (m_{EOO}), acetic acid (m_A), 30% aqueous solution of hydrogen peroxide (m_{aqHP}) and water (m_W) was equipped with condenser, thermometer and magnetic stirrer. Compositions of investigated mixtures are given in Table 1. The mixtures were equilibrated in a thermostatic water bath at 293, 308, 323 and 338 (±1) K for an hour under the constant stirring of 1000 rpm. Without stopping the stirring, six samples of about 10 mL were withdrawn from the mixture and centrifuged (20 min, 1000 rpm). The samples in centrifugation tubes were again thermostated at particular temperature for 20 min. Three samples were used to determine the content of volatile matter in the oil phase. The weighed, in grams, portions of the oil ($m^{s,o}$) and water ($m^{s,w}$) phase of other three samples were titrated to determine the mass fractions of acetic acid and hydrogen peroxide. Sampling of the phases from latter three centrifuge tubes simulated triple determination of the liquid–liquid equilibrium constant for acetic acid.

Methods

To characterize the olive oil and epoxidized olive oil, a standard gravimetric method for the moisture and volatile matter content [13], the Hanus method for the iodine number and standard HBr–acetic acid method for the epoxy oxygen content [14] were applied. All analyses were done in triplicate.

The mass fraction of hydrogen peroxide in the hydrogen peroxide aqueous solution (ω_{HP}^{aqHP}) was determined by permanganometric titration with 0.1 N $KMnO_4$.

The mass fraction of water, acetic acid and hydrogen peroxide in the oil phase ($\omega_{W,A,HP}^{o}$) of the equilibrated mixtures was determined in triplicate according to the standard gravimetric method for the moisture and volatile matter content in plant oils [13], assuming that acetic acid and hydrogen peroxide evaporate together with water.

The mass fractions of acetic acid in the oil (ω_A^o) and water (ω_A^w) phase were determined by the neutralization titration with 0.1 N NaOH, whereas the mass fractions of hydrogen peroxide in the oil (ω_{HP}^{o}) and water (ω_{HP}^{w}) phase were determined by the permanganometric titration with 0.1 N $KMnO_4$. The fractions of component *j* were calculated according to the following expressions:

$$\omega_j^o = \frac{\left(V_t^o - V_{t,cor}^o\right) N_t E_j}{1000 m^{s,o}} \tag{8}$$

$$\omega_j^w = \frac{V_t^w N_t E_j n}{1000 m^{s,w}} \tag{9}$$

where V_t^o and V_t^w (mL) are the volumes of titration solution *t* consumed for titration of the samples of the oil and water phase, respectively; N_t (gE/L) indicates the normality of titration solution *t*; E_j (g/gE) is the mass of component *j* gram equivalent, which for acetic acid is $E_A = M_A$, while for hydrogen peroxide is $E_{HP} = M_{HP}/2$; and *n* is the number of aliquots. $V_{t,cor}^o$ (mL) is the volume of titration solution *t* consumed, in the case of NaOH titration, for the neutralization of the free fatty acids and, in the case of $KMnO_4$ titration, for the oxidation of the minor components in the oil phase sample. It was calculated as follows:

$$V_{t,cor}^o = \frac{m^{s,o}\left(1-\omega_{W,A,HP}^o\right)\left(h_{OO}^t m_{OO}\left(1-\omega_W^{OO}\right) + h_{EOO}^t m_{EOO}\left(1-\omega_W^{EOO}\right)\right)}{m_{OO}\left(1-\omega_W^{OO}\right) + m_{EOO}\left(1-\omega_W^{EOO}\right)} \tag{10}$$

where h_{OO}^t and h_{EOO}^t (mL *t*/g oil) are corrections for the titration of olive oil and epoxidized olive oil, respectively, determined experimentally for both titration solutions as 0.025 mL NaOH/g OO, 0.125 mL NaOH/g EOO, 0.0199 mL $KMnO_4$/g OO and 0.0189 mL $KMnO_4$/g EOO; ω_W^{OO} and ω_W^{EOO} indicate the moisture content in the olive oil and epoxidized olive oil, respectively.

Calculation of the liquid-liquid equilibrium constant for acetic acid using the experimental data

The value of the liquid–liquid equilibrium constant for acetic acid was calculated on the basis of Eqs. (2) and (3).

For calculation of the mole fractions of acetic acid in the oil and water phase, Eq. (2), the masses of the system components were calculated using the mass balance equations and the experimental data i.e. the mass fractions of acetic acid and hydrogen peroxide in both phases and the mass fraction of water, acetic acid and hydrogen peroxide in the oil phase. The calculation proceeds as follows.

Experimentally determined mass fractions of acetic acid and hydrogen peroxide were used to calculate the masses of these components in the equilibrated phases:

$$m_{\mathrm{A}}^{\mathrm{o}} = \omega_{\mathrm{A}}^{\mathrm{o}} m^{\mathrm{o}} \tag{11}$$

$$m_{\mathrm{A}}^{\mathrm{w}} = \omega_{\mathrm{A}}^{\mathrm{w}} m^{\mathrm{w}} \tag{12}$$

$$m_{\mathrm{HP}}^{\mathrm{o}} = \omega_{\mathrm{HP}}^{\mathrm{o}} m^{\mathrm{o}} \tag{13}$$

$$m_{\mathrm{HP}}^{\mathrm{w}} = \omega_{\mathrm{HP}}^{\mathrm{w}} m^{\mathrm{w}} \tag{14}$$

where m^{o} and m^{w} (g) are the masses of the oil and water phases in equilibrium, respectively. Assuming the insolubility of oils in the water phase and knowing weighed masses of olive oil and epoxidized olive oil, as well as measured content of moisture in both oils, the masses of olive oil ($m_{\mathrm{OO}}^{\mathrm{o}}$) and epoxidized olive oil ($m_{\mathrm{EOO}}^{\mathrm{o}}$) in the oil phase are:

$$m_{\mathrm{OO}}^{\mathrm{o}} = m_{\mathrm{OO}}(1 - \omega_{\mathrm{W}}^{\mathrm{OO}}) \tag{15}$$

$$m_{\mathrm{EOO}}^{\mathrm{o}} = m_{\mathrm{EOO}}(1 - \omega_{\mathrm{W}}^{\mathrm{EOO}}) \tag{16}$$

The mass balance of the oil phase is defined as follows:

$$m^{\mathrm{o}} = m_{\mathrm{OO}}^{\mathrm{o}} + m_{\mathrm{EOO}}^{\mathrm{o}} + m_{\mathrm{A}}^{\mathrm{o}} + m_{\mathrm{HP}}^{\mathrm{o}} + m_{\mathrm{W}}^{\mathrm{o}} \tag{17}$$

When Eqs. (11) and (13) are substituted in (17), the mass of water in the oil phase ($m_{\mathrm{W}}^{\mathrm{o}}$) can be calculated as:

$$m_{\mathrm{W}}^{\mathrm{o}} = m^{\mathrm{o}}\left(1 - \omega_{\mathrm{HP}}^{\mathrm{o}} - \omega_{\mathrm{A}}^{\mathrm{o}}\right) - m_{\mathrm{EOO}}^{\mathrm{o}} - m_{\mathrm{OO}}^{\mathrm{o}} \tag{18}$$

The total mass of water in the system, which partitions between the oil and water phase, is the sum of weighed water and water introduced into the system with hydrogen peroxide solution, olive oil and epoxidized olive oil:

$$m_{\mathrm{W}} + m_{\mathrm{aqHP}}\left(1 - \omega_{\mathrm{HP}}^{\mathrm{aqHP}}\right) + m_{\mathrm{OO}}\omega_{\mathrm{W}}^{\mathrm{OO}} + \\ + m_{\mathrm{EOO}}\omega_{\mathrm{W}}^{\mathrm{EOO}} = m_{\mathrm{W}}^{\mathrm{o}} + m_{\mathrm{W}}^{\mathrm{w}} \tag{19}$$

where $\omega_{\mathrm{HP}}^{\mathrm{aqHP}}$ is the mass fraction of hydrogen peroxide in the hydrogen peroxide solution. Therefore, the mass of water in the water phase ($m_{\mathrm{W}}^{\mathrm{w}}$) is:

$$m_{\mathrm{W}}^{\mathrm{w}} = m_{\mathrm{W}} + m_{\mathrm{aqHP}}\left(1 - \omega_{\mathrm{HP}}^{\mathrm{aqHP}}\right) + m_{\mathrm{OO}}\omega_{\mathrm{W}}^{\mathrm{OO}} + \\ + m_{\mathrm{EOO}}\omega_{\mathrm{W}}^{\mathrm{EOO}} - m_{\mathrm{W}}^{\mathrm{o}} \tag{20}$$

The calculation of the mass of each phase in equilibrium was performed as follows. The mass of the oil phase in equilibrium can be calculated as:

$$m^{\mathrm{o}} = \frac{m_{\mathrm{OO}}^{\mathrm{o}} + m_{\mathrm{EOO}}^{\mathrm{o}}}{1 - \omega_{\mathrm{W,A,HP}}^{\mathrm{o}}} \tag{21}$$

while following expression for the mass of the water phase in equilibrium:

$$m^{\mathrm{w}} = \frac{m_{\mathrm{W}}^{\mathrm{w}}}{1 - \omega_{\mathrm{HP}}^{\mathrm{w}} - \omega_{\mathrm{A}}^{\mathrm{w}}} \tag{22}$$

can be derived when Eqs. (12) and (14) are substituted in the equation that describes the mass balance of equilibrated water phase, assuming already accepted insolubility of oils in the water phase:

$$m^{\mathrm{w}} = m_{\mathrm{A}}^{\mathrm{w}} + m_{\mathrm{W}}^{\mathrm{w}} + m_{\mathrm{HP}}^{\mathrm{w}} \tag{23}$$

In order to check the agreement of weighed and experimentally determined contents of acetic acid and hydrogen peroxide, both partitioned between the system phases, an average relative error *ARE* (%) was calculated as follows:

$$ARE = \frac{100}{NEP}\sum_{p=1}^{NEP}\left|\frac{m_{j,p}^{\mathrm{o,exp}} + m_{j,p}^{\mathrm{w,exp}} - m_{j,p}^{\mathrm{weig}}}{m_{j,p}^{\mathrm{weig}}}\right| \tag{24}$$

where *NEP* is the number of experimental points for the liquid–liquid equilibrium constant determination; $m_{j,p}^{\mathrm{o,exp}}$ and $m_{j,p}^{\mathrm{w,exp}}$ are the experimentally determined masses of component *j* in oil (o) and water (w) phase, respectively, for experimental point *p*; and $m_{j,p}^{\mathrm{weig}}$ is the weighed mass of component *j* for experimental point *p*.

RESULTS AND DISCUSSION

The olive oil was characterized with an experimentally measured iodine number (IN_{OO}) of 80.30 and the moisture content of 0.02 wt.%. For epoxidized olive oil were determined the epoxy oxygen content (*EO*) of 4.41 wt.%, the residual iodine number (IN_{EOO}) of 0.36 and the moisture content of 3.40 wt.%. Therefore, the conversion of olive oil double bonds was 99.5% and the selectivity of epoxidation was 91.9%.

For the following fatty acid composition of olive oil: 9.0% palmitic, 6.1% stearic, 77.9% oleic, 6.3% linoleic and 0.7% linolenic acid, the molecular mass of 878.3 g/mol was calculated according to equation:

$$M_{\mathrm{OO}} = 3\sum_{FA=1}^{NFA} M_{FA}x_{FA} + M_{\mathrm{G}} - 3M_{\mathrm{W}} \tag{25}$$

where *NFA* is the number of fatty acids in the olive oil triglycerides; x_{FA} is the mole fraction of particular fatty acid in the olive oil triglycerides; and M_{G} (g/mol) indicates the molecular mass of glycerol. The accepted fatty acid composition of the olive oil corresponds to the experimentally determined iodine number.

The molecular mass of epoxidized olive oil of 934.0 g/mol was calculated *via* following mole balance of olive oil's double bond (D) partial conversion to epoxy group (E) and hydroxyl acetate group (HA), assuming that hydroxyl acetate is generated as the only side product during the epoxidation of olive oil [15,16]:

$$N_{D,OO} = N_{D,EOO} + N_{E,EOO} + N_{HA,EOO} \quad (26)$$

where $N_{D,OO}$ is the number of moles of double bond per mole of olive oil; $N_{D,EOO}$, $N_{E,EOO}$ and $N_{HA,EOO}$ are the numbers of moles of residual double bond, epoxy group and hydroxyl acetate, respectively, per mole of epoxidized olive oil. By expressing $N_{D,OO}$ as a function of iodine number of olive oil, as well as $N_{D,EOO}$ and $N_{E,EOO}$ as functions of residual iodine number and epoxy oxygen content in epoxidized olive oil, respectively, the quantity of the hydroxyl acetate group can be written according to Eq. (26) as follows:

$$N_{HA,EOO} = \frac{IN_{OO}M_{OO}}{200A_I} - \frac{IN_{EOO}M_{EOO}}{200A_I} - \frac{EO\ M_{EOO}}{200A_O} \quad (27)$$

where A_I and A_O are the atomic masses of iodine and oxygen, respectively. Since the molecular mass of epoxidized olive oil can be expressed as enlarged molecular mass of olive oil due to formed epoxy group and hydroxyl acetate group, it can be calculated as:

$$M_{EOO} = M_{OO} + N_{E,EOO}A_O + N_{HA,EOO}(A_O + M_A) \quad (28)$$

After expressing $N_{E,EOO}$ as the function of *EO* and substituting Eq. (27) in Eq. (28), the equation for calculation of the molecular mass of epoxidized olive oil used in this work is established:

$$M_{EOO} = \frac{M_{OO}[1 + IN_{OO}(A_O + M_A)(200A_I)^{-1}]}{1 + EO\ M_A(100A_O)^{-1} + IN_{EOO}(A_O + M_A)(200A_I)^{-1}} \quad (29)$$

The mass fraction of hydrogen peroxide in the hydrogen peroxide aqueous solution (ω_{HP}^{aqHP}) was determined as 0.288.

Experimental values of the liquid-liquid equilibrium constant

The mass fraction of water, acetic acid and hydrogen peroxide as the volatile matter in the oil phase, as well as the mass fractions of acetic acid and hydrogen peroxide in the oil and water phase, are given in Table 1 as the average values of three experimental determinations.

Table 1. Compositions of equilibrated mixtures and experimentally determined mass fraction of water (W), acetic acid (A) and hydrogen peroxide (aqHP), $\omega_{W,A,HP}^{O}$, in the oil phase, mass fractions of acetic acid (ω_A^O) and hydrogen peroxide (ω_{HP}^O) in the oil phase, as well as mass fractions of acetic acid (ω_A^W) and hydrogen peroxide (ω_{HP}^W) in the water phase; OO: olive oil, EOO: epoxidized olive oil

Mixture	*T* K	Weighed mass[a] (m_j), g					$\omega_{W,A,HP}^{O}$	ω_A^O	ω_{HP}^O	ω_A^W	ω_{HP}^W
		OO	EOO	A	aqHP	W					
O1	308	0.00	36.78	4.65	5.03	11.86	0.0664	0.0282	0.00303	0.171	0.0671
	323	0.00	36.88	4.65	5.03	11.86	0.0777	0.0307	0.00297	0.170	0.0672
	338	0.00	36.77	4.66	5.03	11.85	0.0673	0.0300	0.00343	0.171	0.0665
O2	308	0.00	36.80	2.67	10.04	7.56	0.0872	0.0195	0.0105	0.102	0.140
	323	0.00	36.78	2.67	10.05	7.55	0.0621	0.0179	0.00763	0.102	0.139
	338	0.00	36.80	2.68	10.04	7.55	0.0588	0.0175	0.00743	0.101	0.137
O3	293	8.75	27.58	2.66	5.02	11.87	0.0319	0.0134	0.00137	0.111	0.0722
	308	8.76	27.60	2.66	5.02	11.86	0.0443	0.0135	0.00247	0.109	0.0699
	323	8.77	27.61	2.66	5.02	11.85	0.0424	0.0144	0.00240	0.109	0.0735
	338	8.75	27.58	2.66	5.04	11.87	0.3160	0.0135	0.00200	0.110	0.0721
O4	293	17.52	18.41	2.67	10.04	7.54	0.0518	0.0132	0.00433	0.114	0.140
	308	17.55	18.39	2.66	10.05	7.55	0.0510	0.0134	0.00453	0.114	0.145
	323	17.50	18.39	2.66	10.06	7.56	0.0484	0.0126	0.00410	0.111	0.142
	338	17.57	18.40	2.66	10.04	7.55	0.0307	0.0116	0.00337	0.111	0.142
O5	293	17.55	18.40	6.68	5.12	12.07	0.0360	0.0225	0.00113	0.243	0.0634
	308	17.52	18.39	6.67	5.02	11.85	0.0980	0.0409	0.00503	0.249	0.0624
	323	17.51	18.40	6.67	5.02	11.91	0.0481	0.0274	0.00173	0.248	0.0637
	338	17.50	18.43	6.66	5.02	11.86	0.0314	0.0238	0.000967	0.245	0.0616
O6	293	26.29	9.21	4.65	15.22	3.25	0.0207	0.0139	0.00230	0.180	0.191
	308	26.33	9.23	4.66	15.09	3.42	0.0243	0.0141	0.00290	0.183	0.193
	323	26.28	9.12	4.66	15.14	3.28	0.0239	0.0148	0.00277	0.178	0.193
	338	26.26	9.21	4.65	15.07	3.24	0.0325	0.0142	0.00233	0.179	0.190
O7	293	35.08	0.00	6.66	18.84	0.00	0.0206	0.0152	0.00177	0.242	0.214
	308	35.05	0.00	6.65	18.84	0.00	0.0192	0.0155	0.00177	0.243	0.218
	323	35.04	0.00	6.66	18.83	0.00	0.0197	0.0152	0.00177	0.243	0.218
	338	35.06	0.00	6.65	18.84	0.00	0.0200	0.0154	0.00177	0.243	0.212

The total masses of acetic acid and hydrogen peroxide in the system were determined with an average relative error (Eq. (24)) of 2.15 and 2.12%, respectively. Since these masses were calculated *via* the mass balance equations using experimental data determined by five analytical methods, namely method for gravimetric determination of the volatile matter content in the oil phase and four titration methods for determination of acetic acid and hydrogen peroxide contents in both phases, the obtained average relative errors have to be considered as the total error of all analytical measurements.

The olive oil–epoxidized olive oil–acetic acid–hydrogen peroxide-water system was equilibrated at four temperatures for seven compositions. The temperatures, as well as mixture compositions, were varied in the range that is significant for the epoxidation of plant oils. The molar ratio of components was selected as to simulate variation of component concentrations in the epoxidation system with reaction time. However, as the oil phase of the mixtures without olive oil, namely mixtures O1 and O2 in Table 1, became solid during the equilibration at 293 K, only 26 values of the liquid-liquid equilibrium constant for acetic acid were determined. For investigated conditions, these values range from 1.52 to 2.73 and they are presented in Table 2. The defined trend of dependency of the liquid-liquid equilibrium constant for acetic acid neither from temperature nor from composition of examined mixtures of the olive oil–epoxidized olive oil–acetic acid–hydrogen peroxide-water system was observed.

Simplified calculation of the liquid-liquid equilibrium constant

A simplified approach for the calculation of the liquid–liquid equilibrium constant for acetic acid is based on the assumptions that only acetic acid is partitioned between two liquid phases of the epoxidation reaction system and that olive oil and epoxidized olive oil are insoluble in the water. This is described with the following constrains for the masses of components *j* in phase *L*:

$$m_{\mathrm{HP}}^{\mathrm{o}} = m_{\mathrm{W}}^{\mathrm{o}} = 0 \tag{30}$$

$$m_{\mathrm{OO}}^{\mathrm{w}} = m_{\mathrm{EOO}}^{\mathrm{w}} = 0 \tag{31}$$

Therefore, the activity coefficients of acetic acid in both phases are expressed as following functions:

$$\gamma_{\mathrm{A}}^{\mathrm{o}} = f\left(x_{\mathrm{OO}}^{\mathrm{o}}, x_{\mathrm{EOO}}^{\mathrm{o}}, x_{\mathrm{A}}^{\mathrm{o}}, T\right) \tag{32}$$

$$\gamma_{\mathrm{A}}^{\mathrm{w}} = f\left(x_{\mathrm{OO}}^{\mathrm{w}}, x_{\mathrm{EOO}}^{\mathrm{w}}, x_{\mathrm{A}}^{\mathrm{w}}, T\right) \tag{33}$$

As aforementioned, the mass of acetic acid in the system is partitioned between the oil and water phases:

$$m_{\mathrm{A}} = m_{\mathrm{A}}^{\mathrm{o}} + m_{\mathrm{A}}^{\mathrm{w}} \tag{34}$$

By substituting Eqs. (2), (32) and (33) in (1), a non--linear equation with one unknown variable ($m_{\mathrm{A}}^{\mathrm{w}}$) is established:

$$F\left(m_{\mathrm{A}}^{\mathrm{w}}\right) = x_{\mathrm{A}}^{\mathrm{o}}\gamma_{\mathrm{A}}^{\mathrm{o}} - x_{\mathrm{A}}^{\mathrm{w}}\gamma_{\mathrm{A}}^{\mathrm{w}} = 0 \tag{35}$$

In this work, Eq. (35) is solved by the modified Newton method.

Rigorous calculation of the liquid-liquid equilibrium constant

To check the accuracy of the simplified approach, a rigorous flash calculation of the phase equilibrium was performed. For such calculation it is assumed that all components are partitioned between the system phases. The activity coefficients of all components are expressed *via* Eqs. (4) and (5). Using the components' and total mass balance equations, after appropriate substitutions, the mole fraction of the oil phase (φ) in the investigated system has to be determined from the following non-linear equation:

$$\sum_{j=1}^{NC} \frac{z_j}{1+\varphi\left(K_j - 1\right)} = 1 \tag{36}$$

where z_j indicates the mole fraction of component *j* in the system; and K_j is the liquid–liquid equilibrium constant for component *j* in the system. The Newton method was applied to solve Eq. (36).

Modeling of activity coefficients for acetic acid

Due to lack of the interaction parameters for epoxy group with other groups present in the investigated system, none of the models based on the group contribution method for direct calculation of the activity coefficient, such as the UNIFAC (uniquac functional-group activity coefficients) and ASOG (analytical solution of groups) models, were applied in this work. Consequently, the UNIQUAC and NRTL models for the activity coefficient were used to correlate the liquid-liquid equilibrium constant for acetic acid with temperature and composition.

The UNIQUAC structural parameters r_j and q_j, which are the van der Waals volume and area of the molecule of component *j* relative to those of a standard segment, respectively, were calculated using the UNIFAC LLE (liquid–liquid equilibrium) group contribution data [17]:

$$r_j = \sum_{g=1}^{NG} \nu_{g,j} R_g \tag{37}$$

Table 2. Comparison of experimentally determined values of the liquid–liquid equilibrium constant for acetic acid (K_A) in the system olive oil–epoxidized olive oil–acetic acid–hydrogen peroxide–water and those calculated by simplified and rigorous approach when the UNIQUAC and NRTL models for the activity coefficient were applied

T / K	Mixture	Experimental	Calculated		
			Simplified		Rigorous
			UNIQUAC	NRTL	NRTL
293	O1	–	–	–	–
	O2	–	–	–	–
	O3	2.637	2.247	2.259	2.311
	O4	1.657	1.706	1.729	1.726
	O5	1.908	1.907	1.853	1.791
	O6	2.031	1.768	1.859	1.808
	O7	1.561	1.669	1.714	1.685
308	O1	2.212	2.267	2.195	2.108
	O2	1.936	1.982	2.132	2.034
	O3	2.115	2.324	2.365	2.322
	O4	1.725	1.816	1.772	1.819
	O5	1.542	1.866	1.862	1.867
	O6	1.836	1.819	1.828	1.837
	O7	1.672	1.599	1.629	1.649
323	O1	2.115	2.308	2.249	2.242
	O2	2.353	2.154	2.213	2.275
	O3	2.346	2.456	2.512	2.534
	O4	1.706	1.964	1.872	1.904
	O5	1.871	1.865	1.900	1.941
	O6	2.034	1.844	1.813	1.848
	O7	1.609	1.584	1.590	1.602
338	O1	2.376	2.383	2.322	2.342
	O2	2.438	2.369	2.334	2.444
	O3	2.731	2.640	2.689	2.629
	O4	2.213	2.147	2.008	1.983
	O5	2.323	1.895	1.956	1.998
	O6	1.515	1.905	1.842	1.855
	O7	1.626	1.596	1.571	1.552
Objective function, S			0.9485	0.8566	0.7951
Root mean square deviation, $RMSD = \sqrt{\sum_{i=1}^{NE}(K_{A,i}^{calc} - K_{A,i}^{exp})^2}$			0.1910	0.1815	0.1749
Average relative deviation, $ARE\ (\%) = \frac{100}{NE}\sum_{i=1}^{NE}\left\lvert\frac{K_{A,i}^{calc} - K_{A,i}^{exp}}{K_{A,i}^{exp}}\right\rvert$			7.23	7.30	7.24
Average absolute deviation, $AAD = \frac{1}{NE}\sum_{i=1}^{NE}\left\lvert K_{A,i}^{calc} - K_{A,i}^{exp}\right\rvert$			0.1418	0.1438	0.1414

$$q_j = \sum_{g=1}^{NG} \nu_{g,j} Q_g \tag{38}$$

where NG is the total number of group species in the system; $\nu_{g,j}$ is the number of groups of type g in the molecule of component j; and R_g and Q_g are the parameters related to the volume and area of group g, respectively. In order to calculate the structural parameters from the literature data, the molecule of hydrogen peroxide was presented with two hydroxyl groups, whereas the olive oil and epoxidized olive oil, each considered as one pseudo-component, were presented with the following molecular structures, respectively:

$(CH_2COO)_3CH(CH_2)_b(CH{=}CH)_c(CH_3)_3$,
$[(CH_2COO)_3(CH)_d(CH_2)_b(CH{=}CH)_f$ and
$(FCH_2O)_l(OH)_y(CH_3COO)_y(CH_3)_3$.

Since the structural parameters for epoxy group are not available in the literature, an ether group of cyclic ethers, FCH_2O, was included into the pseudo-component molecule of epoxidized olive oil instead. The coefficients in the pseudo-component molecules *b*, *c*, *d*, *f*, *l* and *y* were accepted as 40.904, 2.778, 3.9559, 0.0134, 2.5733 and 0.1913, respectively, on the basis of the iodine numbers, epoxy oxygen content and fatty acid composition of the olive oil and epoxidized olive oil. Although the number of groups in a molecule is usually defined with an integer within UNIFAC model, the decimal numbers have been successfully used for coefficients in the pseudo-component molecules of plant oils when the liquid-liquid equilibrium of the systems similar to the system investigated in this work was studied [7,9]. The calculated values of r_{OO} and q_{OO} parameters are 38.867 and 31.529, respectively, whereas the values of r_{EOO} and q_{EOO} parameters are 40.0194 and 33.1965, respectively.

Binary interaction parameters of both NRTL and UNIQUAC activity coefficient models were determined by minimization of the following objective function *S*:

$$S = \sum_{i=1}^{NE} \left(K_{A,i}^{calc} - K_{A,i}^{exp} \right)^2 \tag{39}$$

where *NE* is the number of experiments; and $K_{A,i}^{calc}$ and $K_{A,i}^{exp}$ are calculated and experimentally determined values, respectively, of the liquid–liquid equilibrium constant for acetic acid for the experiment *i*. The Marquardt method was applied to minimize the objective function [18]. Therefore, the fitting of interaction parameters was based on the algorithm with two loops. The outer loop is the minimization of the objective function, and inner loop is either the simplified or the rigorous calculation of the liquid–liquid equilibrium constant for acetic acid. The determined interaction parameters for simplified and rigorous calculations are given in Tables 3–5.

Table 3. Interaction parameters $u_{j,k}$ (J/mol) of the UNIQUAC model for activity coefficient applied within the simplified calculation of K_A

Component	Olive oil	Epoxidized olive oil	Acetic acid	Hydrogen peroxide	Water
Olive oil	0	–1170.159	6072.516	–	–
Epoxidized olive oil	–2670.553	0	–504.9471	–	–
Acetic acid	–2399.01	5145.97	0	–8082.141	–4950.184
Hydrogen peroxide	–	–	3865.073	0	–8162.745
Water	–	–	15163.77	1847.888	0

Table 4. Interaction parameters $u_{j,k}$ (J/mol) of the NRTL model for activity coefficient applied within the simplified calculation of K_A

Component	Olive oil	Epoxidized olive oil	Acetic acid	Hydrogen peroxide	Water
Olive oil	0	23.00308	–6792.634	–	–
Epoxidized olive oil	5154.96	0	–2190.579	–	–
Acetic acid	1638.673	–5827.824	0	–18728.77	–11964.42
Hydrogen peroxide	–	–	35188.14	0	–22226.66
Water	–	–	24023.41	19073.41	0

Table 5. Interaction parameters $u_{j,k}$ (J/mol) of the NRTL model for activity coefficient applied within the rigorous calculation of K_A

Component	Olive oil	Epoxidized olive oil	Acetic acid	Hydrogen peroxide	Water
Olive oil	0	10764.7	239.1269	–9235.735	–88.59006
Epoxidized olive oil	–6781.327	0	1949.265	34458.26	–472.6696
Acetic acid	–1795.675	–1056.141	0	4409.27	9341.472
Hydrogen peroxide	16563.09	123.3846	1710.127	0	–3772.03
Water	17447.25	36863.31	–1869.315	7440.163	0

Comparison of activity coefficient models and types of calculation

The values of the liquid-liquid equilibrium constant for acetic acid calculated using determined interaction parameters of UNIQUAC and NRTL models for the activity coefficient are presented in Table 2 for both types of calculations.

The simplified approach for calculation of the liquid-liquid equilibrium constant for acetic acid shows good agreement with experimental data since the relative

mean square deviations (*RMSD*) for both UNIQUAC and NRTL activity coefficient models are low, namely 0.1910 and 0.1815, respectively. The rigorous calculation was performed applying only NRTL model for activity coefficient as it showed slightly better correlation in the case of simplified calculation. Although the number of adjustable parameters is higher for rigorous than for simplified calculation, 20 compared to 12, the predicted values of the equilibrium constant are similar, *i.e*., the *RMSD* for rigorous calculation is 3.64% lower than for simplified. This implies that the application of proposed simplified calculation of the liquid-liquid equilibrium constant for acetic acid is acceptable.

As previously mentioned, the applicability of different activity coefficient models for describing the liquid-liquid equilibrium in the systems relevant for epoxidation of plant oils was reported in the literature. Thus, for the system soybean oil-acetic acid-water, the original and three modified UNIFAC models, as well as the UNIQUAC model, were used to correlate the liquid-liquid equilibrium data by assuming the immiscibility of soybean oil and water. For such system, the UNIQUAC model was significantly more accurate than other models [7,8]. The UNIQUAC model was also more adequate than modified UNIFAC model for describing the equilibrium of the system soybean oil-formic acid-water [8]. To estimate the liquid-liquid equilibrium constant for acetic acid in the epoxidized soybean oil-acetic acid-water system, the Wilson, NRTL and UNIQUAC models were used to correlate the experimental data. In spite of all simplifications, the conclusion was that all three models are adequate to predict the equilibrium constant for acetic acid. However, according to the analysis of ARE, the most successful prediction of the liquid–liquid equilibrium constant for acetic acid in the investigated system was obtained with UNIQUAC model when partial miscibility of epoxidized soybean oil and water was assumed [9]. Under the conditions applied in the present investigation, the adequacy of both NRTL and UNIQUAC models for prediction of the liquid-liquid equilibrium constant for acetic acid in the olive oil-epoxidized olive oil-acetic acid-hydrogen peroxide–water system is confirmed, although the computationally less demanding NRTL model slightly better correlates the experimental equilibrium data.

CONCLUSION

The liquid–liquid equilibrium constant for acetic acid in the system olive oil–epoxidized olive oil–acetic acid–hydrogen peroxide–water was experimentally determined and successfully estimated under conditions of temperature and component ratios significant for the process of plant oil epoxidation with peracetic acid generated *in situ*. The experimentally determined values of the constant are better correlated when NRTL than when UNIQUAC model for the activity coefficient was applied, under the accepted simplifications regarding the partitioning and solubility of particular components in the system phases. When the NRTL model was used within the rigorous flash calculation of the equilibrium, slightly better fitting was achieved than with simplified calculation. Since the values of the liquid-liquid equilibrium constant for acetic acid predicted by simplified and by rigorous calculation are comparable, the usage of proposed simplified approach can be recommended when establishing the mathematical model that describes the reaction system for epoxidation of plant oils.

Acknowledgment

This work is part of Project No. III45022 supported by the Ministry of Education, Science and Technological Development of the Republic of Serbia.

List of symbols

A	Acetic acid
A_I,A_O	Atomic mass of iodine i.e. oxygen, respectively
aqHP	Hydrogen peroxide aqueous solution
b	Number of (CH_2) groups present in OO and EOO pseudo-component molecules
c	Number of (CH=CH) groups present in OO pseudo-component molecule
D	Double bond
d	Number of (CH) groups present in EOO pseudo-component molecule
E	Epoxy group
E_j	Mass of component j gram equivalent (g/gE)
EO	Epoxy oxygen content (wt%)
EOO	Epoxidized olive oil
f	Number of (CH=CH) groups present in EOO pseudo-component molecule
$G_{j,k}$	NRTL binary interaction parameter for components j and k in the mixture
h^t_{OO} , h^t_{EOO}	Correction for titration of OO and EOO, respectively, with titration solution t (mL t/g oil)
HA	Hydroxyl acetate group
HP	Hydrogen peroxide
IN_j	Iodine number of component j
K_j	Liquid–liquid equilibrium constant for component j
$K^{calc}_{A,i}$, $K^{exp}_{A,i}$	Calculated, *i.e*., experimentally determined value of K_A, respectively, for experiment i
l	Number of (FCH_2O) groups present in EOO pseudo-component molecule
M_j , M_k	Molecular mass of component j, *i.e*., k, respectively (g/mol)
m_j	Weighed mass of component j (g)
m^o,m^w	Mass of the oil, *i.e*. ,water phase, respectively, in equilibrium (g)

m_j^L, m_k^L Mass of component *j* i.e. *k*, respectively, in phase *L* (g)
$m^{s,L}$ Mass of the sample of phase *L* (g)
$m_{j,p}^{L,\mathrm{exp}}$ Experimentally determined mass of component *j* in phase *L* for experimental point *p* (g)
$m_{j,p}^{\mathrm{weig}}$ Weighed mass of component *j* for experimental point *p* (g)
n Number of aliquots
N_t Normality of titration solution *t* (gE/L)
$N_{\mathrm{D,OO}}$ Number of moles of double bond per mole of olive oil
$N_{\mathrm{D,EOO}}$, $N_{\mathrm{E,EOO}}$, $N_{\mathrm{HA,EOO}}$ Number of moles of residual double bond, epoxy group *i.e.*, hydroxyl acetate, respectively, per mole of epoxidized olive oil
NC Number of components in the system
NE Number of experiments
NEP Number of experimental points
NFA Number of fatty acids in the olive oil triglycerides
NG Total number of group species in the system
OO Olive oil
Q_g Area parameter of group *g*
q_j Area parameter of molecule of component *j*
R Universal gas constant
R_g Volume parameter of group *g*
r_j Volume parameter of molecule of component *j*
S Objective function
T Temperature (K)
$u_{j,k}$ Adjustable binary parameter for components *j* and *k* in the mixture (J/mol)
V_t^L Volume of titration solution *t* consumed for titration of the sample of phase *L* (mL)
$V_{t,\mathrm{cor}}^{\mathrm{o}}$ Correction volume of titration solution *t* consumed for titration of the oil phase sample (mL)
W Water
x_{FA} Mole fraction of fatty acid FA in the olive oil triglycerides
x_j^L Mole fraction of component *j* in phase *L*
y Number of (OH) groups, as well as number of (CH_3COO) groups present in EOO pseudo-component molecule
z_j Mole fraction of component *j* in the system

Greek letters

α Non-randomness parameter in the NRTL model
γ_j^L Activity coefficient of component *j* in phase *L*
$\nu_{g,j}$ Number of groups of type *g* in the molecule of component *j*
$\tau_{j,k}$ UNIQUAC binary interaction parameter for components *j* and *k* in the mixture
φ Mole fraction of the oil phase
ω_j^L Mass fraction of component *j* in phase *L*
$\omega_{\mathrm{HP}}^{\mathrm{aqHP}}$ Mass fraction of hydrogen peroxide in the hydrogen peroxide solution
$\omega_{\mathrm{W}}^{\mathrm{OO}}$, $\omega_{\mathrm{W}}^{\mathrm{EOO}}$ Moisture content in OO, *i.e.*, EOO, respectively
$\omega_{\mathrm{W,A,HP}}^{\mathrm{o}}$ Mass fraction of water, acetic acid and hydrogen peroxide in the oil phase

Superscripts

L Phase
o Oil phase
w Water phase

Subscripts

A Acetic acid
aqHP Hydrogen peroxide aqueous solution
D Double bond
E Epoxy group
EOO Epoxidized olive oil
G Glycerol
HA Hydroxyl acetate group
HP Hydrogen peroxide
OO Olive oil
W Water

REFERENCES

[1] S.G. Tan, W.S. Chow, Biobased epoxidized vegetable oils and its greener epoxy blends: A review, Polym.-Plast. Technol. Eng. **49** (2010) 1581–1590.

[2] S-C. Chua, X. Xu, Z. Guo, Emerging sustainable technology for epoxidation directed toward plant oil-based plasticizers, Process Biochem. **47** (2012) 1439–1451.

[3] B. Rangarajan, A. Havey, E.A. Grulke, P.D. Culnan, Kinetic parameters of a two-phase model for *in situ* epoxidation of soybean oil, J. Am. Oil Chem. Soc. **72** (1995) 1161–1169.

[4] R.L. Musante, R.J. Grau, M.A. Baltanás, Kinetics of liquid-phase reactions catalyzed by acidic resins: the formation of peracetic acid for vegetable oil epoxidation, Appl. Catal., A **197** (2000) 165–173.

[5] E. Santacesaria, R. Tesser, M. Di Serio, R. Turco, V. Russo, D. Verde, A biphasic model describing soybean oil epoxidation with H_2O_2 in a fed-batch reactor, Chem. Eng. J. **173** (2011) 198–209.

[6] E. Santacesaria, A. Renken, V. Russo, R. Turco, R. Tesser, M. Di Serio, Biphasic model describing soybean oil epoxidation with H_2O_2 in a continuous reactors, Ind. Eng. Chem. Res. **51** (2012) 8760–8767.

[7] S. Sinadinović-Fišer, M. Janković, Prediction of the partition coefficient for acetic acid in a two-phase system soybean oil-water, J. Am. Oil Chem. Soc. **84** (2007) 669–674.

[8] A. Campanella, B.A. Mandagarán, E.A. Campanella, Partitioning of a carboxylic acid between oil and water phases. Experimental, correlation, and prediction, J. Am. Oil Chem. Soc. **86** (2009) 513–519.

[9] M. Janković, S. Sinadinović-Fišer, M. Lamshoeft, Liquid-liquid equilibrium constant for acetic acid in an epox-

idized soybean oil-acetic acid-water system, J. Am. Oil Chem. Soc. **87** (2010) 591–600.

[10] D.S. Abrams, J.M. Prausnitz, Statistical thermodynamics of liquid mixtures: a new expression for the excess Gibbs energy of partly or completely miscible systems, AIChE J. **21** (1975) 116–128.

[11] H. Renon, J.M. Prausnitz, Local composition in thermodynamic excess functions for liquid mixtures, AIChE J. **14** (1968) 135–144.

[12] S. Sinadinović-Fišer, M. Janković, Z. Petrović, Kinetics of *in situ* epoxidation of soybean oil in bulk catalyzed by ion exchange resin, J. Am. Oil Chem. Soc. **78** (2001) 725–731.

[13] Method Ca 2c-25 in Official Methods and Recommended Practices, 3rd ed., American Oil Chemists' Society, Champaign, IL, 1987.

[14] Standard Methods for the Analysis of Oils, Fats and Derivatives, Blackwell Scientific Publications, London, 1987.

[15] A. Campanella, M.A. Baltanás, Degradation of the oxirane ring of epoxidized vegetable oil with solvated acetic acid using cation-exchange resin, Eur. J. Lipid Sci. Technol. **106** (2004) 524–530.

[16] A. Campanella. M.A. Baltanás, Degradation of the oxirane ring of epoxidized vegetable oil in a liquid-liquid-solid heterogeneous reaction system, Chem. Eng. Process **46** (2007) 210–221.

[17] T. Magnussen, P. Rasmussen, A. Fredenslund, UNIFAC parameter table for prediction of liquid-liquid equilibria, Ing. Eng. Chem. Process Des. Dev. **20** (1981) 331–339.

[18] D.W. Marquardt, An algorithm for least-squares estimation of nonlinear parameters, J. Soc. Ind. Appl. Math. **11** (1963) 431–441.

IZVOD

KONSTANTA RAVNOTEŽE TEČNO–TEČNO SIRĆETNE KISELINE U SISTEMU MASLINOVO ULJE–EPOKSIDOVANO MASLINOVO ULJE–SIRĆETNA KISELINA–VODONIK-PEROKSID–VODA

Milovan R. Janković, Olga M. Govedarica, Snežana V. Sinadinović-Fišer, Jelena M. Pavličević, Vesna B. Teofilović, Nevena R. Vukić

Tehnološki fakultet, Univerzitet u Novom Sadu, Bul. cara Lazara 1, 21000 Novi Sad, Srbija

(Naučni rad)

Epoksidovanje biljnih ulja se industrijski izvodi perorganskom kiselinom formiranom *in situ* iz odgovarajuće organske kiseline i vodonik peroksida u prisustvu kiselog katalizatora. Kada se kao homogeni katalizator primenjuje neka mineralna kiselina, reakcioni sistem epoksidovanja ulja je dvofazni (ulje–voda), dok pri primeni heterogenog katalizatora, kakva je kisela jonoizmenjivačka smola, pomenuti sistem je trofazni (ulje–voda–katalizator). Pri postavljanju pouzdanog matematičkog modela koji opisuje ovaj višefazni reakcioni sistem, a za potrebe optimizovanja procesa epoksidovanja biljnih ulja, neophodno je uzeti u obzir raspodelu sirćetne kiseline između uljne i vodene faze. U ovom radu je konstanta fazne ravnoteže tečno-tečno sirćetne kiseline u kvinarnom sistemu maslinovo ulje–epoksidovano maslinovo ulje–sirćetna kiselina–vodonik peroksid–voda određena eksperimentalno za temperature u opsegu 293–338 K i za različite odnose komponenata. Odnos komponenata u ispitivanim smešama je odabran tako da odgovara uslovima izvođenja epoksidovanja, ali i da simulira promenu odnosa komponenata u sistemu usled odigravanja reakcija. Za uslove ispitivanja, eksperimentalno određene vrednosti konstante ravnoteže se kreću u opsegu 1,52–2,73. U cilju izračunavanja konstante ravnoteže sirćetne kiseline, eksperimentalne vrednosti konstante su korelisane UNIQUAC (universal quasi-chemical) i NRTL (non-random two liquid) modelima za koeficijent aktivnosti. Binarni interakcioni parametri ovih modela su određeni primenom metode Marquardt-a za fitovanje eksperimentalnih podataka. Pri uprošćenom proračunu, u kom je usvojeno da se maslinovo ulje i epoksidovano maslinovo ulje ne rastvaraju u vodi, kao i da se voda i vodonik peroksid ne rastvaraju u maslinovom i epoksidovanom maslinovom ulju, standardno odstupanje je 0,1910 za UNIQUAC i 0,1815 za NRTL model. Pri rigoroznom flash proračunu, u kojem je pretpostavljeno prisustvo svih komponenata u obe faze, standardno odstupanje za jedino primenjeni NRTL model je 0,1749. Kako je ovo odstupanje manje za samo 3,64% od standardnog odstupanja postignutog pri uprošćenom proračunu, kada se primenjuje isti model za koeficijent aktivnosti, upotreba uprošćenog proračuna je prihvatljiva za modelovanje reakcionog sistema epoksidovanja biljnih ulja.

Ključne reči: Ravnoteža tečno–tečno • Sirćetna kiselina • Biljno ulje • Epoksidovanje

Sinteza, struktura i svojstva biološki aktivnih derivata spirohidantoina

Anita M. Lazić, Nataša V. Valentić, Nemanja P. Trišović, Slobodan D. Petrović, Gordana S. Ušćumlić

Katedra za organsku hemiju, Tehnološko–metalurški fakultet, Univerzitet u Beogradu, Beograd, Srbija

Izvod

Prvu sintezu cikloalkanspiro-5-hidantoina izveli su Bučerer i Lib (Bucherer, Lieb) 1934. godine, reakcijom cikličnog ketona sa kalijum-cijanidom i amonijum-karbonatom u smeši etanola i vode, zagrevanjem uz refluks. U ovom radu su prikazani različiti postupci sinteze derivata spirohidantoina, njihova fizičko–hemijska svojstva i biološka aktivnost. Posebno je istaknut značaj cikloalkanspiro-5-hidantoina sa antikonvulzivnim, antiproliferativnim, antipsihotičkim, antimikrobnim, antiinflamatornim i analgetskim svojstvima kao i njihov značaj kao potencijalnih lekova u lečenju dijabetesa. Pored osnovnih svojstava molekula koja su značajna za aktivnost proučavanih spirohidantoina, navedeni su najznačajniji podaci QSAR (eng. Quantitative Structure–Activity Relationship) studija na osnovu kojih se dobija detaljniji uvid u mehanizam njihovog farmakološkog dejstva.

Ključne reči: *Spirohidantoini; sinteza; fizičko–hemijska svojstva; biološka aktivnost*.

Dostupno na Internetu sa adrese časopisa: http://www.ache.org.rs/HI/

PREGLEDNI RAD

UDK 547.783.057:615

Hem. Ind. **70** (2) 177–199 (2016)

doi: 10.2298/HEMIND150205025L

Uvođenjem različitih supstituenata u *N*-3 i *N*-1 položaje hidantoinskog prstena (u strukturi spirohidantoina) nastaju farmakološki važni molekuli, interesantni kao potencijalni lekovi u tretmanu raznih bolesti. Spirohidantoinska jedinica je gradivni element selektivnih agonista i antagonista serotoninskih 5-HT receptora te su stoga pomenuti derivati spirohidantoina od važnosti kao potencijalni psihoaktivni agensi [1,2]. Spiropiperidino-hidantoinski derivati su modulatori aktivnosti hemokinskih receptora podvrste CCR5 i kao takvi su od značaja za prevenciju ili tretman infektivnih oboljenja (npr. infekcija izazvana HIV-om), imunoregulatornih i inflamatornih oboljenja, reakcije organizma na presađeni organ [3], itd. Molekuli koji pokaziju aktivnost ka aldoza reduktazi enzimu (ALR2) privlače pažnju kao potencijalni lekovi u prevenciji ili lečenju komplikacija koje su posledica dijabetesa [4,5]. Spirohidantoini su važni kao potencijalni lekovi u lečenju kancera [6,7], epilepsije i drugih konvulzivnih poremećaja [8,9] i čitavog niza drugih bolesti. Osim navedenih fizioloških aktivnosti, značajni su i kao polazni reaktanti za sintezu različitih aminokiselina [10].

STRUKTURA SPIROHIDANTOINA

Mnogi derivati spirohidantoina su biološki aktivni molekuli različitih svojstava, a strukture nekih aktivnijih jedinjenja kao i odgovarajuća dejstva data su u tabeli 1.

Prepiska: N.V. Valentić, Tehnološko–metalurški fakultet, Univerzitet u Beogradu, Karnegijeva 4, 11120 Beograd, Srbija.
E-pošta: naca@tmf.bg.ac.rs
Rad primljen: 5. februar, 2015
Rad prihvaćen: 14. april, 2015

FIZIČKA SVOJSTVA SPIROHIDANTOINA

Spirohidantoini su bele kristalne supstance, različitih temperatura topljenja. Spirohidantoini sa supstituentima na atomima azota se tope na nižim temperaturama od nesupstituisanih analoga što je posledica manje polarnosti molekula i smanjene mogućnosti građenja intermolekulskih vodoničnih veza [12,13]. Usled velike koncentracije heteroatoma i karbonilnih grupa u prstenu, spirohidantoini su hidrofilni molekuli; dobro se rastvaraju u vodi, etanolu i etil-acetatu [13].

HEMIJSKA SVOJSTVA SPIROHIDANTOINA

Kiselost

Derivati spirohidantoina sadrže dve NH grupe u položajima 1 i 3 hidantoinskog prstena. N3-H grupa se nalazi između dve elektrofilne karbonilne grupe što znatno povećava njenu kiselost u odnosu na N1-H grupu koja je u susedstvu samo jedne karbonilne grupe. Primenom IR spektroskopije dokazano je da pomenute NH grupe nisu međusobno ekvivalentne, zbog čega derivati spirohidantoina ispoljavaju različita kiselo-bazna svojstva [14].

Hidroliza

Hidroliza hidantoina i spirohidantoina jedan je od najčešće korišćenih postupaka za sintezu neproteinskih aminokiselina. Najefikasniji metod hidrolize spirohidantoinskih derivata je bazna hidroliza upotrebom barijum-hidroksida. Primer je reakcija alkalne hidrolize ciklopentanspiro-5-hidantoina (**1**) do 1-aminociklopentankarboksilne kiseline (**2**, šema 1) [10].

Spirohidantoini su važni intermedijeri za sintezu konformaciono ograničenih α-aminokiselina. Na primer, prva sinteza 1-aminociklopropankarboksilne kiseline izvršena je 1922. godine, alkalnom hidrolizom ciklo-

Tabela 1. Neki fiziološki aktivni derivati spirohidantoina
Table 1. Some of physiological active derivatives of spirohydantoins

Redni broj	Formula	Dejstvo
1	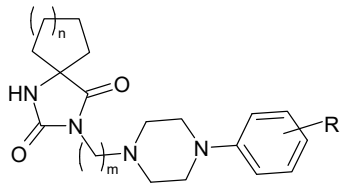 n = 1, 2 m = 3, 4 R = H, *o*-OCH_3	Antidepresiv, antipsihotik [1,11]
2	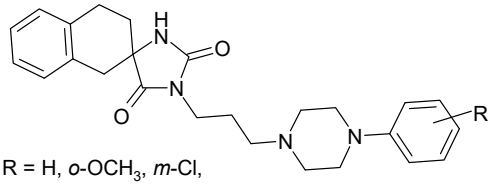 R = H, *o*-OCH_3, *m*-Cl, *o*-F, *p*-F, *m*-CF_3	Anksiolitičko [1,2]
3	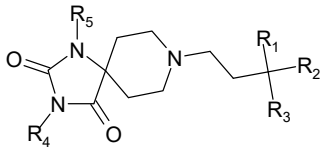 nezavisno R_1, R_4, R_5 = H nezavisno R_1, R_2, R_3, R_4, R_5 = C_{1-10} alkil, C_{2-10} alkenil ili alkinil nezavisno R_1, R_3, R_4, R_5 = C_{6-12} aril nezavisno R_2, R_4, R_5 = 3-10 člani heterocikl R_1 = OH, OC_{1-6} alkil, OC_{6-12} aralkil R_5 = C_{6-12} aralkil	Antiinflamatorno [3]
4	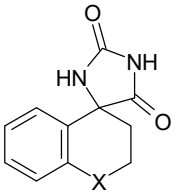 X = CH_2, O, S	Antidijabetik [4]
5	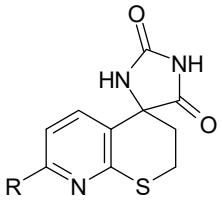 R = H, CH_3	Antidijabetik [5]
6	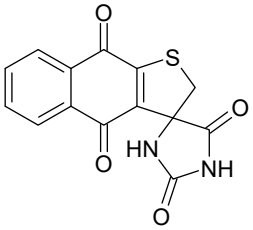	Antikancerogeno [7]

Tabela 1. Nastavak
Table 1. Continued

Redni broj	Formula	Dejstvo
7	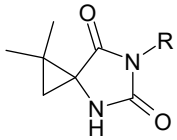 R = H, CH_3, C_6H_5	Antikonvulziv [8]
8	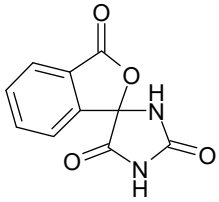	Antikonvulziv [9]

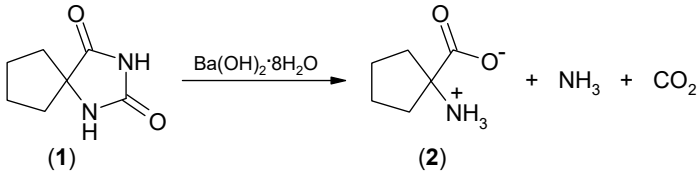

Šema 1. Alkalna hidroliza cikloalkanspiro-5-hidantoina.
Scheme 1. Hydrolysis of cycloalkanespiro-5-hydantoins under alkaline conditions.

propanspiro-5-hidantoina (**3**) [15]. Tretiranjem rezultujuće hidantoinske kiseline (**4**) sa azotastom kiselinom, dobija se karbaminska kiselina (**5**), koja spontano dekarboksiluje dajući 1-aminociklopropankarboksilnu kiselinu (**6**, šema 2) [15].

Cikloalkanspiro-5-hidantoini (**7**) sa voluminoznijim cikloalkil-grupama se prevode u konformaciono ograničene aminokiseline preko intermedijarnog *N,N'*-zaštićenog spirohidantoina (**8**) koji se dobija uvođenjem *terc*-butiloksikarbonil (Boc) zaštitne grupe tretiranjem cikloalkanspiro-5-hidantoina sa di-*terc*-butil-dikarbonatom. Nastali intermedijer (**8**) relativno lako podleže baznoj hidrolizi nakon čega sledi zakišeljavanje (šema 3) [15].

N-3 i *N*-1 supstitucija

Piner (Pinner) je ustanovio da je moguće izvršiti direktno alkilovanje hidantoina u položaju 3, tretiranjem sa alkil-halogenidima u baznom rastvoru. Reakcijom ciklopentanspiro-5-hidantoina (**1**) sa benzil-bromidom u prisustvu kalijum-karbonata, dobija se 3-benzilciklopentanspiro-5-hidantoin (**10**, šema 4) [16].

Primenom istog postupka ne može se izvršiti direktno *N*-1 alkilovanje hidantoina osim ukoliko u položaju 5, pomenutog molekula, nije prisutna dvostruka veza ili fenil grupa. Prisustvo C-5 dvostruke veze aktivira azot u položaju 1, omogućavajući zamenu vodonikovog atoma odgovarajućom alkil-grupom [16].

Berend (Berend) i Nejmer (Niemeyer) prvi su dokazali da reakcija spirohidantoina (**1**) i formaldehida rezultira formiranjem 1,1'-metilendispirohidantoina (**11**) (šema 5), odnosno, *N*-1 supstitucijom [16].

SINTEZA SPIROHIDANTOINA

Prvu sintezu cikloalkanspiro-5-hidantoina izveli su Bučerer i Lib 1934. godine, reakcijom cikličnog ketona, kalijum-cijanida i amonijum-karbonata, uz refluks, u smeši etanola i vode [15]. Opisana metoda sadrži jedan nedostatak. Naime, tokom reakcije izdvaja se cijanovodonična kiselina koja je izuzetno toksična. Potencijalno rešenje predstavlja primena mikrotalasnog zračenja koje obezbeđuje visoke prinose i čistije proizvode [15].

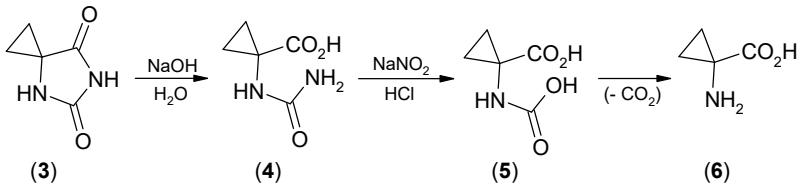

Šema 2. Sinteza 1-aminociklopropankarboksilne kiseline.
Scheme 2. Synthesis of 1-aminocyclopropanecarboxylic acid.

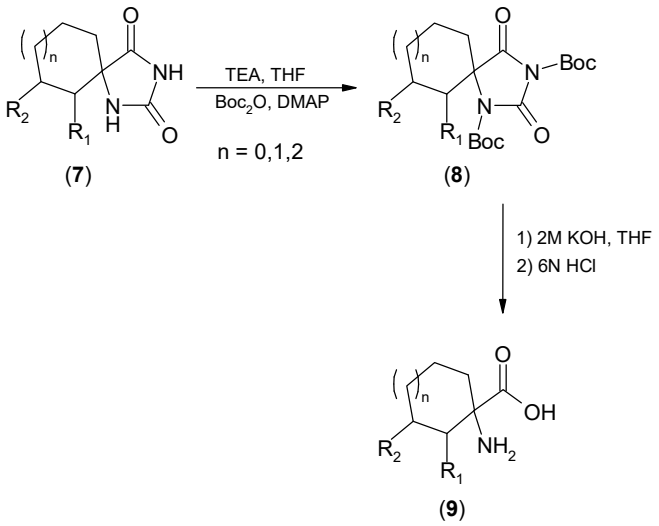

Šema 3. Sinteza konformaciono ograničenih aminokiselina.
Scheme 3. Synthesis of conformationally restricted amino acids.

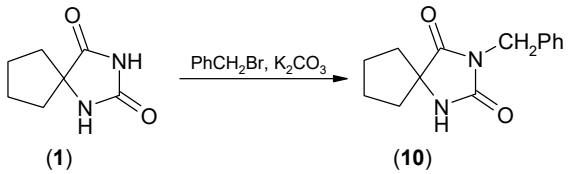

Šema 4. Supstitucija u položaju N-3-hidantoinskog prstena.
Scheme 4. Substitutions at position N-3-hydantoin ring.

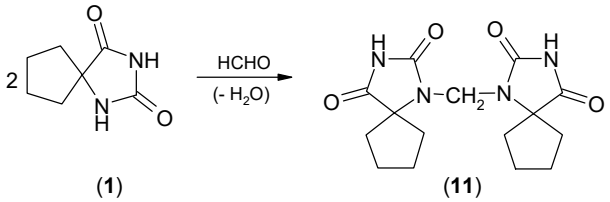

Šema 5. Reakcija spirohidantoina i formaldehida.
Scheme 5. Reaction of spirohydantoin and formaldehyde.

Bučerer–Libova metoda je modifikacija poznatog postupka sinteze hidantoina dejstvom kalijum-cijanida i amonijum-karbonata na aldehide i ketone, odnosno, takozvane Bučerer–Bergsove (Bucherer–Bergs) reakcije [16]. Modifikacija se sastoji u upotrebi 50% vodenog rastvora etanola kao reakcionog medijuma.

Sinteza cikloalkanspiro-5-hidantoina (**13**) Bučerer–Libovim postupkom, iz odgovarajućih cikličnih ketona (**12**), prikazana je na šemi 6 [12].

Ciklopentanspiro-, cikloheksanspiro- i cikloheptanspiro-5-hidantoin, sintetisani su Bučerer–Bergsovim postupkom uz dejstvo mikrotalasnog zračenja (šema 7). Optimalno vreme zračenja koje obezbeđuje visoke prinose je 2–5 min. Nasuprot tome, izlaganje reakcionih komponenata dužem zračenju ima za posledicu razgradnju proizvoda [17].

Na šemi 8, opisana je sinteza farmakološki aktivnog aminokiselinskog nitrogen-mustarda, derivata tetralin-

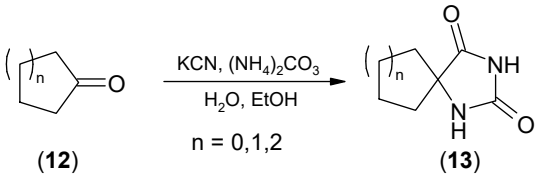

Šema 6. Bučerer–Libova sinteza cikloalkanspiro-5-hidantoina iz cikličnih ketona.
Scheme 6. Bucherer–Libe cycloalkanespiro-5-hydantoin synthesis from cyclic ketones.

spirohidantoin nitrogen-mustarda. Aminokiselinski nitrogen-mustardi su od važnosti kao potencijalni antitumorni agensi s obzirom na veliki značaj L-fenilalaninskih mustarda u terapiji kancerogenih oboljenja [6]. Polazna supstanca je β-tetralon hidantoin (**17**) iz koga nastaje smeša dva tetralin-spirohidantoin nitrogen-mustarda (**18** i **19**). Njihovom hidrolizom se dobijaju finalni produkti DL-2-amino-7-[bis(2-hloretil)amino]-1,2,3,4-tet-

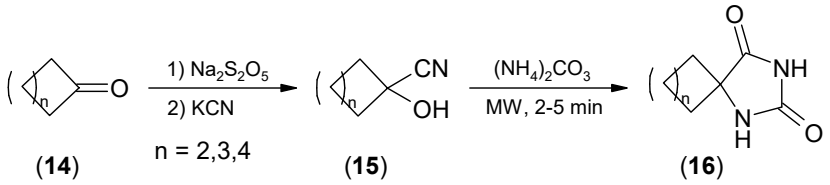

Šema 7. Bučerer–Bergsova sinteza spirohidantoina pod dejstvom mikrotalasnog zračenja.
Scheme 7. Bucherer–Bergs spirohydantoin synthesis under microwave irradiation.

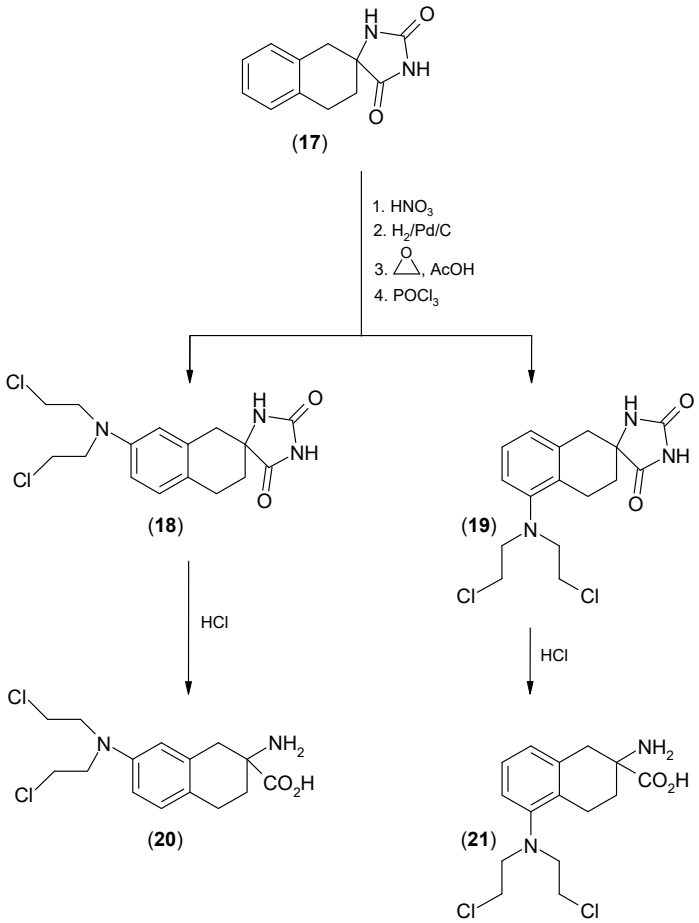

Šema 8. Sinteza L-aminokiselinskog nitrogen-mustarda.
Scheme 8. Synthesis of L-amino acid nitrogen mustard.

rahidro-2-naftenska kiselina (**20**) i DL-2-amino-5-[bis(2--hloretil)amino]-1,2,3,4-tetrahidro-2-naftenska kiselina (**21**), u protonovanom amonijum-karboksilnom obliku [6].

Postupak dobijanja piperidinspirohidantoina (**23**), polazeći iz odgovarajućeg piperidona (**22**), prikazan je na šemi 9 [15].

Analozi sorbinila (**25**) koji pokazuju aktivnost ka inhibiciji aldoza reduktaze enzima (ALR2) (šema 10), proizvod su reakcije 2,3-dihidrotiopirano-(2,3-*b*)-piridin-4(4H)-ona (**24**), kao i njegovog metil analoga, sa kalijum-cijanidom i amonijum-karbonatom u vodeno––alkoholnoj sredini [5].

3-Supstituisani ciklopropanspiro-5-hidantoinski derivati koji imaju antikonvulzivnu aktivnost, dobijeni su prema postupku opisanom na šemi 11. Dietil-2,2--dimetilciklopropan-1,1-dikarboksilat (**26**), sintetizovan Majklovom (Michael) reakcijom ciklizacije, preveden je u monoestar (**27**) pomoću reakcije monosaponifikacije. Kurtiusovom (Curtius) reakcijom, formiran je *in situ* izocijanat (**28**) koji je zatim reagovao sa aminom gradeći α-karboetoksi ureu (**29**). Ciklizacijom *N,N*-asimetričnih molekula uree (**29**) dobijen je spirohidantoinski derivat (**30**) [8].

Štrekerova (Strecker) reakcija predstavlja direktnu metodu za asimetričnu (enantioselektivnu) sintezu derivata cikloalkanspiro-5-hidantoina [18]. Tako se, na primer, klasičnom Štrekerovom reakcijom *N*-supstituisanog-4-piperidona (**31**) sa anilinom i kalijum-cijanidom, u vodenom rastvoru sirćetne kiseline, formira

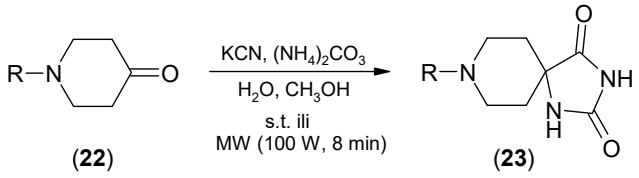

R = H, CH_3, CH_2Ph

Šema 9. Sinteza piperidin spirohidantoina iz piperidona.
Scheme 9. Synthesis of piperidine spirohydantoin from piperidone.

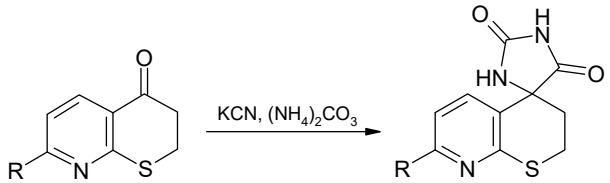

R = H, CH_3

Šema 10. Sinteza spirohidantoinskog derivata 2,3-dihidrotiopirano-(2,3-b)-piridin-4-(4H)-ona.
Scheme 10. Synthesis of spirohdantoin derivative of 2,3-dihydrotiopyrano-(2,3-b)-pyridin-4-(4H)-one.

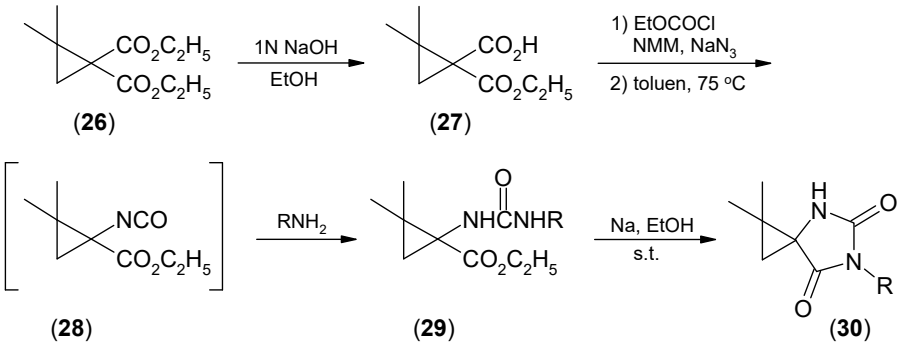

R = H, CH_3, $(CH_3)_2CH$, $CH_3(CH_2)_2CH_2$, $CH_3CH_2(CH_2OH)CH$, $PhCH_2$, Ph, 4-$CH_3C_6H_4$, 4-$CH_3OC_6H_4$, 4-FC_6H_4, 3,5-diClC_6H_3, 4-$NO_2C_6H_4$

Šema 11. Sinteza 3-supstituisanog ciklopropanspiro-5-hidantoinskog derivata.
Scheme 11. Synthesis of 3-substituted cyclopropanespiro-5-hydantoin derivative.

prekursor (**32**, šema 12). Modifikovana Štrekerova reakcija se izvodi u anhidrovanim uslovima, u glacijalnoj sirćetnoj kiselini, korišćenjem tetrametilsilil-cijanida (TMSCN) umesto kalijum-cijanida (šema 12). Luisove (Lewis) kiseline katališu modifikovanu Štrekerovu reakciju adicije TMSCN na imine. Nakon modifikovane Štrekerove sinteze, nastali α-aminonitril (**32**) se kondenzuje sa odabranim izocijanatom, a zatim sledi ciklizacija i nastaje spirohidantoin (**34**).

Postupak sinteze derivata cikloalkanspiro-5-hidantoina koji imaju antikonvulzivnu aktivnost (šema 13), započinje Bučerer–Bergsovom reakcijom *β*-tetralona (**35**) kojom se formira *β*-tetralon hidantoin (**17**). Njegovom daljom reakcijom sa 4-supstituisanim piperazinom i formaldehidom u 96% etanolu, dobijaju se *N*-[(4-(supstituisani fenil)-piperazin-1-il)-metil]-[7,8--*f*]benzo-1,3-diaza-spiro[4.5]dekan-2,4-dioni (**36**) [19].

Prvi korak u sintezi spiromustina (**40**) (šema 14) predstavlja alkilovanje cikloheksanspiro-5-hidantoina (**37**) sa 1-brom-2-hloretanom. Formirani produkt, odnosno, 3-(2-hloretil)cikloheksanspiro-5-hidantoin (**38**) kondenzuje se sa dietanolaminom gradeći 3-[2-[bis(2--hidroksietil)-amino]-etil]cikloheksanspiro-5-hidantoin (**39**) koji u završnoj fazi reakcije reaguje sa $POCl_3$ [20].

Spirohidantoinski derivat sirćetne kiseline (**43**), koji pokazuje slabu aktivnost ka inhibiciji aldoza reduktaze (ALR2) i aldehid reduktaze (ALR1), može se sintetizovati alkilovanjem sulfona (**41**) (šema 15) [5]. Alkilovanje se vrši sa etil-bromacetatom u acetonu, u prisustvu anhidrovanog kalijum-karbonata, zagrevanjem uz refluks. Alkalnom hidrolizom prekursora (**42**) dobija se ciljano jedinjenje.

Široka mogućnost primene cikloalkanspiro-5-hidantoina dovela je, između ostalog, i do proučavanja *N*-supstituisanih derivata cikloheksanspiro-5-hidan-

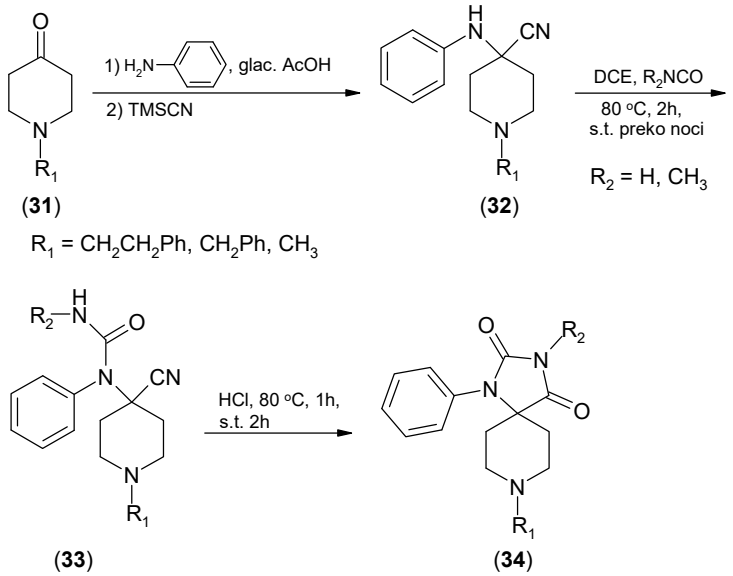

Šema 12. Sinteza asimetričnih spirohidantoinskih derivata.
Scheme 12. Synthesis of asymmetric spirohydantoin derivative.

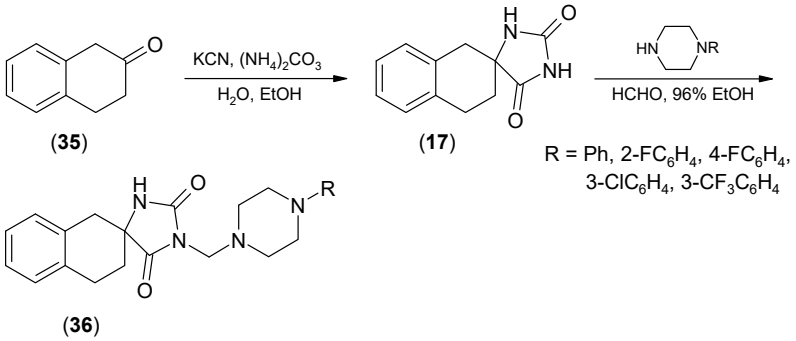

Šema 13. Sinteza N-[(4-(supstituisanih fenil)-piperazin-1-il)-metil]-[7,8-f]benzo-1,3-diaza-spiro[4.5]dekan-2,4-diona.
Scheme 13. Synthesis of N-[(4-(substituted phenyl)-piperazin-1-yl)-methyl]-[7,8-f]benzo-1,3-diaza-spiro[4.5]decane-2,4-diones.

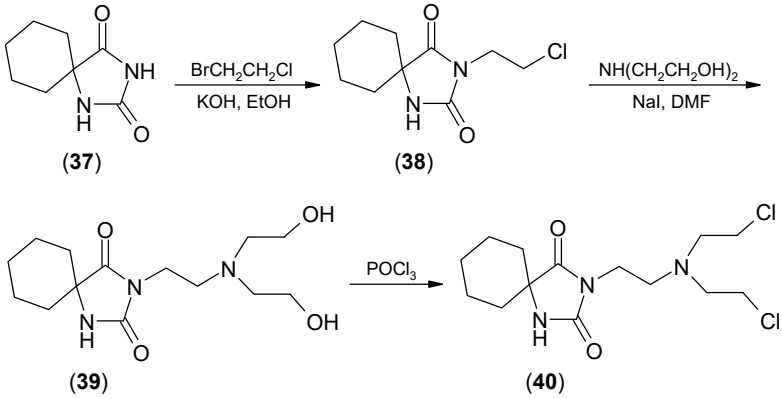

Šema 14. Sinteza spiromustina.
Scheme 14. Synthesis of spiromustine.

toina. Cikloheksanspiro-5-hidantoin (**37**) se može selektivno alkilovati u položaju *N*-3-dejstvom agensa za alkilovanje (agens za alkilovanje/spirohidantoin, 1:1) u prisustvu kalijum-hidroksida u etanolu, zagrevanjem uz refluks (šema 16) [21]. Kada se kao alkilujući agens koristi 1,3-dibrompropan, on se uzima u višku (agens za alkilovanje/spirohidantoin 2:1) [21].

Do alkilovanja u položaju *N*-1 dolazi znatno teže, najčešće u prisustvu natrijum-hidrida u dimetilformamidu. Da bi se izvršilo selektivno alkilovanje u položaju

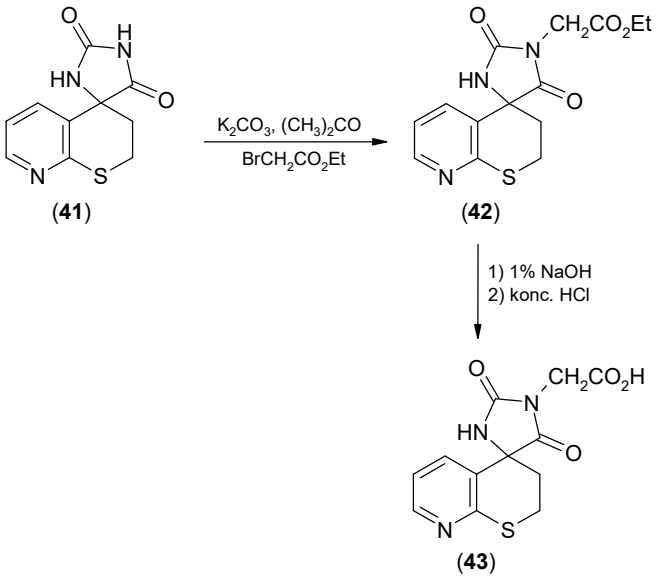

Šema 15. Sinteza acetatnog derivata spirohidantoin 2,3-dihidrotiopirano-(2,3-b)-piridin-4-(4H)-ona.
Scheme 15. Synthesis of spirohydantoin derivative of acetate of 2,3-dihydrotyopyrano-(2,3-b)-pyrdine-4-(4H)-one.

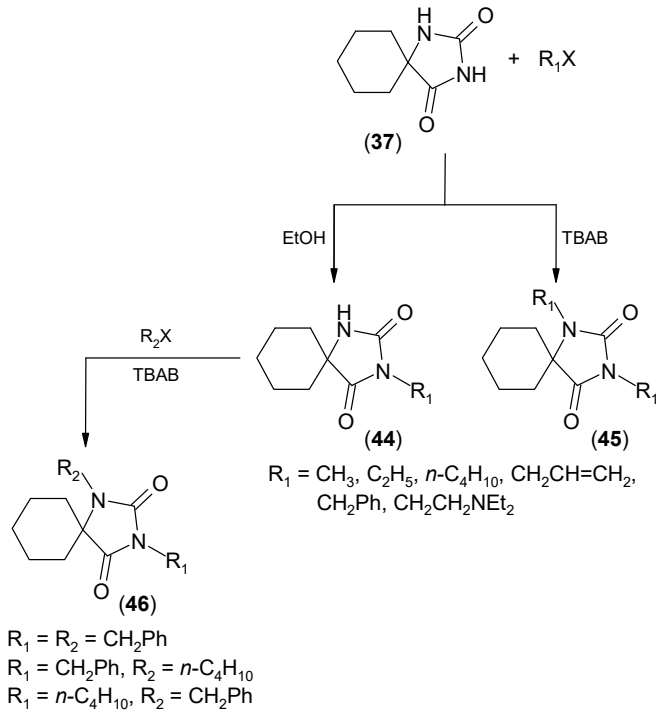

Šema 16. Sinteza disupstituisanih derivata cikloheksanspiro-5-hidantoina.
Scheme 16. Synthesis of disubstituted cyclohehanespiro-5-hydantoin derivatives.

N-1, položaj 3 se mora prethodno zaštititi. Kada se alkilovanje, vrši u sistemu toluen-vodeni alkalni rastvor uz tetrabutilamonijum-bromid (TBAB) kao međufazni katalizator, dobija se di-*N*-alkilovani derivat cikloheksanspiro-5-hidantoina (šema 16) [21].

Cikloheksanspiro-5-hidantoin (**49**) produkt je reakcije supstituisane α-halogensirćetne kiseline (**47**) i simetričnih *N,N'*-dialkilkarbodiimida poput *N,N'*-dicikloheksilkarbodiimida (**48**) (šema 17) [22].

Derivati spirohidantoina sa antikonvulzivnim svojstvima

Epilepsija je poremećaj funkcije mozga koga karakterišu epileptički napadi praćeni epizodnim (privremenim) visokofrekventnim pražnjenjem impulsa koje vrši grupa neurona u mozgu [23]. Napadi imaju različite oblike i različite ishode, u zavisnosti od epizoda neuronskih pražnjenja. Najčešće su praćeni konvulzijama, ali se mogu pojaviti i u mnogim drugim oblicima. Mesto

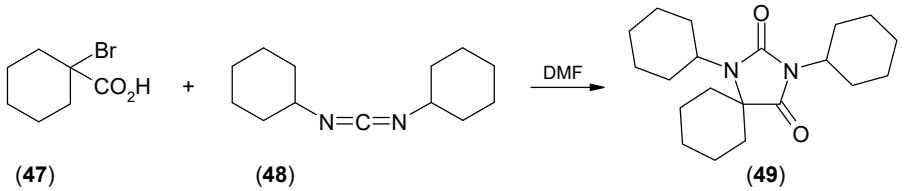

Šema 17. Sinteza cikloheksanspiro-5-hidantoina iz supstituisane α-halogensirćetne kiseline i N,N'-dialkilkarbodiimida.
Scheme 17. Synthesis of cyclohexanespiro-5-hydantoin from substituted α-halogenacetic acide and N,N'-dialcanecarbamide.

primarnog pražnjenja i opseg njegovog širenja određuju simptome koji nastaju prilikom napada.

Epilepsija je jedna od najčešćih hroničnih neuroloških bolesti. Klinička klasifikacija epilepsije definiše dve glavne kategorije napada: parcijalne i generalizovane [23]. Napadi u kojima pražnjenje počinje kao lokalno, i često ostaje lokalizovano, su parcijalni napadi. Generalizovani napadi zahvataju ceo mozak, i zato proizvode poremećenu električnu aktivnost u obe hemisfere. Dva važna klinička oblika generalizovanih epileptičkih napada su toničko-klonički (granda mal) i absansni napadi (petit mal).

Epilepsija se uglavnom leči lekovima, ali se u teškim slučajevima mogu obaviti hirurški zahvati na mozgu. Naziv antiepileptik koristi se istovremeno kao i naziv antikonvulziv, za opis lekova koji se koriste u terapiji epilepsije kao i neepileptičkih konvulzivnih poremećaja [23]. Postoje tri glavna mehanizma delovanja antiepileptika: pojačavanje delovanja *γ*-aminobuterne kiseline (GABA), inhibicija funkcije voltažno-zavisnih kanala Na^+ i Ca^{2+} [23].

Uprkos velikom napretku koji je postignut u oblasti istaživanja vezanih za epilepsiju, i dalje se kod 25% pacijenata konvulzije neadekvatno kontrolišu primenom standardne terapije lekovima. U poslednje vreme se u lečenju epilepsije koriste novi lekovi (tzv. antikonvulzivi druge generacije) poput: felbamata (Felbatol®), lamotrigina (Lamictal®), gabapentina (Neurontin®) i topiramata (Topamax®) [9]. Njihovo mesto u terapiji epilepsije se još uvek određuje. Iako su efikasni u tretmanu epileptičkih sindroma, nisu pokazali superiornost u odnosu na tradicionalne antikonvulzive (antikonvulzivi prve generacije) [9]. Iz tog razloga postoji konstantna potreba za pronalaženjem novih antiepileptika sa većom efikasnošću i manjim nuspojavama.

Većina jedinjenja koja pokazuje antikonvulzivnu aktivnost, u svojoj strukturi sadrži cikličnu ureidnu jedinicu sa fenil ili alkil supstituentima [9,19]. Važan predstavnik antikonvulziva prve generacije je fenitoin (5,5--difenilhidantoin, Dilantin®). Iako je otkriven pre više od sedam decenija i dalje je u širokoj terapijskoj upotrebi, s obzirom da je efikasan u terapiji različitih formi parcijalnih i generalizovanih napada (ali ne absansnih) [23].

Odnos strukture i bioloških svojstava derivata hidantoina intenzivno se proučava sa ciljem da se identifikuju oni strukturni elementi koji su odgovorni za korisnu aktivnost, ali i neželjena dejstva. Uspostavljanje vodoničnih veza sa ciljnim mestima nalazi se u osnovi mehanizma njihovog antikonvulzivnog delovanja. Kristalografska analiza antikonvulziva je pokazala da međusobna orijentacija aromatične grupe i dela molekula koji gradi vodonične veze značajno utiče na efikasnost njihovog delovanja [13,24–26].

Od otkrića 5,5-difenilhidantoina do danas, sintetizovani su mnogi analozi hidantoina, uključujući spirohidantoine [8,9,19], koji pokazuju antikonvulzivnu aktivnost.

U slučaju *N*-3-supstituisanih ciklopropanspiro-5-hidantoina (tabela 2), kao farmakološki najaktivniji pokazali su se derivati koji sadrže nerazgranate alkil i hidroksialkil supstituente (npr. metil-, butil- i (1-hidroksimetil)propil-grupa) [8]. Takođe, uočeno je da prisustvo fluora u *para* položaju *N*-3-fenil-grupe pojačava aktivnost derivata cikloalkanspiro-5-hidantoina, dok disupstitucija hlorom u 3' i 5' položaju *N*-3-fenilnog jezgra, znatno smanjuje antikonvulzivnu aktivnost. Elektron--donorske grupe kao što je metoksi i snažne elektron-akceptorske grupe poput nitro grupe, koje se nalaze u *para* položaju *N*-3-fenilnog jezgra, smanjuju delotvornost derivata ciklopropanspiro-5-hidantoina [8].

Tabela 2. 3-Supstituisani ciklopropanspiro-5-hidantoini sa antikonvulzivnim svojstvima
Table 2. 3-Substituted cyclopropanespiro-5-hydantoins with anticonvulsant properties

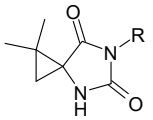

Redni broj	R
1	H
2	CH_3
3	$(CH_3)_2CH$
4	$CH_3(CH_2)_3$
5	$CH_3CH_2(CH_2OH)CH$
6	$C_6H_5CH_2$
7	C_6H_5
8	4-$CH_3C_6H_4$
9	4-$CH_3OC_6H_4$
10	4-FC_6H_4
11	3,5-diClC_6H_3
12	4-$NO_2C_6H_4$

Proučavanje antikonvulzivne aktivnosti u okviru serije *N*-1',*N*-3'-disupstituisanih ftalidil spirohidantoina (tabela 3), ukazalo je da struktura supstituenta na azotu veoma utiče na antikonvulzivnu aktivnost i lipofilnost molekula [9]. Supstituenti na azotu su odabrani tako da pruže uvid u optimalnu dužinu alkil lanca i da povećaju lipofilnost molekula spirohidantoina i tako olakšaju njihov prolaz kroz krvno–moždanu barijeru. Rezultati su pokazali da je u homologoj seriji jedinjenja sa po dve metil-, etil- ili alil-grupe (R_1, R_2 = metil, etil, alil), farmakološki najaktivnji dietil derivat, sa srednjom efektivnom dozom (ED_{50}) od 190 mg/kg u pentilentetrazolskom (scPTZ) testu [9].

Tabela 3. N-1',N-3'-disupstituisani ftalidil spirohidantoini sa antikonvulzivnim svojstvima
Table 3. N-1',N-3'-disubstituted phthalidyl spirohydantoins with anticonvulsant properties

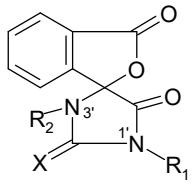

Redni broj	R_1	R_2	X
1	CH_3	CH_3	O
2	C_2H_5	C_2H_5	O
3	Alil	Alil	O
4	CH_3	C_2H_5	O
5	*n*-C_3H_7	*n*-C_3H_7	O
6	*n*-C_4H_9	*n*-C_4H_9	O
7	*i*-C_3H_7	*i*-C_3H_7	O
8	Ciklo-C_6H_{11}	Ciklo-C_6H_{11}	O
9	C_6H_5	CH_3	O
10	C_6H_5	CH_3	S
11	*p*-F-C_6H_4	CH_3	O
12	*p*-CF_3-C_6H_4	CH_3	O
13	C_6H_5	C_2H_5	O
14	*p*-F-C_6H_4	C_2H_5	O
15	*p*-NO_2-C_6H_4	C_2H_5	O
16	*p*-OCH_3-C_6H_4	C_2H_5	O

N-1',*N*-3'-dipropil derivat (tabela 3) se pokazao dva i po puta aktivniji (ED_{50} = 78,5 mg/kg (scPTZ test)) u poređenju sa odgovarajućim dietil analogom. Povećanjem dužine zasićenog supstituentskog alkil lanca do tri ugljenikova atoma, kod oba supstituenta na azotu, znatno raste antikonvulzivna aktivnost, dok povećanje broja ugljenikovih atoma kod samo jednog supstituenta rezultira smanjenim dejstvom. Uvođenjem razgranatih grupa (npr. izopropil-grupa) u prsten hidantoina znatno se umanjuje antikonvulzivna aktivnost jedinjenja. Položaj *N*-3' je kritičan za antikonvulzivnu aktivnost i u skladu sa tim može da sadrži supstituent sa najviše tri ugljenikova atoma, dok *N*-1' može biti supstituisan i aril grupom [9].

Supstituenti na *N*-1'-fenilnom jezgru značajno utiču na aktivnost. Naime, mala lipofilna grupa u *para* položaju (atom fluora) povećava antikonvulzivna svojstva, dok glomaznija CF_3 grupa u *para* položaju smanjuje aktivnost. Elektron-donorske grupe, npr. metoksi u *para* položaju fenilnog jezgra, uzrokuju blago smanjenje aktivnosti, dok duži lanci u istom položaju dovode do velike toksičnosti. U grupi *N*-1'-aril-*N*-3'-alkil disupstituisanih jedinjenja, najaktivniji se pokazao *N*-1'-*p*-nitrofenil-*N*-3'-etil derivat (ED_{50} = 41,8 mg/kg (scPTZ test)). Lipofilnost proučavanih spirohidantoina (izražena preko izračunatog particionog koeficijenta log *P*) sa značajnom antikonvulzivnom aktivnošću kreće se u intervalu 2,4–3,0, dok je lipofilnost farmakološki slabije aktivnog dietil derivata znatno manja (log *P* = 1,457) [9].

Da postoji korelacija između antikonvulzivne aktivnosti derivata hidantoina i njihove lipofilnosti, pokazali su i rezultati proučavanja serija 3,5-disupstituisanih-5--fenilhidantoina [27] i 5-supstituisanih-5-fenilhidantoina [28,29]. U cilju razumevanja antikonvulzivne aktivnosti nekog molekula treba uzeti u obzir fenomen prenosa *in vivo* i interakciju sa receptorom.

Antiproliferativna aktivnost derivata spirohidantoina

Iako je malignitet poznat od nastanka čovečanstva, postao je vodeći uzročnik smrti tek u dvadesetom veku. Pomenuta bolest, može se pojaviti u bilo kom životnom dobu, mada su mnogo veće šanse za njen razvoj u srednjim godinama. Tako se karcinom debelog creva najčešće registruje kod osoba uzrasta 30–50 godina, dok se karcinom rektuma javlja kod osoba od 50–70 godina. Osim leukemije i limfoma koji se dijagnostikuju kod određenog broja maloletnih pacijenata, ostali oblici maligniteta retko se pojavljaju u ovom životnom periodu. Kod dece se takođe, uočavaju tumori na mozgu, nervnom sistemu, kostima, bubrezima, koji se inače retko sreću kod velikog broja odraslih ljudi [30].

Ne postoji univerzalna definicija za sve vrste raka. Karcinom (*gr. karkinos – rak)* je oboljenje koje karakteriše nekontrolisana ćelijska proliferacija [30]. Pripada velikoj porodici bolesti čija je najvažnija odlika formiranje grupe neoplazmi sa svojstvima maligniteta. Neoplazma (tumor) predstavlja skup ćelija koje su pretrpele neregulisani rast pa često formiraju čvorić ili se distribuiraju difuzijom [31].

Tretmani kancera podrazumevaju operacije, radijacije i hemoterapije [30]. Hiruška intervencija je primarni metod lečenja velikog broja čvrstih izolovanih kancera, njena uspešnost u velikoj meri doprinosi preživljavanju. Cilj je odjednom ukloniti celokupnu malignu masu koja u određenim slučajevima uključuje i limfne čvorove. Ponekad je to sve što je neophodno da bi se u potpunosti eliminisao rak [32].

Hemoterapija je pored hirurgije, od izuzetno velike koristi kod brojnih oblika kancera, kao što je karcinom dojke, kolorektalni karcinom, karcinom pankreasa, osteogeni sarkom, rak testisa, rak jajnika. Efikasnost je često ograničena zbog toksičnosti po preostale organe [32].

Radioterapija podrazumeva primenu jonizujućeg zračenja u pokušaju izlečenja ili poboljšanja simptoma raka. Koristi se kod 50% pacijenata, a najpoznatija je brahiterapija koja se odnosi na primenu inertnih izvora zračenja. Bitan je dodatak operaciji i hemoterapiji, dok se kod lečenja kancera glave i vrata može samostalno primenjivati [32].

Hinonska struktura predstavlja osnovu mnogih antitumorskih lekova, kao i antibiotika (doksorubicin (Adriamycin®) i mitoksantron (Mitoxantrone®)) koji se uveliko primenjuju u hemoterapijskoj kontroli brojnih kancera, a takođe su veoma efikasni kod tumora koji se postepeno razvijaju. Klinički značaj opisanih medikamenata, uticao je na razvoj novih antiproliferativnih agenasa kod kojih je zadržano hidantoinsko jezgro. Neoplastična aktivnost hidantoinskih derivata posledica je prisustva planarnog, policikličnog jezgra, sposobnog da se veže za molekul DNA i dva bočna lanca koji sadrže različite supstituente u odnosu na hromoforu [7].

U seriji 3-amino-3-etoksikarbonil-2,3-dihidrotieno-(2,3-*b*)-nafto-4,9-dion derivata supstituisanih u položaju 3 različitim aminokiselinama, najaktivnije jedinjenje je 3-(glicil)-amino-3-etoksikarbonil-2,3-dihidrotieno-(2,3-*b*)-nafto-4,9-dion sa izuzetnom citotoksičnom aktivnošću u submikromolarnim koncentracijama. Efikasan je kod nekoliko tipova leukemije kao i čvrstih tumora [7].

Razvijena je i serija derivata cikloalkanspiro-5-hidantoina, odnosno, 3-(alkil)(supstituisani alkil)spiro[(dihidroimidazo-2,4-dion)-5,3'-(2',3'-dihidrotieno[2,3-*b*]nafto-4',9'-dion)] derivati, kod kojih je policiklična jedinica, preko hidantoinskog prstena povezana sa bočnim alkil lancem (tabela 4) [7].

Derivat sa metil supstituentom (jedinjenje 1, tabela 4) deluje citotoksično na karcinom dojke (MCF-7) i debelog creva (SW 620) sa vrednostima IC_{50} (koncentracija koja izaziva 50% inhibicije) od 0,023 μM prema ćelijskoj liniji MCF-7 i IC_{50} = 0,108 μM prema ćelijskoj liniji SW 620, slično kao doksorubicin (IC_{50} = 0,022 μM (MCF-7); IC_{50} = 0,178 μM (SW 620)). Ostala jedinjenja poseduju smanjenu aktivnost zbog povećane lipofilnosti i sternih smetnji na bočnom lancu. Uvođenje krajnje amino ili dialkilamino grupe u ravan alkil bočni lanac, nema uticaja na citotoksičnost prema ćelijskoj liniji MCF-7, dok se citotoksičnost prema ćelijskoj liniji SW 620 povećava (posmatrano u odnosu na doksorubicin). Pomenuto ukazuje da dužina bočnog niza određena brojem metilenskih grupa koje razdvajaju hromoforu i udaljene amino grupe (unutar lanca) ne utiče značajno na citotoksičnost [7].

Tabela 4. 3-(Alkil)(supstituisani alkil)spiro[(dihidroimidazo-2,4-dion)-5,3'-(2',3'-dihidrotieno[2,3-b]nafto-4',9'-dion)] derivati sa citotoksičnom aktivnošću
Table 4. 3-(Alkyl)(alkyl-substituted)spiro[(dihydroimidazo-2,4-dione)-5,3'-(2',3'-dihydrothieno[2,3-b]naphtho-4',9'-dione)] derivatives with cytotoxic activity

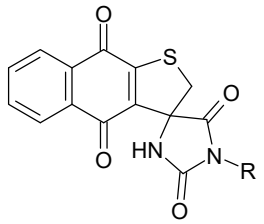

Redni broj	R
1	CH_3
2	CH_2CH_3
3	$(CH_2)_2CH_3$
4	$(CH_2)_3CH_3$
5	$CH(CH_3)CH_2CH_3$
6	$C(CH_3)_3$
7	$(CH_2)_2OH$
8	$(CH_2)_3OH$
9	$(CH_2)_2NH_2$
10	$(CH_2)_3NH_2$
11	$(CH_2)_4NH_2$
12	$(CH_2)_2N(CH_3)_2$
13	$(CH_2)_2N(CH_2CH_3)_2$
14	$(CH_2)_3N(CH_2CH_3)_2$

Uprkos brojnim otkrićima i napredovanjima u terapiji, broj raspoloživih lekova, za tretman leukemije relativno je ograničen. Dejstvo većine antiproliferativnih medikamenata zasniva se na apoptozi (oblik programirane ćelijske smrti koja se javlja u fiziološkim i patološkim procesima u organizmu). Neuspešno odumiranje kancerogenih krvnih ćelija glavni je razlog neizlečenja. Dokazano je da da se primenom ASHD-a (propil-2-(8-(3,4-difluorbenzil)-2',5'-diokso-8-azaspiro[biciklo-[3.2.1]oktan-3,4'-imidazolidin]-1'-il)-acetat) (slika 1), postiže visoka citotoksičnost kod B-ćelijske hronične limfatične leukemije i hronične mijeloidne leukemije [33].

Posredovanje u replikaciji DNA i ćelijskoj deobi predstavlja jedan od načina indukovanja citotoksičnosti od strane ASHD. Takođe, utiče na translokaciju fosfatidilserina iz citoplazme na površinu ćelije, na izmenu potencijala mitohondrijalne membrane, što za posledicu ima povećanje koncentracije proteina koji izaziva apoptozu [33].

Analog somatostatina (slika 2) je modulator aktivnosti G-proteinskih kuplujućih receptora odgovornih za

razvoj maligniteta. Dejstvo se zasniva na inhibiciji ćelijske proliferacije [20].

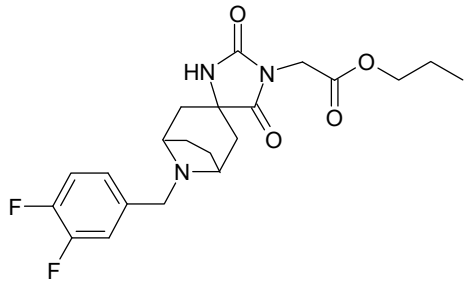

Slika 1. Struktura ASHD-a.
Figure 1. Structure of ASHD.

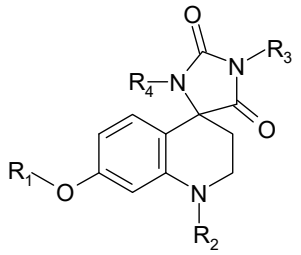

Slika 2. Inhibitor G-proteinskih receptora.
Figure 2. Inhibitor of G-protein receptors.

Azaspiro biciklični derivati hidantoina (tabela 5) su značajni kao potencijalni lekovi u tretmanu karcinoma jajnika (SKOV-3 i OVSAHO), osteosarkoma (LM8 i LM8G7), koji najveći broj metastaza ostvaruju na plućima [34]. Najveću antiproliferativnu aktivnost pokazuje komponenta koja sadrži 3,4-difluorobenzil grupu i 4-(metilsulfonil)benzil grupu, supstituente koji uveliko doprinose aktivnosti [34].

Pri dizajniranju antineoplastika koji bi se primenjivali u terapiji tumora centralnog nervnog sistema, poseban naglasak treba staviti na alkilujuće agense koji su sposobni da prodru kroz krvno-moždanu barijeru [35]. Lipofilnost 5,5-difenilhidantoina zahvaljujući kojoj dobro penetrira kroz krvno-moždanu barijeru i činjenica da ne pokazuje antitumornu aktivnost, bili su podsticaj za proučavanje hidantoina kao potencijalnih nosača nitrogen-mustard farmakofornih grupa u cilju sinteze novih lekova, kandidata za lečenje tumora centralnog nervnog sistema [35]. Tako su nastali antitumorni agensi poput spiromustina (**40**) i cipenhimustina.

Spiromustin (**40**) (spirohidantoin mustard, 3-{2-[bis-(2-hloretil)amino]etil}-1,3-diazaspiro-[4.5]dekan-2,4-dion), je bifunkcionalna alkilujuća supstanca iz grupe nitrogen-mustarda sa antineoplastičnom aktivnošću i lipofilnim svojstvima. U svojoj strukturi sadrži lipofilnu hidantoinsku grupu koja je nosač farmakoforne bis-β-etilamino grupe pri prodiranju kroz krvno-moždanu barijeru. Zbog svoje lipofilnosti, lako prolazi kroz krvno–moždanu barijeru, koncentrišući se u neoplastičnim tkivima. Zahvaljujući navedenoj činjenici, antitumorni je agens u terapiji tumora centralnog nervnog sistema. Veoma brzo uništava monoslojeve, sprečavajući opstanak tumorskih ćelija. Dokazano je da je delotvorniji prema cikličnim ćelijama nego prema ostalim formama. U veoma malim koncentracijama (μM) citotoksičan je prema monoslojevima, dok kod miševa na kojima je testiran ne izaziva smrt [36].

Tabela 5. Azaspirobiciklični derivati hidantoina sa antiproliferativnim svojstvima
Table 5. Azaspirobicyclic hydantoin derivatives with antiproliferative activity

Redni broj	R_1	R_2
1	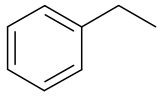	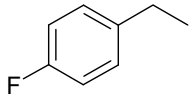
2	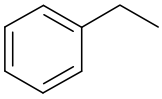	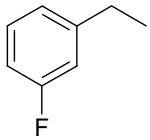
3	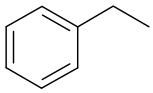	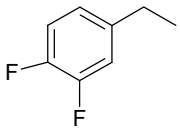
4	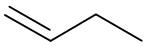	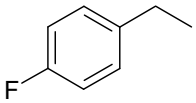
5	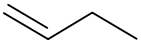	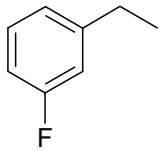
6	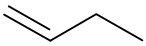	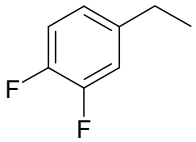
7	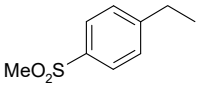	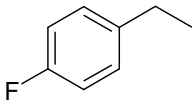
8	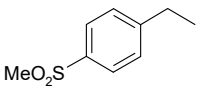	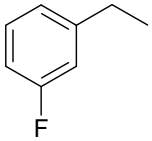
9	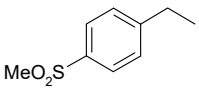	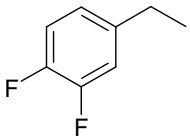

Cipenhimustin (3-{2-[bis-(2-hloretil)amino]etil}-1,3--diazaspiro-[4.4]nonan-2,4-dion), analog je spiromustina (**40**). Modifikacija strukture u odnosu na spiromustin (**40**) sastoji se u zameni spirocikloheksil-grupe spiroalkil-grupom sa jednim C-atomom manje pri čemu je imidazolov prsten molekula hidantoina ostavljen kao nosač *N,N*-bis-(2-hloretil)amino grupe, odnosno, nitrogen-mustard grupe koja je poznata po svojoj antitumornoj funkcionalnosti. Cipenhimustin poseduje značajnu antitumornu aktivnost prema leukemiji L1210, leukemiji P355, melanomu B16, Luisovom (Lewis) karcinomu pluća i intracerebralnom ependimoblastomu [37].

Petočlani prsten kod cipenhimustina je pod naponom u poređenju sa šestočlanim kod spiromustina (**40**), budući da zauzima konformaciju polustolice, dok šestočlani prsten kod spiromustina (**40**) ima stabilnu konformaciju stolice. Utvrđeno je da je cipenhimustin delotvorniji kada se primeni u više doza, nego kada se upotrebi odjednom. Prednost u odnosu na druge nitrogen-mustarde je što prouzrokuje samo blago smanjivanje gustine koštane srži [37].

Karmi (Carmi) je proučavajući antiproliferativnu aktivnost 5-benziliden derivata hidantoina, prema ćelijskoj liniji humanog epidermalnog karcinoma A431, utvrdio da je egzociklična dvostruka veza u položaju 5 hidantoinskog prstena esencijalna za inhibiciju ćelijskog rasta što ukazuje da je krut planaran sistem neophodan za interakciju na ciljnom mestu [38].

Proučavajući antiproliferativnu aktivnost 3-(4-supstituisanih benzil)-5,5-difenilhidantoina i 3-(4-supstituisanih benzil)-5-etil-5-fenilhidantoina, Ušćumlić i saradnici su pokazali značajnu aktivnost ovih molekula prema ćelijskoj liniji humanog karcinoma dojke, MDA--MB-231 i ćelijskoj liniji humanog karcinoma kolona HCT-116. Aktivnost je naročito izražena kada se na fenilnom jezgru kao supstituenti nalaze metil-grupa i halogeni elementi [39–42].

Jedinstvena svojstva fluorovanih molekula dobro su poznata u medicinskoj hemiji [43]. Prisustvo fluora u strukturi biološki aktivnih molekula je od ključne važnosti za njihova farmakološka svojstava. Kod azaspiro bicikličnih sistema, 8-(3,4-difluorbenzil)- i 8-(3,4--dihlorobenzil)-1'-(pent-4-enil)-8-azaspiro[biciklo-[3.2.1]-oktan-3,4'-imidazolidin-2,5-diona (DFH (R_1 = R_2 = = F), DCH (R_1 = R_2 = Cl); slika 3), utvrđeno je da poseduju antitumornu aktivnost prema ćelijskim linijama humane leukemije K562, Reh, CEM i 8E5. Pretpostavka je da pomenuti derivati zaustavljaju rast kancerogenih ćelija preko izmena u DNA replikaciji koje se završavaju apoptozom [43].

Derivati spirohidantoina za lečenje dijabetesa

Dijabetes pripada grupi metaboličkih bolesti. Prati ga hiperglikemija koja je posledica defekta u sekreciji insulina, u delovanju insulina ili u oba procesa. Hronična hiperglikemija stvara oštećenja na mnogim organima, a naročito očima, bubrezima, nervima i srcu. Dugotrajne komplikacije dovode do nastanka retinopatije i mogućnosti gubitka vida, nefropatije koja može završiti otkazivanjem bubrega, periferne nefropatije, gastrointestinalnih i kardiovaskularnih oštećenja. Utvrđeno je da je dijabetes tipa 1 posledica smanjene insulinske sekrecije. Dijabetes tipa 2 (insulinski nezavisni) rezultat je rezistencije na dejstvo insulina u β-ćelijama kao i neadekvatnog izlučivanja insulina. Pored dva najvažnija oblika, razlikuje se i dijabetes koji je posledica genetskog defekta β-ćelija, genetskog defekta u akciji insulina, bolesti pankreasa [44].

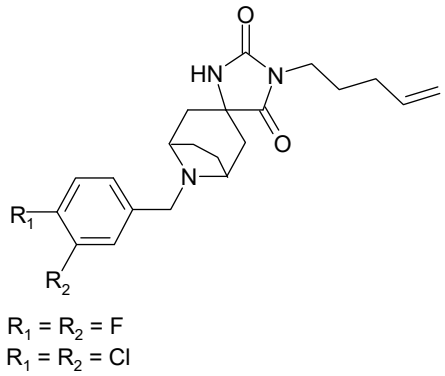

Slika 3. Struktura DFH (R_1 = R_2 = F) i DCH (R_1 = R_2 = Cl).
Figure 3. Structure of DFH (R_1 = R_2 = F) and DCH (R_1 = R_2 = F).

Postoji značajna korelacija između izmenjenog poliolskog puta odgovornog za metabolizam glukoze i dugotrajnog napredovanja komplikacija kao što su: neuropatije, retinopatije, nefropatije i katarakta. Aldoza reduktaza enzim (ARL2) iz familije aldo-keto reduktaza, prvi je enzim na poliolskom putu, koji katalizuje NADPH (nikotinamid adenin dinukleotid fosfat) zavisnu redukciju viška glukoze do sorbitola. Na ovaj način, znatno se povećava koncentracija sorbitola. Njegova akumulacija je spona ka ćelijskom uništenju koje se završava dijabetnim komplikacijama. Inhibitori ALR2 privukli su pažnju kao potencijalni lekovi, obzirom da mogu bezbedno da spreče ili zaustave napredovanje dugotrajnih komplikacija, bez rizika od pojave hipoglikemije jer ne utiču na promenu koncentracije glukoze u krvnoj plazmi [5].

Poznat je veliki broj strukturno različitih komponenata koje inhibiraju aktivnost ALR2, ali su najdelotvorniji derivati spirohidantoina, naročito sorbinil. Dobru inhibitorsku aktivnost poseduju derivati sorbinila kod kojih je atom kiseonika unutar piranskog prstena zamenjen atomom sumpora. Takođe, utvrđeno je da je aktivnost 8-aza analoga sorbinila veća od one koju pokazuje sorbinil [5].

Nesupstituisani i metil supstituisani derivati 2,3-dihidrotiopirano-(2,3-*b*)-piridin-4(4*H*)-ona (jedinjenja 1 i 2, tabela 6) izuzetno su aktivni kao inhibitori ALR2 sa

vrednostima IC_{50} (1, IC_{50} = 0,96 μM; 2, IC_{50} = 0,94 μM) slično onoj kod sorbinila (IC_{50} = 0,65 μM), i za jedan red veličine većoj u odnosu na tolrestat (Tolrestat®) (IC_{50} = = 0,05 μM) [5]. Uvođenjem karboksimetil supstituenta u hidantoinski prsten (jedinjenje 4, tabela 6) smanjuje se aktivnost odgovarajućeg analoga sorbinila. Nesupstituisani derivat (jedinjenje 1, tabela 6) pokazao je izuzetnu *in vivo* aktivnost u sprečavanju nuklearne katarakte kod galaktozemijskih pacova, poput tolrestata [5].

Tabela 6. Spirohidantoinski derivati 2,3-dihidrotiopirano-(2,3--b)-piridin-4-(4H)-ona
Table 6. Spirohydantoin derivatives of 2,3-dihydrothiopyrano--(2,3-b)-piridine-4-(4H)-on

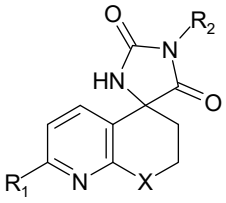

Redni broj	X	R_1	R_2
1	S	H	H
2	S	CH_3	H
3	SO_2	H	H
4	S	H	CH_2COOH

Aktivnost ka inhibiciji aldoza reduktaze pokazali su i derivati spirohidantoina koji su sintetisani iz petočlanih i šestočlanih cikličnih ketona kondenzovanih sa benzenovim prstenom (tabela 7). Nagli pad aktivnosti je uočen kod derivata spirohidantoina sa cikloheptanskom jedinicom [4].

Pravi međusobni odnos aromatičnog i spirohidantoinskog prstena su od ključne važnosti za dobru fiziološku aktivnost. Hidrogenizacija ili uklanjanje benzenovog prstena kao i pomeranje mesta spiro čvora u odnosu na čvorna mesta u kondenzovanom bicikličnom delu sistema, uzrokuje drastičan pad aktivnosti (tabela 7). Benzenov prsten aktivnog jedinjenja je moguće zameniti nekom drugom aromatičnom jedinicom poput: tiofena, furana, piridina. Zamena pirolom se pokazala kao štetna. Supstitucija halogenom u položaju 6 benzodihidropiranskog (hroman) i benzodihidrotiopiranskog (tiohroman) hidantoinskog derivata izuzetno povećava aktivnost [4].

Snažni inhibitori aldoza reduktaze na bazi spiroimidazolona (tabela 8) su od važnosti kao potencijalni agensi u lečenju ili prevenciji određenih komplikacija koje su posledica dijabetesa ili galaktozemije [20].

Derivati spirohidantoina sa antipsihotičkim svojstvima

Depresija je veoma često psihijatrijsko stanje o kojem postoji mnogo različitih neurohemijskih teorija, i za koju se u terapiji koristi veliki broj različitih vrsta lekova. Depresija je najčešći afektni poremećaj. Kreće se od vrlo blagog stanja koje se graniči sa normalnim pa sve do psihotičkih depresija praćenih halucinacijama i deluzijama. Depresija ima dve vrste simptoma: emocionalne (ojađenost, apatija i pesimizam, nedostatak samopouzdanja, neodlučnost, gubitak motivacije) i biološke (usporenost misli i delovanja, gubitak libida, poremećaj sna i gubitak apetita). Postoje dva različita tipa depresivnog sindroma, a to su unipolarna depresija (promene raspoloženja se kreću uvek u istom smeru) i bipolarni afektni poremećaj (depresija se smenjuje sa manijom) [23].

Tabela 7. Derivati spirohidantoina, inhibitori aktivnosti aldoza reduktaze
Table 7. Spirohydantoin derivatives aldose reductase inhibitors

Redni broj	Struktura
1	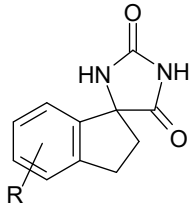
2	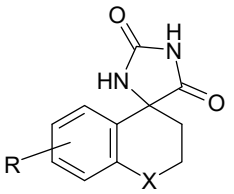 X = CH_2, CH_2CH_2, O, S, SO_2
3	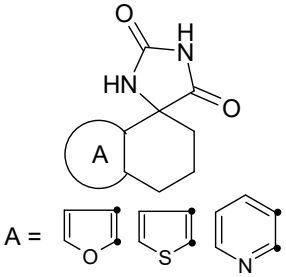
4	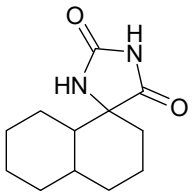
5	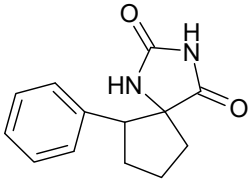

Prema monoaminskoj hipotezi (najvažnija biohemijska teorija depresije), depresiju izaziva funkcionalni manjak monoaminskih transmitera (noradrenalina (NA) i/ili serotonina (5-hidroksitriptamina, 5-HT)) u određenim delovima mozga, dok je manija rezultat njihovog funkcionalnog viška [23]. U terapiji depresije koristi se nekoliko tipova antidepresiva, i to: inhibitori preuzimanja monoamina (triciklični antidepresivi (TCA), selektivni inhibitori preuzimanja 5-HT (SSRI i dr.), inhibitori monoaminooksidaze (MAOI) i atipični antidepresivi (uglavnom neselektivni antagonisti receptora) [23].

Tabela 8. Novi spiro-vezani hidantoini korisni u tretmanu komplikacija kao posledica dijabetesa (diabetes mellitus)
Table 8. A novel spiro-linked hydantoins useful in the treatment of complications arising from diabetes mellitus

Redni broj	Formula
1	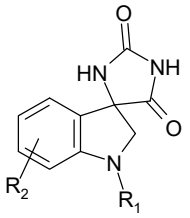
2	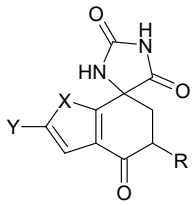 X = O, S Y = H, halogen, alkil-grupa R = H, CH_3, CH_3CH_2

Nezavisno od mehanizma delovanja, zajedničko za sve antidepresive je da se njihovi antidepresivni efekti ispoljavaju tek nakon nekoliko sedmica. Pretpostavka je se da se ovo kašnjenje u delovanju može objasniti inicijalnim porastom ekstracelularnog (vanćelijskog) 5-HT-a rafe jedara (*raphe nuclei*) moždanog stabla (glavni serotonergični izvor) što smanjuje otpuštanje serotonergičnih neurona aktiviranjem somatodendritičkih 5-HT_{1A} autoreceptora (kontrolišu oslobađanje 5-HT) [45]. Nivo serotonina, 5-HT-a, u centralnom nervnom sistemu i regulisanje njegove neurotransmisije povezuje se sa serotoninskim transporterom (SERT), posrednikom u vanćelijskom preuzimanju serotonina iz sinaptičkih pukotina. Po hemijskoj strukturi, SERT je protein čije dejstvo veoma zavisi od koncentracije Na^+. Serotonin, Na^+, Cl^-, formiraju kvaternerni kompleks sa SERT-om, pre nego što budu transportovani preko membrane, potom grade kompleks sa K^+, za transport u suprotnom smeru [46].

Važni pomaci na polju razvoja antidepresiva vode ka uvođenju selektivnih inhibitora preuzimanja 5-HT-a (grupa SSRI) zajedno sa razvojem novih agonista i antagonista sa pre- i post-sinaptičkim adrenergičkim, serotonergičkim i dopaminergičkim dejstvom [45]. Aktuelan pravac u procesu otkrivanja i dizajniranja antidepresiva je dizajniranje liganada sa više ciljeva. Rezultati preklinička ispitivanja ukazuju da bi npr. antidepresiv SSRI tipa koje je ujedno i 5-HT_{1A} antagonist imao poželjne terapijske efekte [46].

5,5-Disupstituisani hidantoini i njihovi *N*-3 modifikovani derivati, pokazuju širok spektar aktivnosti vezanih za centralni nervni sistem, posredstvom raznih receptora poput 5-HT_{1A}, 5-HT_{2A}, dopaminskog D_2, α_1-adrenergičkog, itd. [1]. Rezultati proučavanja 3-(ω-aminoalkil)-5,5-dialkil- (ili 1',5-spirocikloalkil-) hidantoina koji sadrže 1-fenil- ili 1-(2-metoksifenil)piperazin fragment u položaju 3, ukazuju na veliki značaj terminalne hidantoinske jedinice u stabilizaciji 5-HT_{1A} i 5-HT_{2A} receptor/ligand kompleksa [1]. 1',5-ciklopentanspiro-[3-(4-fenil-1-piperazinil)propil]hidantoin (jedinjenje 1; n = 1, m = 3, R = H; tabela 1) i njegov 1',5-cikloheksanspiro analog (jedinjenje 1; n = 2, m = 3, R = H; tabela 1), pokazali su veliki afinitet za 5-HT_{2A} receptor (selektivni 5-HT_{2A} receptor ligandi). 1',5-Cikloheksanspiro-{3-[4-(2-metoksifenil)-1-piperazinil]butil}-hidantoin (jedinjenje 1; n = 2, m = 4, R = *o*-OCH_3; tabela 1) je pokazao veliku aktivnost za 5-HT_{1A} receptore (selektivan 5-HT_{1A} receptor ligand) [11].

Ranih osamdesetih godina dvadesetog veka, počela je terapijska upotreba nove generacije anksiolitičkih lekova. Prvi anksiolitik druge generacije je bio buspiron (Buspar®), arilpiperazinski derivat sa velikim afinitetom prema 5-HT_{1A} i D_2 receptorima. Funkcionalno deluje kao parcijalni antagonist 5-HT_{1A} receptora [2]. Derivati arilpiperazina spadaju u najvažniju grupu 5-HT_{1A} receptorskih liganada [46]. Osim pomenute grupe jedinjenja, treba pomenuti i derivate 2-aminotetralina i benzopiranska jedinjenja [47]. U slučaju arilpiperazinskih derivata kondenzovanih biciklohidantoina, veliki afinitet ka 5-HT_{1A} receptorima je uočen kod derivati sa *o*-OCH_3 i *m*-CF_3 supstituentima na arilpiperazinskom fragmentu (slika 4; R = *o*-OCH_3, *m*-CF_3) [47,48]. Važna strukturna karakteristika pomenutih sistema je prisustvo tri ili četiri metilenske grupe koje razdvajaju biciklohidantoinsku jedinicu od arilpiperazinskog dela. Arilpiperazinski derivati 3-propil-β-tetalonohidantoina (jedinjenje 2, tabela 1) su pokazali umerenu do nisku aktivnost za 5-HT_{1A} receptore [1]. Naglo smanjenje aktivnosti je uočeno kod derivata sa fluor supstituisanom arilpiperazinskom jedinicom [1]. Derivat sa *m*-CF_3 suptituentom na fenilnom jezgru koji je pokazao zadovoljavajuću 5-HT_{1A}/5-HT_{2A} receptorski afinitet, je parcijalni 5-HT_{1A} agonist i antagonist 5-HT_{2A} receptora što ga čini interesantnom potencijalnom psihoaktivnom supstancom [1].

Spiropiperidini pripadaju dobro poznatoj klasi farmakološki važnih molekula koji pokazuju biološku aktiv-

nost prema različitim ciljnim grupama, od inhibitora enzima do blokatora jonskih kanala. Spiropiperidinski molekulski skelet je od posebnog značaja u oblasti G protein-spregnutih receptora (sedam-transmembranski domen receptori) [49]. Zbog toga se ove grupe hemijskih motiva često nazivaju „privilegovane strukture“. Jedna od reprezentativnih grupa spiropiperidina je spiropiperidino-hidantoin, dobro poznati motiv u oblasti serotoninskih receptora [49]. Među važnim analozima spiropiperidino-hidantoina, svakako, treba pomenuti antipsihotik spiperon (Spiroperidol®) koji se koristi u terapiji shizofrenije.

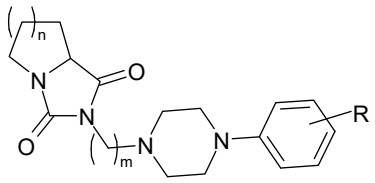

n = 1, 2
m = 3, 4

Slika 4. Biciklohidantoin-arilpiperazini sa afinitetom za 5-HT$_{1A}$ receptore.
Figure 4. Bicyclohydantoin-arylpiperazines with affinity for 5-HT1A receptors

Neurokininski receptori (NK-1, NK-2 i NK-3), poput serotoninskih, pripadaju ciljanoj grupi G protein-spregnutih receptora tako da nije iznenađujuće što neki NK-1 antagonisti sadrže spiropiperidino-hidantoinski fragment kao gradivnu jedinicu [50]. NK-1 receptor je atraktivan cilj za razvoj novih lekova poput analgetika, antidepresiva i antiemetika, koji bi se koristili u terapijskim područjima u rasponu od bola, povraćanja i plućnih bolesti do depresije i anksioznosti [51]. 3,5-Bis(trifluormetil)fenil grupa je u funkciji bioizostera pomenuta u kontekstu nekoliko NK-1 receptorskih liganada. Njena kombinacija sa spiropiperidino-hidantoinskim fragmentom kao središnjim skeletom, bila je osnova za dizajniranje novih potencijalnih neurokininskih-1 receptorskih liganada (tabela 9) [49].

Melanin-koncentrirajući hormonski receptor 1 (MCH-R1) i melanin-koncentrirajući hormon (MCH) koji ga aktivira, su kod sisara uključeni u regulaciju načina ishrane, raspoloženja i energetskog bilansa [52]. S obzirom na to da su oralno aktivni MCH-R1 antagonisti efikasni u kontroli telesne težine kod glodara, za očekivanje je da bi selektivni antagonisti MCH-R1 mogli biti uspešni u tretmanu gojaznosti kod ljudi. U cilju pronalaženja malih molekula koji bi bili pogodni kao selektivni antagonisti MCH-R1, proučavani su i derivati spirohidantoina (tabela 10), koji su pokazali visok afinitet vezivanja i funkcionalnu aktivnost za MCH-R1 [52].

Antimikrobna aktivnost derivata spirohidantoina

Termin antibiotik (antibakterijski lek) odnosi se na supstance koje su metaboliti mikroorganizama kao prirodni proizvodi ili su njihovi polusintetski i sintetski analozi. Deluju antimikrobno, inhibiraju rast (bakteriostatsko dejstvo) ili ubijaju mikroorganizme (baktericidno dejstvo) sa tolerantnom toksičnošću prema domaćinu [53]. Prema mehanizmu dejstva, antibiotike delimo na: antibiotike koji deluju na zid ćelije mikroorganizma, antibiotike koji deluju na membranu citoplazme i antibiotike koji inhibiraju sintezu proteina i nukleinskih kiselina [53].

Tabela 9. Neurokininski-1 receptorski ligandi sa spiropiperidinil-hidantoinskim skeletom
Table 9. Neurokinin-1 receptor ligands with spiropiperidino-hydantoin scaffold

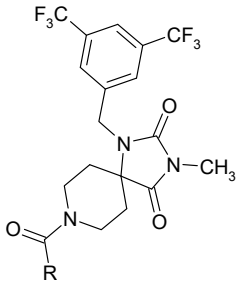

Redni broj	R
1	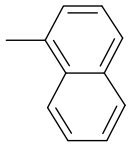
2	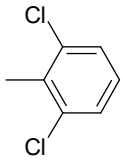
3	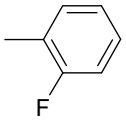
4	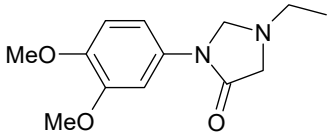
5	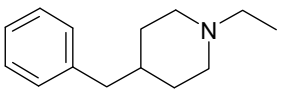

Veoma značajan i složen problem u antimikrobnoj terapiji predstavlja rezistencija (otpornost) patogenih mikroorganizama na dejstvo široko primenjivanih antibiotika. Stoga se u hemijskoj strukturi antibiotika vrše

strukturne modifikacije u cilju povećanja hemijske stabilnosti, proširenja antimikrobnog spektra, povećanja aktivnosti, poboljšanja farmakokinetičkih svojstava i smanjenja toksičnosti [53]. Među sintetskim antimikrobnim lekovima koji su u terapijskoj upotrebi nalazi se i nitrofuranski derivat hidantoina, nitrofurantoin (Furadantin®), antibiotik koji se koristi u terapiji infekcija urinarnog trakta.

Spirofluorenil derivati hidantoina i tiohidantoina (slika 5) se nalaze među malobrojnim derivatima spirohidantoina čija je antimikrobna aktivnost proučavana. 3-Amino-9'-fluorenspiro-5-hidantoin (slika 5; X = O, R = = NH_2) je pokazao izrazitu aktivnost prema Gram-negativnoj bakteriji *Escherichia coli*, dok prema Gram-pozitivnoj bakteriji *Staphylococcus aureus* i gljivici *Candida albicans* nije bio aktivan [54]. 3-Metil-9'-fluorenspiro-5-

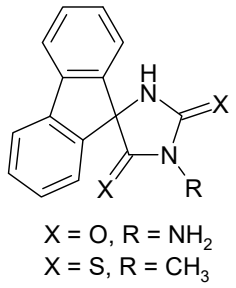

Slika 5. Derivati fluorenilspirohidantoina sa antimikrobnom aktivnošću.
Figure 5. Fluorenylspirohydantoin derivatives with antimicrobal activity.

-(2,4-ditio)hidantoin (slika 5; X = S, R = CH_3) je pokazao potencijal kao antimikrobni agens prema Gram-pozi-

Tabela 10. Derivati spirohidantoina kao antagonisti MCH-R_1 receptora
Table 10. Spirohydantoin derivatives as antagonist of MCH-R_1 receptors

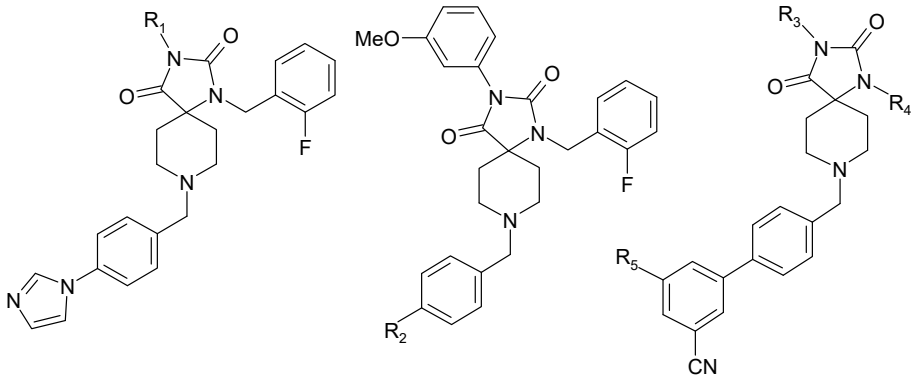

	(**I**)	(**II**)	(**III**)		
Redni broj	R_1	R_2	R_3	R_4	R_5
1	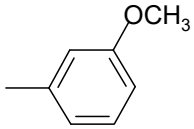	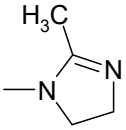	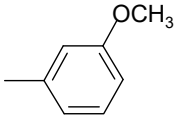	H	H
2	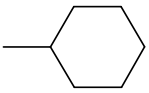	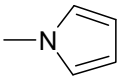	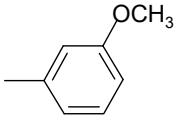	CH_3	H
3	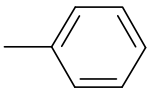	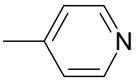	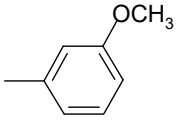	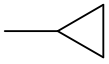	H
4	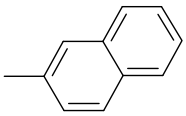	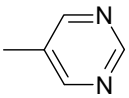	H	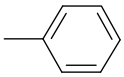	H
5	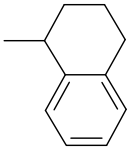	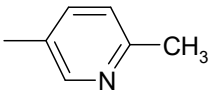	H	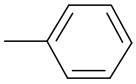	Cl

tivnim bakterijama (*Staphylococcus aureus* i *Bacillus subtilis*), umerenu aktivnost prema gljivici *Candida albicans*, a malu ili nikakvu aktivnost prema Gram-negativnim bakterijama (*Escherichia coli, Salmonella enterica subsp enterica, Pseudomonas aeruginosa*) [55].

Derivati spirohidantoina sa antiinflamatornim svojstvima

Suočen sa napadom patogena, odnosno, organizama koji prouzrokuju bolest (bakterije, virusi, gljivice, prioni, paraziti), organizam sisara može da angažuje odbrambene odgovore čiji razvoj stvara akutnu zapaljensku/imunu reakciju [23]. Kada odbrambene snage nedostaju (na primer u sindromu stečene imunodeficijencije, AIDS) ili su suzbijene lekovima, organizmi koji normalno nisu patogeni, mogu da prouzrokuju oboljenje (oportunističke infekcije) [23]. Osim patogenih agenasa, agensi koji izazivaju zapaljenje mogu biti fizičke (toplota, hladnoća, jonizujuća zračenja i mehanička oštećenja), hemijske (kiseline, baze, toksične supstance) ili traumatske (telesna rana ili povreda) prirode.

Štetni agensi izazivaju direktno oštećenje ćelija, a materije nastale usled poremećenog metabolizma ćelija izazivaju početak procesa zapaljenja [56]. Inflamacija je osnovni i najčešći patološki proces pri kome se lokalno javljaju promene na krvnim sudovima, poremećaji u razmeni tečnosti i izlazak belih krvnih ćelija iz krvi [56]. Ćelije tkiva u kome se odigrava proces inflamacije pokazuju promene od lakih degenerativnih do izumiranja. Ove promene su bitne za početak vaskularnih, eksudativnih (eksudacija – izlazak tečnosti iz ćelija, kapilara i sitnih vena kao i pojava veće količine sluzi na površinama sluznice) i reparativnih procesa koji slede. Oblik, težina i tok zapaljenjskog procesa zavise od vrste i intenziteta štetnog agensa, vrste tkiva i opšteg stanja organizma [56].

U kontekstu NK-1 receptorskih liganada, već je pomenut značaj spiropiperidinskog molekulskog skeleta u oblasti G protein-spregnutih receptora [49]. Hemokinski receptori, takođe, spadaju u G protein-spregnute receptore. Uopšteno govoreći, supstance koje su modulatori hemokinskih receptora su od značaja za prevenciju ili tretman inflamatornih oboljenja, imunoregulatornih oboljenja, reakcije organizma na transplantirani organ, infektivnih oboljenja poput infekcije izazvane HIV-om (virus humane imunodesuficijencije) itd. [3]. Spiropiperidino-hidantoinski fragment se pojavljuje kao središnja jedinica u strukturi molekula koji su modulatori aktivnost hemokinskih receptora podvrste CCR5 (jedinjenje 3, tabela 1) [3]. Ti spirohidantoinski derivati su od potencijalnog značaja za prevenciju ili tretman oboljenja koja su povezana sa modulacijom aktivnosti CCR5 hemokinskih receptora. CCR5 je glavni HIV-1 koreceptor koji kontroliše osjetljivost prema HIV-1 infekciji i bolesti [57]. Interakcija CCR5 koreceptora i virusa HIV-a može da blokira ulaz HIV-a u ćeliju [3].

Derivati spirohidantoina sa analgetskim svojstvima

Bol je subjektivan osećaj koji je teško definisati. Jedan je od najčešćih simptoma uopšte, i predstavlja veliki zdravstveni problem. Prema Međunarodnoj asocijaciji za proučavanje bola (IASP), bol je neprijatno senzorno i emocionalno iskustvo povezano sa stvarnim ili potencijalnim oštećenjem tkiva [58]. Pomenuta definicija uzima u obzir i fizičku i psihičku komponentu bola. Bol je obično direktan odgovor na štetnu pojavu koja prati oštećenje tkiva poput povreda, upala ili karcinoma [23]. Takođe, nezavisno od bilo kog predisponirajućeg faktora može nastati jak bol (npr. trigeminalna neuralgija) ili može trajati dugo nakon izlečenja povrede (npr. fantomski bol u predelu ekstremiteta koji je amputiran). Bol može nastati i bez direktne povrede tkiva, a usled oštećenja mozga i nerava (npr. nakon šloga ili herpesne infekcije) [23]. Ovakav bol je neuropatski po prirodi i ima ga veliki procenat bolesnika. Prema IASP, neuropatski bol je izazvan primarnom lezijom ili disfunkcijom u nervnom sistemu [59]. U osnovi, kad se nerv ošteti, promene u nervnim putevima mogu rezultirati hroničnim bolom čak i u odsustvu daljih podražaja. U slučaju bola kao poremećaja neurološke funkcije malo pomažu standardni analgetici, za razliku od bola čiji je neposredni uzrok poznat [23].

Migrena je čest, hronični, veoma onesposobljavajući neurovaskularni poremećaj, okarakterisan napadima jake, pulsirajuće glavobolje u jednoj polovini glave, disfunkcijom autonomnog nervnog sistema, i (kod nekih pacijenata) pojavom neuroloških simptoma pre ili tokom glavobolje (tzv. aura) [60,61]. Napadi tipično traju od 4 do 72 sata. Ovo neurološko oboljenje pogađa više od 12% odraslih osoba. Kod migrene bez aure, napadi glavobolje su obično praćeni mučninom, povraćanjem, ili osetljivošću na svetlo, zvuk ili pokret [60].

Terapijski pristup u lečenju migrene je individualan. Terapija akutnog napada migrene uključuje nespecifične i specifične lekove. Od nespecifičnih lekova se koriste aspirin, analgetici, nesteroidni antiinflamatorni lekovi itd. Specifična terapija akutnog napada migrene uključuje triptane (derivati triptamina). To su selektivni serotonin receptor agonisti koji aktiviraju 5-HT_{1B} i 5-HT_{1D} receptore [60].

Mnoga istraživanja ukazuju da je ključni igrač u patologiji migrene peptid srodan kalcitoninu (CGRP) [61]. Klinička istraživanja su pokazala da u tretmanu akutne migrene intavenozno primenjeni CGRP receptor antagonist BIBN4096BS ima uporedivu efikasanost sa triptanima [61]. Dakle, dizajn malih molekula koji su oralno raspoloživi nepeptidni CGRP receptor antagonisti značio bi veliki napredak u terapiji akutne migrene.

Benzodiazepinon tetralin-spirohidantoin (slika 6) je prepoznat kao slabo aktivan CGRP receptor antagonist sa konstantom inhibicije CGRP K_i = 4800 nM [62]. Ovaj molekul je poslužio kao osnova za dizajniranje nove

grupe oralno raspoloživih nepeptidnih benzimidazolinon indan-spirohidantoinskih CGRP receptor antagonista (tabela 11) koji su sintetizovani i ispitivana je njhova aktivnost i oralna bioraspoloživost na eksperimentalnim životinjama (pacovi, psi, rezus majmuni) [61]. Osnovna ideja pri dizajniranju ovih molekula je bila da se uz retenciju hidantoinske farmakofore izvrši modifikacija u strukturi benzodiazepinon tetralin-spirohidantoina (slika 6), sa ciljem da se dobije moćan bioraspoloživi CGRP receptor antagonist za lečenje migrene [61].

Svi proučavani derivati su pokazali znatno veću aktivnost u odnosu na benzodiazepinon. Posebno treba istaći 2-piridil supstituisani derivat (jedinjenje 3, tabela 11) koji se pokazao kao moćan CGRP receptor antagonist (CGRP K_i = 21 nM), jedinjenje sa dobrom kombinacijom aktivnosti i farmakokinetike [61]. Osim benzimidazolinon indan-spirohidantoinskih derivata, sintetizovani su i neki benzoksazolinon tetralin- i indan-spirohidantoini koji su imali znatno manju aktivnost u odnosu na benzimidazolinone [61].

Tabela 11. Komponente benzimidazolinona kao antagonisti CGRP receptora
Table 11. Components of benzimidazolinone as antagonists of CGRP receptors

Redni broj	R	Redni broj	R
1	H	7	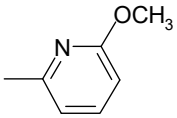
2	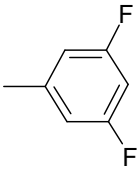	8	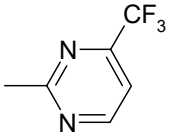
3	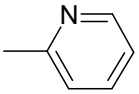	9	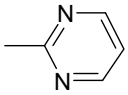
4	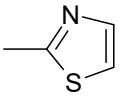	10	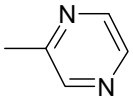
5	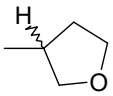	11	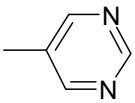
6	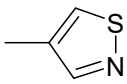	–	–

Derivat indolilspirohidantoina (slika 7) kao inhibitor aktivnosti vaniloidnog receptora 1 (VR1 ili TRPV1), intersantan je u domenu lečenja stanja koja su povezana sa pomenutim receptorom (akutan i hroničan bol, akutan i hroničan neuropatski bol, bol pri akutnoj i hroničnoj upali) [63].

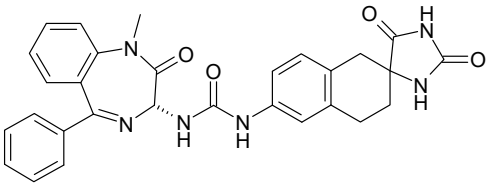

Slika 6. Struktura benzodiazepinon tetralin-spirohydantoina.
Figure 6. Structure of benzodiazepinone tetralin-spirohydantoine.

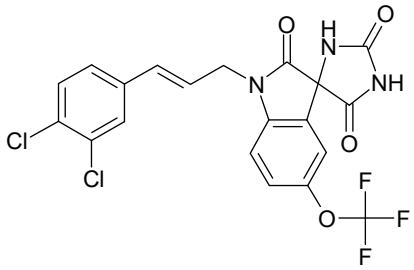

Slika 7. Derivat indolilspirohidantoina, inhibitor aktivnosti vaniloidnog receptora 1 (VR1 ili TRPV1).
Figure 7. Indolylspirohydantoin derivative, compound with vanilloid receptor 1 (VR1 or TRPV1) inhibitor activity.

Zaključak

Spirohidantoin je u osnovi petočlani ciklični ureid koji je lako moguće funkcionalizovati velikim brojem farmakofornih grupa što doprinosi raznovrsnoj fiziološkoj aktivnosti derivata spirohidantoina i njegovih analoga. Zadovoljavajuća lipofilnost supstituisanih spirohidantoina zahvaljujući kojoj dobro prodiru kroz krvno-moždanu barijeru u ćelijske membrane, podsticaj je za proučavanje ovih molekula kao potencijalnih nosača različitih farmakofornih grupa u cilju sinteze novih, potencijalnih lekova u tretmanu različitih bolesti centralnog nervnog sistema. Spirohidantoini i njihovi analozi su važni kao potencijalni antibiotici, antipsihotici, antikonvulzivi, antidijabetici, antiinflamatorni i antikancerogeni lekovi. Od posebnog je značaja postavljanje opštih farmakoloških modela koji bi detaljno prikazali mehanizme farmakološkog delovanja derivata spirohidantoina. Danas se veoma intenzivno radi na dizajniranju postojećih lekova kao i uvođenju novih farmakološki aktivnih supstanci, postavljanjem QSAR modela, koji omogućuju kvantitativnu procenu fiziološke aktivnosti spirohidantoina na osnovu njihovih strukturnih karakteristika.

Zahvalnica

Autori se zahvaljuju Ministarstvu prosvete, nauke i tehnološkog razvoja Republike Srbije na finansijskoj pomoći tokom izrade ovog rada (Projekat 172 013).

LITERATURA

[1] H. Byrtus, M. Pawlowski, B. Duszyńska, A. Wesolowska, E. Chojnacka-Wójcik, A.J. Bojarski, Arylpiperazine derivatives of 3-propyl-β-tetralonohydantoin as new 5-HT_{1A} and 5-HT_{2A} receptor ligands, Pol. J. Pharmacol. **53** (2001) 396–401.

[2] J. Kossakowski, T. Zawasowski, J. Turbo, J. Kleps, Synthesis of *N*-(4-aril-1-piperazinylbutyl)-substituted 7,8-benzo-1,3-diazaspiro-(4,5)-decane 2,4-dione derivatives with potential anxiolytic activity, Farmaco **53** (1998) 169–171.

[3] L.C.C. Kong, C. Moinet, L. Vaillancourt, M. Bubenik, Spirohydantoin compounds and methods for the modulation of chemokine receptor activity, US 2006/0014769 A1 (2006).

[4] R. Sarges, R.C. Schnur, J.L. Belletire, M.J. Peterson, Spirohydantoin aldose reductase inhibitors, J. Med. Chem. **31** (1988) 230–243.

[5] F. Da Settimo, G. Primofiore, C. La Motta, S. Salerno, E. Novellino, G. Greco, A. Lavecchia, S. Laneri, E. Boldrini, Spirohydantoin derivatives of thiopyrano (2,3-*b*)-pyridin-4-(4H)-one as potent *in vitro* and *in vivo* aldose reductase inhibitors, Bioorg. Med. Chem. **13** (2005) 491–499.

[6] D.R. Haines, R.W. Fuller, S. Ahmad, D.T. Vistica, V.E. Marquez, Selective cytotoxity of a system L specific amino acid nitrogen mustard, J. Med. Chem. **30** (1987) 542–547.

[7] I.G. Monterrey, G. Santelli, P. Campiglia, D. Califano, F. Falasconi, C. Pisano, L. Vesci, T. Lama, P. Grieco, E. Novellino, Synthesis and cytotoxic evaluation of novel spirohydantoin derivatives of the dihydrothieno-(2,3-b)-naphtho-4,9-dione system, J. Med. Chem. **48** (2005) 1152–1157.

[8] Q. Zhu, Y. Pan, Z. Hu, R. Li, G. Qiu, W. Xu, X. Ke, L. Wu, X. Hu, Synthesis and potential anticonvulsant activity of new *N*-3- substituted 5,5-cyclopropanespirohydantoins, Eur. J. Med. Chem. **44** (2009) 296–302.

[9] H.J. Patel, J. Sarra, F. Caruso, M. Rossi, U. Doshi, R.A. Stephani, Synthesis and anticonvulsant activity of new *N*-1',*N*-3'-disubstituted-2'*H*,3*H*,5'*H*-spiro-(2-benzofuran--1,4'-imidazolidine)-2',3,5'-triones, Bioorg. Med. Chem. Lett. **16** (2006) 4644–4647.

[10] N. Stoyanov, M. Marinov, Two мethods for spirothiohydantoin synthesis, Acta Chim. Slov. **59** (2012) 680––685.

[11] H. Byrtus, M. Pawlowski, S. Charakchieva-Minol, B. Duszynska, M.J. Mokrosz, J.L. Mokrosz, A. Zejc, 3-(*ω*-Aminoalkyl)-5,5-dialkyl(or spirocycloalkyl-1',5-)hydantoins as New 5-HT1A and 5-HT2A Receptor Ligands, Arch. Pharm. (Weinheim) **329** (1996) 283–290.

[12] E. Naydenova, N. Pencheva, J. Popova, N. Stoyanov, M. Lazarova, B. Aleksiev, Aminoderivatives of cycloalkane-spirohydantoins: synthesis and biological activity, Farmaco **57** (2002) 189–194.

[13] N. Trišović, G. Ušćumlić, S. Petrović, Hydantoins: synthesis, properties and anticonvulsant activity, Hem. Ind. **63** (2009) 17–31.

[14] T. Kimura, Y. Nagao, N-H Stretching vibrations of hydantoin (2,4-imidazolidinedione), its derivatives and related compounds, Bull. Fac. Sci. Tech. Hirosaki Univ. **5** (2003) 11–13.

[15] I. Rivero, E.R. Soto, A.O. Teran, Microwave-assisted synthesis of cycloalkanespirohydantoins and piperidine-spirohydantoins as precursors of restricted α-amino acids, ARKIVOC (2011) 260–271.

[16] E. Ware, The chemistry of the hydantoins, Chem. Rev. **46** (1950) 403–470.

[17] K. Faghihi, K. Zamani, A. Mobinikhaledi, Facile synthesis of hydantoin derivatives under microwave irradiation, Turk. J. Chem. **28** (2004) 345–350.

[18] M. Nieto, A. Philip, J. Poupaert, C. McCurdy, Solution-Phase parallel synthesis of spirohydantoins, J. Comb. Chem. **7** (2005) 258–263.

[19] J. Obniska, H. Byrtus, K. Kaminski, M. Pawlowski, M. Szczesio, J.K. Wojciechowska, Design, synthesis, and anticonvulsant activity of new N-Mannich bases derived from spirosuccinimides and spirohydantoins, Bioorg. Med. Chem. **18** (2010) 6134–6142.

[20] L.K. Abdulrahman, M.M. Al-Mously, M.L. Al-Mosuli, K.K. Al-Azzawii, The biological activity of 5,5'-imidazolidine-2,4-dione derivatives, Int. J. Pharm. Pharm. Sci. **5** (2013) 494–504.

[21] C. Pedregal, G.G. Trigo, J. Eiguero, E.-J. Vincent, R. Faure, Etude de quelques derives N-3-substitues et N-l,N-3-disubstitues de la cyclohexanospirohydantoine, J. Hetero. Chem. **21** (1984) 477–480.

[22] F. Olimpieri, M.C. Bellucci, T. Marcelli, A. Volonterio, Regioselective multicomponent sequential synthesis of hydantoins, Org. Biomol. Chem. **10** (2012) 9538–9555.

[23] H.P. Rang, M.M. Dale, J.M. Ritter, P.K. Moore, Farmakologija, 5. izdanje (urednik srpskog izdanja Todorović, Z.), Data status, Beograd, 2005.

[24] N. Trišović, N. Valentić, G. Ušćumlić, Solvent effects on the structure-property relationship of anticonvulsant hydantoin derivatives: A solvatochromic analysis, Chem. Cent. J. **5** (2011) 1–11.

[25] N. Trišović, T. Timić, J. Divljaković, J. Rogan, D. Poleti, M. Savić, G. Ušćumlić, Synthesis, structural and biological characterization of 5-phenylhydantoin derivatives as potential anticonvulsant agents, Monatsh. Chem. **143** (2012) 1451–1457.

[26] T. Đaković-Sekulić, A. Mandić, N. Trišović, G. Ušćumlić, Structure-Retention Relationship Strudy of HPLC Data of Antiepileptic Hydantoin Analogs, Curr. Comput. Aided Drug Des. **8** (2012) 3–9.

[27] T. Đaković-Sekulić, A. Smolinski, N. Trišović, G. Ušćumlić, Multivariate evaluation of the correlation between retention data and molecular descriptions of antiepicleptic hydantoin analogs, J. Chemometr. **26** (2012) 95––107.

[28] T. Đaković-Sekulić, Z. Lozanov-Cvetković, A. Mandić, G. Ušćumlić, S. Keleman, Quantitative-Structure-Retention Relationship Study of Some 5-Substituted-5-Phenyl Hydantoins, Chromatographia **73** (2011) 51–57.

[29] N. Trišović, N. Valentić, M. Erović, T. Đaković-Sekulić, G. Ušćumlić, I. Juranić, Synthesis, structure and solvato-

chromic properties of pharmacologically active 5-substituted-5-phenylhydantoins, Monatsh. Chem. **142** (2011) 1227–1234.

[30] G.M. Cooper, Elements of human cancer, Jones & Bartlett Learning, Boston, MA, 1992.

[31] Online Cancer Glossary, Amer. Cancer Society, 2015, http://www.cancer.org/cancer/cancerglossary/index (pristupljeno 21/01/2015).

[32] D.W. Kufe, R.E. Pollock, R.R. Weichselbaum R.C. Bast, T.S. Gansle, J.F. Holland, E. Frei (Eds.), Holland-Frei Cancer Medicine, 6th ed., BC Decker, Hamilton, 2003.

[33] C.V. Kavitha, M. Nambiar, P.B. Narayanaswamy, E. Thomas, U. Rathore, C.S.A. Kumar, B. Choudhary, K.S. Rangappa, S.C. Raghavan, Propyl-2-(8-(3,4-difluorobenzyl)-2',5'-dioxo-8-azaspiro[bicyclo[3.2.1]octane-3,4'-imidazolidine]-1'-yl) acetate induces apoptosis in human leukemia cells through mitochondrial pathway following cells cycle arrest, PLoS One **8** (2013) 1–8.

[34] Basappa, C.S. Ananda Kumar, S. Nanjunda Swamy, K. Sugahara, K.S. Rangappa, Anti-tumor and anti angiogenic activity of novel hydantoin derivatives: Inhibition of VEGF secretion in liver metastatic osteosarcoma cells, Bioorg. Med. Chem. **17** (2009) 4928–4934.

[35] G.W. Peng, V.E. Marquez, J.S. Driscoll, Potential central nervous system antitumor agents. Hydantoin derivatives, J. Med. Chem. **18** (1975) 846–469.

[36] Y. Sano, T. Hoshino, R. Bjerkvig, D. F. Deen, The relative resistance of non-cycling cells in 9L Multicellular spheroids to spirohydantoin mustard, Eur. J. Cancer Clin. Oncol. **19** (1983) 1451–1456.

[37] U. Sanyal, S. Bhattacharya, U. Sadhu, S. Dutta, H. Das, M. Ghosh, Evaluation of cypenhymustine, a new anticancer compound, in murine tumour models, Cancer Lett. **70** (1993) 1–6.

[38] C. Carmi, A. Cavazzoni, V. Zuliani, A. Lodola, F. Bordi, P.V. Plazzi, 5-Benzylidene hydantoins as new EGFR inhibitors with antiproliferative activity, Bioorg. Med. Chem. Lett. **16** (2006) 4021–4025.

[39] S. Hmuda, N. Trišović, J. Rogan, D. Poleti, Ž. Vitnik, V. Vitnik, N. Valentić, B. Božić, G. Ušćumlić, New derivatives of hydantoin as potential antiproliferative agents: biological and structural characterization in combination with quantum chemical calculations, Monatsh. Chem. **145** (2014) 821–833.

[40] N. Trišović, B. Božić, A. Obradović, O. Stefanović, S. Marković, Lj. Čomić, B. Božić, G. Ušćumlić, Structure-activity relationship of 3-substituted-5,5-diphenylhydantoins as potential antiproliferative and antimicrobial agents, J. Serb. Chem. Soc. **76** (2011) 1597–1606.

[41] S. Hmuda, N. Trišović, V. Valentić, G. Ušćumlić, Solvent effects on the Structure-Property Relationship of Some Potentially Pharmacologically Active 3-(4-Substituted Benzyl)-5-Ethyl-5-Phenyl and 3-(4-Substituted Benzyl)-5,5-Dyfenilhydantoins, J. Solution. Chem. **40** (2011) 307–319.

[42] A. Obradović, J. Žižić, N. Trišović, B. Božić, G. Ušćumlić, B. Božić, S. Marković, Evaluation of antioxidative effects twelve 3-substituted-5,5-diphenylhydantoins on human colon cancer cell line HCT-116, Turk. J. Biol. **37** (2013) 741–747.

[43] C.V. Kavitha, M. Nambiar, C.S. Ananda Kumar, B. Choudhary, K. Muniyappa, K.S. Rangappa, S.C. Raghavan, Novel derivatives of spirohydantoin induce growth inhibition followed by apoptosis in leukemia cells, Biochem. Pharmacol. **77** (2009) 349–350.

[44] Diagnosis and classification of diabetes mellitus, Diabetes Care **35** (2012) 64–71.

[45] H. Pessoa-Mahana, R. Araya-Maturana, C.B. Saitz, D.C. Pessoa-Mahana, A synthetic overview of molecules with 5-HT1A binding affinities, Mini Rev. Med. Chem. **3** (2003) 77–93.

[46] A. Zagórska, A. Czopek, M. Pawlowski, M. Dybala, A. Siwek, G. Nowak, Serotonin transporter activity of imidazolidine-2,4-dione and imidazo[2,1-f]purine-2,4-dione derivatives in aspect of their acid-base properties, Med. Chem. Res. **11** (2012) 3455–3459.

[47] S.J. Oh, H.J. Ha, D.Y. Chi, H.K. Lee, Serotonin receptor and transporter ligands – Current status, Curr. Med. Chem. **8** (2001) 999–1034.

[48] M.L. Lopez-Rodriguez, M.L. Rosado, B. Benhamu, M.J. Morcillo, A.M. Sanz, L. Orensanz, M.E. Eneytez, J.A. Fuentes, J. Manzanares, Synthesis and structure-activity relationships of a new model of arylpiperazines. 1. 2-[[4-(*o*-Methoxyphenyl)piperazin-1-yl]methyl]-1,3-dioxoperhydroimidazo[1,5-*a*]pyridine: A selective 5-HT_{1A} receptor agonist, J. Med. Chem. **39** (1996) 4439–4450.

[49] K. Bleicher, Y. Wutrich, M. De Boni, S. Kolczewski, T. Hoffmann, A. Sleihgt, Parallel solution- and solid-phase synthesis of spirohydantoin derivatives as neurokinin-1 receptor ligands, Bioorg. Med. Chem. Lett. **12** (2002) 2519–2522.

[50] G. Galley, T. Godel, A. Goergler, T. Hoffmann, S. Kolczewski, S. Roever, 1,3,8-Triazaspiro[4.5]decan-4-one derivatives as neurokinin receptor antagonists, WO 0194346 (2001).

[51] J.M. Humphrey, Medicinal Chemistry of Selective Neurokinin-1 Antagonists, Curr. Top. Med. Chem. **3** (2003) 1423–1435.

[52] M.W. Rowbottom, T.D. Vickers, J. Tamiya, M. Zhang, B. Dyck, J. Grey, D. Schwarz, C.E. Heise, M. Hederick, J. Wen, H. Tang, H. Wang, A. Fisher, A. Aparicio, J. Saunders, V.S. Goodfellow, Synthesis and structure-activity relationships of spirohydantoin-derived small-molecule antagonists of the melanin-concentrating hormone receptor-1 (MCH-R1), Bioorg. Med. Chem. Lett. **17** (2007) 2171–2178.

[53] S. Velimirov, S. Živanov-Stakić, Farmaceutska hemija 2. deo, Farmaceutski fakultet, Beograd, 2006.

[54] P. Marinova, M. Marinov, Y. Feodorova, M. Kazakova, D. Georgiev, V. Lekova, P. Penchev, N. Stoyanov, Synthesis, cytotoxicity and antibacterial activity of 3-amino-9'-fluorenespiro-5-hydantoin, Compt. Rend. Acad. Bulg. Sci. **67** (2014) 513–518.

[55] P. Marinova, M. Marinov, Y. Feodorova, M. Kazakova, A. Slavchev, D. Blazheva, V. Sarafian, I. Nikolova, N. Stoyanov, Synthesis, characterization, *in vitro* antiproliferative and antimicrobial study of 3-methyl-(9'-fluorene)-

spiro-5-(2,4 dithiohydantoin), Sci. Technol. **4** (2014) 112–117.

[56] Medicinski leksikon (glavni urednik Kostić, A), 6. doštampano izdanje, Medicinska knjiga, Beograd – Zagreb, 1988.

[57] P.M. Murphy, M. Baggiolini, I.F. Charo, C.A. Hébert, R. Horuk, K. Matsushima, L.H. Miller, J.J. Oppenheim, C.A. Power, International Union of Pharmacology. XXII. Nomenclature for Chemokine Receptors **52** (2000) 145––176.

[58] J. Ivanušić, A. Harangozo, Psihološko-psihijatrijski aspekti lijecenja boli, Medicus **23** (2014) 15–22.

[59] M. Cvijanović, S. Simić, S. Banić-Horvat, Z. Jovin, P. Slankamenac, M. Ilin, Savremeni tretman neuropatskog bola, Med. Pregl. **64** (2011) 443–447.

[60] P.J. Goadsby, R.B. Lipton, M.D. Ferrari, Migraine – Current understanding and treatment, N. Eng. J. Med. **346** (2002) 257–270.

[61] I.M. Bell, R.A. Bednar, J.F. Fay, S.N. Gallicchio, J.H. Hochman, D.R. McMasters, C. Miller-Stein, E.L. Moore, S.D. Mosser, N.T. Pudvah, A.G. Quigley, C.A. Salvatore, C.A. Stump, C.R. Theberge, B.K. Wong, C.B. Zartman, X.-F. Zhang, S.A. Kane, S.L. Graham, J.P. Vaccaa, T.M. Williams, Identification of novel, orally bioavailable spirohydantoin CGRP receptor antagonists, Bioorg. Med. Chem. Lett. **16** (2006) 6165–6169.

[62] T.M. Williams, C.A. Stump, D.N. Nguyen, A.G. Quigley, I.M. Bell, S.N. Gallicchio, C.B. Zartman, B.-L. Wan, K. Della Penna, P. Kunapuli, S.A. Kane, K.S. Koblan, S.D. Mosser, R.Z. Rutledge, C. Salvatore, J.F. Fay, J.P. Vacca, S.L. Graham, Non-peptide calcitonin gene-related peptide receptor antagonists from a benzodiazepinone lead, Bioorg. Med. Chem. Lett. **16** (2006) 2595–2598.

[63] L. Horoszok, C. Leung, M. Tomaszewski, C. Walpole, Use of spiro [imidazolidine-4, 3'-indole] 2, 2', 5' (lH) triones for treatment of conditions associated with vanilloid receptor 1, WO 2007/091946 Al (2007).

SUMMARY

SYNTHESIS, STRUCTURE AND PROPERTIES OF BIOLOGICAL ACTIVE SPIROHYDANTOIN DERIVATIVES

Anita M. Lazić, Nataša V. Valentić, Nemanja P. Trišović, Slobodan D. Petrović, Gordana S. Ušćumlić

Department of Organic Chemistry, Faculty of Technology and Metallurgy, University of Belgrade, Karnegijeva 4, 11120 Belgrade, Serbia

(Review paper)

Spirohidantoins represent an pharmacologically important class of heterocycles since many derivatives have been recognized that display interesting activities against a wide range of biological targets. First synthesis of cycloalkanespiro-5-hydantoins was performed by Bucherer and Lieb 1934 by the reaction of cycloalkanone, potassium cyanide and ammonium-carbonate at reflux in a mixture of ethanol and water. QSAR (Quantitative Structure–Activity Relationship) studies showed that a wide range of biological activities of spirohydantoin derivatives strongly depend upon their structure. This paper describes different methods of synthesis of spirohydantoin derivatives, their physico-chemical properties and biological activity. It emphasizes the importance of cycloalkanespiro-5-hydantoins with anticonvulsant, antiproliferative, antipsychotic, antimicrobial and antiinflammatory properties as well as their importance in the treatment of diabetes. Numerous spirohydantoin compounds exhibit physiological activity such as serotonin and fibrinogen antagonist, inhibitors of the glycine binding site of the NMDA receptor also, antagonist of leukocyte cell adhesion, acting as allosteric inhibitors of the protein-protein interactions. Some spirohydantoin derivatives have been identified as antitumor agents. Their activity depends on the substituent presented at position *N*-3 of the hydantoin ring and increases in order alkene > ester > ether. Besides that, compounds that contain two electron withdrawing groups (*e.g.*, fluorine or chlorine) on the third and fourth position of the phenyl ring are better antitumor agents than compounds with a single electron withdrawing group.

Keywords: Spirohydantoins • Synthesis • Physicochemical properties • Biological activity

Automatski uredjaji za elektohemijsku dezinfekciju vode sa pothlađivanjem elektolita

Tomislav Lj. Trišović[1], Miroslav D. Spasojević[2], Milica M. Gvozdenović[3], Branimir Z. Jugović[1], Lidija D. Rafailović[4]

[1]*Institut tehničkih nauka Srpske akademije nauka i umetnosti, Beograd, Srbija*
[2]*Agronomski fakultet, Univerzitet u Kragujevcu, Čačak, Srbija*
[3]*Tehnološko-metaluruški fakultet, Univerzitet u Beogradu, Beograd, Srbija*
[4]*Center of Electrochemical Surface Technology CEST, Wr.Neustadt, Austria*

Izvod

Dezinfekciona sredstva za tretman voda koja se najčešće primenjuju zasnivaju se na hloru i jedinjenjima hlora. Sva jedinjenja hlora se tokom skladištenja raspadaju i gube punu efikasnost u procesu dezinfekcije. Osim razgranje, dodatni problemi su transport, skladištenje i rukovanje ovim hemikalijama. U svetu se poslednjih godina dosta radi na razvoju *in situ* uređaja za proizvodnju jedinjenja hlora, posebno uređaja razvijenim da *in situ* proizvode hlor-dioksid ili natrijum-hipohlorit. Najjednostavniji uređaji za dobijanje hipohlorita se sastoje od izvora jednosmerne struje, elektolizera, rezervoara razblaženog rastvora natrijum-hlorida i sistema za doziranje rastvora. Projektovanje samog uređaja podrazumeva određivanje i održavanje optimalnih parametara za elektrohemijsku sintezu u samom elektrolizeru tokom kontinualne proizvodnje. Komercijalni aspekt izrade uređaja podrazumeva optimizaciju sklopa sa aspekta odnosa cene, kvaliteta i efikasnosti u cilju konkurentnosti uređaja na tržištu. Cilj rada je bio da se dodatno razvije elektohemijski uređaj koji proizvodi hipohlorit na osnovu novog tehnološkog projekta koji podrazumeva i ugradnju novih komercijalnih komponenti koje su sastavni delovi kompletnog uređaja. Ovakav uređaj je ispitivan u ekstremnim uslovima eksploatacije (temperatura ulazne vode preko 20 °C, sobna temperatura preko 38 °C i vlažnosti vlazduha od 90%), što je uslov za njegovu uspešnu komercijalizaciju. Rezultati dobijeni u takvim uslovima pokazuju da je moguće dobiti neophodnu koncentraciju hipohlorita u izlaznom rastvoru od 0,85%.

Ključne reči: *dezinfekcija, elektohlorinatori, aktivan hlor, elektohemijski tretman vode*.

Dostupno na Internetu sa adrese časopisa: http://www.ache.org.rs/HI/

STRUČNI RAD

UDK 628.166:544.6:546.13

Hem. Ind. **70** (2) 201–207 (2016)

doi: 10.2298/HEMIND140822026T

Postupak dezinfekcije pomoću aktivnog hlora (dinamička smeša hipohloraste kiseline i natrijum-hipohlorita) proizvedenog elektrolizom 3% rastvora NaCl na mestu upotrebe je pogodniji od ostalih postupaka dezinfekcije vode, ne samo sa aspekta ekonomske isplativosti i efikasnosti, već i sa ekološkog aspekta. Uređaji koji proizvode aktivan hlor procesom elektrolize su razvijani u poslednjih dvadesetak godina, posebno od 1998. Godine, kada je Evropska zajednica donela zakonsku zabranu transporta gasovitog i tečnog hlora. Iz ovog razloga će sadašnji konvencionalni postupak upotrebe hlora morati da se ukine i u Srbiji. Elektroliza ne zahteva posebne mere zaštite, a efikasnost nastalog natrijum-hipohlorita je jednaka ili bolja od učinka gasovitog hlora. Prema proračunima, sam postupak je, iako zahteva konstrukciju i izradu elektrolizera, dugoročno gledano isplativiji, i u smislu početne investicije kao i zbog troškova kontinualne eksploatacije, od konvecionalnog postupka hlorisanja koji se trenutno koristi kod nas. Ovi elektrolizeri se, u zavisnosti od konstrukcionih zahteva, mogu koristiti u javnim i privatnim vodovodima, bazenima za rekreaciju i za industrijske potrebe.

Proizvodnja „hlora“ na mestu korišćenja predstavlja najjeftiniju, pouzdanu i sigurnu alternativu postojećim sredstvima za dezinfekciju. Poznato je nekoliko konstrukcija elektolizera [1–4] za *in situ* proizvodnju aktivnog hlora, kao što su: protočna, šaržna i recirkulaciona. Postoje i rešenja uređaja sa lagerovanjem dobijenog proizvoda – aktivnog hlora, i bez njega. Primena ovih uređaja zavisi od zahteva mesta, kapaciteta i tehno-ekonomske analize isplativosti svakog uređaja ovog tipa. Generalno se može konstatovati da, ukoliko je potrebno koristiti uređaje manjeg kapaciteta, konstrukcija zahteva uređaje protočnog tipa sa nižim nivoom automatike i bez lagerovanja dobijenog proizvoda jer su takvi uređaji jeftiniji i mogu se lakše komercijalizovati.

Cilj rada je da se unapredi uređaj za proizvodnju natrujum-hipohlorita jednostavne konstrukcije sa što manje merno-regulacionih komponenata, ali tako da se ne ugrozi njegova funkcionalnost, pouzdanost i eks-

Prepiska: T.Lj. Trišović, Institut tehničkih nauka Srpske akademije nauka i umetnosti, Knez Mihajlova 35/4, 11000 Beograd, Srbija.
E-pošta: tomislav.trisovic@itn.sanu.ac.rs
Rad primljen: 22. avgust, 2014
Rad prihvaćen: 5. maj, 2011

ploatacioni vek. U svetu postoje rešenja za proizvodnju natrijum-hipohlorita elektolizom razblaženih rastvora hlorida u standardnom elektolizeru sa visokim nivoom automatike, kao i membranskom elektolizom kao najsloženiji uređaji. Najjeftinija, i sa aspekta bezbednosti najprihvatljivija za potrošačko tržište, je elektoliza razblaženih rastvora hlorida sa standardnim elektolizerima. Iz ovog razloga je odlučeno da se projektuje nova konstrukcija uređaja sa elektolizom razblaženih rastvora hlorida sa standardnim elektolizerom.

Uređaj se sastoji iz nekoliko desetina komponenata (elektodni materijali, releji, programabilni logički kontroleri, strujna napajanja, senzorski elementi, pretvarači, rashladni sistemi, izmenjivači toplote, dozirni uređaji, itd.) koje se mogu pronaći na tržištu. Proizvođači ovih komponenata stalno unapređuju svoje stare i nude nove proizvode. U tom smislu neophodna je stalno osvežavanje uređaja sa novim komponentama i konstruisanje savremenijih uređaja. Pored izbora komponenti isto tako je važno i konstruktorsko rešenje koje će pored jednostavnosti kostrukcije biti pouzdano i konkurentno na tržištu. S obzirom na to da je cena instalacije izmenjivača toplote uz elektolizer i cena uređaja za klimatizaciju prostora visoka, ideja je da se u konstruisanju novog uređaja ova komponenta uređaja zameni sa jednostavnim rashladnim uređajem sa koaksijalnim izmenjivačem toplote koji ima podhlađuje rastvor neposredno na ulasku u sam elektolizer. Ovo konstukciono rešenje omogućilo bi da se uređaj instalira u neklimatizovanim prostorijama a da se ne odigrava termohemijska reakcija (temperature iznad 38 °C) prevođenja hipohlorita u hlorat.

EKSPERIMENTALNI DEO

Naše konstrukciono rešenje se sastoji od nekoliko celina: elektolizer, podhlađivač, elektoormar sa ispravljačkom stanicom i automatikom, dozirni sistem, rezervoar kuhinjske soli, rezervoar hipohlorita, pomoćna posuda sa omekšanom vodom, ventilacioni sistem i uređaj za hemijsku pripremu vode. Blok shema uređaja je data na slici 1. Omekšana voda i zasićen rastvor NaCl se mešaju u odnosu 10:1 tako da se kontinualno pravi 3% rastvor. Takav rastvor se neposredno pred ulazak u elektolizer podhlađuje u koaksijalnom izmenjivaču do temperature od oko 5 °C. U elektolizeru se kuhinjska so, tj. hloridi, na anodi oksiduju, hidrolizuju u natrijum-hipohlorit, dok se na katodi redukuje vodai izdvaja gasoviti vodonik. Oba proizvoda gravitacionim strujanjem ulaze u rezervoar sa hipohloritom. Na vrhu rezervoara, u praznoj zoni, nalazi se ejektor koji, uz pomoć ventilatora, pravi podpritisak u rezervoaru sa hipohloritom sa ciljem da se odstrani gasoviti vodonik iz rezervoara. Razblaženi rastvor aktivnog hlora se pomoću dozirnog sistema dozira iz rezervoara u cevovod u količini neophodnoj da je ostvari proces dezinfekcije vode (najčešće 1 mg aktivnog hlora po litru vode). Ispitivanja uređaja su obuhvatila funkcionalnost pojedinih komponenata kao i funkcionalnost uređaja za *in situ* dezinfekciju aktivnim hlorom. Glavni cilj je bio da se ispita rad elektolizera u smislu dobijanja najvećeg iskorišćenja u najekstremnijim uslovima povišene temperature i vlage. U slučaju porasta temperature rastvora preko 38 °C dolazi do neželjene reakcije prelaska natrijum-hipohlorita u hlorat. Vlaga nepovoljno utiče na vek svih električnih komponenata. Iz tih razloga, ispitivanja su izvršena u uslovima povišene sobne temperature, 38

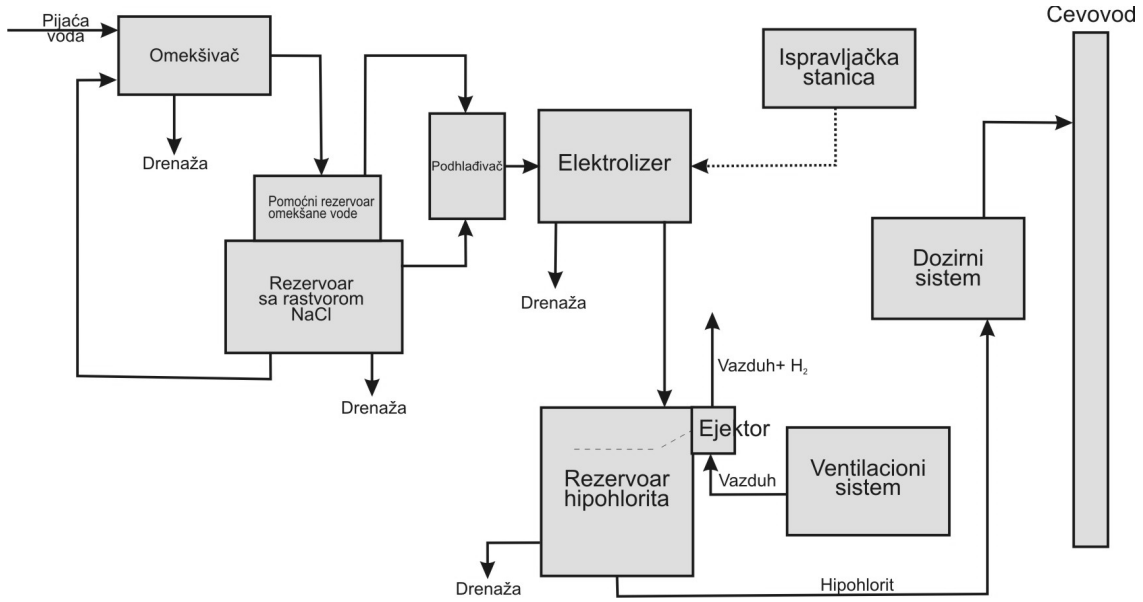

Slika 1. Blok shema uređaja za kontinualnu proizvodnju natrijum-hipohlorita sa pothlađivanjem elektolita.
Figure 1. Block diagram of the device for the continuous production of active chlorine with cooling of the electrolyte.

°C, i relativne vlažnosti 90% u mašinskoj prostoriji gde je smešten uređaj. Po startovanju uređaja merena je temperatura vode za hlađenje na ulazu i izlazu iz koaksijalnog izmenjivača toplote i temperatura rastvora aktivnog hlora na izlazu iz elektolizera. Takođe je praćena i jačina struje svakog pojedinačnog seta elektoda u elektolizeru (ukupno dva seta elektoda, slika 2) u periodu od trenutka uključenja elektolizera do dostizanja stacionarne temperature rastvora na izlazu iz elektolizera.

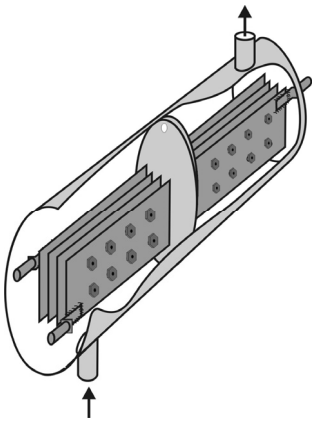

Slika 2. Sklop – presek dupleks elektolizera kapaciteta 2×30 g natrijum-hipohlorita/h.
Figure 2. Assembly –Cross-section of duplex elektolyzer, 2×30 g/h, for the continuous production of active chlorine.

Komercijalni elektrolizeri su obično tipa ramske filer prese ili cevni elektrolizeri. Za potrebe ispitivanog uređaja projektovan je i izrađen elektrolizer na osnovu tehničkih karakteristika komercijalnih katalizatora anoda i katoda, $RuO_2/IrO_2/TiO_2$ (SC-DSA) na sledeći način. Konstruisan je cevni elektrolizer sa dve komore i dva seta elektroda. Svaki set elektroda se sastoji od četiri ploče koje su obostrano aktivirane $RuO_2/IrO_2/TiO_2$ katalizatorom. Sklopni crtež elektolizera je dat na slici 2. Elektrolizer – generator natrijum-hipohlorita, predstavlja osnovnu komponentu uređaja. U njemu se vrši elektroliza 3% rastvora NaCl pri čemu se dobija 0,8–1,0% rastvor NaClO.

Merenjem osnovnih parametara rada elektolizera usklađeni su parametri tehnološkog procesa [4,5] kao što su koncentracija hlorida i protok elektolita kroz elektolizer, optimalna temperatura na ulazu i izlazu elektrolizera i gustina struje.

Elektrolizer cevnog tipa sa plastičnim kućištem sadrži anode i katode sa aktivnom prevlakom specijalno razvijenom za primenu u elektrolizi razblaženih rastvora NaCl, koja omogućava iskorišćenje struje do 85%. Elektrodni razmak je 3 mm, dok su elektode vezane bipolarno. Na sredini cilindričnog kućišta nalazi se perforirana pregrada koja deli kućište elektrolizera na dva jednaka dela, slika 1. Elektolizer se postavlja u horizontalni položaj. Na dnu cilindričnog kućišta elektolizera ulazi podhlađeni rastvor, a na suprotnom kraju, na vrhu elektrolizera, izlazi. Na samom izlazu iz elektrolizera ugrađena je temperaturna sonda koja je povezana sa automatikom na kontrolnoj tabli, koja omogućava prestanak rada elektrolizera kada se dostigne gornja grnica temperature elektrolita od 38 °C.

Napajanje koaksijalnog izmenjivača toplote elektrolitom, ostvaruje se dozirnim pumpama, a iz njega elektolit gravitaciono ulazi u elektrolizer, slika 2.

Dva nezavisna seta elektroda napajaju se pomoću dva nezavisna izvora jednosmerne struje. Ovakva konstrukcija omogućava da u slučaju bilo kakvog kvara na elektrolizeru ili napajanju, bar jedan set bude u funkciji dok se ne ostvari popravka drugog modula sa neispravnim setom. Neophodno je takođe izabrati i pouzdane dozatore (dozir pumpe, regulatore protoka, ejektore,...) koji će kontinualno dozirati rastvor kuhinjske soli (30 g L^{-1}) kako bi iskorišćenje struje bilo maksimalno. Sa smanjenjem koncentracije NaCl u rastvoru, favorizuje se oksidacija vode pa zbog toga opada iskorišćenje struje za dobijanje natrijum-hipohlorita i raste utrošak energije po jedinici dobijenog proizvoda. Kontinualno napajanje odgovarajućom strujom i kontinualno napajanje elektolitom su dva najvažnija faktora za visoko iskorišćenje struje i dobijanje 1,0% rastvora hipohlorita.

Pored jačine struje elektrolize i koncentracije NaCl, važan faktor je i temperatura elektrolita zbog uticaja na vrednost anodnog potencijala i na anodno iskorišćenje struje po natrijum-hipohloritu. Anodni potencijal opada sa povišenjem temperature dok iskorišćenje struje po hipohloritu raste do 50 °C, a potom opada zbog intenziviranja konverzije hipohlorita u hlorat [5,6]. Optimalan temperaturni interval za proizvodnju hipohlorita je od 25 do 38 °C. S obzirom na to da se deo električne energije u elektrolizeru konvertuje u toplotu neophodno je da temperatura elektrolita na ulazu bude bar za 15 °C niža u odnosu na optimalan temperaturni interval, tj. najviše 20 °C, kako bi na izlazu iz elektrolizera bila od 35 do 38 °C.

Elektrohemijski reaktor je projektovan na osnovu analize komercijalnih anodnih i katodnih materijala koje proizvode poznate multinacionalne kompanije (DeNora, Eltech, itd.), kao i kinetičkih i operativnih parametara: elektrodne prenapetosti, pada napona u elektrolitu, katodnog, anodnog i ukupnog iskorišćenja struje i potrošnje energije po jedinici proizvoda natrijum-hipohlorita. Utvrđena je optimalna konstrukcija i optimalne vrednosti tehnoloških parametara procesa. Ustanovljeno je iz literaturnih podataka [7] da najbolja elektrohemijska svojstva poseduje titanska anoda sa prevlakom rutenijum-, iridijum- i titan-oksida [8]. Pri elektolizi rastvora sastava 30 g L^{-1} NaCl na 25 °C i pH 7,0, pri gustini struje od 1000 A m^{-2} postiže se visoko anodno iskorišćenje struje od 85% [9,10].

U tom cilju, projektovan je uređaj kojim se elektroliza izvodi pri gore navedenim parametrima uzimajući u obzir varijacije temperature okoline i temperature ulaznog elektrolita koje mogu biti i preko 40 °C. Da bi se održali optimalni parametri procesa elektrolize, a s obzirom na to da temperatura tokom rada uređaja raste i da su u mašinskim prostorijama gde se uređaji obično instaliraju veoma visoke sobne temperature, čak i preko 40 °C, projektovan je uređaj sa pothlađivanjem elektolita dat u blok shemi na slika 1.

Na slici 1 je prikazan hidraulički tok rastvora koji prolazi kroz komponente uređaja. Voda iz vodovodne mreže ulazi u omekšivač, gde se uklanjaju joni kalcijuma i magnezijuma. Preko nivostat plovka se napaja rezervoar sa koncentrovanim rastvorom NaCl. Dozirna pumpa manjeg kapaciteta dozira koncentrovani rastvor NaCl u pothlađivač sa jedne strane, dok sa druge strane dozirna pumpa većeg kapaciteta dozira iz omekšanu vodu. Mešanjem vode i rastvora soli dobija se 3% rastvor koji se u rashladnom uređaju ohladi tako da temperatura rastvora nije viša od 10 °C. Ohlađeni rastvor gravitaciono struji kroz elektrolizer. Pod uticajem jednosmerne električne struje niskog napona dolazi do oksido–redukcijskih procesa koji na izlazu iz uređaja proizvedu 0,8 do 1,0% rastvor natrijum-hipohlorita. Vodonik se kao sporedni proizvod ejektorom odstranjuje u atmosferu pomoću ventilacionog sistema. Nastali hipohlorit se skladišti u rezervoaru hipohlorita koji može imati zapreminu za višednevno korišćenje. Koncentrovan rastvor sadrži oko 10000 mg L^{-1} aktivnog hlora, koji se pomoću dozirnog sistema injektira u vodu koja se dezinfikuje. Ukoliko se dezinfekcija sprovodi na vodovodu, sa jednim litrom rastvora aktivnog hlora može se dezinfikovati 16000 L vode dostižući koncentraciji aktivnog hlora od oko 0,5 mg L^{-1}.

Da bi se proces kontuinualno odigravao i održavao u projektovanim parametrima neophodna je automatika koja omogućuje kontinualan rad bez nadzora čoveka (slika 3).

Omekšanom vodom se kontinualno snabdeva rezervoar i rezervoar sa NaCl. Iz rezervoara vode se dozirnom pumpom 1 voda dozira u podhlađivač elektrolita – hladnjak. Na posudi sa vodom su montirana dva nivostata za minimum i maksimum. Minimum nivostat alarmira i zaustavlja rad uređaja u slučaju da je iz nekog razloga nestalo snabdevanje omekšanom vodom, čime se sprečava rad pumpe na prazno i sprečava se i da elektrolizer radi, a da ne postoji optimalan protok elektrolita kroz njega. Maksimum nivo indicira da je došlo do kvara nivostat plovka i da voda ulazi nekontrolisano u pomoćnu posudu. Koncentrovani rastvor NaCl se transportuje pomoću pumpe 2 u koaksijalni izmenjivač toplote. Na potisu pumpe 2 se nalazi indikator protoka pomoću kog se prati da li pumpa radi. Ovo je neophodno kao zaštita elektrolizera koji bi se trajno oštetio ukoliko se ne snabdeva projektovanom protokom rastvora NaCl. Na izlazu iz koaksijalnog izmenjivača nalazi se sonda termoregulatora koji upravlja radom rashladnog uređaja koji bi trebalo stalno da obezbeđuje temperaturu ulaznog hloridnog rastvora najviše 10 °C. Uređaj za pothlađivanje rastvora potpuno nezavisno radi od automatike uređaja i sa njime upravlja samo termoregulator. Na izlazu iz elektolizera se nalazi termo sonda „T-max“ koja meri temperaturu dobijenog aktivnog hlora. Ukliko je temperatura izlaznog rastvora aktivnog hlora veća od 38 °C uređaj se isključuje. Razlog isključenja može biti neispravnost pumpe 1 ili 2, ili neispravnost uređaja za pothlađivanje.

U rezervoaru sa natrijum-hipohloritom se nalaze tri nivostata. Najniži, „nivostat minimum“, sprečava da

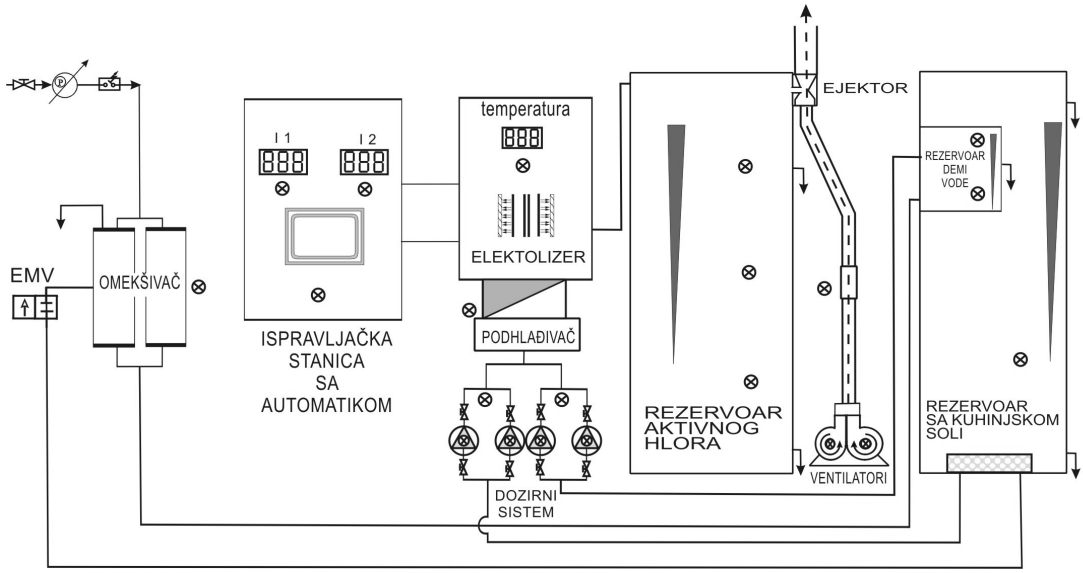

Slika 3. Memo-shema uređaja za kontinualnu proizvodnju natrijum-hipohlorita sa pothlađivanjem elektolita.
Figure 3. Memo-scheme of the device for continuous production of active chlorine with cooling of the electrolyte.

dozirna pumpa 3 koja dozira natrijum-hipohlorit u vodovod radi "na suvo". Ovo je slučaj ekstremno velike potrošnje kada uređaj ne može da proizvede dovoljno natrijum-hipohlorita. Srednji, „nivostat startni minimum", uključuje uređaj sve dok se nivo natriujum-hipohlorita u rezervoaru aktivnog hlora ne podigne do nivoa „zaustavni maksimum" kada se uređaj isključuje.

Sam elektrolizer i rezervoar natriujum-hipohlorita se održavaju pod blagim podpritiskom zahvaljujući ventilacionom sistemu sa ejektorom. Ventilacioni sistem poseduje indikator protoka vazduha. U slučaju da nema protoka vazduha kroz ventilacioni vod, vodonik se ne odstranjuje u dovoljnoj meri pa se u tom slučaju uređaj isključuje i ulazi se u „alarmno stanje 2" (isključuje se samo proizvodnja natrijum-hipohlorita dok se njegovo doziranje nesmetano obavlja).

Proizvedeni natrijum-hipohlorit se iz rezervoara aktivnog hlora transportuje dozirnom membranskom pumpom 3 i ubrizgava u vodovodnu cev. Kontrola nivoa rezidualnog hlora se obavlja pomoću redoks elektrode i prikazuje na displeju kontrolera koji upravlja radom dozirne pumpe na osnovu podešene gornje i donje vrednosti redoks potencijala.

Dva nezavisna seta elektroda elektrolizera napajaju se iz dva nezavisna izvora struje tipa SPS (prekidački izvor jednosmerne struje) sa strujom od 14 A pri naponu od oko 12 V. Indikacija rada svakog napajanja pa time i elektrolizera se prati na digitalnim ampermetrima koji pokazuju trenutnu vrednost jačine struje.

Kompletno automatsko vođenje procesa rada uređaja koordinira programabilni logički kontroler PLC koji je programiran da održi proces elektrolize i zaštiti rad svake komponente uređaja. Zahvaljujući ovim konstrukcijama, temperaturni režim rada uređaja je takav da se ne dostiže kritična temperatura elektrolita na izlazu od preko 38 °C.

REZULTATI I DUSKUSIJA

Uređaj za kontinualnu proizvodnju natrijum-hipohlorita sa pothlađivanjem elektolita je projektovan i konstruisan sa novim komponentama tako da je njegova cena znatno niža od uređaja koji se pojavljuju na našem tržištu. Pomenuti uređaj je testiran u mašinskoj prostoriji gde se nalazi i ostala oprema za održavanje vode u bazenu (toplotne pumpe, izmenjivači toplote, cirkulacione pumpe i filtri). U mašinskoj prostoriji se posle nekoliko dana rada kompletne opreme uspostavila stacionarna temperatura od 38 °C i relativna vlažnost od 86%. U takvim, veoma nepovoljnim uslovima za uređaj za kontinualnu proizvodnju natrijum-hipohlorita, startovan je sam uređaj sa pothlađivanjem elektrolita pod pomenutim eksploatacionim uslovima: i ulaznom temperaturom omekšane vode iz vodovodne mreže od 24 °C. Praćena je temperatura rastvora aktivnog hlora neposredno na izlasku iz elektrolizera tokom vremena. Maksimalna temperatura izlaznog rastvora natrijum-hipohlorita bila je 35,3 °C. Dobijeni rezultati su prikazani na slici 4.

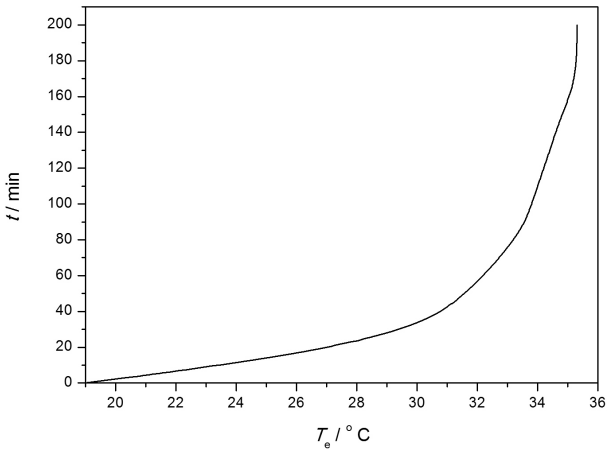

Slika 4. Zavisnost temperature izlaznog elektolita od vremena pri konstantnoj temperaturi u mašinskoj prostoriji od 36 °C i temperaturi ulazne vode od 24 °C.
Figure 4. Time dependence of outlet electrolyte temperature at constant room temperature of 36 °C and inlet water temperature of 24 °C.

Kao što se sa dijagrama na slici 4 može videti, stacionarno stanje temperature se uspostavljanja posle 40 min. Temperatura ne prelazi 36 °C što je u okviru optimalnih parametara sinteze i lagerovanja aktivnog hlora. Ovo znači da i u najnepovoljnijim uslovima elektrohemijske sinteze, povećane temperature okoline i ulaznog elektrolita i vlažnosti vazduha, temperatura izlaznog rastvora aktivnog hlora na izlazu iz uređaja ne prelazi kritičnu temperaturu od 38 °C. Ukoliko se u mašinskoj prostoriji uvede bilo kakvo provetravanje i snizi temperatura i vlažnost vazduha, uslovi za rad uređaja za kontinualnu proizvodnju aktivnog hlora sa pothlađivanjem elektolita će biti još bolji.

Na osnovu dosadašnjih istraživanja [7–9] i ovde navedenih, osnovne prednosti korišenja uređaja za *in situ* dobijanje aktivnog hlora su sledeci: bezbedan rad za ljude i okolinu tokom proizvodnje; smanjeni troškovi proizvodnje i jednostavno održavanje; zadovoljeni su svi uslovi zdravstvenog i sigurnosnog zakonodavstva; poboljšan je kvalitet vode; smanjene su količine sporednih proizvoda pri dezinfekciji; rad uređaja ne zavisi od nabavke specijalnih hemikalija; najjeftiniji dezinficijens.

ZAKLJUČAK

Ispitivani uređaj za elektrohemijsku dezinfekciju vode najnovije generacije sa pothlađivanjem elektolita u koji su ugrađene najnovije komponente radi u oblasti projektovanih parametara. Novougrađene komponente uređaja (strujna napajanja, programbilni logički kontroleri, senzorski elementi kao i samo konstruktorsko re-

šenje) omogućuju, pored pouzdane funkcionalnosti, i nižu cenu uređaja od sličnih dosadašnjih (cena je niža oko 20%). Prema proračunima, dobijeni proizvod je jeftiniji od gasovitog hlora kako u početnoj investiciji tako i u eksploataciji. Dobijeni natrijum-hipohlorit po svojim karakteristikama može biti efikasna alternativa sredstvima za dezinfekciju na bazi hlora ili hlor-dioksida. Mogućnost proizvodnje natrijum-hipohlorita *„in situ"* elektrolizom rastvora NaCl, efikasnost u uklanjanju patogenih mikroorganizama, niski stepen sigurnosnih mera i niska cena troškova proizvodnje predstavljaju glavne prednosti. Elektroliza ne zahteva posebne mere zaštite, a efikasnost nastalog hipohlorita je jednaka ili bolja od efikasnosti gasovitog hlora. U najekstremnijim uslovima eksploatacije (visokih atmosferskih temperatura i/ili visokih temperatura u prostoriji gde je instaliran uređaj, kao i vlažnosti vazduha u mašinskoj prostoriji) dobija se željeni proizvod odgovarajućeg kvaliteta, prvenstveno zahvaljujući novom tehničkom rešenju uređaja sa pothlađivanjem ulaznog elektolita.

ZAHVALNICA

Ovaj rad je urađen uz finansijsku pomoć Ministarstva prosvete, nauke i tehnološkog razvoja Republike Srbije, projekat broj 172046.

LITERATURA

[1] D.J. Pickett, Electrochemical Reactor Design, 2nd ed., Elsevier, Amsterdam, 1979.

[2] K. Scott, Electrochemical Reaction Engineering, Academic Press, London, 1991.

[3] M.D. Spasojević, N.V. Krstajić, M.M. Jakšić, Optimization of on anodic electrocatalyst: RuO_2/TiO_2 on titanium, J. Res. Inst. Catalysis Hokkaido Univ. **31** (1983) 77–94.

[4] N. Krstajić, V. Nakić, M. Spasojević, Hypochlorite production. I. A model of the cathodic reactions, J. Appl. Electrochem. **17** (1987) 77–81.

[5] Lj. Gajić-Krstajić, T.Lj. Trišović, N.V. Krstajić, Spectrophotometric study of the anodic corrosion of Ti/RuO_2 Electrode in acid sulfate solution, Corr. Sci. **46** (2006) 65–74.

[6] M.D. Spasojević, T.Lj. Trišović, L. Ribić-Zelenović, P.M. Spasojević, Development of RuO_2/TiO_2 titanium anodes and a device for *in situ* active chlorine generation, Hem. Ind. **67** (2013) 313–321.

[7] A. Kraft, Electrochemical Water Disinfection: A Short Review, Platinum Metals Rev. **52** (2008) 177–185.

[8] N. Trišović, Lj. Gajić-Krstajić, T. Trišović, Aparat za proizvodnju aktivnog hlora, patent YU 716 MP (2005).

[9] T. Trišović, B. Jugović, M. Gvozdenović, N. Trišović, Universal Modular Device for Electrochemical Synthesis of the Disinfectant, J. Trends Dev. Mach. Assoc. Technol. **16** (2012) 187–190.

SUMMARY

AUTOMATIC DEVICES FOR ELECTROCHEMICAL WATER TREATMENT WITH COOLING OF ELECTROLYTE

Tomislav Lj. Trišović[1], Miroslav D. Spasojević[2], Milica M.Gvozdenović[3], Branimir Z. Jugović[1], Lidija D. Rafailović[4]

[1]*Institute of Technical Sciences of SASA, Knez-Mihailova 35/IV, 11000 Belgrade, Serbia*
[2]*Faculty of agronomy Čačak, University of Kragujevac, Cara Dušana 34, 32000 Čačak, Serbia*
[3]*Faculty of Technology and Metallurgy, University of Belgrade, Karnegijeva 4, 11120 Belgrade, Serbia*
[4]*Center of Electrochemical Surface Technology CEST, Vitor Kaplan Strasse 2, 2700 Wr.Neustadt, Austria*

(Professional paper)

The most common disinfectants for water treatment are based on chlorine and its compounds. Practically, water treatments with chlorine compounds have no alternative, since they provide, in comparison to other effective processes such as ozonization or ultraviolet irradiation, high residual disinfection capacity. Unfortunately, all of chlorine-based compounds for disinfection tend to degrade during storage, thus reducing the concentration of active chlorine. Apart from degradation, additional problems are transportation, storage and handling of such hazardous compounds. Nowadays, a lot of attention is paid to the development of electrochemical devices for *in situ* production of chlorine dioxide or sodium hypochlorite as efficient disinfectants for water treatment. The most important part of such a device is the electrochemical reactor. Electrochemical reactor uses external source of direct current in order to produce disinfectants in electrochemical reactions occurring at the electrodes. Construction of an electrochemical device for water treatment is based on evaluation of optimal conditions for electrochemical reactions during continues production of disinfectants. The aim of this study was to develop a low-cost electrochemical device for the production of disinfectant, active chlorine, at the place of its usage, based on newly developed technical solutions and newest commercial components. The projected electrochemical device was constructed and mounted, and its operation was investigated. Investigations involved both functionality of individual components and device in general. The major goal of these investigations was to achieve maximal efficiency in extreme condition of elevated room temperature and humidity with a novel device construction involving coaxial heat exchanger at the solution inlet. Room operation of the proposed device was investigated when relative humidity was set to 90% and the ambient temperature of 38 °C. The obtained results in such extreme operation conditions reveled that it was possible to obtain required concentration of 0.85% of active chlorine with maximal temperature of outlet electrolyte of 35.3 °C, which is within the limits of optimal temperatures.

Keywords: Disinfection • Electrochlorination • Active chlorine • Electrochemical treatment of water

Kvantifikacija akrilamida u izabranim namirnicama primenom gasne hromatografije u tandemu sa masenom spektrometrijom

Veselin M. Delević[1], Refik M. Zejnilović[2], Biljana S. Jančić-Stojanović[3], Brižita I. Đorđević[4], Zorana N. Tokić[5], Milica D. Zrnić-Ćirić[4], Ivan M. Stanković[4]

[1]*Institut za javno zdravlje, Podgorica, Crna Gora*
[2]*Univerzitet Crne Gore, Farmaceutski fakultet, Podgorica, Crna Gora*
[3]*Univerzitet u Beogradu, Farmaceutski fakultet, Katedra za analitiku lekova, Srbija*
[4]*Univerzitet u Beogradu, Farmaceutski fakultet, Katedra za bromatologiju, Srbija*
[5]*Univerzitet u Beogradu, Farmaceutski fakultet, Katedra za Organsku hemiju, Srbija*

NAUČNI RAD

UDK 613.263:547–327:661.717.53: 543

Hem. Ind. **70** (2) 209–215 (2016)

doi: 10.2298/HEMIND150225027D

Izvod

Akrilamid je toksično i verovatno kancerogeno jedinjenje koje nastaje termičkim tretmanom namirnica bogatih ugljenim hidratima na visokim temperaturama. U ovom radu prikazana je unapređena metoda za ekstrakciju i kvantifikaciju akrilamida iz namirnica proizvedenih na bazi kukuruznog brašna koje su zastupljene u našoj tradicionalnoj ishrani. Derivatizacija akrilamida sa bromom je izvedena sa smanjenom zapreminom zasićenog rastvora bromne vode čime je značajno smanjena toksičnost ovog dela pripreme uzoraka. Kvantifikacija je urađena osetljivom GC-MS metodom. Kvantifikaciji akrilamida GC–MS metodom predhodile su: homogenizacija uzorka, ekstrakcija akrilamida vodom, prečišćavanje ekstrakta pomoću ekstrakcije na čvrstoj fazi, bromovanje (koristeći smanjenu zapreminu rastvora bromne vode), dehidrobromovanje sa natrijum-tiosulfatom i prevođenje 2,3-dibrompropenamida u 2-brompropenamid pomoću trietilamina. Kalibracija je vršena u opsegu koncentracija 5–80 μg/kg. Dobijena je sledeća jednačina prave $y = 0{,}069x + 0{,}038$ sa koeficijentom determinacije $R^2 > 0{,}999$. Dobijena granica detekcije bila je 6,86 μg/kg, a granica kvantifikacije 10,78 μg/kg. Takođe, ispitana je i tačnost metode a dobijene *Recovery* vrednosti bile su prosječno od 97 do 110%. Predložena GC–MS metoda je jednostavna, pouzdana i precizna za određivanje akrilamida u uzorcima termički tretiranih namirnica. Dobijeni rezultati pokazuju da se u ispitivanim namirnicama kvantifikuje prisustvo akrilamida u koncentracijama od 18 do 77 μg/kg u zavisnosti da li je namirnica pripremljena kuvanjem ili pečenjem.

Ključne reči: akrilamid, optimizacija bromovanja, GC–MS metoda, termički tretirane namirnice.

Dostupno na Internetu sa adrese časopisa: http://www.ache.org.rs/HI/

Grupa istraživača Švedske Agencije za bezbednost hrane i Univerziteta u Stokholmu 2002. godine obavijestili su naučnu javnost da su kvantifikovali visoke koncentracije akrilamida u termički tretiranim namirnicama bogatim ugljenim hidratima, što je privuklo veliku pažnju jer je akrilamid od strane međunarodne Agencije za istraživanje kancera (eng. *International Agency for Research on Cancer,* IRAC) svrstan u grupu 2A kao verovatno kancerogen za ljude [1,2].

Akrilamid (2-propenamid, slika 1) nastaje tokom termičkih tretmana namirnica na visokim temperaturama reakcijom između redukujućih šećera i amino kiseline asparagina takozvanom Maillard-ovom reakcijom. Danas je pokrenuto nekoliko naučnih inicijativa da bi se u potpunosti razumela njegova hemija i toksikologija,

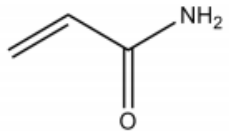

Slika 1. Molekulska struktura akrilamida.
Figure 1. Molecular structure of acrylamide.

fokusirajući se prvenstveno na njegove mehanizme formiranja i moguće posledice po ljude. Ispitivanja na životinjama su pokazala da visoke doze akrilamida (> 203 μg/kg) imaju nepoželjne efekte na razvojne funkcije u neonatalnom periodu kod glodara. S druge strane, epidemiološke studije za različite vrste kancera nijesu pokazale vezu između ishranom unešenog akrilamida i pojave kancera [3,4]. Međutim, došlo se do zaključka da standardne epidemiološke studije imaju nisku statističku validnost kako bi se utvrdila povezanost pojave raka sa izloženošću akrilamidu [5]. Imajući ovo u vidu Zajednički FAO/WHO ekspertski komitet za aditive (eng. Joint FAO/WHO Expert Committee on

Prepiska: V.M. Delević, Institut za javno zdravlje, ulica Džona Džeksona b.b., 20000 Podgorica, Crna Gora.
E-pošta: delevic@t-com.me
Rad primljen: 25. februar, 2015
Rad prihvaćen: 6. maj, 2015

Food Additives, JECFA) istakao je važnost dobijanja što više validnih podataka o sadržaju akrilamida u namirnicama koje se konzumiraju u zemljama u razvoju kao vredan instrument u obavljanju procene unosa, kako bi se redukovala izloženost ljudi [6].

Akrilamid nastaje u namirnicama tokom termičkih tretmana na visokim temperaturama kao što je pečenje ili prženje u ulju. Na formiranje akrilamida u namirnicama pored termičkih tretmana utiče i prisustvo amino kiselina (asparagina) i redukujućih šećera. Amino kiselina asparagin je glavni prekursor za nastajanje akrilamida u prisustvu redukujućih šećera. Međutim, neke studije su pokazale da akrolein, akrilne kiseline i druge amino kiseline kao što su alanin i arginin su takođe mogući prekursori nastanka akrilamida [5].

Poslednjih deset godina u svetu se intenzivno radi na razvoju analitičkih metoda za kvantifikaciju akrilamida u različitim vrstama termički tretiranih namirnica koje su dominantno HPLC ili GC metode [9], kao i u namirnicama koje nisu termički tretirane, vodi za piće i biološkom materijalu [7,8]. Prikaz GC i HPLC metoda, kao i elektroforeckih metoda za određivanje akrilamida u različitim uzorcima dat je u preglednom radu [10]. Pored toga, opisani su i različiti postupci pripreme uzoraka kao što su ekstrakcija sa *n*-propanolom [11], ekstrakcija sa *n*-heksanom i vodenim rastvorom natrijum-hlorida [12], ekstrakcija na čvrstoj fazi (eng. Solid Phase Exstaction – SPE) [13,14], ekstrakcija sa metanolom, prečišćavanje sa rastvorom Carrez I i II [15], itd. Za kvantifikaciju akrilamida pomoću GC–MS (eng. gas chromatography–mass spectrometry) ili LC–MS-MS (eng. Liquid chromatography–tandem mass spectrometry) metode većina istraživača predlaže pripremu uzoraka u više faza. Sve do sada publikovane GC–MS metode za određivanje akrilamida u namirnicama možemo podeliti u dve kategorije, one koje uključuju derivatizaciju i one bez primene derivatizacije. Metode za određivanje akrilamida bez derivatizacije zahtevaju dugotrajne ekstrakcije koje mogu trajati u nekim slučajevima i do deset dana [16]. Metode sa derivatizacijom imaju prednosti jer omogućavaju kvantifikaciju akrilamida i do nivoa tragova [17–19]. Međutim, derivatizacija bromovanjem podrazumeva upotrebu broma u laboratorijskom radu čije pare ako se udišu mogu biti opasne po analitičara, stoga, čini se da brom treba koristiti što je moguće manje u laboratorijskim eksperimentima. Gasna hromatografija sa masenom spektrometrijom (GC–MS) je jedna od najosetljivijih metoda korištenih za kvantifikaciju akrilamida u uzorcima životnih namirnica [20].

Cilj ovog rada bio je da se unapredi GC–MS metoda za određivanje akrilamida iz termički tretiranih namirnica. U tom cilju urađena je optimizacija postupka bromovanja čime je potvrđeno da se sa manjim zapreminama broma mogu dobiti tačni i precizni rezultati. Postupak pripreme uzoraka podrazumevao je četiri faze nakon šega je primenjena GC–MS metoda. GC–MS metoda je validirana i primenjena za analizu različitih uzoraka.

EKSPERIMENTALNI DEO

Aparatura i reagensi

Za određivanje akrilamida korišćen je gasni hromatograf Shimadzu GC–MS model QP2010 plus (Shimadzu Inc., Koyoto, Japan), sa kapilarnom kolonom HP-5 MS (30 m×0,25 mm×0,25 µm, J&W Scientific, Folsom, CA, USA). Obrada podataka i kontrola GC–MS sistema vršena je pomoću softvera „Lab solution“ (Shimadzu Inc., Koyoto, Japan). Kao standard korišćen je rastvor akrilamida (čistoće > 99,8%) proizvođača Sigma-Aldrich (St. Louis, MO, USA). Kao interni standard korišćen je rastvor izotopa akrilamida – [$^{13}C_3$], koncentracije 1mg/ml u metanolu ($H_2{}^{13}C={}^{13}CH{}^{13}CONH_2$) proizvođača Sigma–Aldrich, (St. Louis, MO, USA). Organski rastvarači: *n*-heksan, metanol, etil-acetat, kao i kalijum-bromid, natrijum-tiosulfat, trietilamin i anhidrovani natrijum-sulfat takođe su od proizvođača Sigma–Aldrich (St. Louis , MO, USA). Kertriđži za ekstrakciju na čvrstoj fazi (SPE) su OASIS MCX 3cc (60 mg) i tečna faza OASIS HLB 6cc (200 mg) su od proizvođača Waters Corporation (Massachusetts, USA). Kalijum-bromid i natrijum-sulfat su ižareni na 600 °C u trajanju od 6 sati pomoću peći za žarenje (Carbolite Furnaces; Chelmsford/Esser, England). Ostali reagensi su korišteni bez daljeg prečišćavanja.

Priprema rastvora

Osnovni standard akrilamida koncentracije 1 mg/ml pripremljen je rastvaranjem u etil-acetatu. Radni rastvor pripremljen je rastvaranjem osnovnog rastvora standarda u opsegu koncentracija od 5 do 80 µg/dm^3 u etil-acetatu.

Interni standard izotopa akrilamida [$^{13}C_3$] koncentracije 4 mg/dm^3 dodat je ispitivanom uzorku u količini od 10 µl i dobijena je koncentracija internog standarda od 40 µg/dm^3.

Postupak optimizacije zapremine bromne vode u postupku derivatizacije akrilamida

U ovoj fazi istraživanja optimizirana je potrebna količina broma za pripremu uzoraka. U cilju određivanja optimalne zapremine broma, vršeno je opterećivanje uzorka kukuruznog hleba koji je sadržao 29,5 µg/kg akrilamida sa 40 µg akrilamida koji je pripremljen sa 5 različitih zapremina bromne vode (1, 2, 5, 10 i 15 ml). Kao odgovor, praćen je prinos ekstrakcije izražen kao Recovery vrednost. Dobijeni rezultati prikazani su u tabeli 1.

Tabela 1. Recovery vrednost za akrilamid u uzorku pripremljenom sa 5 različitih zapremina bromne vode
Table 1. Recovery value for acrylamide in a specimen prepared from 5 different brominated flame-volume water

Zapremina bromne vode, mL	Opseg Recovery vrijednosti, %	Srednja vrijednost za Recovery ± SD, %
15	103,8–105,7	105,3±1,42
10	99,1–104,1	101,6±1,70
5	93,1–106,3	98,1±4,90
2	83,5–99,1	89,2±6,19
1	53,1–92,5	70,6±13,7

Postupak pripreme uzoraka

Akrilamid je kvantifikovan kao derivat 2-brompropen amida (2-BPA) po metodi Pittet i dr. [20] i Yong i dr. [21] uz određene modifikacije koje su urađene u cilju unapređenja metode.

Prvo unapređenje jeste smanjena zapremina bromne vode u fazi bromovanja. Drugo unapređenje sastoji se u upotrebi SPE ekstrakcije umesto rastvora Carrez I i II kako je to bilo u predhodno publikovanoj metodi [20].

Kompletan postupak se sastoji iz četiri faze koje su u ovom delu detaljno opisane. Uzorci koji su analizirani bili su proizvodi na bazi kukuruznog brašna, prikupljeni od strane službe sanitarne inspekcije u okviru redovnog sanitarnog nadzora nad kuhinjama dečijih vrtića u Podgorici.

Faza 1. Homogenizacija i dodavanje internog standarda: Izmeri se 20 g dobro homogenizovanog uzorka i ostavi da bubri upijajući 200 ml dejonizovane vode (70±1 °C) u trajanju od najmanje 60 min. Smeša se ponovo dobro izhomogenizuje pomoću homogenizatora Ultra-turrax (IKA-T25 Basel, Switzerland). 1 g homogenizovane smeše se prenese u kivetu za centrifugiranje, doda se 3 ml 2M NaCl i smeša se ponovo homogenizuje. Zapremina od 10 µl internog standard koncentracije 4 mg/dm^3 izotopa [$^{13}C_3$] akrilamida doda se u smešu i smeša se homogenizuje na vorteks mikseru (Stuart Scientific, Manchester, England) u toku 1 min. U smešu se doda 40 µg/kg odnosno 40 ng/g internog standarda.

Faza 2. Prečišćavanje: Smeša koja sadrži interni standard centrifugira se na 10000 obrtaja pomoću centrifuge (Sigma, Gillingham Dorset, UK) u trajanju od 30 min. Dobijeni supernatant se profiltrira kroz stakleni filter pora 0,45µm (Witeg Labortechnik GmbH, Germany) kako bi se izdvojila eventualno zaostala mast. Kolone za ekstrakciju na čvrstoj fazi (HLB, MCX) kondicioniraju se najprije sa 3 ml metanola zatim sa 3 ml vode. Nakon kondicioniranja, na kolonu se nanosi uzorak filtrata, a zatim se vrši eluiranje sa 50 ml dejonizovane vode. U eluat se zatim doda 7,5 g kalijum-bromida čija je pH vrednost podešena na pH 2,0 dodavanjem oko 15 kapi 47% bromovodonične kiseline.

Faza 3. Bromovanje: Ekstraktima uzoraka se uz mešanje doda po 2 ml zasićenog rastvora bromne vode (1,6 vol.%). Uzorci se čuvaju na 0 °C u trajanju od 24 h kako bi se završila reakcija bromovanja.

Faza 4. Finalno prečišćavanje za GC–MS određivanje: Nakon završetka reakcije bromovanja višak broma ukloni se dodavanjem 5 kapi 1 M natrijum-tiosulfata dok nestane žuta boja. Zatim se doda po 10 g anhidrovanog natrijum-sulfata i smeša se dobro izmeša. Smeša se prenese u levak za odvajanje zapremine 250 ml, doda se 20 ml smeše etil-acetat/heksan (4:1, *V*/*V*) i dobro se izmeša. Organska faza se zatim prenese u kivetu za centrifugiranje u kojoj je odmereno 4 g anhidrovanog natrijum-sulfata. Ovaj korak se ponovi dva puta sa po 20 ml smeše etil-acetat/heksan (4:1, *V*/*V*). Smeša se centrifugira i dekantuje kroz stakleni filter papir i upari do suva pomoću rotacionog vakum uparivača (Rotavapor R-124; Buchi, Switzerland). Suvi ostatak se rastvori u 50 µl trietilamina i 450 µl etil-acetata. Pripremljeni ekstrakti se čuvaju u zamrzivaču na –20 °C do GC–MS analize.

Postupak GC–MS analize

Nakon stabilizovanja GC–MS sistema uradi se kalibracija. Svi potrebni parametri (vremenske funkcije, izbor metode izračunavanja, atenuacije i dr.) unesu se softverskom metodom koja omogućava praćenje razdvajanja akrilamida. Hromatografski uslovi su navedeni u tabeli 2.

Tabela 2. Uslovi hromatografskog postupka
Table 2. Terms chromatographic procedure

Mobilna faza	He, 99,999% (1,6 ml/min)
Temperaturni program	50–240 °C (5 °C/min); 8 min
Temperatura injektora	200 °C, splitles mod

Statistička analiza

Za statističku obradu podataka korišćeni su programi Microsoft Office Excel i Statistica. Primijenjene su regresiona i korelaciona analiza.

REZULTATI I DISKUSIJA

Za određivanje sadržaja akrilamida u termički tretiranim uzorcima proizvedenim na bazi kukuruznog brašna primenjena je GC–MS metoda. Kao što je navedeno u uvodu, cilj je bio da se razvije metoda koja će

biti brža i ekonomičnija od uobičajenih metoda i koja će zahtevati manju količinu broma za fazu derivatizacije akrilamida. Iz tog razloga, urađena je optimizacija bromovanja prema proceduri opisanoj u Eksperimentalnom delu, a korišćene zapremine bromne vode, kao i dobijeni rezultati za *Recovery* vrednosti prikazane su u tabeli 1.

Na osnovu rezultata zaključeno je sledeće: srednja Recovery vrednost za 1 ml bromne vode bila je 70,6% što je dosta nisko dok je Recovery vrednost za zapreminu bromne vode od 2 ml, bio prihvatljivih 89,2%. Dalje povećanje zapremine bromne vode dovodi do povećanja Recovery vrednosti, ali kako su sa zapreminom od 2 ml bromne vode dobijene reproduktivne vrednosti sa zadovoljavajućom Recovery zaključeno je da nije potrebno raditi sa većim zapreminama. Za izvođenje ekstrakcije akrilamida iz različitih vrsta namirnica, drugi istraživači koristili su 15 ml bromne vode [2,7,18––21]. Na ovaj način postignuto je značajno unapređenje s obzirom na činjenicu da je ovaj reagens toksičan za okolinu.

Pouzdanost metode je testirana kvantifikacijom akrilamida u 6 ponavljanja, a nakon tog procesa, dalje je vršena validacija metode i određivanje akrilamida u ostalim uzorcima.

Validacija metode

Pod zadatim hromatografskim uslovima snimljeni su maseni spektri za 2-BPA i 2-BP[$^{13}C_3$] A koji su prikazani na slici 2.

Dalje, urađena je verifikacija vrednosti LoD i LoQ. Za verifikaciju *LoD* i *LoQ* pripremljen je radni standard (veštački uzorak) koji sadrži 5 µg kg^{-1} akrilamida. Dobijeni rezultati prikazani su u tabeli 3.

Tabela 3. Verifikacija granice detekcije i granice kvantifikacije
Table 3. Verification of limits of detection and limit of quantification

Parametar	Koncentracija, µg/kg
Radni rastvor akrilamida koncentracije 5 µg/kg	4,46
	5,54
	5,53
	5.58
	5,54
	4.44
X_{sr}	5,18
RSD	0,56

Vrednosti *LoD* i *LoQ* izračunate su primjenom formula (1) i (2):

$$LoD = X_{sr} + 3SD = 5{,}18\ \mu g/kg + 3\times 0{,}56 = 6{,}86\ \mu g/kg \quad (1)$$

$$LoQ = X_{sr} + 10SD = 5{,}18\ \mu g/kg + 10\times 0{,}56 = 10{,}78\ \mu g/kg \quad (2)$$

U narednoj fazi urađena je procjena linearnosti metode. Zavisnost odnosa površina pikova *m/z* 151 i 154) i koncentracije akrilamida ispitana je regresionom analizom i dobijena je linearna kalibraciona kriva sa

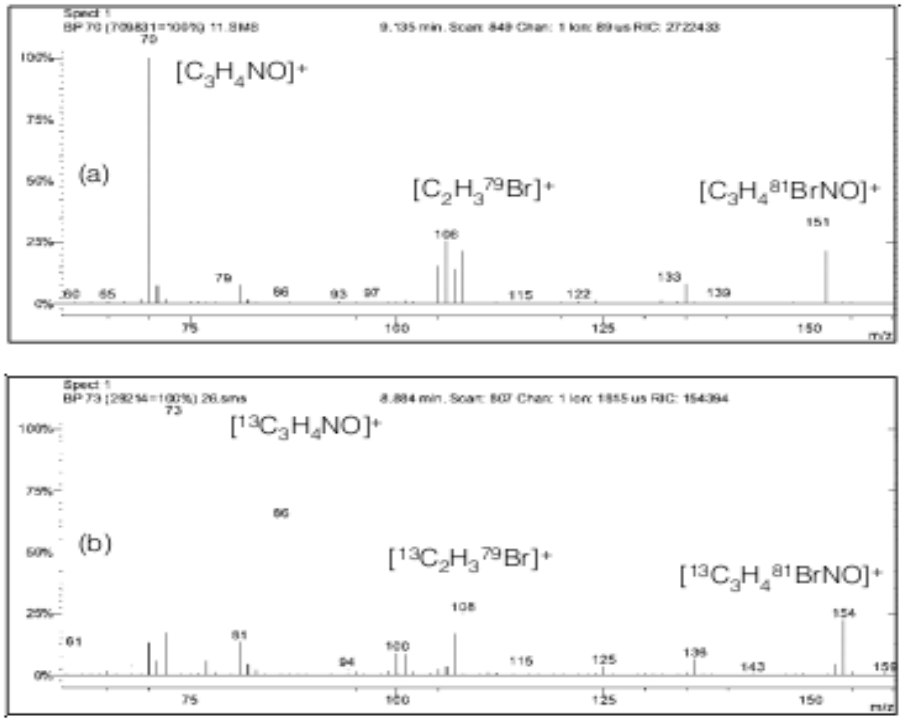

Slika 2. GC–MS spektri za: a) 2-brompropenamid (2-BPA) i b) 2-BP[$^{13}C_3$]A.
Figure 2. GC–MS spectra of a) 2-brompropenamid (2-BPA) and b) 2-BP[13C3]A.

koeficjentom determinacije R^2 > 0,999. Kalibracija je vršena u opsegu koncentracija od 5–80 µg/kg (5, 20, 40, 60 i 80 µg/kg) i dobijena je jednačina prave: $Y = 0{,}069x + 0{,}038$.

Tačnost metode procenjena je na taj način što je uzorak kukuruznog hleba koji je sadržao 29,5 µg/kg akrilamida opterećen sa 10, 20 i 40 µg/kg akriamida i dobijene vrijednosti su prikazane u tabeli 4. Vrijednosti dobijene iz šest paralelno urađenih ekstarkcija kvantitativno su obrađene GC–MS postupkom.

Vrijednosti za Recovery dobijene za tri nivoa koncentracija potvrđuju da je metoda tačna. Dobijeni rezultati za ispitivane parametre validacije potvrđuju pouzdanost metode pa je validirana GC–MS metoda primenjena za određivanje sadržaja akrilamida u izabranim namirnicama proizvedenim na bazi kukuruznog brašna kao što su kukuruzni hleb, kornfleks, palenta, projice sa sirom i projice sa sirom i spanaćem. U tabeli 5 prikazana je koncentracija akrilamida u ispitivanim namirnicama. Rezultati ispitivanja pokazuju da je akrilamid detektovan u svim uzorcima, minimalna vrednost akrilamida (18,1 µg/kg) je detektovana je kod palente, a maksimana (77,5 µg/kg) kod kornfleksa. Ove vrijednosti su značajno niže nego kod namirnica proizvedenih dominantno od pšeničnog brašna što je posledica smanjenog sadržaja sirovih proteina u kukuruznom brašnu, pa je i mogućnost sinteze akrilamida manja.

ZAKLJUČAK

U ovom radu prikazana je GC-MS metoda za određivanje sadržaja akrilamida u termički tretiranim namirnicama. U radu je opisano unapređenje faze bromovanja u smislu smanjenja upotrebe reagensa koji se smatra toksičnim. Takođe, primenjena je SPE metoda u fazi pripreme uzorka čime je postupak značajno pojed-

Tabela 4. Recovery vrednost za akrilamid u opterećenim uzorcima kukuruznog hleba
Table4. Recovery value for acrylamide in loaded samples cornbread

Početna konc. AA, mg/kg	Dodata količna AA, mg/kg	Dobijena konc. AA, mg/kg	Očekivana konc. AA, mg/kg	Tačnost, %
28,9	10,0	43,1	38,9	110,8
29,0		42,8	39,0	109,7
30,8		44,6	40,8	109,3
29,9		44,2	39,9	110,7
28,7		42,4	38,7	109,8
29,5		43,4	39,5	110,0
c_{sr} = 29,5				110,0
28,9	20,0	50,2	48,9	102,6
29,0		49,7	49,0	101,5
30,8		51,0	50,8	100,4
29,9		50,4	49,9	101,1
28,7		48,2	48,7	98,9
29,5		49,1	49,5	99,3
c_{sr} = 29,5				100,6
28,9	40,0	67,9	68,9	98,5
29,0		67,0	69,0	97,1
30,8		70,3	70,8	99,4
29,9		67,7	69,9	96.9
28,7		65,7	68,7	95,7
29,5		66,1	69,5	95,1
c_{sr} = 29,5				97,1

Tabela 5. Koncentracija akrilamida u ispitivanim namirnicama
Table 5. The concentration of acrylamide in foods tested

Uzorak	Broj uzoraka	Opseg konc. akrilamida, µg kg^{-1}	Sradnja vrijednost±SD, , µg kg^{-1}	*SD* / %
Kukuruzni hleb	13	26,7–31,5	27,0±1,7	1,7
Kornfleks	7	69,0–77,5	72,8±4,2	4,2
Palenta	5	18,1–23,8	20,4±1,9	1,9
Projice sa sirom i spanaćem	8	29,0–35,8	31,6±2,3	2,3
Projice sa sirom	9	27,9–35,0	31,1±2,4	2,4

nostavljen i veoma je prihvatljiv za praktičnu primenu. GC–MS metoda je validirana sa limitom detekcije 6,86 µg/kg čime je potvrđena i njena osetljivost. Na kraju, metoda je uspešno primenjena za ispitivanje sadržaja akrilamida u različitim uzorcima kao sto su krompir, čips, hleb, itd.

LITERATURA

[1] IARC. Monographs on the evalution of carcinogen risk to humans [serial on the Internet]. 2011. Avaliable from: http:// monographs.iarc.fr/

[2] Swedish National Food Administration (SNFA). Information about acrylamide in food Uppsala [serial on the Internet]. Avaliable from: http://www.slv.se

[3] H. Mojska, I. Gielecinska, L. Zsponar, M. Oltarzewski, Estimation of the dietary acrylamide exposure of the Polish population, Food. Chem. Toxicol. **48** (2010) 2090–2096.

[4] Food Standards Agency. Stady of acrylamide in food [serial on the Internet], 2010, Avaliable from: http://www.food.gov.uk

[5] Scientific Committee on food. Opinon of the SCF on new findings regarding the presence of acrylamide in food [serial on the Internet]. 2010. Avaliable from: http://www.europa.eu.int

[6] FAO/WHO (Food and Agricultural Organisation/World HealthOrganization).Summary and conclusions report of the seventy-second meeting of the Joint FAO/WHO Expert Committee on Food Additives (JECFA) 1-16, 2010, Available from http://www.fao.org/ag/agn/agns/jecfa output en.Asp

[7] N. Marchettini, S. Focardi, M. Guarnieri, C. Guerranti, G.Perra, Determination of acrylamide in local and commercial cultivar of potatoes from biological farm, Food Chem. **136** (2013) 1426–1428.

[8] C. Laurence, E. Sune, Analytical methods used to measure acrylamide concentrations in Foods, J. AOAC. Int. **88** (2005) 274–284.

[9] Y.Zhang, G. Zhang, Occurrence and analytical methods of acrylamide in heat-treated foods review and recent developments, J. Chromatogr., A **1075** (2005) 1–21.

[10] S.E. Kepekci Tekkeli, C. Onal, A. Onal, A Review of current methods for the determination of acrylamide in food products, Food. Anal. Methods. **5** (2012) 29–39.

[11] L. Dunovska, T. Cajka, J. Hajslova, K. Holadova, Direct determination of acrylamide in food by gas chromatography-high-resolution time-of-flight mass spectrometry, Anal. Chim. Acta **578** (2006) 234–240.

[12] Y.Zhang, Y. Dong, Y. Ren, Y. Zhang, Rapid determination of acrylamide contaminant in conventional fried foods by gas chromatography with electron capture detector, J. Chromatogr., A **1116** (2006) 209–216.

[13] C.M. Soares, R.C. Alves, S.Casal, M.B. Oliveira, J.O. Fernandes, Development and validation of a matrix solid-phase dispersion method to determine acrylamide in coffee and coffee substitutes, J. Food. Sci. **75** (2010) 57–63.

[14] E.K. Paleologos, M.G.Kontominas, Determination of acrylamide and methacrylamide by normal phase high performance liquid chromatography and UV detection, J. Chromatogr., A **1077** (2005) 128–135.

[15] V. Gokmen, H.Z. Senyuva, J. Acar, K. Sarioglu, Determination of acrylamide in potato chips and crisps by high-performance liquid chromatography, J. Chromatogr., A **1088** (2005) 193–199.

[16] J.R. Pedersen, J.O. Olsson, Soxhlet extraction of acrylamide from potato chips. Analyst **128** (2003) 332–334.

[17] L. Castle, M.J. Campos, J. Gilbert, Determination of acrylamide Monomer in hydroponically grown tomato fruits by capillary gas chromatography-mass spectrometry. J. Agric. Food Chem. **54** (1991) 549–555.

[18] L. Castle, Determination of acrylamide monomer in mushrooms grown on polyacrylamide gel. J. Agric. Food Chem. **41** (1993) 1261–1263.

[19] J.S. Ahn, L. Castle, D.B. Clarke, A.S. Lloyd, M.R. Philo, D.R. Speck, Verification of findings of acrylamide in heated foods. Food Addit. Contam., A **19** (2002) 1116–1124.

[20] A. Pittet, A. Périsset, J.M. Oberson, Trace level determination of acrylamide in cereal-based foods by gas chromatography–mass spectrometry, J. Chromatogr., A **1035** (2004) 123–130.

[21] M.S. Young, K.S. Jenkins, C.R. Mallet, Solid–phase extraction and cleanup procedures for determination of acrylamide in fried potato products by liquid chromatography/mass spectrometry, J. AOAC Int., B **87** (2004) 961–964.

[22] Scientific Committee on food. Opinion of the SCF on new findings regarding the presence of acrylamide in food [serial on the Internet]. 2010, Avaliable from: http://www.europa.eu

[23] International Conference on Harmonization, Q2B: Validation of Analytical Procedures: Methodology; Availability, Federal Register **62** (1997) 27463–27467.

SUMMARY

QUANTIFICATION OF ACRYLAMIDE IN FOODS SELECTED BY USING GAS CHROMATOGRAPHY TANDEM MASS SPECTROMETRY

Veselin M. Delević[1], Refik M. Zejnilović[2], Biljana S. Jančić-Stojanović[3], Brižita I. Đorđević[4], Zorana N. Tokić[5], Milica D. Zrnić-Ćirić[4], Ivan M. Stanković[4]

[1]*Institute of Public Health, Podgorica, Montenegro*
[2]*Faculty of Pharmacy, Podgorica, Montenegro*
[3]*Department of of Drug Analysis, Faculty of Pharmacy, University of Belgrade, Belgrade, Serbia*
[4]*Department of Bromatology, Faculty of Pharmacy, University of Belgrade, Belgrade, Serbia*
[5]*Department of Organic Chemistry, Faculty of Pharmacy, University of Belgrade, Belgrade, Serbia*

(Scientific paper)

Acrylamide is toxic and probably carcinogenic compound, made as a result of high-temperature thermal treatment of carbohydrate-rich foodstuffs. In this article a method is improved for the extraction and quantitation of acrylamide in foods produced based on corn flour that are represented in our traditional diet. Acrylamide extraction was carried out using reduced volume of saturated solution of bromine water and the GC–MS method for the quantification was shown. Quantification of acrylamide was preceded by: sample homogenization, acrylamide extraction using water, extract purification using solid phase extraction, bromination, using a reduced volume of bromine water solution, dehydrobromination with sodium thiosulfate and transformation of dibromopropenamide in 2,3,2-bromopropenamide using triethylamine. Regression and correlation analysis were applied for the probability level of 0.05. Calibration is performed in the concentration range 5–80 ug/kg with a detection limit 6.86 mg/kg and the limits of quantification 10.78 ug/kg and the coefficient of determination R^2 > 0.999. Calibration curve was obtained: $y = 0.069x + 0.038$. Recovery values were an average from 97 to 110%. Proposed GC–MS method is simple, precise and reliable for the determination of acrylamide in the samples of thermal treated foods. Our results show that the tested foods quantify the presence of acrylamide in concentrations of 18 to 77 mg/kg acrylamide depending on whether the food was prepared by cooking or baking.

Keywords: Acrylamide • Foods • GC–MS

Immobilization of horseradish peroxidase onto kaolin by glutaraldehyde method and its application in decolorization of anthraquinone dye

Nataša Ž. Šekuljica[1], Nevena Ž. Prlainović[1], Jelena R. Jovanović[2], Andrea B. Stefanović[2], Sanja Ž. Grbavčić[1], Dušan Ž. Mijin[2], Zorica D. Knežević-Jugović[2]

[1]*University of Belgrade, Innovation Center, Faculty of Technology and Metallurgy, Belgrade, Serbia*
[2]*University of Belgrade, Faculty of Technology and Metallurgy, Belgrade, Serbia*

Abstract
The problem of environmental pollution becomes more worrisome day by day, primarily due to the large amounts of wastewater contaminated with various harmful organic compounds, discharged untreated or partially clean into the environment. Feasibility of use of horseradish peroxidase (*Amoracia rusticana*) in the synthetic dyes decolorization was approved by many researchers. Among a number of supports used for the immobilization, it was found that natural clay, kaolin, has excellent features which are a precondition for obtaining biocatalysts with the excellent performances. For this reason, a horseradish peroxidase was immobilized onto kaolin using glutaraldehyde as a cross-linking agent. Obtained biocatalyst was applied in the decolorization of anthraquinone dye C.I. acid violet 109. Under determined optimal conditions (pH 4.0, hydrogen peroxide concentration 0.6 mM, dye concentration 30 mg L^{-1}, temperature 24 °C) around 76% of dye decolorization was achieved. Reusability study showed that resulting biocatalyst was possible to apply four times in the desired reaction with relatively high decolorization percentage.

Keywords: horseradish peroxidase, immobilization, wastewater, dyes.

Available online at the Journal website: http://www.ache.org.rs/HI/

SCIENTIFIC PAPER

UDC 628.3:577.152.1:58:66:54

Hem. Ind. **70** (2) 217–224 (2016)

doi: 10.2298/HEMIND150220028S

The global water crisis has become worrisome problem because it is leading worldwide cause of deaths and diseases [1]. The textile industry is the main consumer of water in the production process, and therefore generates a large amount of wastewater. Wastewater from the textile industry is colored, rich in suspended particles, heavy metals, organic matter and other pollutants and often untreated or partially treated discharged into the environment. Complex composition of textile wastewater requires special treatment methods and many of them are high in energy demands and expensive. Around 2–20% of untreated wastewater is directly discharged in to the environment causing direct contamination of ground and surface water [1,2]. Different types of dyes (azo, anthraquinone and reactive) are applied in the textile processing technology and they represent the biggest problem in the textile wastewater. Most of them, like anthraquinone dyes, have steadfast structure based on the fused aromatic rings which make them difficult to remove and wastewater stay colored for a long period. Colored wastewater leads to impaired photosynthesis, inhibition of growth, development and reproduction of aquatic organisms [3,4]. Besides, the presence of dyes and their degradation products cause serious human health problems such as hemorrhage nausea, reproductive system, liver, brain and central nervous system damage [5]. Traditional methods for wastewater treatment can be divided into three groups: physical, chemical and biological and because of the complexity and variability in the composition of the wastewater they cannot adequately respond to stringent regulations for water purity [6]. Stringent standards for the discharge of wastewater into the environment motivated researchers to develop alternative methods for the treatment of wastewaters. Usage of oxidoreductive enzymes (manganese, lignin, horseradish, turnip and tomato peroxidase) is on the first place, because they show merit in converting complex chemical compounds under mild environmental conditions with high efficiency [5]. Horseradish peroxidase (EC: 1.11.1.7, HRP) applied in the treatment of wastewater can act on the harmful compounds by converting them into innocuous products or changing the characteristics of a given waste making it more favorable for the treatment [7]. The wastewater is characterized with high temperatures, high or low pH, high ionic strength, high reactant concentrations and presence of inhibitors which can all alter the catalytic conformation of the enzyme. Because of this it is necessary to convert enzyme into immobilized form which leads to increased stability, ease of handling, possibility to reuse and a consequent decrease in running cost [8,9].

In this paper in order to develop a sustainable and eco-friendly biocatalyst for the decolorization of col-

Correspondence: D.Ž. Mijin, Faculty of Technology and Metallurgy, University of Belgrade, Karnegijeva 4, 11000 Belgrade, Serbia.
E-mail: kavur@tmf.bg.ac.rs
Paper received: 20 February, 2015
Paper accepted: 12 May, 2015

ored wastewater a simple method for the immobilization was applied. HRP was immobilized onto kaolin using glutaraldehyde (GA) as a cross-linking agent. Influence of the initial glutaraldehyde concentration as well as the initial enzyme concentration on the enzyme coupling yield and the activity of resulting biocatalyst was examined. The obtained immobilized biocatalyst was tested in the decolorization of the model dye C.I. acid violet 109 (AV 109).

EXPERIMENTAL

Materials

Anthraquinone dye C.I. acid violet 109 was provided by Lanaset (Lanaset Violet B). Horseradish peroxidase, glutaraldehyde and pyrogallol were obtained from Sigma–Aldrich (USA). Kaolin was supplied from Carlo Erba, and hydrogen peroxide was purchased from Merck (Darmstadt). All other chemicals used in this study were of analytical grade.

Methods

Support activation

In order to increase the reactivity of the support, prior to immobilization, kaolin was activated using thermal treatment [10–12]. Thermal activation was accomplished after heating the kaolin paste (50% of moisture) in the oven for 2 h at 550 °C.

The effect of the initial glutaraldehyde concentration on the immobilized mass and enzyme activity

100 mg of thermally activated support was suspended in 0.5 mL of different glutaraldehyde solution concentrations 0.12–1.0% and gently mixed at room temperature for 1 h [13]. After the reaction was finished excess of glutaraldehyde was washed several times with distilled water. Prepared support was used for the HRP immobilization.

Immobilization of HRP

Immobilization of HRP was carried out by immersing 100 mg of GA–kaolin into 0.5–5.0 mg mL^{-1} of HRP solution in phosphate buffer (100 mM, pH 7.0) and suspension was incubated for 4h at room temperature. Biocatalyst was separated from the supernatant and washed with immobilization buffer until no activity was detected in the washings. Immobilized enzyme was stored at 4 °C until use.

Measurement of the enzyme activity

Activity of the free and immobilized HRP was measured using standard substrates, hydrogen peroxide and pyrogallol. The reaction mixture for measuring the activity of free enzyme consisted of: 1 mL of 13 mM pyrogallol in the potassium-phosphate buffer pH 7.0, 10 µL of 3% hydrogen peroxide and 10 µL of diluted enzyme solution. The reaction rate was monitored spectrophotometrically at 420 nm by following the change in absorbance values every 30 s for 3 min. The reaction mixture for measuring the activity of immobilized HRP consisted of: 3 mL of 13 mM pyrogallol prepared in the potassium phosphate buffer pH 7.0, where few milligrams of immobilized biocatalyst were suspended. After adding 30 µL of hydrogen peroxide, magnetic stirrer was set on the maximum and reaction rate was recorded each 60 s for 3 min in the samples obtained after centrifugation. One unit of the activity was defined as the amount of peroxidase that will form 1.0 mg of purpurogallin from pyrogallol in 20 s at pH 7.0 and 20 °C [14].

Protein content determination

Immobilization yield was calculated after protein content determination in the initial solution, supernatant and washings. Protein content was determined using modified method of Lowry [15]. The difference between the offered, protein in the supernatant and washings represent the mass of bound protein.

Dye decolorization in batch process

Optimal pH was evaluated by incubating the free and immobilized HRP with equal activity in AV 109 solution (30 mg L^{-1}) at pH 3.0–12.0 under 25 °C. Influence of hydrogen peroxide concentration on the decolorization was examined by varying the hydrogen peroxide concentration in the range 0.05–2.0 mM. In the third set of experiments, dye concentration influence was examined by varying the dye concentration in the range 10–50 mg L^{-1}, on the decolorization. In order to compare the properties, all experiments were performed with both forms of free and immobilized HRP under similar reaction conditions. In defined time intervals aliquots were collected from the reaction mixtures and residual dye amount was followed using UV–Vis spectrophotometer (UV Shimadzu 1700, Shimadzu Corporation, Kyoto, Japan) at maximum wavelength for the tested dye (λ_{max} 590 nm, AV 109).

Decolorization percentage was calculated using following mathematical expression [16]:

$$\text{Decolorization} = \frac{100\left(A_0 - A_t\right)}{A_0} \quad (1)$$

where A_0 is the initial absorbance of the untreated dye solutions (control) and A_t is the absorbance of the dye solution after enzymatic treatment.

RESULTS AND DISCUSSION

The influence of the initial glutaraldehyde concentration

Support activation using glutaraldehyde was studied intensively because the method is simple, inexp-

ensive and efficient [17]. Glutaraldehyde used in the activation step has a role of a spacer arm and may prevent direct contact of the enzyme with the support. However, the excess of the glutaraldehyde can randomly attach the amino groups of the enzyme resulting in the hindering of the enzyme active center and inactivation [18]. Because glutaraldehyde is prone to cross linking and forming dimmers its initial concentration can greatly affect the amount of free aldehyde groups on the activated support at thus the immobilization and the activity yield. Influence of the initial glutaraldehyde dose on the protein loading and the activity of the immobilized preparation is presented in Figure 1.

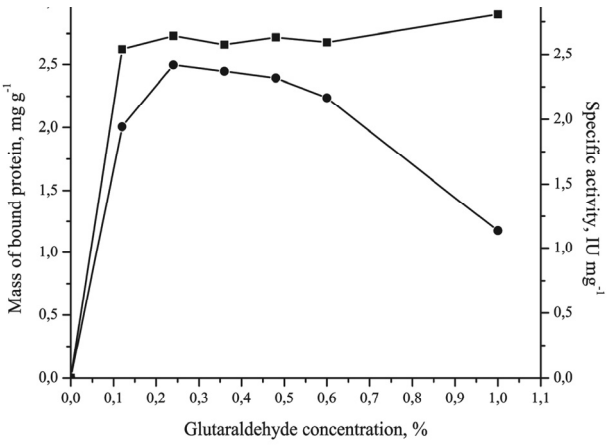

Figure 1. Initial glutaraldehyde concentration (GA) influence on mass of bound protein (square) and specific activity of immobilized preparation (circle).

It can be seen from the Figure 1 that, in the tested range, increasing the initial glutaraldehyde concentration did not have effect on the protein loading which is almost constant (2.7 mg g^{-1}), while the increase in GA concentration up to 0.24% leads to increase in the activity of the immobilized enzyme (2.4 IU mg^{-1}). Further increase resulted in the reduction of the activity which falls more than double at GA concentration of 1%. The explanation for such behavior lays in the fact that high concentration of aldehyde groups can lead to multi-point covalent attachment that can change the active enzyme conformation and transform it into inactive form [19]. Similar results were given in the literature. Chen *et. al* immobilized β-galactosidase using GA and obtained the most active biocatalyst at GA concentration of 0.3%. Increase the GA concentration above 0.3% GA significantly reduced the obtained preparation activity, as a consequence of multipoint attachment between enzyme and support [13].

Immobilization of HRP

After activation, support was used for the immobilization of HRP. Herein, in order to examine the support capacity and the activity of immobilized preparations, offered enzyme concentration was varied.

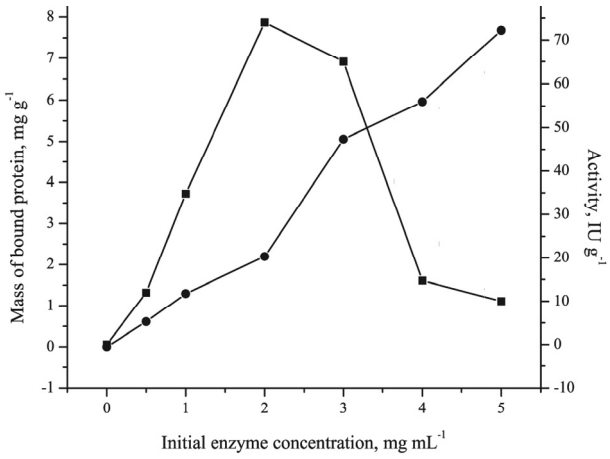

Figure 2. Initial enzyme concentration influence on mass of bound protein (circle) and specific activity of immobilized preparation (square) (reaction conditions: reaction time 4 h, pH 7.0, glutaraldehyde concentration 0.24%, temperature 24 °C).

It is evident from the Figure 2 that, in the investigated range, increasing the offered mass of protein resulted in almost linear increase of protein loading. This indicates a large number of available aldehyde groups on the support surface. However, the increase in the mass of bound proteins does not necessarily mean the activity increase. From the Figure 2 it can be observed that the increase in the offered enzyme concentration from 0.5–2.0 mg mL^{-1} leads to activity increase up to 74.2 IU g^{-1}. Further increase in the offered enzyme concentration resulted in a sharp activity decrease and was negligible for the initial concentration of 5.0 mg mL^{-1}. Due to increase in the mass of loaded protein enzyme molecules become more densely packed which increases the possibility of steric hindrances and limits the mass diffusion as well [17]. Also, at higher protein loading activity of the immobilized preparation was significantly impaired mainly due protein-protein interactions. The protein–protein interactions are the consequence of deficiently space between adsorbed proteins which leads to structural rearrangements and activity decrease [20,21].

Dye decolorization in batch process

Optimum pH

Obtained immobilized biocatalyst with the specific activity of 2.4 IU mg^{-1} was used for the optimization of process parameters for the AV 109 decolorization in the batch reactor. As a batch reactor glass vial with magnetic stirrer was used. Because of its intrinsic influence on the acidic-basic behavior of the substrate and protonation state of histidine and arginine involved in the catalytic cycle, pH is one of the most important

parameters for the efficient performing of the desired reaction [23]. Optimum pH for the decolorization of AV 109 with the free and immobilized HRP was performed by measuring the decolorization at different pH values using the same amount of the free and immobilized HRP and similar reaction conditions. The experimental pH region from 3.0 to 12.0 is chosen because pH conditions of textile effluent are in that range [24]. The activity of the immobilized and free biocatalyst under different pHs is depicted in the Figure 3.

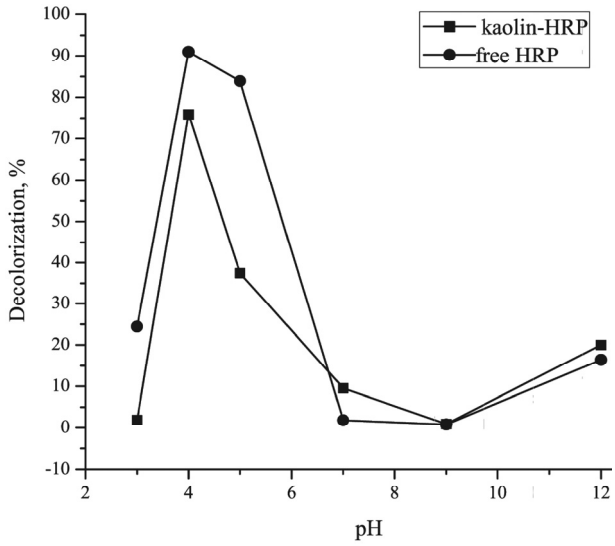

Figure 3. pH influence on the decolorization of AV 109 by free and kaolin-HRP (dye concentration 30 mg L^{-1}, temperature 24 °C, hydrogen peroxide concentration 0.4 mM, enzyme concentration 0.1 U).

From the Figure 3 it can be seen that the optimum pH for the immobilized as well as for the free peroxidase corresponds to pH 4. A small degree of decolorization below pH 4.0 can be interrelated with the loss of heme group, which occurs much faster in this pH range, and the conversion of HRP into catalytically inactive form [25]. Under defined conditions after 60 min immobilized HRP oxidized 75.9%, meanwhile free oxidized 95% of AV 109 dye. This can be correlated with the steric effect of the support which hides the enzyme active center and the substrate may be difficult to approach. The obtained optimal pH corresponds to the reported value for HRP decolorization of Lanaset Blue 2R, where 59% of dye decolorization was achieved at pH 4.0 [26]. As it can be observed from the Figure 3, an increase in pH above 6.0 significantly decreased the decolorization. Similar results were obtained after applying HRP in the decolorization of Remazol Blue and Red Cibacron, where above pH 6.0 HRP activities were significantly smaller [27]. Performances of the immobilized biocatalyst are extremely dependent on the carrier selected for the immobilization. Thus, for example, Mohan *et al.* showed that HRP optimum pH for decolorization of Acid Black 10 BX dye was 2.0, but Karim *et al.* approved that pH 6.0–8.0 was optimal for azo dye removal from textile effluent, when HRP was immobilized in acrylamide gel and β-cyclodextrin-chitosan complex, respectively [28,29]. Besides, free HRP exhibited highest activity in acidic pH, meanwhile immobilized biocatalyst showed stability against alkaline conditions unlike free HRP whose activity was negligible under these conditions. Also a sharp decline in the activity under alkaline conditions to pH 12.0 and thereafter abrupt increase can be seen on the Figure 3. This arise from the structural changes in the distal pocket of the heme cavity where movement of distal histidine leads to its binding to the metal ion or from the changes in spin state of iron, from high to low [30,31].

Optimum hydrogen peroxide dose

It is clear from the Figure 4 that catalytic yield is favored by the low hydrogen peroxide concentration. Increase in the H_2O_2 concentration above 0.6 mM induced a slight decrease in the decolorization efficiency. Inhibitory effect of coadjutant was noticed by other researchers too. For example, HRP immobilized in β-cyclodextrin-chitosan matrix showed the highest activity with 0.6 mM hydrogen peroxide concentration; where upon the decolorization percentage of tested azo dye was reduced significantly [32]. This phenomenon could be explained with the fact that excess of hydrogen peroxide leads to higher generation of intermediate species that inhibit the activity of the enzyme [7]. Besides horseradish peroxidase, other peroxidases used in the decolorization reactions also showed increased sensitivity against hydrogen peroxide [16,7,33].

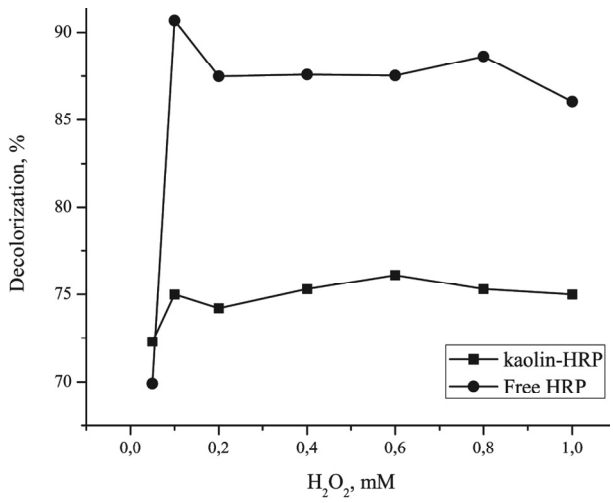

Figure 4. Initial H_2O_2 dose influence on the AV 109 decolorization by free and kaolin-HRP (dye concentration 30 mg L^{-1}, temperature 24 °C, pH 4.0, enzyme concentration 0.1 U).

However, Figure 4 also shows a higher sensitivity of free HRP than its immobilized counterpart against suicide effect of the peroxide. The optimum dose for performing the decolorization of AV109 using immobilized HRP was 0.6 mM, meanwhile free HRP exhibited highest activity at peroxide concentration of 0.1 mM. This suggests that the immobilization protected active center and the enzyme is active in a much wider range of hydrogen peroxide concentrations.

Optimum dye dose

Figure 5 represents the dependence of decolorization percentage of the dye concentration. It is evident that the dye had inhibitory influence on HRP, too. For both, free and immobilized enzyme optimal concentration for the highest decolorization percentage (92.3% for free HRP and 76.5% for kaolin-HRP) was 30 mg L^{-1}. Decolorization decreased thereafter, but the inhibitory influence of the dye is much more pronounced on the free than on the kaolin-HRP. Up to a concentration of 100 mg L^{-1} immobilized enzyme retained almost constant decolorization potential (around 70%) while steep decreased for the free enzyme can be observed and the decolorization percentage falls to 21.3%. Immobilization had positive influence on the HRP since under determined conditions the free HRP retained 23%, while the kaolin-HRP retained 92% of the activity.

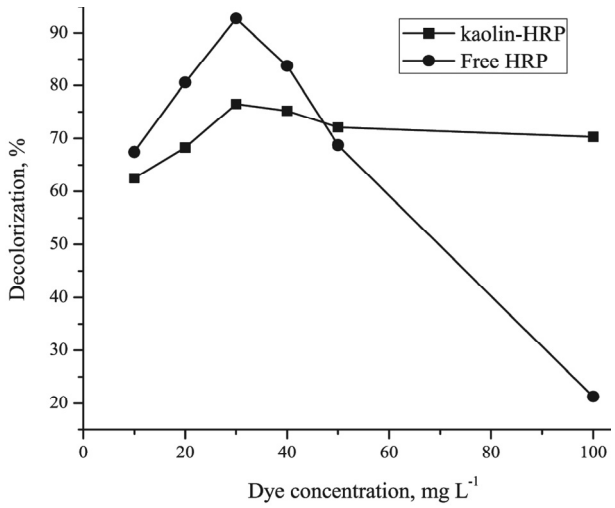

Figure 5. Initial dye concentration influence on the AV 109 decolorization by free and kaolin-HRP (hydrogen peroxide concentration 0.1 mM and 0.6 mM for free and kaolin-HRP, respectively, temperature 24 °C, pH 4.0, enzyme concentration 0.1 U).

The negative effect of the high dye concentration was observed in the decolorization reactions by other peroxidases [34,35]. Lower substrate concentrations were very effective in the suppression of the enzyme inactivation. Explanation for this can be found in the HRP catalytic cycle. Namely, in the HRP catalytic cycle there are tree similar forms of the enzyme HRP E, E-I and E-II so there is the same possibility for dye binding for E-I as well as for E-II and form dead-end complex. With dye concentration increase the possibility for inactivate complex formation also increases [36–38]. When enzyme is immobilized by GA method, this formation of inactivate complex is almost absent.

It can be concluded that the optimal conditions are: enzyme concentration 0.1 U, pH 4.0, hydrogen peroxide and dye concentration 0.6 mM and 30 mg L^{-1}, 1 h of contact time. Under the optimal conditions the immobilized biocatalysts decolorized 76.5%, meanwhile free HRP 92.3% of AV 109 dye.

Reusability study

In addition, the possibility of application of obtained biocatalyst at industrial scale was evaluated trough reusability study. Results are presented in the Figure 6.

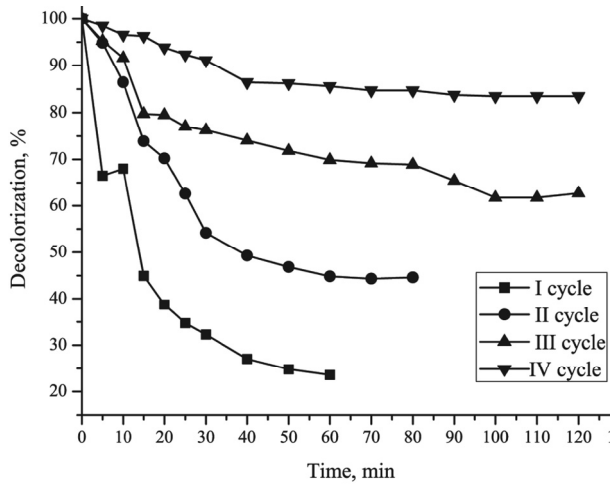

Figure 6. Reusability study (enzyme concentration 0.1 U, dye concentration 30 mg L^{-1}, pH 4.0, hydrogen peroxide concentration 0.6 mM, temperature 24 °C).

Biocatalyst applied under determined optimum conditions after first cycle was separated from the reaction mixture, rinsed with the reaction buffer and assessed for its left over catalytic activity. It was possible to apply the immobilized HRP four times in the reaction; where after each cycle progressive decrease in the decolorization was observed. For example, after fourth cycle immobilized HRP retained 15% of its original activity. Jiang *et.al* found that HRP encapsulated in phospholipid-templated titania retained around 50% of the activity after 6 consecutive cycles, meanwhile mesoporous materials did not show such good properties in terms of reusability and the immobilized enzyme was possible to apply only twice in the decolorization of dye Remazol Brilliant Blue R [39,40]. This behavior was explained by forming the reaction products layer across the enzyme active site, which thus became inaccessible for the substrate [40]. Immobil-

ization of HRP onto kaolin by GA method approved to be a good immobilization technique because 0.1 IU of immobilized HRP decolorized 55.7 mg L^{-1}, meanwhile free HRP only 27.7 mg L^{-1}.

CONCLUSION

After multiple set of experiments listed above, the kaolin has proven to be a good choice as the support for the immobilization of HRP. Obtained biocatalyst is characterized by good performances in terms of continuous use and the retained activity. The high degree of tested dye decolorization and improved properties in terms of pH, the impact of dye and hydrogen peroxide, indicated the possibility of this biocatalyst application as a clean alternative in wastewater treatment. In order to apply the immobilized enzyme in the continuous wastewater treatment plants further experiments should be focused on the stability increase.

Acknowledgement

The authors acknowledge the financial support of the Ministry of Education, Science and Technological Development of the Republic of Serbia (project number III-46010 and 172013).

REFERENCES

[1] M. Rizwana, M. Darshan, D. Nilesh, Phytoremediation of textile wastewater using potential wetland plant: Eco sustainable approach, Int. J. Interdiscip. Multidiscip. Stud. **1** (2014) 130–138.

[2] D.H.Y. Yanto, S. Tachibana, K. Itoh, Biodecolorization of textile dyes by immobilized enzymes in a vertical bioreactor system, Procedia Environ. Sci. Eng. Manage. **20** (2014) 235–244.

[3] M.B. Ibrahim, N. Poonam, S. Datel, M. Roger, Microbial decolorization of textile dye-containing effluents: a review, Bioresour. Technol. **58** (1996) 217–227.

[4] S. Wijetunga, X.F. Li, C. Jian, Effect of organic load on decolourization of textile waste-water containing acid dyes in up flow anaerobic sludge blanket reactor, J. Hazard. Mater. **177** (2010) 792–798.

[5] Q. Husain, Peroxidase mediated decolorization and remediation of wastewater containing industrial dyes: a review, Rev. Env. Sci. Biotechnol. **9** (2010) 117–140.

[6] Md. A. Arafath, M. Hossain, S.S. Alam, R. Sourav, Studies on the adsorption efficiency and kinetics of dye removal from textile effluent using some natural bio-adsorbent, Int. J. Sci. Eng. Technol. **2** (2013) 853–856.

[7] F. Jamal, S. Sinhg, T. Qidwai, D. Singh, P.K. Pandey, G.C. Pandey, M.Y. Khan, Catalytic activity of soluble versus immobilized cauliflower (*Brassica oleracea*) bud peroxidase-concavalin A complex and its application in dye color removal, Biocatal. Agric. Biotechnol. **2** (2013) 311–321.

[8] K. Poonkuzhal, T. Palvannan, Comparation of biopolymers for immobilization of lacasse: Ecotoxicity assessment of azo dye, Indian J. Biotechnol. **12** (2013) 395–401.

[9] A. Mugdha, M. Usha, Enzymatic treatment of wastewater containing dyestuffs using different delivery systems, Sci. Rev. Chem. Commun. **2** (2012) 31–40.

[10] A.M. Rashad, Metakaolin as cementitious material: History, scours, production and composition – A comprehensive overview, Constr. Build. Mat. **41** (2013) 303–318.

[11] G. Kakali, T. Perraki, S. Tsilvis, E. Badogiannis, Thermal treatment of kaolin: the effect on mineralogy on the pozzolanic activity, Appl. Clay Sci. **20** (2001) 73–80.

[12] B. Plešingerova, G. Sučik, M. Fabian, Surface area change of kaolin causing annealing, Acta Metallurg. Slov.**17** (2011) 169–176.

[13] H. Chen, Q. Zhang, Y. Dang, G. Shu, The effect of glutaraldehyde cross-linking on the enzyme activity of immobilized β-galactosidase on chitosan bed, Adv. J. Food. Sci. Technol. **5** (2013) 932–935.

[14] T. Cvetić, A. Sabovljević, J. B. Pristov, M. Sabovljević, M, Effects of day length on photosynthetic pigments and antioxidative metabolism of *in vitro* cultured moss *Atrichum undulatum* (Hedw.) P. Beauv. (*Bryophyta*), Bot. Serb. **33** (2009) 83–88.

[15] E.F. Hartree, Determination of protein: A modification of the Lowry method that gives a linear photometric response, Anal. Biochem. **48** (1972) 422–427.

[16] N. Šekuljica, N. Prlainović, A. Stefanović, M. Žuža, D. Čičkarić, D. Mijin, Z. Knežević-Jugović: Scientiffic World J. (2015), Article ID 371625.

[17] J. Zhu, G. Sun, Lipase immobilization on glutaraldehyde-activated nanofibrous membranes for improved enzyme stabilities and activities, React. Funct. Polym. **72** (2012) 839–845.

[18] H.J. Chae, E.Y. Kim, Man-Jin In, Improved immobilization yields by addition of protecting agents in glutaraledhyde induced immobilization of protease, J. Biosci. Bioeng. **89** (2000) 377–379.

[19] J.L. House, E.M. Anderson, W.K. Ward, Immobilization techniques to avoid enzyme loss from oxidase-based biosensors: A one year study, J. Diab. Sci. Technol. **1** (2007) 18–27.

[20] A. Sethuraman, G. Belfort, Protein structural perturbation and aggregation on homogenous surfaces, Biophys. J. **88** (2005) 1322–1333.

[21] A. Sethuraman, G. Vendanthan, T. Imoto, T. Przybycien, G. Belfort, Protein unfolding and interfaces: Slow dinamics of alpha-helix to beta-sheet transition, Proteins **56** (2004) 669–678.

[22] E. Laurenti, E. Ghibaudi, S. Ardissone, R.P. Ferrari, Oxidation of 2,4-dichlorophenol catalyzed by horseradish peroxidase: characterization of the reaction mechanism by UV-visible spectroscopy and mass spectrometry, J. Inorg. Biochem. **95** (2003) 171–176.

[23] A. Cordoba, I. Magario, M.L. Ferreira, Evaluation of hematin-catalyzed Orange II degradation as a potential alternative to horseradish peroxidase, Inter. Biodeteor. Biodegr. **73** (2013) 60–72.

[24] T. Thongsook, D.M. Barrett, Purification and partial characterization of broccoli (*Brassica oleracea Var. Italica*) peroxidases, J. Agric. Food. Chem. **53** (2005) 3206–3214.

[25] S.M.A.G.U. de Souza, E. Forgiarini, A.A.U. de Souza, Toxicity of textile dyes and their degradation by the enzyme horseradish peroxidase (HRP), J. Hazard. Mater. **147** (2007) 1073–1078.

[26] K. Knutson, S. Kirzan, A. Ragauskas, Enzymatic biobleaching of two recalcitrant paper dyes with horseradish and soybean peroxidase, Biotechnol. Lett. **27** (2005) 753–758.

[27] S.V. Mohan, K.K. Prasad, N.C. Rao, P.P. Sarma, Acid azo dye degradation by free and immobilized horseradish peroxidase (HRP) catalyzed process, Chemosphere **58** (2005) 1097–1105.

[28] Z. Karim, R. Adnan, Q. Husain, A β-cyclodextrin-chitosan complex as the immobilization matrix for horseradish peroxidase and its application for the removal of azo dyes from textile effluent, Int. Biodeterior. Biodegrad. **72** (2012) 10–17.

[29] T.K. Das, S. Mazumdar, S. Mitra, Heme CD as a probe for monitoring local structural changes in heme-proteins: Alkaline transition in heme proteins, Proc. Indian Acad. Sci. (Chem. Sci.) **107** (1995) 497–503.

[30] A. Mandan, S. Modi, A. Saxena, D.V. Behere, S. Mitra, Nature of distal amino acid residue responsible for acid-alkaline transition in HRP: Circular dichroism studies, Proc. Indian Acad. Sci. (Chem. Sci.) **102** (1990) 431–503.

[31] M. Celebi, M. Altikatoglu, Z.M. Akdeste, H. Yildrim, Determination of decolorization properties of Reactive Blue 19 using horseradish peroxidase enzyme, Turkish J. Biochem. **37** (2012) 200–206.

[32] S. Akhtar, Q. Husain, Potential applications of immobilized bitter gourd (*Momordica charantia*) peroxidase in the removal of phenols from polluted water, Chemosphere **65** (2006) 1228–1235.

[33] M.Z. Alam, M.F. Mansor, K.C. Jalal, Optimization of decolorization of methylene blue by lignin peroxidase produced from sewage sludge with *Phanerocheate chryosporium*, J. Hazard. Mater. **162** (2009) 708–715.

[34] G. Yu, X. Wen, R. Li, Y. Qian, In vitro degradation of a reactive azo dye by crude lignolytic enzymes from nonimmersed culture of *Phanerocheate chryosporium*, Process Biochem. **41** (2006) 1987–1993.

[35] A.N.P. Hiner, E.L. Raven, R.N.F. Thorneley, F. Garcia-Canovas, J.N. Rodrigez-Lopez, Mechanisms of compound I formation in heme peroxidases, J. Inorg. Chem. **91** (2002) 27–34.

[36] F. Deyhimi, F. Nami, Peroxidase-Catalyzed Electrochemical Assay of Hydrogen Peroxide: A Ping-Pong Mechanism, Int. J. Chem. Kinet. **44** (2012) 699–704.

[37] U. Bandyopadhyay, S. Adak, R.K. Banerjee, Role of active site residues in peroxidase catalysis: Studies on horseradish peroxidase, PINSA **B65** (1999) 315–330.

[38] Y. Jang, W. Tang, J. Gao, L. Zhou, Y. He, Immobilization of horseradish peroxidase in phospholipid-templated titania and its application in phenolic compounds and dye removal, Enzyme Microb. Technol. **55** (2014) 1–6.

[39] M. Guo, L. Fuping, L. Minyao, L. Tuoping, P. Jun, N. Wang, P. Liang, C. Zhang, Purification of recombinant lacasse from *Trametes Versicolor* in *Pichia methanolica* and its use for the decolorization of anthraquinone dye, Biotechnol. Lett. **30** (2008) 2091–2096.

IZVOD

IMOBILIZACIJA PEROKSIDAZE IZ RENA GLUTARALDEHIDOM NA KAOLIN I PRIMENA U DEKOLORIZACIJI ANTRAHINONSKIH BOJA

Nataša Ž. Šekuljica[1], Nevena Ž. Prlainović[1], Jelena R. Jovanović[2], Andrea B. Stefanović[2], Sanja Ž. Grbavčić[1], Dušan Ž. Mijin[2], Zorica D. Knežević-Jugović[2]

[1]*Inovacioni centar, Tehnološko–metalurški fakultet, Univerzitet u Beogradu, Karnegijeva 4, 11000 Beograd, Srbija*
[2]*Tehnološko–metalurški fakultet, Univerzitet u Beogradu, Karnegijeva 4, 11000 Beograd, Srbija*

(Naučni rad)

Očuvanje životne sredine, predstavlja jedan od vodećih izazova s obzirom na količinu otpadnih voda koje se svakodnevno generišu. Opšte je poznato da je voda jedan od polaznih uzroka mnogih bolesti, te je stoga akcenat stavljen na razvoj ekološki prihvatljivih, ali i održivih metoda prečišćavanja. Umesto tradicionalnih metoda prečišćavanja koje ne mogu da se primene na širok spektar jedinjenja, čijom primenom nastaje sekundarni problem zagađenja u obliku aktivnog mulja, koriste se enzimi. U ovom radu pažnja je usmerena na primenu peroksidaze biljnog porekla u dekolorizaciji sintetičkih boja. Sintetičke boje se primenjuju u svim granama industrije (kozmetičkoj, prehrambenoj, farmaceutskoj, tekstilnoj) koje zahtevaju velike količine procesne vode, koja napušta proizvodni proces kao otpadna voda bogata bojama, površinski aktivnim materijama, deterdžentima, teškim metalima itd. Otpadna voda sadrži sintetičke boje koje su toksične, kancerogene i mutagene i u cilju zaštite vodenih sistema i čoveka neophodno je adekvatno prečišćavanje pre ispuštanja u vodotokove. U ovom radu je ispitana mogućnost imobilizacije peroksidaze iz rena na prirodnu glinu, kaolin, koja je široko rasprostranjena u zemljištu, kako bi se dobio biokatalizator sa potencijalnom primenom u dekolorizaciji sintetičkih boja. Pre samog postupka imobilizacije, kaolin je obrađen termički (2 h, 550 °C) kako bi se izvršila fazna transformacija i dobio znatno reaktivniji nosač. Metakaolin, nastao termičkom obradom kaolina je tretiran različitim početnim koncentracijama glutaraldehida, kako bi se ispitao uticaj koncentracije glutaraldehida na masu vezanih proteina i aktivnost dobijenog imobilizata. Nakon optimizacije koncentracije glutaraldehida, ispitan je uticaj koncentracije enzima na masu vezanih proteina i aktivnost. Nakon imobilizacije, ispitana je potencijalna primena biokatalizatora u dekolorizaciji sintetičke boje AV 109. Dobijeni biokatalizator se pokazao znatno efikasnijim u pogledu stabilnosti u sredinamarazličitih pH, naročito alkalnoj; znatno je manje osetljiv na dejstvo inhibirajućih supstrata, vodonik-peroksida i boje. Pored toga, ispitivanjem reciklacije imobilisane peroksidaze, utvrđeno je da je ovaj biokatalizator moguće primeniti i u kontinualnom režimu.

Ključne reči: Peroksidaza iz rena • Imobilizacija • Otpadna voda • Boje